UNIVERSIDAD NACIONAL
AUTÓNOMA DE MÉXICO

UNAM POSGRADO

FACULTAD DE QUÍMICA

PROGRAMA DE MAESTRÍA Y DOCTORADO
EN CIENCIAS BIOQUÍMICAS

CONTROL DE LA GLUCÓLISIS EN CÉLULAS TUMORALES DE RÁPIDO CRECIMIENTO

T E S I S

QUE PARA OBTENER EL GRADO DE:

DOCTOR EN CIENCIAS (BIOQUÍMICAS)

P R E S E N T A:

M. EN C. ALVARO MARÍN HERNÁNDEZ

Tutor: DR. RAFAEL MORENO SÁNCHEZ

MÉXICO, D. F. Febrero 2011

CONTROL DE LA GLUCÓLISIS EN CÉLULAS TUMORALES DE RÁPIDO CRECIMIENTO

RECONOCIMIENTOS

Esta tesis doctoral se realizó bajo la dirección del Dr. Rafael Moreno Sánchez en el Departamento de Bioquímica del Instituto Nacional de Cardiología "Ignacio Chávez".

El Comité Tutoral que asesoró el desarrollo de esta tesis estuvo formado por:

Dra. Irma Ofelia Bernal Lugo	Facultad de Química, UNAM
Dr. Jesús Adolfo García Sáinz	Instituto de Fisiología Celular, UNAM
Dr. Rafael Moreno Sánchez	Instituto Nacional de Cardiología

Se reconoce la colaboración de la Dra. Emma Cecilia Saavedra Lira, del departamento de Bioquímica del Instituto Nacional de Cardiología, en el desarrollo de los modelos cinéticos.

Se reconoce la colaboración de la Dra. Marina Macías Silva, del Instituto de Fisiología Celular, quien nos proporcionó hepatocitos de rata.

Se reconoce la colaboración del Dr. Alejandro Zentella Dehesa, del Instituto de Investigaciones Biomédicas, quien nos proporcionó células endoteliales de cordón umbilical.

El proyecto fue apoyado parcialmente por CONACYT (43811-Q, 80534, 123636). Durante los estudios de doctorado gocé de una beca otorgada por CONACYT para la realización de la presente tesis.

El Jurado de Examen Doctoral estuvo constituido por:

Presidente	Dr. Armando Gómez Puyou	Instituto de Fisiología Celular, UNAM
Vocal	Dr. Jesús Adolfo García Sáinz	Instituto de Fisiología Celular, UNAM
Secretario	Dr. Alejandro Zentella Dehesa	Instituto de Inv. Biomédicas, UNAM
Suplente	Dr. Juan Pablo Pardo Vázquez	Facultad de Medicina, UNAM
Suplente	Dr. Marco Antonio Cerbón Cervantes	Facultad de Química, UNAM

DEDICATORIAS

A mi esposa, una mujer incansable que me apoya incondicionalmente y de la cual estoy profundamente enamorado.

A mis hijos, esas personitas a las que amo.

A mis padres, por darme la vida y por inculcarme el sentido de la responsabilidad y de la honradez.

A mi hermano por su apoyo.

A las familias: Marín y Robles

A todos mis amigos por su amistad.

AGRADECIMIENTOS

Quiero expresar mi agradecimiento:

A mi tutor el Dr. Rafael Moreno Sánchez por apoyar mi formación, por su confianza y por haberme permitido ser parte de su grupo.

A cada una de las personas que forman parte del Departamento de Bioquímica.

A mis alumnas, por la confianza que depositaron en mí.

Al Instituto Nacional de Cardiología " Ignacio Chávez".

Al CONACYT por el financiamiento del proyecto y por la beca que me otorgo.

"La alegría de ver y entender es el
más perfecto don de la naturaleza".

"La mayoría de las ideas fundamentales de la ciencia
son esencialmente sencillas y, por regla general pueden
ser expresadas en un lenguaje comprensible para todos".
Albert Einstein

"El principio de la investigación
necesita más cabezas que medios".
Severo Ochoa

INDICE **página**

“CONTROL DE LA GLUCÓLISIS EN CÉLULAS TUMORALES DE RÁPIDO CRECIMIENTO”

RESUMEN

Un incremento significativo en la velocidad de la glucólisis se observa en la mayoría de las células tumorales con respecto a sus tejidos de origen. Dada la constante duplicación de las células tumorales, se considera que la glucólisis es una vía metabólica de gran importancia, ya que proporciona los esqueletos de carbono necesarios para la síntesis de proteínas, DNA y triglicéridos. Además puede contribuir en la síntesis de ATP cuando las células se ven sometidas a bajas concentraciones de oxígeno o cuando la mitocondria es disfuncional.

Este incremento en la glucólisis se atribuye a un aumento en la expresión de todas las enzimas y transportadores de esta vía, promovido por algunos oncogenes (C-*MYC*) o por el factor inducido por hipoxia (HIF-1α). Además, la hexocinasa (HK) y la fosfofructocinasa tipo 1 (PFK-1) presentan cambios en sus mecanismos de regulación. Estos antecedentes nos llevaron a proponer que la distribución de control en la glucólisis de las células tumorales era diferente a lo que se observa en las células normales.

Para evaluar nuestra propuesta inicialmente se caracterizó la glucólisis en células normales (hepatocitos de rata) y en células tumorales (AS-30D). En ambos modelos se midió el flujo, la concentración de algunos metabolitos y la actividad de cada una de las enzimas de la glucólisis. Los resultados indicaron que en las células tumorales (en comparación a las células normales) había un incremento en la actividad de la mayoría de las enzimas de la glucólisis de 1 a 4 veces, aunque el cambio más significativo que se observó fue el incremento en la actividad de la HK y de la PFK-1 de 306 y 56 veces, respectivamente. En consecuencia, también hubo un aumento en las concentraciones intracelulares de sus productos: la glucosa 6-fosfato (G6P) y la fructosa 1,6-bifosfato (FBP) entre 5 y 250 veces; y un incremento en el flujo glucolítico de 9 veces.

Posteriormente, para determinar la distribución de control se empleo el análisis de elasticidades y el modelado cinético, y se encontró que el control de la glucólisis en las células AS-30D, recae en el transportador de glucosa (GLUT) (C^J_{Ei}= 0.2), en la HK (C^J_{Ei}= 0.44) y en la hexosa fosfato isomerasa (HPI) (C^J_{Ei}= 0.4). Asimismo, el modelado cinético de la glucólisis en las células tumorales humanas HeLa determinó que los principales sitios de control son el GLUT (C^J_{Ei}= 0.4) y la degradación de glucógeno (C^J_{Ei}= 0.57). Estas diferencias en la distribución de control entre ambos tipos de células tumorales se atribuyeron a la expresión de diferentes isoformas del GLUT y al mayor contenido de glucógeno en las células HeLa.

Esta distribución de control apoyó parcialmente nuestra propuesta, pues la PFK-1 no ejerció un control significativo en las células tumorales mientras que en células normales esta enzima es uno de los sitios principales de control. La razón mecanística residió en la presencia de una alta concentración de los principales activadores de la enzima en el citosol de las células tumorales como son la fructosa 2-6 bisfosfato, el AMP y el fosfato (Pi), los cuales, por un lado, llevan a la enzima a su máxima actividad y, por otro, bloquean la inhibición que ejercen el ATP y el citrato. Por otra parte, la HK mantiene un control significativo de la glucólisis tumoral debido a que independiente de su localización (citosol o membrana externa mitocondrial) continua siendo fuertemente inhibida por la G6P.

Una vez que determinamos que la HK era uno de los principales sitios de control de la glucólisis en AS-30D, se planteó disminuir el flujo de esta vía al inhibir a esta enzima. Sin embargo, no se observó una baja en el flujo glucolítico, por lo que concluimos que era necesario inhibir a más de una enzima para poder observar una disminución significativa en la glucólisis.

ABSTRACT

A significant increase in the rate of glycolysis is observed in most tumor cells with respect to their tissue of origin. Due to the continuous duplication of tumor cells, it is thought that glycolysis is an essential metabolic pathway, providing the carbon skeletons necessary for the synthesis of macromolecules (proteins, DNA and triglycerides). Additionally, it can help in the synthesis of ATP when cells are subjected to low concentrations of oxygen or when the mitochondrion is dysfunctional.

This increase in glycolysis is attributed to an increase in the expression of all enzymes and transporters of this pathway, promoted by some oncogenes (*C-MYC*) or the hypoxia-induced factor (HIF-1α). In addition, hexokinase (HK) and phosphofructokinase type 1 (PFK-I) undergo changes in their regulatory mechanisms. Our proposal was that the distribution of control in glycolysis of tumor cells was different from that observed in normal cells.

To evaluate our proposal we began characterizing glycolysis in both non-tumor cells (rat hepatocytes) and tumor cells (AS-30D). In both models the fluxes, concentration of some metabolites and activity of each of the enzymes of glycolysis were determined. The results indicated that in tumor cells (with respect to normal cells) all glycolytic enzymes increase their activity by 1 to 4 times, although the most significant change was observed in HK and PFK-1 activities with increases of 306 and 56 times, respectively. As a consequence, the intracellular concentrations of glucose 6-phosphate (G6P) and fructose 1,6-bisphosphate (F1,6BP), which are products of HK and PFK-1, respectively, increased by 5- and 250-fold as well as the glycolytic flux (9 fold).

To determine the distribution of control two approaches were used: elasticity analysis and kinetic modeling. Thus, it was established that the main control of the

glycolytic flux in AS-30D cells resided in the glucose transporter (GLUT) (C^J_{Ei}= 0.2), HK (C^J_{Ei}= 0.44) and hexose phosphate isomerase (HPI) (C^J_{Ei}= 0.4) whereas in HeLa cells were the glycogen degradation pathway (C^J_{Ei}= 0.57) and GLUT (C^J_{Ei}= 0.4). The differences in the distribution of control between tumor cells were attributed to the expression of different GLUT isoforms, the over-expression levels of HK, and the glycogen content.

This distribution of control partially supported our original proposal because the PFK-1 did not exert significant control in tumor cells, in marked contrast to non-tumor cells in which this enzyme is one of the main controlling steps. The mechanistic reason was that the high cytosolic concentration of the PFK-1 activators in tumors cells fructose 2-6, bisphosphate, AMP and Pi brought about both an increased PFK-1 activity and protection against ATP and citrate inhibition. Moreover, HK maintained significant control because regardless of their location (cytosol or mitochondrial outer membrane), it was strongly inhibited by G6P.

Finally, considering that HK was one of the main controlling steps of glycolysis in AS-30D, it was examined the possibility of inhibiting tumor HK with the anti-cancer drug casiopeina II-gly to thus blocking the glycolytic flux. However, the glycolytic flux was not significantly diminished leading to the conclusion that it is necessary to inhibit more than one enzyme to observe a significant decrease in tumor glycolysis.

CONTENIDO

Esta tesis está dividida en 6 capítulos. En el capítulo 1 se describen generalidades sobre la glucólisis tumoral. El capítulo 2 comprende los mecanismos que inducen el incremento de la glucólisis en las células tumorales y aquí se incluye un artículo de revisión sobre el factor inducido por la hipoxia (HIF-1α) publicado en la revista *Mini Reviews in Medicinal Chemistry* (Manuscrito No. 1). En el capítulo 3 se relatan las generalidades de la teoría de control metabólico, mientras que el plantemiento del problema, la hipótesis y los objetivos se incluyen en el capítulo 4. El capítulo 5 comprende los resultados que se dividen en tres partes. En la primera y en la segunda parte se establecen las enzimas que controlan el flujo de la glucólisis tumoral, mediante dos herramientas experimentales del análisis de control métabolico: el análisis de elasticidades (Manuscrito No. 2: *FEBS J.* 2006, 273:1975-1988) y el modelado cinético (Manuscrito No. 3: *BBA-Bioenergetics*, 2010). La tercera parte trata de la inhibición de la hexocinasa para reducir la glucólisis; este trabajo se encuentra en preparación y se muestra la primera versión del artículo (Manuscrito No. 4). Finalmente, el capítulo 6 incluye la discusión general, las conclusiones, las perspectivas, las referencias y un apéndice.

ABREVIATURAS

1,3BPG: 1,3 bisfosfoglicerato

2PG: 2-fosfoglicerato

3PG: 3-fosfoglicerato

ALD: Aldolasa

AMPK: AMP cinasa

DHAP: Dihidroxiacetona fosfato

ENO: Enolasa

F1,6BP: Fructosa 1,6 bisfosfato

F2,6BP: Fructosa 2,6 bisfosfato

F6P: Fructosa 6-fosfato

G3P: Gliceraldehído 3-fosfato

G6P: Glucosa 6-fosfato

GAPDH: Gliceraldehído 3-fosfato deshidrogenasa

GLUT: Transportador de glucosa

HIF-1α: El factor inducido por la hipoxia

HK: Hexocinasa

HPI: Hexosa fosfato isomerasa

LDH: Lactato deshidrogenasa

MTC: Transportador de monocarboxilatos

PEP: Fosfoenolpiruvato

PFK-1: Fosfofructocinasa tipo 1

PFKFB3: Fosfofructocinasa tipo 2

PGAM: Fosfoglicerato mutasa

PGK: Fosfoglicerato cinasa

Pi: Fosfato

PYK: Piruvato cinasa

TPI: Triosa fosfato isomerasa

Capítulo 1. La glucólisis en el cáncer

1.1 Introducción

El cáncer es una enfermedad que surge de una serie de alteraciones genéticas (mutaciones, amplificaciones y pérdidas de genes) producidas por defectos genéticos o agentes ambientales (radiación, carcinógenos y virus oncogénicos), que dejan sin regulación la proliferación y la diferenciación celular, propiciando que una célula pueda llegar a generar un tumor (Vogelstein y Kinzler, 2004; Tysnes y Bjerkvig, 2007). Este proceso involucra la activación de oncogenes (HER2, Src, H-Ras, c-Myc) y la inactivación de genes supresores de tumores (PTEN, p53, pRb) los cuales intervienen en la regulación del ciclo celular y la proliferación (Vogelstein y Kinzler, 2004; Gillies et al., 2008).

Durante el 2007, en México, el cáncer ocupó el tercer lugar como causa de muerte con 514, 420 defunciones. Entre las tres principales causas de muerte por tumores en hombres se encuentran el cáncer de próstata, el de pulmón y el de estómago. En las mujeres, las muertes correspondieron principalmente a el cáncer de mama, al de cuello del útero (cérvico-uterino) y al de hígado (INEGI, 2009).

El tratamiento del cáncer se basa en la mayor susceptibilidad que tienen las células tumorales (con respecto a las células normales) al daño inducido por la radiación y la quimioterapia, que dejan severos efectos secundarios y en muchos casos los tumores son refractarios. Esto hace indispensable la búsqueda de nuevas estrategias terapéuticas que sean más selectivas y eficientes contra el cáncer (Hornberg et al., 2007). Por ello, encontrar diferencias a nivel molecular entre las células no tumorales y las células tumorales es esencial (Pelicano et al., 2006).

A este respecto, una de las alteraciones que se mantiene en la mayoría de las células tumorales, es un alto consumo de glucosa en comparación a las células normales, que las lleva a excretar una gran cantidad de lactato, fenómeno conocido como efecto “Warburg”, el cual resulta del aumento en la expresión de todas las enzimas y transportadores de la glucólisis inducido por algunos oncogenes y por el factor inducible por hipoxia-1 (HIF-1) (Walenta y Mueller-Klieser, 2004; Moreno-Sánchez et al., 2007).

El incremento en la velocidad de la glucólisis tumoral puede favorecer la síntesis de macromoléculas (DNA, trigliceridos, proteínas) necesarias para una constante duplicación. Además puede contribuir en la generación de ATP cuando la mitocondria tumoral se encuentra dañada (Carew y Huang, 2002) o cuando las células tumorales se encuentran bajo hipoxia (Xu et al., 2005).

Por lo anterior, diversos grupos de investigación consideran que inhibir a la glucólisis tumoral podría ser una adecuada estrategia en el tratamiento del cáncer (Pedersen et al., 2002; Pelicano et al., 2006; Bartrons y Caro, 2007; Clem et al., 2008; Evans et al., 2008; Kumagai et al., 2008). Sin embargo, para que dicha inhibición sea más efectiva se debe considerar inhibir solo a las enzimas que la controlan. El análisis de control metabólico permite identificar a este tipo de enzimas aplicando diferentes estrategias experimentales (Moreno-Sánchez et al., 2008).

Mediante el empleo del análisis de control metabólico, en este trabajo de tesis se determinaron los principales sitios de control de la glucólisis en las células tumorales.

1.2 La glucólisis

La vía de Embden-Meyorhof-Parnas, mejor conocida como glucólisis, fue descubierta por Eduard Buchner en 1897, aunque fue hasta 1930 cuando se describió la vía completa gracias a los estudios de Otto Warburg, Hans von Euler-Chelpin, Gustav Embden, Otto Meyerhof y Jacob Parnas (Nelson y Cox, 2005). Esta vía metabólica genera, a partir de una molécula de glucosa, dos moléculas de piruvato, y la energía liberada en esta conversión se conserva en forma de ATP y NADH. En aerobiosis, el piruvato formado es oxidado casi por completo por la mitocondria a CO_2 y H_2O. En cambio, cuando no hay suficiente oxígeno para soportar la oxidación del piruvato y del NADH, el piruvato se reduce a lactato, aceptando electrones del NADH y formándose el NAD^+ necesario para mantener a la glucólisis funcionando (Figura 1.1).

Es interesante señalar que aunque en los libros de texto, en general, no se consideran como parte de la glucólisis a los transportadores de glucosa y de monocarboxilatos, ambos transportadores son esenciales, ya que de ellos depende la entrada de la glucosa y la salida del lactato (que bajo anaerobiosis es el producto final) (Figura 1.1).

1.3 La glucólisis tumoral

Las células tumorales presentan como característica común un incremento significativo en la velocidad de glucólisis con respecto a sus tejidos de origen, que se ve reflejado en un aumento en el consumo de glucosa y en la producción de una gran cantidad de lactato (aún en presencia de oxígeno). Este fenómeno fue descrito por Warburg de ahí que sea conocido como efecto “Warburg” (Pedersen, 1979; Eigenbrodt, et al., 1985; Walenta y Mueller-Klieser, 2004; Moreno-Sánchez et al., 2007).

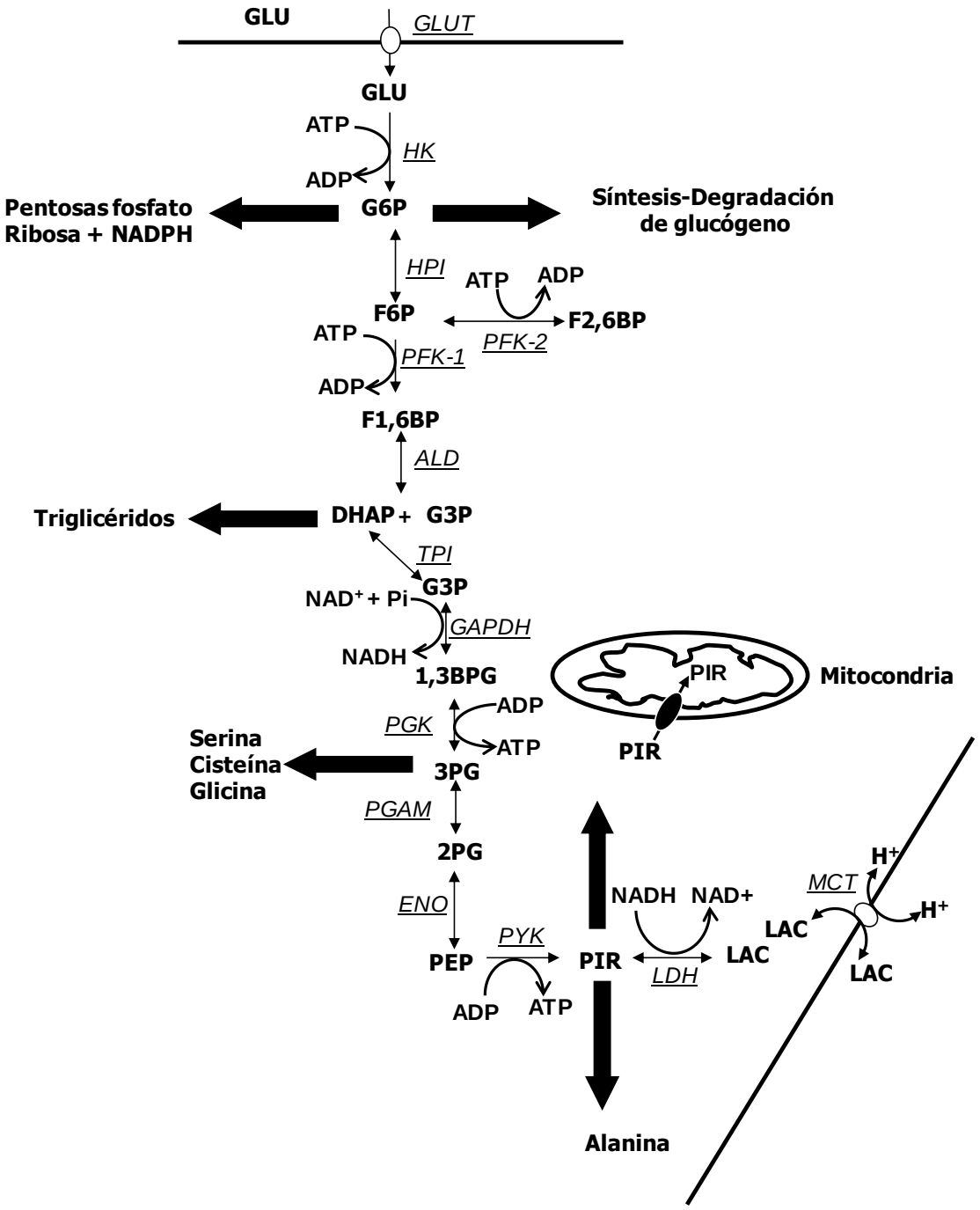

Figura 1.1 La glucólisis y su contribución en la síntesis de algunos intermediarios. GLUT, transportador de glucosa; GLU, glucosa; HK, hexocinasa; G6P, glucosa 6P; HPI, hexosa fosfato isomerasa; F6P, fructosa 6P; PFK-1, fosfofructocinasa tipo 1; F1,6BP, fructosa 1,6 bifosfato; PFK-2, fosfofructocinasa tipo 2; F2,6BP, fructosa 2,6 bifosfato; ALD, aldolasa; DHAP, dihidroxiacetona fosfato;G3P, gliceraldehído 3P; TPI, triosa fosfato isomerasa; GAPDH, gliceraldehído 3P deshidrogenasa; 1,3BPG, 1,3 bifosfoglicerato, PGK, fosfoglicerato cinasa; 3PG, 3-fosfoglicerato; PGAM, fosfoglicerato mutasa; 2PG, 2-fosfoglicerato; ENO, enolasa; PEP, fosfoenolpiruvato; PYK, piruvato cinasa; PIR, piruvato; LDH, lactato deshidrogenasa; LAC, lactato; MTC, transportador de monocarboxilatos. Modificado de *Mini. Rev. Med. Chem*. 2009, 9:1084-1101.

En células tumorales de rata (Novikoff, H-91, Jensen, Rous y Erlich) la producción de lactato llega a ser de 5 a 28 veces mayor que en los tejidos normales (riñón, hígado, músculo, cerebro y placenta) (Pedersen, 1979). En diversos tipos de carcinomas humanos (cervico-uterino, cabeza y cuello, colon-rectal) la concentración de lactato alcanzan los 40 µmol por gramo de tejido (peso húmedo), la cual es muy elevada considerando que los tejidos sanos mantienen una concentración de lactato de alrededor de 2.5 µmol/g de tejido (peso húmedo) (Walenta y Mueller-Klieser, 2004). En el suero de pacientes el lactato alcanza una concentración de hasta 9 mM, concentración 4 veces mayor a la concentración que se encuentra en individuos sanos (Nishijima, et al., 1997; Fisher, et al., 2007).

El incremento de la glucólisis se ha relacionado con el grado de malignidad de los tumores. En hepatomas de rata (tumores experimentales) se ha encontrado que en aquellos con una baja malignidad (reducida velocidad de crecimiento) mantienen una producción de láctico similar al tejido de origen (hígado) (0.16 nmol/min * mg de peso húmedo), mientras que en tumores malignos (elevada velocidad de crecimiento) mantienen una producción de láctico entre 7 a 27 veces mayor (1.6-4.3 nmol/min*mg de peso húmedo) con respecto al tejido normal (Pedersen et al., 1978; Stubbs et al., 2003).

En tumores humanos de cerebro, mama, pulmón, hígado, cérvix, cabeza y cuello niveles altos de lactato tienen pobre prognosis (Gillies et al., 2008), además de que este incremento se asocia con una alta incidencia de metástasis (Walenta et al., 2004). Asimismo, la expresión de la LDH-A está relacionada con la agresividad, metástasis y pobre prognosis en los tumores de colon, pulmón, endometrio y estómago (Giatromanolaki et al., 2006).

Por último, es importante señalar que el incremento en la glucólisis no es exclusivo de las células tumorales ni ocurre en todos los tipos de cáncer (próstata; Liu et al., 2010). Este aumento en la glucólisis también se observa en células proliferativas normales (linfocitos y otras células hematopoyéticas) (DeBerardinis et al., 2008).

1.4 ¿Qué ventajas ofrece a las células tumorales el incremento de la glucólisis?

La mayor parte de las macromoléculas requeridas para la proliferación se generan a partir de intermediarios de la glucólisis (Bauer et al. 2005). Por ejemplo, la glucosa 6-P (G6P) es el precursor de la ribosa 5P (R5P), metabolito necesario para la síntesis de ácidos nucleicos; en paralelo se genera NADPH, útil en la destoxificación de radicales libres, en la síntesis de lípidos y de la desoxirribosa; también hay síntesis de UDP-glucoronato usado en la producción de proteo-glicanos, glicoproteínas y en la detoxificación de xenobióticos. La síntesis de triglicéridos y fosfolípidos comienza con la dihidroxiacetona fosfato (DHAP). A partir del 3-fosfoglicerato (3PG) y del piruvato (PIR) se sintetizan varios aminoácidos (serina, cisteína, glicina y alanina) para la generación de proteínas (Figura 1.1).

Por otra parte, la glucólisis puede ser una fuente muy valiosa de ATP cuando las células se ven sometidas a bajas tensiones de oxígeno como ocurre cuando el tumor aumenta de tamaño y el crecimiento desorganizado de los nuevos vasos (angiogénesis) deja grandes zonas hipóxicas (Gatenby y Filies, 2004) o cuando la mitocondria deja de ser funcional debido a la alta velocidad de mutaciones que se presentan en el ADN-mitocondrial (Carew and Huang, 2002).

Las grandes cantidades de láctico (producto de la glucólisis) expulsado por las células tumorales acidifica los alrededores del tumor, lo que induce la muerte de las

poblaciones vecinas de células normales que son incapaces de adaptarse a la acidosis, esto permite que las células tumorales invadan otros tejidos y además incrementa la radio-quimio resistencia y las metástasis (Gatenby y Gillies, 2004). Asimismo, se ha descrito que el láctico afecta el funcionamiento del sistema inmune, lo cual protege a las células tumorales. La acidificación puede inhibir la actividad de las células NK y la migración de los polimorfonucleares (Lardner, 2001) permitiendo que las células tumorales no sean eliminadas. El lactato también reduce la proliferación, la producción de citocinas y la citotoxicidad en los linfocitos T (Fisher et al., 2007). Al mismo tiempo, el lactato puede permitir la estabilización del HIF-1α, factor muy importante en el desarrollo tumoral.

Capítulo 2. Mecanismos que inducen el incremento de la glucólisis

2.1 El factor inducido por la hipoxia (HIF-1α)

HIF-1α tiene una función muy importante en el incremento de la glucólisis ya que induce la transcripción de la mayoría de los genes de las enzimas y transportadores de la glucólisis. Además como se indicará posteriormente, los genes supresores de tumores y los oncogenes puede indirectamente incrementar la glucólisis, al permitir la estabilización de este factor de transcripción (aun bajo condiciones no hipóxicas). En la siguiente revisión, se discute la importancia de este factor en el metabolismo energético de las células tumorales.

***Mini Reviews in Medicinal Chemistry* 2009, 9: 1084-1101**

Reviews in Medicinal Chemistry, 2009, 9, 1084-1101

HIF-1α Modulates Energy Metabolism in Cancer Cells by Inducing Over-Expression of Specific Glycolytic Isoforms

Alvaro Marín-Hernández[1], Juan C. Gallardo-Pérez[1], Stephen J. Ralph[2], Sara Rodríguez-Enríquez[1] and Rafael Moreno-Sánchez[1,*]

[1]*Instituto Nacional de Cardiología, Departamento de Bioquímica, Tlalpan, México D.F. 14080, México;* [2]*Griffith University, School of Medical Sciences, Southport, Queensland, Australia*

Abstract: To develop new and more efficient anti-cancer strategies it will be important to characterize the products of transcription factor activity essential for tumorigenesis. One such factor is hypoxia-inducible factor-1α (HIF-1α), a transcription factor induced by low oxygen conditions and found in high levels in malignant solid tumors, but not in normal tissues or slow-growing tumors. In fast-growing tumors, HIF-1α is involved in the activation of numerous cellular processes including resistance against apoptosis, over-expression of drug efflux membrane pumps, vascular remodeling and angiogenesis as well as metastasis. In cancer cells, HIF-1α induces over-expression and increased activity of several glycolytic protein isoforms that differ from those found in non-malignant cells, including transporters (GLUT1, GLUT3) and enzymes (HKI, HKII, PFK-L, ALD-A, ALD-C, PGK1, ENO-α, PYK-M2, LDH-A, PFKFB-3). The enhanced tumor glycolytic flux triggered by HIF-1α also involves changes in the kinetic patterns of expressed isoforms of key glycolytic enzymes. The HIF-1α induced isoforms provide cancer cells with reduced sensitivity to physiological inhibitors, lower affinity for products and higher catalytic capacity ($Vmax_f$) in forward reactions because of marked over-expression compared to those isoforms expressed in normal tissues. Some of the HIF1α-induced glycolytic isoforms also participate in survival pathways, including transcriptional activation of H2B histone (by LDH-A), inhibition of apoptosis (by HKII) and promotion of cell migration (by ENO-α). HIF-1α action may also modulate mitochondrial function and oxygen consumption by inactivating the pyruvate dehydrogenase complex in some tumor types, or by modulating cytochrome *c* oxidase subunit 4 expression to increase oxidative phosphorylation in other cancer cell lines. In this review, the roles of HIF-1α and HIF1α-induced glycolytic enzymes are examined and it is concluded that targeting the HIF1α-induced glucose transporter and hexokinase, important to glycolytic flux control, might provide better therapeutic targets for inhibiting tumor growth and progression than targeting HIF1α itself.

Key Words: Glucose transporters, hexokinases, HIF-1α, glycolysis, mitochondria, glycolytic inhibitors, mitochondrial inhibitors.

INTRODUCTION: HIF-1

The development of hypoxic regions in solid tumors is a recurrent feature which is linked to the processes of malignant transformation, metastasis and resistance to chemo-, immuno- and radio-therapy [1, 2]. The hypoxia-inducible factor (HIF) is a key transcriptional regulator that plays a role in these processes by modulating expression of proteins involved in angiogenesis, erythropoiesis, cellular proliferation and survival, vascular remodeling, vasomotor control, and catecholamine, iron and energy metabolic pathways, thereby allowing tissues to adjust to low oxygen concentrations [3].

Although several isoforms of HIF exist including HIF-1, -2 and -3 (see below for more detail), the focus of this review will be on HIF-1 because its functions are the most well defined in relation to modifying glycolysis. The molecular biological mechanisms whereby HIF-1 acts as a transcriptional activation factor regulating gene expression have been extensively studied, since the seminal publication of Semenza *et al.*, [4], and reviewed [5,6]. Thus, the present review focuses on those proteins that play key roles in controlling the changes in glycolytic flux inside cancer cells and whose isoforms are modulated by HIF-1 and hypoxia.

HIF-1 is a heterodimer that binds to promoter regions containing the DNA sequence 5'-RCGTG-3' (R= A or G) [3, 4, 7], called hypoxic responsive elements (HRE) (Fig. 1). This transcriptional factor is comprised of two subunits, HIF-1α and HIF-1β, which both contain one beta Helix-Loop-Helix (bHLH) and two (PER-ARNT (arylhydrocarbon receptor nuclear translocator)-SIM) PAS domains in their N-terminal segments (Fig. 1). The bHLH domain regulates DNA binding; the PAS domains regulate HIF (α + β) subunit heterodimerization and are likely to participate in the target gene selection (Fig. 1) [7]. As HIF-1β is constitutively expressed, the activity of HIF-1 is regulated by varying the levels of HIF1α expression. Under normoxia (21 % O_2 in air ≈ 250 μM O_2 dissolved in water at sea level and 37ºC), HIF-1α content is negligible, given its half-life of 5 min, whereas treatment with desferrioxamine, an iron chelator

*Address correspondence to this author at the Instituto Nacional de Cardiología, Departamento de Bioquímica, Juan Badiano No. 1, Sección XVI, Tlalpan, México D.F. 14080, Mexico; Tel: (5255) 5573 2911, ext. 1298; E-mail: morenosanchez@hotmail.com, rafael.moreno@cardiologia.org.mx

1389-5575/09 $55.00+.00

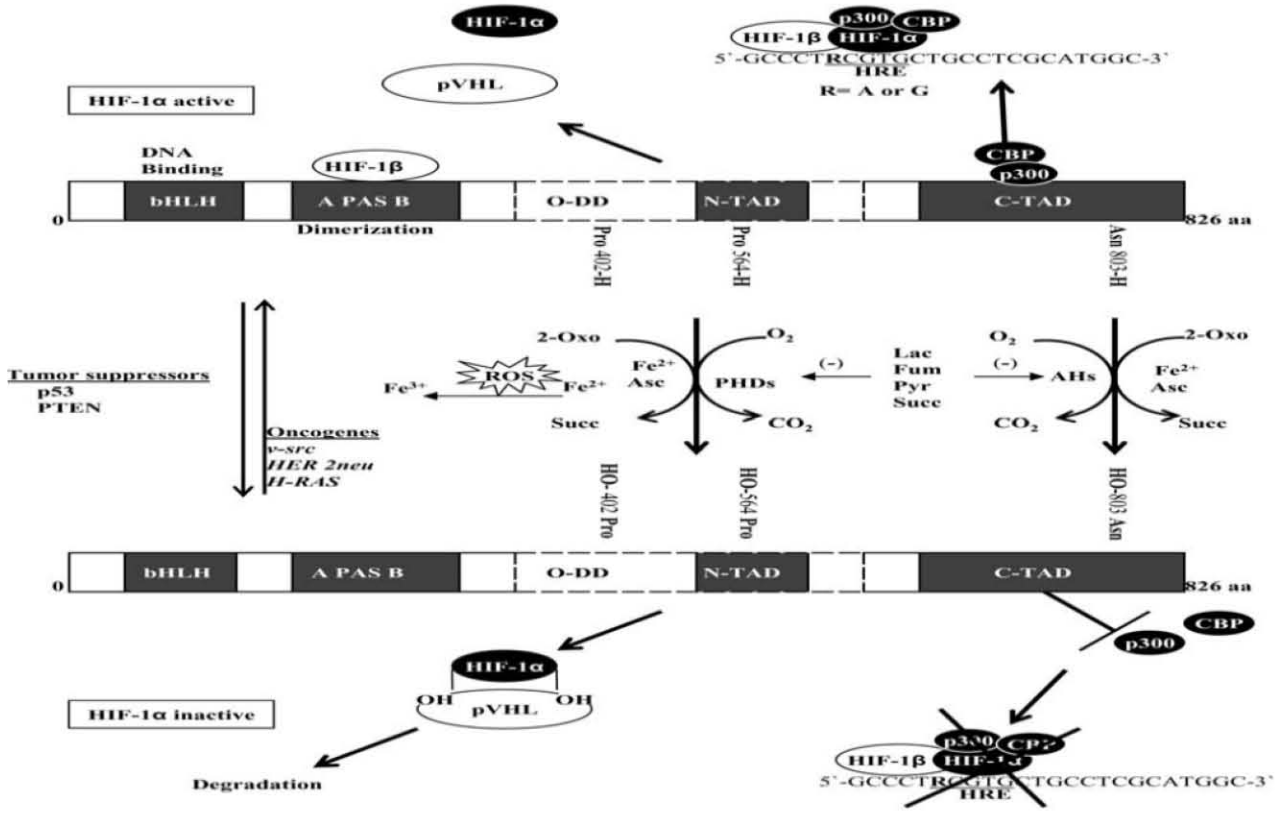

Fig. (1). Regulation of HIF-1α stability and activity.

Under normoxia, prolyl hydroxylase (PHD) hydroxylates proline (Pro) residues (402 and 564) of HIF-1α in a region called the oxygen-dependent degradation (O-DD) domain, which facilitates its interaction with the von Hippel-Lindau protein (pVHL) and hence with an ubiquitin-protein ligase complex that marks HIF-1α for destruction by the proteasome. Asparaginyl-aspartyl hydroxylases (AHs) by hydroxylating an Asn residue (803) in the carboxy-terminal transcriptional activation domain (C-TAD) of HIF-1α, inhibits the binding of cofactors, such as p300 and CBP that are required for the transcription of target genes. HIF-1α is a heterodimer that binds to hypoxic responsive elements (HRE) contained in the promoter region of the glycolytic genes. Abbreviations: 2-oxo, 2-oxoglutarate; Succ, succinate; N-TAD, amine-terminal transcriptional activation domain; Lac, lactate; Fum, fumarate; Pyr, pyruvate; Asc, ascorbate, (-), inhibition.

that mimics hypoxic conditions, the half-life becomes increased to 30 min [8].

In particular, enhanced HIF-1 expression has been detected in the majority of brain, pancreas, mammary gland, colon, ovary, lung and prostate primary tumors, and in their metastasis, but not in the majority of benign tumors or normal tissues [9-15]. Higher expression of HIF-1α correlates with poor survival in breast, head and neck, esophagus, stomach and lung cancers, although for cervical cancer this association is not so clear [15]. Both the biological complexity of the HIF system and methodological difficulties such as the criteria used to identify HIF positive cells, immunohistochemical protocols and source of tumor tissue for its experimental evaluation most probably account for any conflicting data [15].

Regulatory Mechanisms Controlling HIF-1 Activity

The von Hippel-Lindau protein (pVHL), a component of the ubiquitin ligase E3 complex, regulates HIF-1α degradation (Fig. **1**). For pVHL-HIF interaction, HIF-1α must first be hydroxylated at prolines 402 and 564 in the oxygen-dependent degradation (O-DD) domain by prolyl-4-hydroxylases (PHDs). HIF-1α transcriptional activity can also be directly inhibited by Asn 803 hydroxylation catalyzed by asparaginyl-aspartyl hydroxylases (AHs; also known as factors inhibiting HIF-1, FIHs). Hydroxylation prevents recruitment of p300/CBP co-activators that would otherwise combine together with HIF-1α, forming the active transcriptional complex [7] that binds target genes (Fig. **1**).

PHD and AH enzymatic activities both require Fe^{2+}, 2-oxoglutarate, ascorbate and oxygen (Fig. **1**). Hence, one way to reduce HIF hydroxylation would be by decreasing the oxygen level below to that required for PHDs. In this manner, it was proposed that these enzymes sense intracellular oxygen levels [16, 17] and that under hypoxic conditions, PHDs and AHs are inactivated with the result that HIF-1α becomes stabilized and activated [16].

The role of PHDs as an intracellular oxygen sensing system remains uncertain because the hydroxylase *Km* values for O_2 are reported to be much higher (> 90 μM) [18, 19] than the actual O_2 concentration that exists in the cytosol (12.5-25 μM) and in the capillaries and arterioles (20-50

μM) [17, 20-22]. Consequently, HIF-1α should not be inactivated by hydroxylation at an [O_2] of 10 μM. Under such conditions, hydroxylase activity, with a *Km* value of 100 μM should only be 9% of maximal velocity (*Vm*), which is most likely not sufficient to inactivate HIF-1α. In this regard, HIF-1α stabilization has been reported to occur in intact cells at [O_2] below 50 μM [17].

Several possibilities have been suggested to explain the apparent discrepancy between the high *Km* values of PHDs determined for O_2 and the fact that HIF-1α hydroxylation and associated degradation occurs under normoxia. For instance, kinetic studies have not taken into account the contribution of the length of the peptide substrates used in assaying PHD activity nor the role that HIF-1α substrate binding plays in facilitating oxygen binding, which may lower the actual *Km* (O_2) to more physiologically relevant values (reviewed in [23]). In addition, the expression levels of PHD2 and PHD3 are themselves increased under hypoxic conditions by HIF-1α [24, 25]. Therefore, increased PHD expression would be expected to also help reduce HIF-1α levels. In this regard, PHD2 was shown to be the most prominently expressed isoform in a large range of cancer cell lines with potent activity towards HIF-1α [24].

Mitochondrial Involvement in the Regulation of HIF-1α

An additional mechanism explaining how HIF-1α levels are increased during hypoxia is that the decrease in [O_2] causes an increase in the generation of radical oxygen species (ROS) in mitochondria by respiratory complexes I and III [26, 27]. The increased ROS induces oxidation of Fe^{2+} to Fe^{3+}, which would function to diminish the hydroxylase activity of PHD and AH (Fig. **1**). In agreement with this hypothesis, HIF-1α is not stabilized in anti-oxidant treated cells (hepatoma, smooth muscle, cardiomyocytes, gastric epithelium, renal tubule epithelium, macrophages) under hypoxia. In contrast, where ROS production is low, such as in cells lacking (a) mitochondrial DNA (rho zero, ρ^o cells), (b) cytochrome *c*, or (c) complex III Rieske iron-sulfur protein, and (d) in cells treated with stigmatellin, an inhibitor of complex III [28], HIF-1α hydroxylation proceeds efficiently under hypoxia [22, 29, 30].

Regarding the role of the respiratory chain, it has been proposed that the reduction in [O_2] during hypoxia leads to a decrease in cytochrome c oxidase (COX; complex IV) activity [31], resulting in the accumulation and overloading of the reduced intermediates, ubiquinol and semiquinone, particularly the latter, which then promote superoxide generation (see Fig. **3** for chemical structures). Specific inhibition of the respiratory complexes, by either cyanide (COX), antimycin (complex III; cytochrome b-c_1 complex), thenoyltrifluoroacetone (TTFA) or α-tocopheryl succinate (complex II; succinate dehydrogenase) or rotenone (complex I) (Fig. **3**), can also promote the generation of ROS under normoxia, because these respiratory inhibitors affect the electron transport by respiratory chain complexes to induce increased levels of semiquinone (and other free radical molecules) [32-34]. In contrast, blocking entry of energy substrates to inhibit the respiratory chain at the electron entrance level, by using malonate to inhibit complex II, phenylsuccinate or n-butylmalonate to block transport of succinate and other dicarboxylate Krebs cycle intermediates, or α-cyano-hydroxycinnamates to prevent pyruvate uptake into mitochondria (Figs. **2** and **3**), is not expected to induce generation of ROS, as these inhibitors do not directly modify the respiratory chain at the level of electron flow.

Changes in the Krebs cycle are also likely to contribute to the regulation of HIF-1α activity. The enzyme2 of the 2-oxoglutarate dehydrogenase complex (2-OGDH) can be targeted for ubiquitination-dependent degradation by Siah2, the RING finger ubiquitin-protein isopeptide ligase [35]. As Siah2 is induced by hypoxia, disruption of mitochondrial metabolism by affecting 2-OGDH would lead to loss of mitochondrial stability and cell death.

How is HIF-1α Maintained Stable and Active in Cancer Cells?

It is thought that HIF-1α in tumor cells is stabilized due to the hypoxic environment developed in certain regions, particularly in solid tumors 1 mm diameter or larger [36, 37]. Although tumors may have an active angiogenesis, unorganized, thin and fragile new vessels are formed that affect the normal dynamics of the blood flux. Consequently, some tumor sections will become excluded, leading to hypoxic regions [15, 38]. HIF-1α stabilization is also promoted by activation of certain oncogenes such as *v-src*, HER 2^{neu} and H-RAS, or by inactivation of some tumor suppressors such as p53 and PTEN [3, 6]. However, the molecular mechanisms operating in these processes have not been elucidated. A high incidence of pVHL mutations is associated with kidney and central nervous system tumors. These pVHL mutations modify or delete either the α-domain in the C-terminal region which binds to elongin-C in the proteasome, or the β-domain that interacts with the HIF-1α O-DD domain and is required for nuclear/cytosolic trafficking, preventing HIF-1α degradation (Fig. **1**) [3, 39].

Under normoxia, HIF-1α can be stabilized by the high lactate and pyruvate levels generated by active tumor glycolysis. It has been shown that these monocarboxylates, and oxaloacetate, inhibit PHD activity by competing with 2-oxoglutarate for binding [29, 40]. Similarly, mutations or down-regulation of succinate dehydrogenase (SDH) and fumarate hydratase (FH) induce a state of pseudo-hypoxia that makes cancer cells behave as if they were hypoxic, which leads to HIF-1α stabilization and enhancement [41-43]. These mutations inhibit SDH and FH activities, leading to succinate and fumarate accumulation, without associated ROS production, and to product-inhibition of hydroxylases [41-43] (Fig. **1**). Moreover, SDH and FH mutations, or their down-regulation, are associated with development of phaeochromocytomas, paragangliomas, leiomyomas, leiomyosarcomas, renal cell, gastric and colon carcinomas, and papillary thyroid cancer [22, 29, 41-43].

Additional HIF Isoforms

Three isoforms of HIF-α have been described (HIF-1α, HIF-2α/EPAS1 and HIF-3α/IPAS) and three HIF-1β isoforms (HIF-1ß/ARNT1, HIF-2ß/ARNT2, and HIF-3ß/ARNT3), although their exact relationships in forming heterodimers are not known. HIF-1α and HIF-2α/EPAS1 share similar structure, hypoxic stabilization and exclusive dimeri-

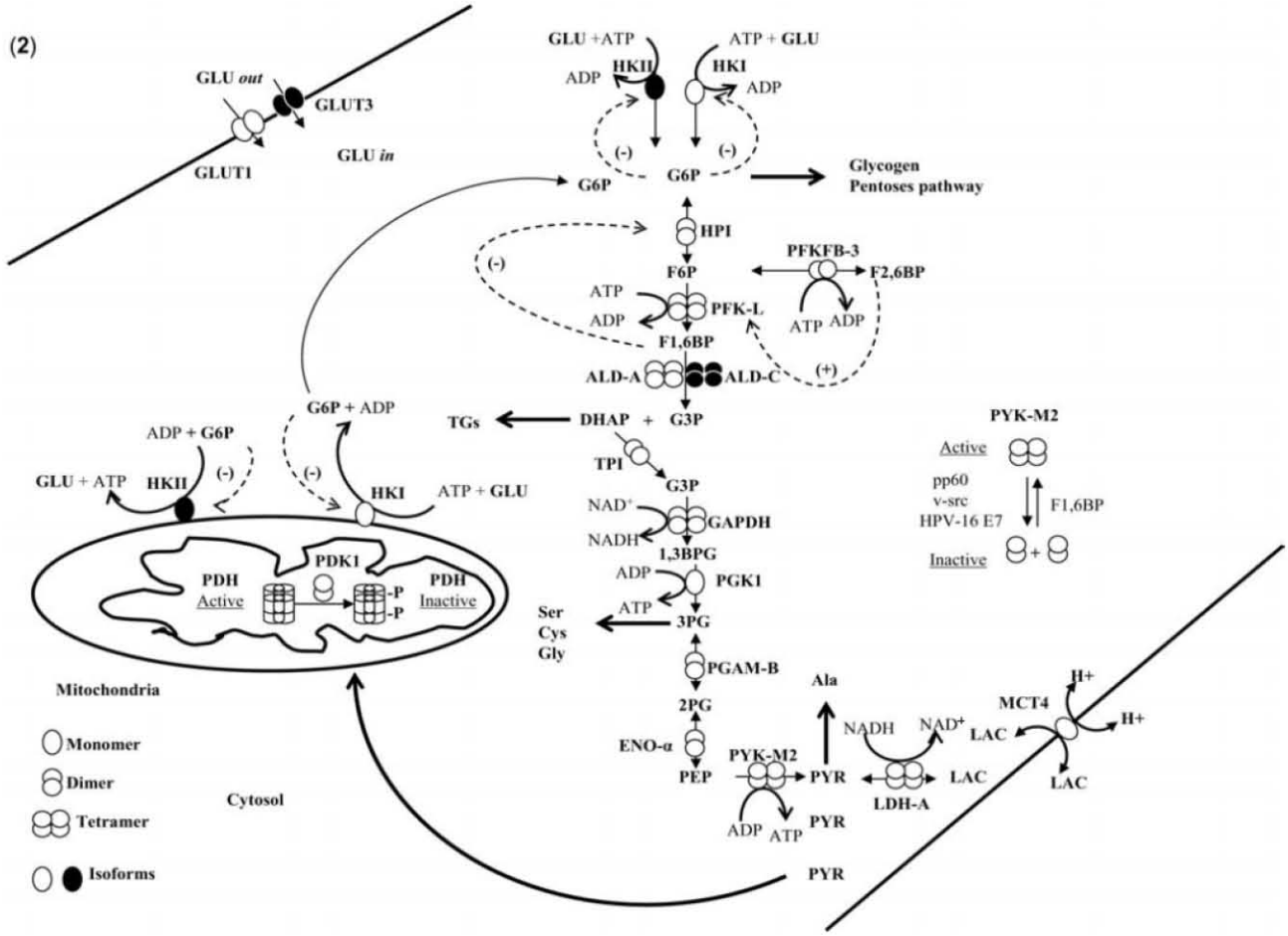

Fig. (2). Glycolytic isoforms upregulated by HIF-1 in cancer cells.

GLUT, glucose transporter; HK, hexokinase; HPI, hexosephosphate isomerase; PFK1, phosphofructokinase type 1; ALD, aldolase; PFKFB3, phosphofructokinase type II; TPI, triosephosphate isomerase; GAPDH, glyceraldehyde-3-phosphate dehydrogenase; PGK, phosphoglycerate kinase; PGAM, phosphoglycerate mutase; ENO, enolase; PYK, pyruvate kinase; LDH, lactate dehydrogenase; MCT, monocarboxylate transporter; PDH, pyruvate dehydrogenase complex; PDK, pyruvate dehydrogenase kinase; GLU, glucose ; G6P, glucose 6-phosphate, F6P, fructose 6-phosphate; F2,6BP, fructose-2,6-bisphosphate; F1,6BP, fructose 1,6 bisphosphate; DHAP, dihydroxyacetone phosphate; G3P, glyceraldehyde-3-phosphate; 1,3BPG, 1,3 bisphosphoglycerate; 3PG, 3-phosphoglycerate; 2PG, 2-phosphoglycerate; PEP, phosphoenolpyruvate; PYR, pyruvate; LAC, lactate; TGs, triacylglycerides; Ser, serine; Cys, cysteine; Gly, glycine; Ala, alanine; (+) activation; (-) inhibition.

zation with HIF-1β [44]. HIF-1β may also dimerize with aryl hydrocarbon receptors, allowing cross-talk with xenobiotic metabolism. However, complexes containing HIF-2α activate a distinct subset of genes, compared to HIF-1α, that are not involved in regulating glycolytic genes [45]. HIF-2α tissue expression occurs in a limited number of non-parenchymal cells (in kidney, pancreas and brain) and parenchymal cells (in liver, intestine and heart) [45]. However, HIF-2α is also involved in tumor progression and increased expression has been observed in diverse solid tumors, including bladder, brain, breast, colon, ovary, prostate and renal carcinomas [13, 45].

The role of HIF-3α is not clear. Three splice variants can be produced from the HIF-3α gene. Isoform-2, also called IPAS (inhibitory PAS domain, a natural HIF-1α antagonist), lacks an Asn-containing transactivation domain (C-TAD), such that it acts in a dominant negative manner forming transcriptionally inactive hetero-dimers with HIF-1β, thereby preventing HIF-1α dimerizing with HIF-1β [44]. In the corneal epithelium, where the IPAS concentration is high, corneal neo-vascularization is inhibited [46]. On the other hand, HIF-1β is constitutively expressed under normoxic conditions and is slightly increased by the same effectors that upregulate HIF-1α expression (hypoxia, EGF, $CoCl_2$) [47].

GLYCOLYSIS AND HIF-MEDIATED REGULATION

Most cancer cells show enhanced glycolytic capacity compared to their tissues of origin [48, 49]. This occurs because many of the glycolytic enzymes can be expressed as several different isoforms (Table **1**) and the isoforms expressed in cancer cells are different. This process is regulated by HIF-1α which acts as a transcriptional factor for most of the glycolytic enzymes and transporters (Figs. **1** and **2**)

GLYCOLYTIC INHIBITORS

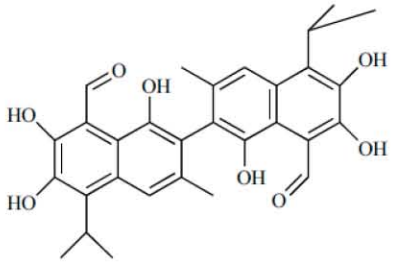

Gossypol

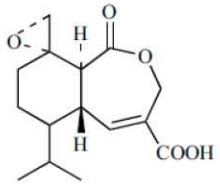

Koningic acid

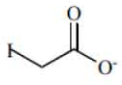

Iodoacetate

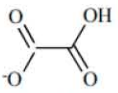

Oxalate

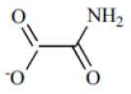

Oxamate

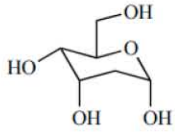

2-deoxyglucose

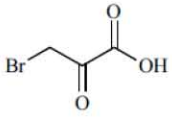

3-bromopyruvate

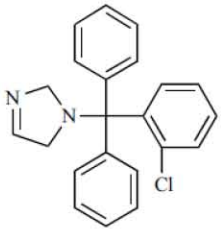

Clotrimazole

MITOCHONDRIAL INHIBITORS

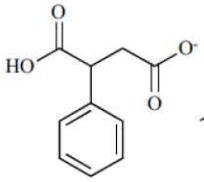

Phenylsuccinate

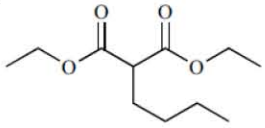

n-buthylmalonate

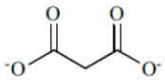

Malonate

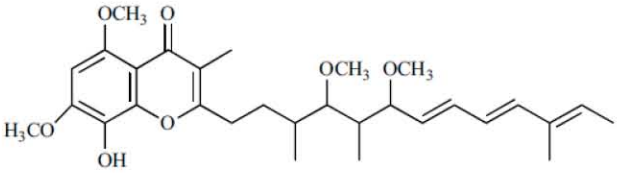

Stigmatellin

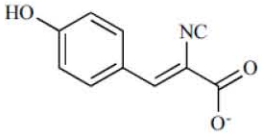

a-cyano-4-hydroxycinnamate

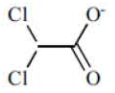

Dicloroacetate

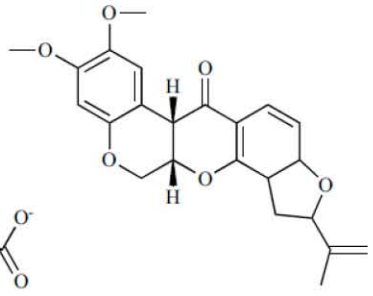

Rotenone

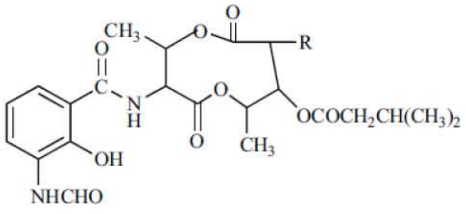

R= Hexyl: Antimycin A_1
R= Butyl: Antimycin A_3

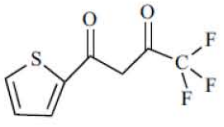

Thenoyltrifluoroacetone

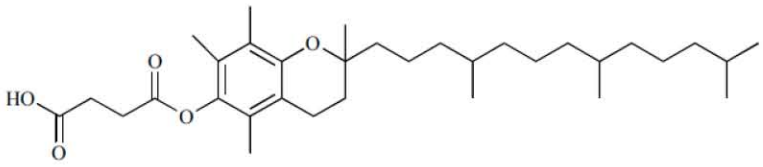

α-tocopheryl succinate

(Fig. 3. Contd....)

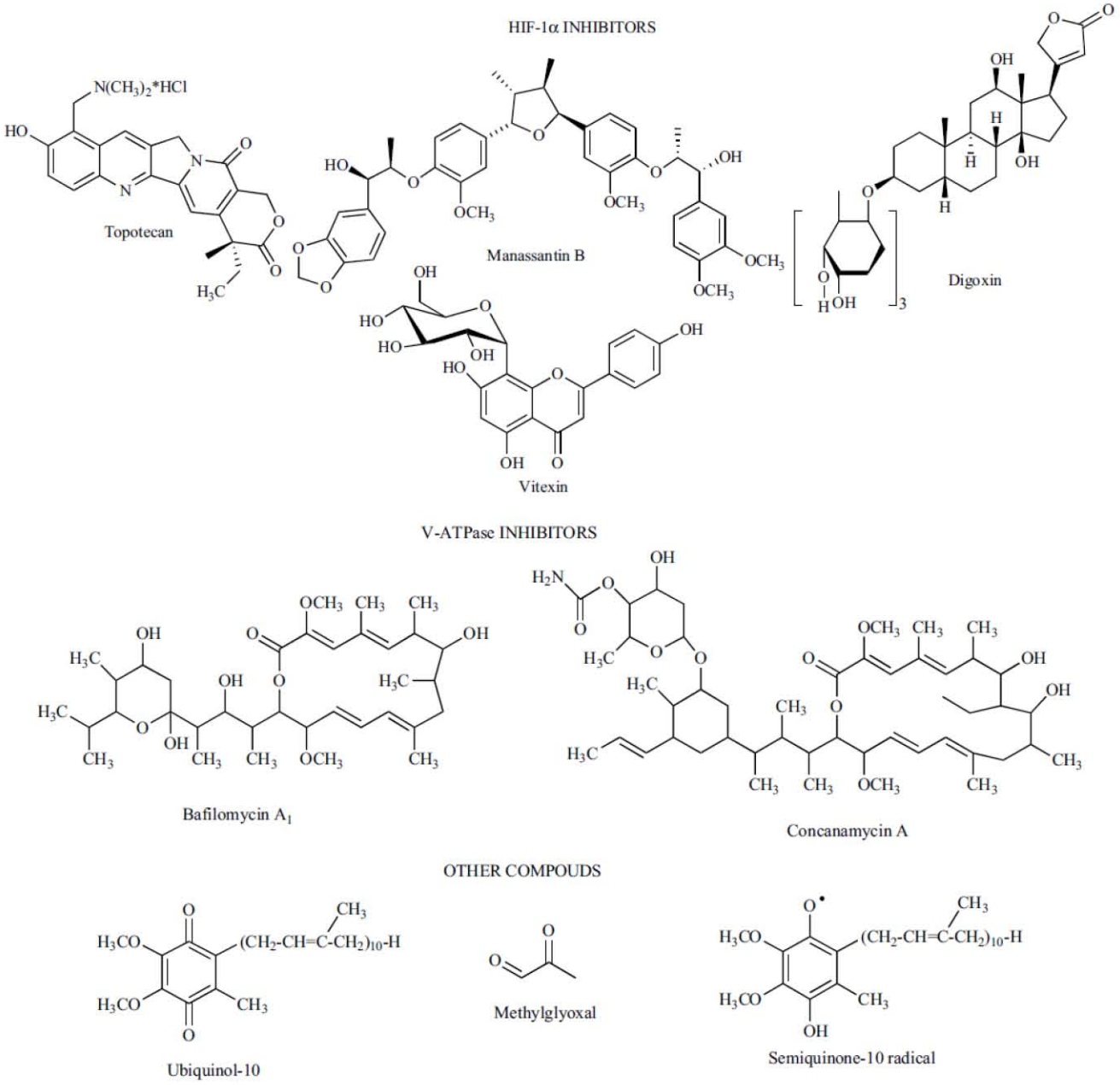

Fig. (3). Chemical structures of some anticancer drugs that block energy metabolism.

[4, 44, 50-54]. Interestingly, HIF-1α activation only increases the transcription of one particular isoform for each of the HIF-1α regulated glycolytic proteins. The following section discusses the specific HIF-1α mediated regulation of glycolysis and why some of the glycolytic isoforms may prove to be suitable drug targets for cancer therapy.

Glucose Transporters (GLUTs)

The glucose transporter family consists of three different classes. Class 1 contains four members, GLUT1-GLUT4 (Table **1**) whose preferential substrate is glucose. Class 2 and 3 transporters are selective for other carbohydrates [55]. GLUT1 and GLUT3 expression is up-regulated by HIF-1α (Fig. **2**). GLUT1 is expressed in all tissue types, whereas GLUT3 is preferentially expressed in the brain. Apparently, GLUT1 can form dimers and tetramers [56]. It has been argued that the HIF-1α-mediated GLUT1 and GLUT3 overexpression in cancer cells is related to their high glucose affinity (low *Km*) [57]. However, it is somewhat surprising that the kinetic parameters of glucose transporters have been determined only for glucose analogues such as 2-deoxyglucose(2-DOG) or 3-*O*-methyl glucose, but not for glucose itself; hence, substantial differences in the kinetic parameters have been reported: GLUT1, *Km* = 6.9-50 mM, *Vm* = 6.5-

Table 1. Isoforms of Glycolytic Proteins

Transporter or Enzyme	Genes	Isoforms	Oligomeric State	Anticancer Drugs
GLUT	4	GLUT1, GLUT2, GLUT3, GLUT4	M?, D, T	
HK	4	HKI, HKII, HKIII, HKIV	M, T	3-BrPyr, clotrimazole
HPI	1	No isoforms	D	2-DOG
PFK-1	3	PFK-L, PFK-M, PFK-P	T	clotrimazole
ALD	3	ALD-A, ALD-B, ALD-C	T	clotrimazole
TPI	1	No isoforms	D	
GAPDH	2	GAPD1, GAPD2	T	Arsenite,Goss, IAA, 3-BrPyr, Koningic acid
PGK	2	PGK1, PGK2	M	3-BrPyr
PGAM	2	PGAM-A, PGAM-B	D	Oxamate, Oxalate
ENO	3	ENO-α, ENO-β, ENO-γ	D	
PYK	2	PYK-R, PYK-L, PYK-M1, PYK-M2	T	Oxamate, Oxalate
LDH	3	LDH-A, LDH-B, LDH-C	T	Goss, Oxamate, Oxalate
PFK-2	4	PFKFB1, PFKFB2, PFKFB3, PFKFB4	D	
MCT	4	MCT1, MCT2, MCT3, MCT4	M?	

M, monomer; D, dimer; T, tetramer. IAA, iodoacetate; 2-DOG, 2-deoxyglucose; 3-BrPyr, 3-bromopyruvate; Goss, gossypol. Data taken from [55, 56, 63, 65, 73, 77, 78, 81, 100, 107, 109, 111, 116, 121, 124, 128, 130, 132].

700 pmol/min/oocyte; GLUT2, *Km* = 17-42 mM, *Vm* = 3.1-900 pmol/min/oocyte; GLUT3, *Km* = 1.8-10 mM, *Vm* = 2.2-850 pmol/min/oocyte; GLUT4, *Km* = 4.6-100 mM, *Vm* = 150 pmol/min/oocyte) [58-60]. Based on the kinetic parameters determined for 2-DOG, and the assumption that the *Km* values for 2-DOG are close to those for glucose, it can be concluded that GLUT3 is the transporter with the highest affinity and catalytic efficiency (*Vm*/*Km*; GLUT3>GLUT1> GLUT2>GLUT4), while GLUT2 over-expression would be physiologically irrelevant at normal blood glucose levels of around 5 mM.

GLUT1 is the transporter most widely over-expressed in cancer cells (Table **2**), particularly in highly proliferative and malignant tumors [55, 61]. GLUT3 is also over-expressed in lung, colon, ovary, larynx and mammary gland tumors (Table **2**); high levels of GLUT1 or GLUT3 have been used as indicators of bad prognosis [55]. Interestingly, GLUT1 and GLUT3 are one of the main controlling steps of glycolysis in some fast-growth tumor cells [62; Rodríguez-Enríquez S., Marín-Hernández A, Gallardo-Pérez J.C., Moreno-Sánchez R., unpublished data], and hence it provides a suitable therapeutic target for glycolytic and hypoxic tumors. However, inhibitors of GLUT that specifically target cancer cells have not yet been developed.

Hexokinase (HK)

Monomeric HK has four isoforms (Table **1**) with molecular masses of 100 KDa for HKI, HKII and HKIII or 50 KDa for HKIV, or glucokinase (GK). Their *Km* values for glucose range from 0.003 to 8 mM in the order of relative affinity (1/*Km*): HKIII>HKI>HKII>HKIV. The activity of isoforms I-III is strongly inhibited by the product, G6P, whereas GK is fully insensitive to this metabolite [63]. HKI and HKII genes are HIF-1α targets (Fig. **2**) [44]. HKII over-expression occurs in the majority of tumors, although in brain, testis, and head and neck tumors HKI is preferentially over-expressed (Table **2**) [64] and may form tetramers [65]. These two isoforms can bind to the external mitochondrial membrane by means of a 15 hydrophobic amino acid segment, MIASHLLAYFFTELN, in the amino-terminal region [66]. In some tumor cells, the mitochondria-bound HK accounts for 50-70% of total cellular HK [62]. However, in the majority of kinetic studies in cancer cells, the analysis of HK activity has been derived from the free or cytosolic isoform, while the contribution of membrane-bound HK has often not been evaluated, thereby underestimating the total HK activity.

Apparently, HK preferentially interacts with the membrane permeability transition (MPT) pore through the voltage-dependent anion channel (VDAC), which leads to the blocking of cytochrome c release induced by the pro-apoptotic proteins Bax and Bid and protection of cancer cells from apoptosis [66, 67]. In turn, inactivation of cyclophilin D, a matrix component of the MPT pore, induces the release of HKII from mitochondria and enhances Bax-mediated apoptosis in cancer cells [68].

Mitochondrial HKI and HKII have preferential access to ATP produced by oxidative phosphorylation because of their

Table 2. Isoforms of Glucose Transporters and Glycolytic Enzymes Expressed in Human Tumors

Isoforms	Types of tumor																								
	Liver	Pancreas	Mg	Esophagus	Brain	Kidney	Lung	Skin	Colon	Endo.	Ovarian	Cervix	Larynx	Testis	H/N	LN	Prostate	Stomach	Úterus	NS	Placenta	Eye	RL	Cartilage	BM	Thyroid
GLUT1	X	X	X	X	X	X	X	X	X	X	X	X														
GLUT3			X				X		X		X		X													
HKI					X									X	X											
HKII	X	X	X	X	X	X	X	X	X	X	X	X														
HPI	X	X			X	X	X	X			X			X	X	X	X	X	X	X						
PFK-L					X	X	X	X								X	X				X	X				
ALD-A	X	X	X			X	X	X			X			X	X		X	X	X	X	X	X				
TPI	X	X	X		X	X	X	X			X			X		X	X	X	X			X				
GAPDH	X	X	X		X	X	X	X	X		X	X		X	X	X	X	X	X	X		X	X	X		
PGK1	X	X	X		X				X					X		X	X	X	X	X	X	X			X	
PGAM-B	X		X				X		X																	
ENO-α	X	X			X	X	X	X	X		X	X		X			X	X	X	X		X				
PYK-M2	X	X	X		X	X	X	X	X		X			X	X	X	X	X	X	X	X	X	X	X		
LDH A	X		X			X		X						X	X	X	X	X	X		X	X	X			
PFKFBP3			X						X		X						X									X
MTC4	there are not reports																									

Data taken from [55, 61, 113, 114, 165, 166]. Mg, Mammary gland; Endo, endometrium; H/N, head and neck; LN, lymphatic nodules; NS, nervous system; RL, reticular lymphoma ; BM, bone marrow.

proximal location to mitochondria (Fig. **2**) [64] and, as a result, are reportedly less sensitive to inhibition by G6P [69]. However, results from our laboratory have revealed strong G6P inhibition of both mitochondrial and cytosolic HK [62] when enzyme activity was assayed under near-physiological conditions (37°C, pH 7 and concentrations of glucose and G6P ≥ 1 mM). The G6P concentration has been reported at 0.6-5 mM in tumors [62] and the inhibition constant (*Ki*) or IC_{50} values for HK vary between 20 and 210 μM [63, 70]. Consequently, the HK activity would be predicted to be strongly G6P-inhibited under such conditions (Fig. **2**). Furthermore, G6P (1 mM) induces the release of mitochondrially bound HK in both malignant and non-malignant cells [71, 72]. Hence, HK would be predominantly free in the cytosol in cancer cells with high [G6P] such as AS-30D hepatocarcinoma (G6P ≥ 5 mM), whereas in tumors with low G6P such as HeLa cells (G6P=0.6 mM), HK may be predominantly bound to mitochondrial external membrane.

It should also be pointed out that, in some studies, the relative levels of HKI and HKII activity in cytosolic fractions have very likely been under-estimated, because the ATP concentration used (3-5 mM) was not saturating given the *Km* values of 0.4-1 mM. In order to correctly estimate HK activity (*Vmax*), at least 10 times the *Km* value (≥ 10 mM ATP) should have been used for these kinetic assays. This provides an additional uncertainty in interpreting the data from the studies of others when determining the overall ratio of HK and relative contributions from cytosolic *versus* mitochondrial activity.

HKI and HKII binding to mitochondria inhibit apoptosis and ensure that mitochondrial ATP is preferentially used for hexose phosphorylation, thereby contributing to the survival advantage of tumor cells. This regulatory mechanism of tumor HK supports an essential role for the enzyme in the control of the glycolytic flux [62]. Moreover, HKII overexpression promotes enhanced glycolytic flux because HKII, together with GLUT, exerts the main control on the glycolytic rate in tumor cells [62]. Therefore, mitochondrial HKI and II make attractive targets for therapeutic intervention to suppress tumor growth.

Apparent specific inhibition of HK by 3-bromopyruvate (Table **1**; Fig. **3**) has been reported [73]. However, the cytotoxic activity against cancer cells was of low potency (IC_{50}~

50 μM) [74, 75] and other glycolytic (150 μM induces 70% inhibition of GAPDH and PGK) (Table **1**) and mitochondrial (PDH, SDH, glutamate dehydrogenase, pyruvate transporter) proteins [76, 77], as well as the mitochondrial proton leak, are also sensitive to similar low concentrations of this compound [77]. Clotrimazole (Fig. **3**) induced HK detachment from mitochondria in B16 melanoma cells, but also detached PFK-1 and ALD from the cytoskeleton in mouse LL/2 Lewis lung cancer cells, leading to diminished G6P, F1,6BP, and ATP levels, and glycolytic flux [78]. Clotrimazole reduces cellular proliferation and viability of human CT-26 colon, Lewis lung and breast MCF-7 carcinomas (IC_{50}= 50- 80 μM) [78, 79]; and the size and development of intracranial gliomas (C6 and 9L), prolonging survival in rodents [80]. Clearly, although more specific HK inhibitors are required, some of the already known HK inhibitors might assist treatment by sensitizing cancer cells to other anti-cancer drugs.

Hexosephosphate Isomerase (HPI)

HPI is a homodimer with 63 KDa subunits and with no isoforms (Table **1**) [81]. HPI is over-expressed under hypoxia through a mechanism not directly dependent on HIF-1α [54]; HIF-1 specific consensus sequence for binding in the HPI gene has not been described (Fig. **2**). Moreover, the enzyme does not seem to exert significant flux control over glycolysis [62], and hence HPI over-expression in cancer cells (Table **2**) may be related to its other less well-known functions. In addition to participating in glycolysis, HPI also promotes cell migration, proliferation and metastasis [82]. In tumor cells, HPI is expelled to the extracellular space where acts as a cytokine (*i.e.*, autocrine motility factor, AMF) thus altering several functions including tumor progression and metastasis.

HPI is inhibited by erythrose 4-phosphate (ERI4P) and F1,6 BP (*Ki* values of 0.7 and 170 μM, respectively) [83; Marín-Hernández A, Moreno-Sánchez R, Saavedra E, manuscript in preparation], which may exist at relatively high concentrations inside tumor cells (16 μM and 10-25 mM, respectively) [62, 84]. Hence, HPI modulation by ERI4P and F1,6BP can be proposed as one mechanism for limiting excessive flux through the glycolytic pathway, regulating the supply of G6P for the pentose phosphate and glycogen synthesis pathways.

2-DOG is a glucose analog recognized by glucose transporters, phosphorylated by HK and dehydrogenated by glucose 6-phosphate dehydrogenase (G6PDH). However 2-DOG (as 2-DOG6P after HK phosphorylation) is not isomerized by HPI, which it inhibits, thereby diminishing glycolytic flux (Table **1**). In addition, 2-DOG effectiveness is drastically reduced in the presence of glucose, due to the competition for GLUT, HK and G6PDH. The 2-DOG primary effect is on HPI because HPI inhibition by 2-DOG6P (*Ki*=5 mM) [85] induces, in turn, the accumulation of G6P, which is a more potent HK inhibitor (*Ki*=20-200 μM [63, 70]) than 2-DOG (*Ki*=0.4 mM) and 2DOG6P (*Ki*=4.3 mM) [86]. In consequence, glycolytic flux in the presence of 2-DOG diminishes because HK is inhibited by G6P and HPI is inhibited by 2-DOG6P.

Interestingly, 2-DOG is more toxic for osteosarcoma ρ^o cells than for the parental osteosarcoma cells (IC_{50} values of 32-100 μM and 0.6-6 mM, respectively), presumably because the ρ^o cells are only dependent on glycolysis for ATP generation [87]. 2-DOG (500 mg/kg weight) does not exhibit anticancer activity in osteosarcoma nude mouse xenografts and non-small cell lung cancer [88], which may be because they rely more on OxPhos for their energy supply. However, 2-DOG significantly enhances the anticancer activity of etoposide, camptothecin, and Hoechst-33342 in a range of other cancers, including cerebral glioma BMG-1, squamous carcinomas 4451 and 4197, and malignant glioma U-87 cells [89]. It is possible that cells treated with the other agents become heavily reliant on glycolysis and therefore become more sensitive to 2-DOG. Combining 2-DOG with adriamycin, paclitaxel or etoposide diminishes the size and proliferation of human osteosarcoma, xeno-transplanted MV522 lung carcinoma and Ehrlich hepatoma-bearing mice in comparison with tumors treated with 2-DOG or anticancer drugs, separately [88-90]. This increased sensitivity towards anticancer drugs induced by 2-DOG is attributed to the high glycolysis-dependence of the tumor for ATP supply and may result from increased demands for ATP made by the cell damaging agents.

2-DOG also affects protein glycosylation, induces accumulation of mis-folded proteins in the endoplasmic reticulum, leads to a decrease in the amount of HK associated with mitochondria and induces the expression of P-glycoprotein [91, 92]. Therefore, the drug is not a specific glycolysis inhibitor and its anticancer activity may as a result be limited.

Phosphofructokinase Type 1 (PFK-1)

PFK-1 is a homo- or hetero-tetramer of 380 KDa, with three isoforms (Table **1**). The main isoforms expressed in liver and platelets are PFK-L and PFK-P (or C), respectively, whereas skeletal muscle only has PFK-M. A mixture of the three isoforms is found in all other tissues [81], but HIF-1α only increases expression of the PFK-L isoform [4, 44].

PFK-M shows the highest affinity for F6P ($K_{0.5}$=0.6-2 mM) and it is the least sensitive to ATP inhibition. PFK-L is the least sensitive isoform to inhibition by the Krebs cycle intermediate, citrate (IC_{50}=0.18 mM). PFK-P has the lowest affinity for F6P ($K_{0.5}$=1.4-4 mM) and is more sensitive to citrate inhibition (IC_{50}=0.08 mM) [93]. Therefore, to increase flux through this enzyme (and hence increase glycolysis and ATP synthesis) tumors preferentially over-express M and L, over the P isoform, exploiting their reduced sensitivity to feed-back inhibition by ATP and citrate. A lower pH also inhibits PFK-1 activity, decreasing both the affinity for F6P and *Vm* [Moreno-Sánchez R, Marín-Hernández A, Encalada R, Saavedra E, unpublished data]. Due to their higher glycolytic flux resulting in lactic acid production, cancer cells have a more acidic cytosol and extracellular pH [94], which would decrease PFK-1 activity. Hence, it is not surprising that tumors express greater levels of PFK-1 induced by HIF-1α to compensate for the lower pH.

The role for activators such as F2,6BP and AMP, which would also be expected to promote an increased flux *via* the L and M isoforms, is currently unclear because unfortunately, detailed kinetic studies on PFK-1 are scarce. The systematic kinetic analysis of AS-30D and HeLa PFK-1 are

currently under investigation in our laboratory [Moreno-Sánchez R, Marín-Hernández A, Encalada R, Saavedra E, unpublished data]. The results have shown that the *Ki* values for ATP and citrate are 1.7 and 4-17 mM, whereas the *Ka* values for F2,6BP and AMP are 0.1-33 μM and 0.4-3 mM, respectively, in a K^+-based medium; K^+ is also a PFK-1 activator with a *Ka* of 11.5-13.5 mM. Usually, these affinity constants have been determined in reaction medium with no K^+.

The physiological concentrations of ATP (1.4-9.2 mM), AMP (0.15-3.3 mM), citrate (0.4-1.7) and F2,6BP (5-50 μM) present in tumor cells [62, 95-97] would indicate that ATP inhibition is more likely to be relevant than citrate inhibition, and that F2,6BP would prevail over AMP activation. Furthermore, it has been established that PFK-1 activation by F2,6BP overcomes ATP and citrate inhibition [62]. Hence, the high F2,6BP levels present in cancer cells [96, 97] does not support a major role for activated PFK in the flux-control of glycolysis [62]. On the other hand, PFK-1 in tumors with low expression or low F2,6BP content might still exert significant flux control of glycolysis [Marín-Hernández A, Moreno-Sánchez R, Saavedra E, manuscript in preparation].

Aldolase (ALD)

ALD is a homo-tetramer of 40 KDa subunits, with three isoforms (Table **1**). ALD-A, B, and C predominate in skeletal muscle, liver and brain, respectively. Combinations of the three isoforms are found throughout all tissues [81].

ALD-A and C are more efficient (10-20 times) than B in the forward (glycolytic) reaction [98]. ALD-B shows higher affinity for G3P and DHAP, which facilitates the reverse reaction. Thus, ALD-A and C are preferentially localized in tissues with high glycolysis such as skeletal muscle, erythrocytes and brain, whereas ALD-B is in gluconeogenic tissues such as liver and kidney. Therefore, HIF-1α up-regulates the expression of ALD-A and C (Fig. **2**) [4, 44] with ALD-A predominantly expressed in tumors (Table **2**) [61].

Triosephosphate Isomerase (TPI)

TPI is a homodimeric enzyme of 27 KDa subunits without isoforms (Table **1**), although post-translational regulation has been described [81]. TPI gene is a HIF-1α target [51] (Fig. **2**). Enzymatic activity of TPI is one of the highest found in nature and in tumors its activity is 6-61 U/mg protein, whereas other glycolytic enzymes have much lower activities in the 0.003-0.8 U/mg protein range [62]. Therefore, TPI does not exert flux control of glycolysis [62], and its elevated content in cancer most likely have a still unknown function.

TPI deficiency in patients induces an increase in DHAP concentration. The DHAP accumulation favors its non-enzymatic decomposition to methylglyoxal (Fig. **3**), which is a highly reactive aldehyde that modifies proteins and DNA. Interestingly, some studies have suggested that methylglyoxal has anticancer properties. In particular, it inhibits glycolysis and mitochondrial respiration in human leukaemia cells, but not in normal cells [99]. Therefore, the physiological meaning of an increased expression of TPI in tumor cells, induced by HIF-1α, may be related to avoiding the accumulation of DHAP, and the generation of methylglyoxal.

Glyceraldehyde-3-Phosphate Dehydrogenase (GAPDH)

GAPDH is a homo-tetramer of 37 KDa subunits [100] with no isoforms, except for a second gene (*gapd2*) exclusively expressed in spermatozoa [101]; post-translational regulation has also been described. Its *Km* values for G3P and NAD^+ are 240 and 80 μM, respectively [Marín-Hernández A, Moreno-Sánchez R, Saavedra E, manuscript in preparation]. HIF-1α up-regulates its expression. In addition to glycolysis and gluconeogeneis, GAPDH participates in transcriptional regulation as a nuclear tRNA export protein, and in replication and repair of DNA (acting as uracyl-DNA glycosylase, by removing uracyl residues). GAPDH can also mediate endocytosis by its interaction with tubulin and it can be required for programmed neuronal cell death [82, 100]. However, the role of its nuclear translocation in cancer development and growth has not yet been established.

GAPDH is a house-keeping protein that is used in numerous studies as a cytosolic marker or control for protein loading in SDS-PAGE. However, this protein is over-expressed to variable degrees in cancer cells, and its subcellular localization varies with the cellular growth state. In quiescent cells, GAPDH is localized in the cytosol but, in proliferating cells, GAPDH is detected also in the nucleus [100]. Therefore, it is not ideal to use the GAPDH protein or mRNA as a loading control for western or northern blotting studies or as a cytosolic marker in studies with tumor cells.

Gossypol, a polyphenolic aldehyde derived from cotton seeds (Table **1**; Fig. **3**), is an inhibitor of GAPDH, but it also inhibits other NAD^+-dependent enzymes such as LDH (Table **1**) and some mitochondrial dehydrogenases (*e.g.*, isocitrate dehydrogenase). Gossypol can also affect a number of cellular functions associated with cellular proliferation, including ion transport, membrane properties, glycolysis, respiration, glucose uptake, and calcium homeostasis by inhibiting calcineurin [102]. At 1-9 μM, gossypol induces growth inhibition of several human cancer cell lines (breast, cervix, melanoma, ovary, and colon) [102, 103]. Structural data and molecular modeling studies have shown the direct interaction of gossypol with Bcl-2 and Bcl-XL and support its ability to inhibit the pro-survival activity of these proteins in cancer cells, promoting apoptosis [104]. At low doses (30 mg/kg), the drug reduced tumor size by 65%, and mortality was reduced to 8% in nude mice with the human SW-13 adrenocortical carcinoma [105]. In a phase I clinical trial, gossypol decreased glial and adrenal tumor size by 10-50% [106].

Koningic acid (heptelidic acid, avocettin) is a sesquiterpene antibiotic (Fig. 3) that inhibits GAPDH activity by reacting with the essential thiol group (cysteine 149). The type of inhibition is competitive against G3P (*Ki*=1.1 μM) [107]. At 1 mg/Kg, it suppresses tumor growth of Erlich ascites *in vivo*, whereas at 36 μM (10 μg/mL), it inhibits the growth of several cancer cell lines with high glycolysis but not the growth of normal cells lines with low glycolysis [108]. However, koningic acid also shows acute toxicity in mice (at 31.5 mg/Kg or about 600 μg *per* mouse) and deleterious effects on normal cells with high glycolysis (erythrocytes) [108].

For other GAPDH inhibitors, such as arsenite (AsO_2^{1-}) and iodoacetate (Table **1**; Fig. **3**), information about their

effects on tumor cells are scarce. Arsenate ($H_2AsO_4^{1-} \leftrightarrow HAsO_4^{2-}$ at neutral pH) can also block glycolytic flux because GAPDH may use it, instead of phosphate, to form 1-arseno-3-phosphoglycerate, which is spontaneously and rapidly hydrolyzed in water back to G3P with no associated synthesis of ATP (Table **1**) [for further details see 109].

Phosphoglycerate Kinase (PGK)

PGK is a monomer of 48 KDa with two isoforms (Table **1**). PGK1 is expressed in all somatic and cancer cells (Table **2**), whereas PGK2 only appears in spermatozoids [81]. HIF-1α up-regulates expression of PGK1 (Fig. **2**) [4, 44]. As PGK does not have significant flux control of glycolysis, its over-expression in tumor cells may have other functions. Tumor cells secrete PGK, and extracellular disulfide bond reduction of plasminogen by PGK acting as a disulfide reductase leads to production of angiostatin by promoting autoproteolytic cleavage of plasminogen [110]. Angiostatin inhibits the plasma membrane FoF_1-ATPase, normally present in mitochondria but found expressed in cancer cells. As a result cytosolic acidification occurs and both angiogenesis and metastasis are inhibited.

Phosphoglycerate Mutase (PGAM)

PGAM is a dimeric enzyme consisting of A or B isoforms (AA, AB and BB) (Table **1**) each requiring 2,3-bisphosphoglycerate (2,3BPG) as a cofactor [111]. PGAM-B (homodimer of B subunits) shows a higher affinity for 3PG and 2,3BPG (*Km*= 0.5 mM and 25 μM) than PGAM-A (*Km*=0.8 mM and 60 μM, respectively) whereas the affinity for 2PG is similar in both isoforms (*Km*=0.28 mM) [112]. PGAM-B over-expression has been reported in liver, lung, colon, and mammary gland tumors (Table **1**) [113, 114]; in addition, HIF-1α regulation of PGAM-B expression has been indicated [50], suggesting that PGAM-B may play an important role in malignancy. Furthermore, it has been reported that increased expression of the two PGAM isoforms favors the proliferation and immortalization of fibroblasts, whereas decreased expression induces premature senescence [115]. This observation suggests that PGAM promotes the immortalization of cancer cells rather than affecting increased glycolysis, as this enzyme is not a flux-controlling step [62]. Hence, PGAM is not highly relevant to the theme of this review.

Enolase (ENO)

ENO is a dimeric enzyme formed from three different subunits of 82-100 KDa (Table **1**). The main isoforms are αα, αβ, ββ, αγ and γγ [116]. ENO-α (homodimer of α subunits) is distributed in most tissues whereas ENO-β and ENO-γ are expressed preferentially in skeletal muscle and brain, respectively [116]. The three isoforms show similar affinity for 2PG (*Km*= 30 μM) [117]. ENO has an essential requirement for divalent metal ions in the following order of potency: $Mg^{2+} > Zn^{2+} > Mn^{2+} > Fe^{2+} > Cd^{2+} > Co^{2+} > Ni^{2+} > Sm^{3+} > Tb^{3+}$ [116].

HIF-1α up-regulates ENO-α expression [4, 44] to significant levels in several tumor types (Table **1**). ENO-α acts as a receptor for plasminogen which favors tumor growth and metastasis [116]. Considered together with the role of PGK discussed above as a facilitator of plasminogen activation by autoproteolysis to plasmin, which is involved in catalyzing the degradation of fibrin aggregates, the evidence suggests that the combination of these two glycolytic enzymes is likely to facilitate cancer metastasis. Again, however, these enzymes are not highly relevant to the purpose of this review.

Pyruvate Kinase (PYK)

PYK is a homo-tetramer with four isoforms (Table **1**). PYK-L is localized mainly in liver and kidney (gluconeogenic tissues) and PYK-R is expressed in erythrocytes. These two isoforms are encoded by the same gene (which has 12 exons), but are expressed from alternative promoters such that specific promoters for L and R isoforms are in exon1 and 2, respectively. The two other isoforms are PYK-M1, localized in brain, heart and skeletal muscle, and PYK-M2, which is expressed in embryonic and stem cells, leukocytes, platelets, and cancer cells (Fig. **2**). The M1 and M2 isoforms are also encoded by the same gene through alternative splicing [81].

PYK-M1 is the only isoform with no cooperative kinetics in relation to its substrate, PEP, but has the highest affinity (*Km* = 0.08 mM) whereas PYK-R exhibits the lowest affinity (*Km* = 1.4 mM) [118]. The three other isoforms (R, L and M2) that exhibit cooperative kinetics are also potently activated by F1,6BP (*Ka*= 0.06-0.4 μM), an upstream glycolytic intermediary that establishes a feed-forward regulatory mechanism. ATP strongly inhibits the activity of the L and R isoforms (*Ki*= 0.1 and 0.04 mM, respectively) but only mildly inhibits M1 and M2 activity (*Ki*= 3 and 2.5 mM, respectively). Phosphorylation of the L and R isoforms by protein kinases fully abolishes activity, whereas the M1 and M2 isoforms are not susceptible to phosphorylation and hence are not directly regulated by the action of hormone binding [118]. The kinetic properties of the M2 isoform suggests that it is highly active in tumor cells at physiological concentrations of PEP (0.1-0.3 mM), F1,6BP (0.6-25 mM) and ATP (1.4- 9.2 mM) [64, 96] and, therefore, this is not a controlling step of glycolysis [62].

HIF-1α only up-regulates PYK-M2 expression, which is the main isoform found in tumors (Table **2**). As this isoform is relatively insensitive to ATP inhibition and it is not regulated by phosphorylation, it seems clear that its over-expression is favored in tumors to attain an enhanced glycolytic flux. Furthermore, PYK-M2 undergoes a dimer (inactive)- tetramer (active) transition (Fig. **2**) which is modulated by F1,6BP and the oncoproteins pp60 -v-src and HPV-16 E7 [119]. PYK-M2 binds to tyrosine-phosphory-lated peptides which are induced in growth factor-stimulated cells [120]. The interaction of these peptides and oncoproteins with PYK-M2 induces the release of the allosteric activator F1,6BP, promoting PYK-M2 dimerization and inactivation [119, 120] (Fig. **2**); the less active dimer seems to predominate in cancer cells [119].

It has been proposed that the increase in the inactive enzyme lead to accumulation of upstream glycolytic intermediaries which are in turn channeled to synthesis of ribose and nucleic acids, proteins and lipids essential for cellular prolif-

eration [119, 120]. However, no experimentation has been performed to support this conclusion. Kinetic analysis of PYK, carried out in different rodent and human cancer cell lines, reports higher activity than in their normal counterparts, which suggests that PYK in cancer cells is not inactive and it is not in a dimeric form. Furthermore, glycolytic flux is unaffected in cancer cells by PYK inhibition because this enzyme does not exert significant flux-control [62] due to a marked over-expression, null ATP inhibition and potent F1,6BP activation; in other words, the PYK-M2 tetramer might be less abundant than the dimer, but it would still exceed the pathway demands.

Lactate Dehydrogenase (LDH)

LDH is a homo- or hetero-tetrameric enzyme of 33.5 KDa subunits with two main isoforms. LDH-A (also LDH-5 or LDH-M) is abundant in skeletal muscle, LDH-B in heart, and five other subunit combinations have been found in other tissues (Table **1**): LDH1(B_4), LDH-2 (B_3A), LDH-3 (B_2A_2), LDH-4 (BA_3) and LDH-5 (A_4). LDH-C4 is expressed exclusively in the testis and spermatozoids [121].

In glycolytic tissues such as liver and skeletal muscle, LDH-4 and 5 (isoforms with high subunit A content) are predominant. In contrast, in tissues that consume lactate (heart, kidney, erythrocytes), LDH-1 and 2 (isoforms with high subunit B content) predominate, because of their higher lactate affinity (*Km* = 4 mM) compared to the LDH-4 and 5 isoforms (*Km* = 7 mM) [122]. Not surprisingly, HIF-1α upregulates LDH-A (LDH-5) expression [4, 44] (Fig. **2**) favoring an enhanced glycolytic flux. A high LDH-A level correlates with aggressive forms of several different tumor types [123].

In addition, LDH-A over-expression stimulates other non-glycolytic functions. GAPDH and LDH-A bind to single-stranded DNA. NADH addition diminishes the formation of GAPDH- or LDH-DNA complexes indicating that the $NADH/NAD^+$ ratio may regulate DNA binding of these glycolytic enzymes [82]. GAPDH and LDH-A constitute the transcription factor complex OCA-S, which increases histone transcription (H2Bgene) to maintain the replication process and function of eukaryotic chromosomes [82].

Oxamate and oxalate (Table **1**; Fig. **3**) are classical LDH inhibitors. Oxamate is a competitive inhibitor of LDH that inhibits glycolysis (albeit at very high concentrations with an IC_{80}= 80 mM) [124], but which is much more potent as an inhibitor of tumor cell growth (IC_{50}=10-47 μM) [87]. In monolayer leukemia cultures, tumor micro-spheroids, and *in vivo* tumor models (mouse melanoma), oxalate and oxamate induce apoptosis and cellular death at sub-millimolar doses [125, 126]. Unfortunately, in these studies, the inhibitory effect on LDH and glycolysis was not determined. Oxamate and oxalate are not very specific for LDH, as they also affect other glycolytic (PGAM, PYK), and non-glycolytic enzymes including transaminases, PDH, pyruvate carboxylase and the mitochondrial pyruvate transporter [127, 128]. This makes it difficult to define the importance of LDH inhibition in the control of the glycolytic flux in cancer cells.

However, LDH-A knock down in breast cancer cells increases mitochondrial respiration and decreases mitochondrial membrane potential, compromising the ability of these tumor cells to proliferate under hypoxia [129]. The tumorigenicity of the LDH-A-deficient cells was severely diminished, and this phenotype was reversed by complementation with the human ortholog LDH-A protein. These results demonstrated that LDH-A plays a role in tumor maintenance [129], although it remains to be determined whether similar knock-down of other glycolytic steps also induces the same described phenotype.

Phosphofructokinase Type 2 (PFK-2)

PFK-2 is a bi-functional homodimeric enzyme with 52-58 KDa subunits. The enzyme, through its kinase and phosphatase activities regulates the concentration of F2,6BP, the most potent activator of PFK-1. Therefore, the PFK-2 kinase/phosphatase activity ratio determines the actual F2,6BP cellular level and the degree of PFK-1 activation. The PFK-2 activities are oppositely regulated by PEP, α-glycero-phosphate and citrate, and by protein kinase C phosphorylation, all of which inhibit the kinase activity and stimulate the phosphatase activity [130].

There are four genes (*pfkfb-1, 2, 3, and 4*) in the rat and human genomes that encode four different PFK-2 isoforms (liver, heart, placenta, and testis, respectively). It seems that HIF-1α regulates the expression of the four genes, although the specific consensus sequence for HIF-1α binding has only been described for *pfkfb-3* [53], consistent with the over-expression of the placenta-type PFK-2 in a great variety of tumors (Table **1**). A high content of the placenta-type PFK-2 promotes an increased level of F2,6BP, because the phosphatase activity of this isoform is very low (0.2 mU/mg recombinant protein), but its kinase activity is relatively high (140 mU/mg recombinant protein). The placenta-type PFK-2 kinase/phosphatase activity ratio is therefore about 710, which is the highest compared to the other isoforms (0.4-4.1). Moreover, the placenta-type PFK-2 kinase activity cannot be inhibited by phosphorylation because it lacks the required Ser residue [130].

The high F2,6BP level in cancer cells [96, 97], brought about by over-expression of the placenta–type PFK-2 overcomes ATP and citrate inhibition and induces full activation of PFK-1 [62] which favors an increased glycolytic flux.

Monocarboxylate Transporter (MCT) and Plasma Membrane H^+-ATPase

Enhanced glycolysis elevates levels of lactate and H^+, which must be actively expelled from cancer cells to keep the cytosolic pH and osmotic balance under control [131]. The MCT family consists of 9-14 members from which MCT1-MCT4 catalyze the reversible co-transport of lactate, pyruvate or ketone bodies and H^+ (Table **1**; Fig. **2**). Lactate extrusion is favored by an acidic cytosolic pH, or an alkaline extracellular pH [131, 132].

MCT1 is in all types of tissues, whereas MCT2 is mainly expressed in the liver, stomach, skin, kidney and brain, MCT3 is exclusive to the retina and MCT4 is abundantly expressed in tissues with high glycolysis such as skeletal muscle, leukocytes, testis, lung, placenta and heart. The affinity for lactate and pyruvate (*Km*= 0.7-28 mM; and 0.1-150

mM, respectively) differs among the four isoforms with MCT4 showing the lower affinity [131, 132]. MCT4 is the predominant isoform expressed in some breast cancer cell lines [133] but in oxidative tumor cells such as CaCo-2, WiDr, FaDu, SiHa and PC-3 cells and primary human cancers it is MCT1 [134, 135]. HIF-1α only up-regulates MCT4 expression [52], although inhibition of MCT1 decreases tumor growth and renders it sensitive to irradiation [135], suggesting that both isoform transporters play a relevant role in the operation of glycolysis in tumors.

A second system used to regulate the cytosolic pH is the plasma membrane V-type H^+-ATPase [132, 136]. This enzyme is over-expressed in tumors and is involved in the tumor interstitium acidification from pH 6.8 to pH 6.5 [137], which in turn promote metastasis [138]. Thus, inhibition of the V-type ATPase and cytosolic acidification can induce cell death and could constitute a promising and novel therapeutic approach. For instance, inhibiting V-ATPase with macrolide antibiotics, bafilomycins or concanamycins (Fig. **3**) [139], or down-regulating its expression [140], induce cancer cell death. Blocking other cytosolic pH regulators such as the Na^+/H^+ antiporter, the MCT family described above, or the Na^+-dependent Cl^-/HCO_3^- exchanger might also be suitable anti-cancer targets and some specific inhibitors have been found [132].

HIF-1α AND REGULATION OF MITOCHONDRIAL ENZYMES, CYTOCHROME C OXIDASE AND PYRUVATE DEHYDROGENASE KINASE

This section discusses the two mitochondrial enzymes, cytochrome c oxidase (COX; complex IV) and PDK, known to be regulated by HIF-1α. COX is the respiratory complex that consumes O_2 and is inhibited by cyanide (Fig. **3**), H_2S, CO, CO_2 or NO. COX is a dimer in which each monomer comprises 13 subunits. Subunits 1-3 are encoded by the mitochondrial DNA, are highly conserved, and constitute the catalytic core. Subunit 4 participates in the initial steps of COX assembly and binds ATP, which induces COX inhibition. HIF-1α regulates COX subunit 4-1 expression, causing an isoform switch from the usual subunit 4-2 to 4-1. The net effect is an increase in COX activity, but only a slight increase in O_2 consumption and ATP levels [141, 142], in agreement with the negligible role of COX in the control of the respiratory flux and oxidative phosphorylation rates [143].

The pyruvate dehydrogenase complex (PDH) is inhibited by phosphorylation in a reaction catalyzed by PDH kinase (PDK). Four PDK isoforms have been identified in mammalian cells (PDK1-4). These enzymes are dimers with subunits of 46 KDa [144]. PDK1 is expressed almost exclusively in heart. PDK2 is found in heart, skeletal muscle, placenta, lung, brain, kidney, pancreas and liver. Heart and skeletal muscle also express PDK3 and PDK4 [145, 146].

PDKs phosphorylate three serine residues (site 1, Ser-264; site 2, Ser-271; site 3, Ser-203) of the PDH-E1 α subunit. PDK1 can phosphorylate all three sites whereas the other isoforms only phosphorylate sites 1 and 2 [147, 148]. HIF-1α up-regulates PDK1 and has been proposed to play a major role in the inactivation of the PDH enzyme complex, thereby decreasing pyruvate oxidation through the Krebs cycle, oxygen consumption, and mitochondrial function in cancer cells [149, 150]. However, this proposal [5, 149-152] assumes that pyruvate is the main oxidizable substrate in hypoxic cancer cells and that PDH is the rate-limiting step of Krebs cycle. Moreover, complete PDH phosphorylation and inhibition has not been demonstrated. Neither has a PDK induced significant diminution in the rate of mitochondrial respiration or OxPhos nor an associated enhancement in glycolysis been shown to occur. Dichloroacetate (DCA; Fig. **3**) has been used as an inhibitor of PDK as a means to highlight the importance of PDK in tumor cell metabolism [152]. In this study, DCA was shown to induce cancer cell death by increasing ROS production and apoptosis. However, DCA probably also affects other cellular functions and hence, the role of PDK is less than certain based on these results. Furthermore, tumor mitochondria are able to oxidize several alternative energy substrates, such as glutamine, glutamate, fatty acids and ketone bodies [49], at high rates and independently of PDH complex activity.

CAN SMALL DRUG INHIBITORS OF HIF-1α ACTIVATION BE DESIGNED AND DEVELOPED AS NOVEL CANCER THERAPIES?

Given the obvious importance of HIF-1α activity to the enhanced proliferation, promotion and survival of cancer cells, it follows that inhibitors of HIF-1α would likely be important cancer therapies (reviewed in [153]). Unfortunately, many of the substances found to inhibit HIF-1α have proven too cytotoxic to be useful as drug candidates. A considerable effort has been made to identify therapeutically useful HIF-1α small drug inhibitors, many of which are natural products or synthetic compounds based on natural products. Among the most recent interesting developments are the manassantins [154] such as manassantin B (Fig. **3**), a complex dineolignan extracted from *Saururus chinensis* and *cernuus*, herbs used in Chinese and Korean folk medicine. It inhibits both the growth of hypoxic cancer cells and HIF-1α activation with nM IC_{50} values. Unlike other compounds that attack hypoxic cancer cells manassantin B has very low toxicity, and as such, is a lead compound in the development of new non-toxic anti-cancer therapeutic agents. The second interesting development is the discovery that cardiac glycosides, such as digoxin (Fig. **3**), are potent inhibitors of HIF-1α synthesis (in the submicromolar range) [155]. At low concentrations, these drugs have also been shown to inhibit tumor growth *in vivo*. These results suggest that previously difficult to treat hypoxic tumors with high HIF-1α activity may now be targeted.

CONCLUSIONS

HIF-1α is a major transcription factor regulating the genes encoding glycolytic enzymes and transporters. Its activity is mainly targeted to those glycolytic isoforms that increase pathway flux but also on other functions such as regulation of gene transcription, DNA repair, cellular migration, invasion and metastasis, and inhibition of apoptosis to favor tumor development and growth. For these reasons, HIF-1α is a logical therapeutic target for the treatment of cancer [156].

HIF-1α inhibition by either RNA interference or by the drugs vitexin or topotecan (Fig. **3**) induces a reduction in tumor growth and metastasis [157-159]. Hypoxia depresses proliferation of tumor from HIF-1α positive embryonic stem cells but, in marked contrast, it does not affect proliferation of HIF-1α-deficient (HIF-1$\alpha^{-/-}$) tumors from embryonic stem cells [160]. In contrast, HIF-1$\alpha^{-/-}$ astrocytes can generate tumors in the vascular-rich brain parenchyma but not in the poorly vascularized subcutaneous environment [161]. Thus, HIF-1α may have different roles in tumor growth and development. HIF-1α also participates in the developing heart and vascular system, in the working skeletal muscle, in the adaptation of ischemic cardiovascular disease, in the female reproductive tract and in osteoblast development in addition to being one of the key transcriptional factors for embryonic development and maintenance of the immune system [3, 162, 163]. Therefore, given the wide-ranging activities and potential for HIF-1α targeted drug induced toxicity, it will be essential that the multiple functions of this transcription factor should be fully elucidated before embarking on clinical trials targeting HIF-1α for the treatment of cancer. General inhibition of HIF-1α activity certainly promotes pronounced side effects [10].

The complete characterization of the HIF-1α regulated mitochondrial proteins and their functions should first be undertaken to better understand why certain isoforms are preferentially synthesized in cancers and to facilitate the identification of the best therapeutic targets.

From the perspective of flux control analysis, it appears that GLUT and HK, but not PFK-1 and PYK, provide the best targets for therapeutic intervention at the level of energy metabolism in hypoxic and glycolytic tumors. It follows that specific, potent and cell permeable inhibitors of these two controlling steps of glycolysis may prove to be preferred targets rather than HIF-1α. For specificity, it is also desirable that putative drugs should only interact with the tumor proteins and not with the non-tumor proteins. It may also be possible to exploit the more acidic extracellular pH in tumors because some compounds such as α-tocopheryl-succinate become more potent anticancer drugs at lower pH than at neutral pH [164]. For potency, preferred compounds will be those with low nanomolar range *Ki* values and drug design should consider that the compound has to penetrate into the cancer cells, for which a hydrophobic chemical segment may prove beneficial.

ACKNOWLEDGEMENTS

The present work was partially supported by CONACyT-México grant No. 80534. The authors wish to thank Prof. P.K. Ralph for his stimulating and helpful observations. AMH was the recipient of CONACyT-México fellowship 159991.

ABBREVIATIONS

HIF	=	Hypoxia-inducible factor
HRE	=	Hypoxic responsive elements
pVHL	=	Von Hippel-Lindau protein
PHDs	=	Prolyl-4-hydroxylases
AHs	=	Asparaginyl-aspartyl hydroxylases
ROS	=	Radical oxygen species
O-DD	=	Oxygen-dependent degradation
C-TAD	=	Asparagine-containing transactivation domain
TTFA	=	Thenoyltrifluoroacetone
SDH	=	Succinate dehydrogenase
FH	=	Fumarate hydratase
MPT	=	Membrane permeability transition
VDAC	=	Voltage-dependent anion channel
OxPhos	=	Oxidative phosphorylation
GLUT	=	Glucose transporter
HK	=	Hexokinase
HPI	=	Hexosephosphate isomerase
PFK-1	=	Phosphofructokinase type 1
PFK-2	=	Phosphofructokinase type 2
ALD	=	Aldolase
TPI	=	Triosephosphate isomerase
GAPDH	=	Glyceraldehyde-3-phosphate dehydrogenase
PGK	=	Phosphoglycerate kinase
PGAM	=	Phosphoglycerate mutase
ENO	=	Enolase
PYK	=	Pyruvate kinase
LDH	=	Lactate dehydrogenase
MCT	=	Monocarboxylate transporter
PDH	=	Pyruvate dehydrogenase complex
PDK	=	Pyruvate dehydrogenase kinase
G6PDH	=	Glucose 6-phosphate dehydrogenase
G6P	=	Glucose 6-phosphate
F6P	=	Fructose 6-phosphate
F2,6BP	=	Fructose 2, 6 bisphosphate
F1,6BP	=	Fructose 1,6 bisphosphate
DHAP	=	Dihydroxyacetone phosphate
G3P	=	Glyceraldehyde-3-phosphate
1,3BPG	=	1,3 bisphosphoglycerate
2,3BPG	=	2,3-bisphosphoglycerate
3PG	=	3-phosphoglycerate
2PG	=	2-phosphoglycerate
PEP	=	Phosphoenolpyruvate
PYR	=	Pyruvate

LAC = Lactate

ERI4P = Erythrose 4-phosphate

2-DOG = 2-deoxyglucose

REFERENCES

[1] Knowles, H.J.; Harris, A.L. Hypoxia and oxidative stress in breast cancer. Hypoxia and tumourigenesis. *Breast Cancer Res.*, **2001**, *3*, 318-22.

[2] Lu, C.W.; Lin, S.C.; Chen, K.F.; Lai, Y.Y.; Tsai, S.J. Induction of pyruvate dehydrogenase kinase-3 by hypoxia-inducible factor-1 promotes metabolic switch and drug resistance. *J. Biol. Chem.*, **2008**, *283*, 28106-14.

[3] Weidemann, A.; Johnson, R.S. Biology of HIF-1alpha. *Cell Death Differ.*, **2008**, *15*, 621-7.

[4] Semenza, G.L; Roth, P.H.; Fang, H.M.; Wang, G.L. Transcriptional regulation of genes encoding glycolytic enzymes by hypoxia –inducible factor 1. *J. Biol. Chem.*, **1994**, *269*, 23757-63,

[5] Denko, N. C. Hypoxia, HIF1 and glucose metabolism in the solid tumour. *Nat. Rev. Cancer*, **2008**, *8*, 705-13.

[6] Kim, J.W.; Gao, P.; Dang, C.V. Effects of hypoxia on tumor metabolism. *Cancer Metastasis Rev.*, **2007**, 26, 291-8.

[7] Lisy, K; Peet, D.J. Turn me on: regulating HIF transcriptional activity. *Cell Death Differ.*, **2008**, *15*, 642-9.

[8] Huang L.E.; Gu, J.; Schau, M.; Bunn, H.F. Regulation of hypoxia-inducible factor 1alpha is mediated by an O2-dependent degradation domain *via* the ubiquitin-proteasome pathway. *Proc. Natl. Acad. Sci. USA*, **1998**, *95*, 7987-92.

[9] Zhong, H,; De Marzo, A.M.; Laughner, E; Lim, M.; Hilton, D.A.; Zagzag, D.; Buechler, P.; Isaacs, W.; Semenza, G.L.; Simons, J.W. Overexpression of hypoxia-inducible factor 1alpha in common human cancers and their metastases. *Cancer Res.*, **1999**, *59*, 5830-5.

[10] Lundgren, K.; Holm, C.; Landberg, G. Hypoxia and breast cancer: prognostic and therapeutic implications. *Cell Mol. Life Sci.*, **2007**, *64*, 3233-47.

[11] Sun, H.L.; Liu, Y.N.; Huang, Y.T.; Pan, S.L.; Huang, D.Y.; Guh, J.H.; Lee, F.Y.; Kuo, S.C.; Teng, C.M. YC-1 inhibits HIF-1 expression in prostate cancer cells: contribution of Akt/NF-kappaB signaling to HIF-1alpha accumulation during hypoxia. *Oncogene*, **2007**, *26*, 3941-51.

[12] Shyu, K.G.; Hsu, F.L.; Wang, M.J.; Wang, B.W.; Lin, S. Hypoxia-inducible factor 1alpha regulates lung adenocarcinoma cell invasion. *Exp. Cell. Res.*, **2007**, *313*, 1181-91.

[13] Talks, K.L.; Turley, H.; Gatter, K.C.; Maxwell, P.H.; Pugh, C.W.; Ratcliffe, P.J.; Harris, A.L. The expression and distribution of the hypoxia-inducible factors HIF-1alpha and HIF-2alpha in normal human tissues, cancers, and tumor-associated macrophages. *Am. J. Pathol.*, **2000**, *157*, 411-21.

[14] Monsef, N.; Helczynski, L.; Lundwall, A.; Pahlman, S.; Anders-Bjartell . Localization of immunoreactive HIF-1alpha and HIF-2alpha in neuroendocrine cells of both benign and malignant prostate glands. *Prostate*, **2007**, *67*, 1219-29.

[15] Vaupel, P.; Mayer, A. Hypoxia in cancer: significance and impact on clinical outcome. *Cancer Metastasis Rev.*, **2007**, *26*, 225-39.

[16] Fong, G.H.; Takeda, K. Role and regulation of prolyl hydroxylase domain proteins. *Cell Death Differ.*, **2008**, *15*, 635-41.

[17] Ward, J.P. Oxygen sensors in context. *Biochim. Biophys. Acta*, **2008**, *1777*, 1-14.

[18] Koivunen, P.; Hirsilä, M.; Kivirikko, K.I.; Myllyharju, J. The length of peptide substrates has a marked effect on hydroxylation by the hypoxia-inducible factor prolyl 4-hydroxylases. *J. Biol. Chem.*, **2006**, *281*, 28712-20.

[19] Ehrismann, D.; Flashman, E.; Genn, D.N.; Mathioudakis, N.; Hewitson, K.S., Ratcliffe, P.J.; Schofield, C.J. Studies on the activity of the hypoxia-inducible-factor hydroxylases using an oxygen consumption assay. *Biochem. J.*, **2007**, *401*, 227-34.

[20] Tsai, A.G.; Johnson, P.C.; Intaglieta, M. Is the distribution of tissue pO(2) homogeneous? *Antioxid. Redox Signal.*, **2007**, *9*, 979-84.

[21] Cabrales, P.; Tsai, A.G.; Frangos, J.A.; Intaglieta, M. Role of endothelial nitric oxide in microvascular oxygen delivery and consumption. *Free Radic. Biol. Med.*, **2005**, *39*, 1229-37.

[22] Lee, K.; Roth, R.A.; LaPres, J.J. Hypoxia, drug therapy and toxicity. *Pharmacol. Ther.*, **2007**, *113*, 229-46.

[23] Fandrey, J.; Gorr, T.A.; Gassmann, M. Regulating cellular oxygen sensing by hydroxylation. *Cardiovasc. Res.*, **2006**, *71*, 642-51.

[24] Appelhoff, R.J.; Tian, Y.M.; Raval, R.R.; Turley, H.; Harris, A.L.; Pugh, C.W.; Ratcliffe, P.J.; Gleadle, J.M. Differential function of the prolyl hydroxylases PHD1, PHD2, and PHD3 in the regulation of hypoxia-inducible factor. *J. Biol. Chem.*, **2004**, *279*, 38458-65.

[25] Stiehl, D.P.; Wirthner, R.; Köditz, J.; Spielmann, P.; Camenisch, G.; Wenger, R.H. Increased prolyl 4-hydroxylase domain proteins compensate for decreased oxygen levels. Evidence for an autoregulatory oxygen-sensing system. *J. Biol. Chem.*, **2006**, *281*, 23482-91.

[26] Klimova, T.; Chandel, N.S. Mitochondrial complex III regulates hypoxic activation of HIF. *Cell Death Differ.*, **2008**, *15*, 660-6.

[27] Taylor, C.T. Mitochondria and cellular oxygen sensing in the HIF pathway. *Biochem J.*, **2008**, *409*, 19-26.

[28] Covian, R.; Pardo, J.P.; Moreno-Sánchez, R. Tight binding of inhibitors to bovine bc1 complex is independent of the Rieske protein redox state. Consequences for semiquinone stabilization in the quinol oxidation site. *J. Biol. Chem.*, **2002**, 277, 48449-55.

[29] Pouysségur, J.; Mechta-Grigoriou, F. Redox regulation of the hypoxia-inducible factor. *Biol. Chem.*, **2006**, *387*, 1337-46.

[30] Bell, E.L.; Klimova, T.A.; Eisenbart, J.; Moraes, C.T.; Murphy, M.P.; Budinger, G.R.S.; Chandel, N.S. The Qo site of the mitochondrial complex III is required for the transduction of hypoxic signaling *via* reactive oxygen species production. *J. Cell Biol.*, **2007**, *177*, 1029-36.

[31] Horvat, S.; Beyer, C.; Arnold, S. Effect of hypoxia on the transcription pattern of subunit isoforms and the kinetics of cytochrome c oxidase in cortical astrocytes and cerebellar neurons. *J. Neurochem.*, **2006**, *99*, 937-51.

[32] Neuzil, J.; Dyason, J.C.; Freeman, R.; Dong, L. F.; Prochazka, L.; Wang, X. F.; Scheffler, I.; Ralph, S.J. Mitocans as anti-cancer agents targeting mitochondria: lessons from studies with vitamin E analogues, inhibitors of complex II. *J. Bioenerg. Biomembr.*, **2007**, *39*, 65-72.

[33] Pitkanen, S.; Robinson, B.H. Mitochondrial complex I deficiency leads to increased production of superoxide radicals and induction of superoxide dismutase. *J. Clin. Invest.*, **1996**, *98*, 345-51.

[34] Dong, L.F.; Freeman, R.; Liu, J.; Zobalova, R.; Marín-Hernández, A.; Stantic, M.; Rohlena, J.; Rodríguez-Enríquez, S.; Valis, K.; Butcher, B.; Goodwin, J.; Brunk, U.T.; Witting, P.K.; Moreno-Sánchez, R.; Scheffler, I.E.; Ralph, S.J.; Neuzil, J. Suppression of tumor growth *in vivo* by the mitocan alpha-tocopheryl succinate requires respiratory complex II. *Clin. Cancer. Res.*, **2009**, *15*, 1593-600.

[35] Habelhah, H.; Laine, A.; Erdjument-Bromage, H.; Tempst, P.; Gershwin, M.E.; Bowtell, D.D.; Ronai, Z. Regulation of 2-oxoglutarate (alpha-ketoglutarate) dehydrogenase stability by the RING finger ubiquitin ligase Siah. *J. Biol. Chem.*, **2004**, *279*, 53782-8.

[36] Li, X.F.; Carlin, S.; Urano, M.; Russell, J.; Ling, C.C.; O'Donoghue, J.A. Visualization of hypoxia in microscopic tumors by immunofluorescent microscopy. *Cancer Res.*, **2007**, *67*, 7646-53.

[37] Leo, C.; Horn, L.C.; Einenkel, J.; Hentschel, B.; Höckel, M. Tumor hypoxia and expression of c-met in cervical cancer. *Gynecol. Oncol.*, **2007**, *104*, 181-5.

[38] Liao, D.; Johnson, R.S. Hypoxia: a key regulator of angiogenesis in cancer. *Cancer Metastasis Rev.*, **2007**, *26*, 281-90.

[39] Bonicalzi, M.E.; Groulx, I.; Paulsen, N.; Lee, S. Role of exon 2-encoded beta -domain of the von Hippel-Lindau tumor suppressor protein. *J. Biol. Chem.*, **2001**, *276*, 1407-16.

[40] Lu, H.; Dalgard, C.L.; Mohyeldin, A.; McFate, T.; Tait, A.S.; Varma, A. Reversible inactivation of HIF-1 prolyl hydroxylases allows cell metabolism to control basal HIF-1. *J. Biol. Chem.*, **2005**, *280*, 41928-39.

[41] Selak, M.A.; Armour S.M.; MacKenzie, E.D.; Boulahbel, H.; Watson, D.G.; Mansfield, K.D.; Pan, Y.; Simon, M.C.; Thompson, C.B.; Gottlieb, E. Succinate links TCA cycle dysfunction to oncogenesis by inhibiting HIF-alpha prolyl hydroxylase. *Cancer Cell*, **2005**, *7*, 77-85.

[42] Pollard, P.J.; Brière, J.J.; Alam, N.A.; Barwell, J.; Barclay, E.; Wortham, N.C.; Hunt, T.; Mitchell, M.; Olpin, S.; Moat, S.J.; Hargreaves, I.P.; Heales, S.J.; Chung, Y.L.; Griffiths, J.R.; Dalgleish,

A.; McGrath, J.A.; Gleeson, M.J.; Hodgson, S.V.; Poulsom, R.; Rustin, P.; Tomlinson, I.P. Accumulation of Krebs cycle intermediates and over-expression of HIF1alpha in tumours which result from germline FH and SDH mutations. *Hum. Mol. Genet.,* **2005**, *14*, 2231-9.

[43] Lee, S.; Nakamura, E.; Yang, H.; Wei, W.; Linggi, M.S.; Sajan, M.P.; Farese, R.V.; Freeman, R.S.; Carter, B.D.; Kaelin, W.G. Jr.; Schlisio, S. Neuronal apoptosis linked to EglN3 prolyl hydroxylase and familial pheochromocytoma genes: developmental culling and cancer. *Cancer Cell*, **2005**, *8*, 155-67.

[44] Rankin, E.B.; Giaccia, A.J. The role of hypoxia-inducible factors in tumorigenesis. *Cell Death Differ.*, **2008**, *15*, 678-85.

[45] Patel, S.A.; Simon, M.C. Biology of hypoxia-inducible factor-2alpha in development and disease. *Cell Death Differ.*, **2008**, *15*, 628-34.

[46] Jang, M.S.; Park, J.E.; Lee, J.A.; Park, S.G.; Myung, P.K.; Lee, D.H.; Park, B.C.; Cho, S. Binding and regulation of hypoxia-inducible factor-1 by the inhibitory PAS proteins. *Biochem. Biophys. Res. Commun.*, **2005**, *337*, 209-15.

[47] Zhong, H.; Hanrahan, C.; van der Poel, H.; Simona, J.W. Hypoxia-inducible factor 1alpha and 1beta proteins share common signaling pathways in human prostate cancer cells. *Biochem. Biophys. Res. Commun.,* **2001**, *284*, 352-6.

[48] Pedersen, P.L. Mitochondrial events in the life and death of animal cells: a brief overview. *J. Bioenerg. Biomembr.*, **1999**, *31*, 291-304.

[49] Moreno-Sánchez, R.; Rodríguez-Enríquez, S.; Marín-Hernández, A.; Saavedra, E. Energy metabolism in tumor cells. *FEBS J.*, **2007**, *274*, 1393-418.

[50] Takahashi, Y.; Takahashi, S.; Yoshimi, T.; Miura, T. Hypoxia-induced expression of phosphoglycerate mutase B in fibroblasts. *Eur. J. Biochem.,* **1998**, *254*, 497-504.

[51] Gess, B.; Hofbauer, K.H.; Deutzmann, R.; Kurtz, A. Hypoxia up-regulates triosephosphate isomerase expression *via* a HIF-dependent pathway. *Pflugers Arch.*, **2004**, *448*, 175-80.

[52] Ullah, M.S.; Davies, A.J.; Halestrap, A.P. The plasma membrane lactate transporter MCT4, but not MCT1, is up-regulated by hypoxia through a HIF-1alpha-dependent mechanism. *J. Biol. Chem.* **2006**, *281*, 9030-7.

[53] Obach, M.; Navarro-Sabate, A.; Caro, J.; Kong, X.; Duran, J.; Gómez, M.; Perales, J.C.; Ventura, F.; Rosa, J.L.; Bartrons, R. 6-Phosphofructo-2-kinase (pfkfb3) gene promoter contains hypoxia-inducible factor-1 binding sites necessary for transactivation in response to hypoxia. *J. Biol. Chem.*, **2004**, *279*, 53562-70.

[54] Funasaka, T.; Yanagawa, T.; Hogan, V.; Raz, A. Regulation of phosphoglucose isomerase/autocrine motility factor expression by hypoxia. *FASEB J.*, **2005**, *19*, 1422-30.

[55] Macheda, M.L.; Rogers, S.; Best, J.D. Molecular and cellular regulation of glucose transporter (GLUT) proteins in cancer. *J. Cell. Physiol.*, **2005**, *202*, 654-62.

[56] Pessino, A.; Hebert, D.N.; Woon, C.W.; Harrison, S.A.; Clancy, B.M.; Buxton, J.M.; Carruthers, A.; Czech, M.P. Evidence that functional erythrocyte-type glucose transporters are oligomers. *J. Biol. Chem.*, **1991**, *266*, 20213-7.

[57] Zhao, F.Q.; Keating, A.F. Functional properties and genomics of glucose transporters. *Curr. Genomics*, **2007**, *8*, 113-28.

[58] Burant, C.F.; Bell, G.I. Mammalian facilitative glucose transporters: evidence for similar substrate recognition sites in functionally monomeric proteins. *Biochemistry*, **1992**, *31*, 10414-20.

[59] Gould, G.W.; Thomas, H.M.; Jess, T.J.; Bell, G.I. Expression of human glucose transporters in *Xenopus* oocytes: kinetic characterization and substrate specificities of the erythrocyte, liver, and brain isoforms. *Biochemistry*, **1991**, *30*, 5139-45.

[60] Liu, Q.; Vera, J.C.; Peng, H.; Golde, H. The predicted ATP-binding domains in the hexose transporter GLUT1 critically affect transporter activity. *Biochemistry*, **2001**, *40*, 7874-81.

[61] Alterberg, B.; Greulich, K.O. Genes of glycolysis are ubiquitously overexpressed in 24 cancer classes. *Genomics*, **2004**, *84*, 1014-20.

[62] Marín-Hernández, A.; Rodríguez-Enríquez, S.; Vital-González, P.A.; Flores-Rodríguez, F.L.; Macías-Silva, M.; Sosa-Garrocho, M.; Moreno-Sánchez, R. Determining and understanding the control of glycolysis in fast-growth tumor cells. Flux control by an over-expressed but strongly product-inhibited hexokinase. *FEBS J.* **2006**, *273*, 1975-88.

[63] Wilson, J.E. Isozymes of mammalian hexokinase: structure, subcellular localization and metabolic function. *J. Exp. Biol.*, **2003**, *206*, 2049-57.

[64] Pedersen, P.L.; Mathupala, S.; Rempel, A.; Geschwind, J.F.; Ko, Y.H. Mitochondrial bound type II hexokinase: a key player in the growth and survival of many cancers and an ideal prospect for therapeutic intervention. *Biochim. Biophys. Acta*, **2002**, *1555*, 14-20.

[65] Xie, G.; Wilson, J.E. Tetrameric structure of mitochondrially bound rat brain hexokinase: a crosslinking study. *Arch. Biochem. Biophys.*, **1990**, *276*, 285-93.

[66] Pastorino, J.G.; Shulga, N.; Hoek, J.B. Mitochondrial binding of hexokinase II inhibits Bax-induced cytochrome c release and apoptosis. *J. Biol. Chem.*, **2002**, *277*, 7610-8.

[67] Majewski, N.; Nogueira, V.; Robey, R.B.; Hay, N. Akt inhibits apoptosis downstream of BID cleavage *via* a glucose-dependent mechanism involving mitochondrial hexokinases. *Mol. Cell. Biol.*, **2004**, *24*, 730-40.

[68] Machida, K.; Ohta, Y.; Osada, H. Suppression of apoptosis by cyclophilin D *via* stabilization of hexokinase II mitochondrial binding in cancer cells. *J. Biol. Chem.*, **2006**, *281*, 14314-20.

[69] Nakashima, R.; Paggi, M.; Scott, L.J.; Pedersen, P.L. Purification and characterization of a bindable form of mitochondrial bound hexokinase from the highly glycolytic AS-30D rat hepatoma cell line. *Cancer Res.*, **1988**, *48*, 913-9.

[70] Ardehali, H.; Printz, R.L.; Koch, S.; Whitesell, R.R.; May, J.M.; Granner, D.K. Functional interaction between the N- and C-terminal halves of human hexokinase II. *J. Biol. Chem.*, **1999**, *274*, 15986-9.

[71] White, T.K.; Wilson, J.E. Rat brain hexokinase: location of the allosteric regulatory site in a structural domain at the N-terminus of the enzyme. *Arch. Biochem. Biophys.,* **1987**, *259*, 402-11.

[72] Radojkovic, J.; Ureta, T. Hexokinase isoenzymes from the Novikoff hepatoma. Purification, kinetic and structural characterization, with emphasis on hexokinase C. *Biochem. J.,* **1987**, *242*, 895-903.

[73] Ko, Y.H.; Pedersen, P.L.; Geschwind, J.F. Glucose catabolism in the rabbit VX2 tumor model for liver cancer: characterization and targeting hexokinase. *Cancer Lett.,* **2001**, *173*, 83-91.

[74] Ko, Y.H.; Smith, B.L.; Wang, Y.; Pomper, M.G.; Rini, D.A.; Torbenson, M.S.; Hullihen, J.; Pedersen, P.L. Advanced cancers: eradication in all cases using 3-bromopyruvate therapy to deplete ATP. *Biochem. Biophys. Res. Commun.*, **2004**, *324*, 269-75.

[75] Xu, R.; Pelicano, H.; Zhou, Y.; Carew, J.S.; Feng, L.; Bhalla, K.N.; Keating, M.J.; Huang, P. Inhibition of glycolysis in cancer cells: a novel strategy to overcome drug resistance associated with mitochondrial respiratory defect and hypoxia. *Cancer Res.*, **2005**, *65*, 613-21

[76] Jones, A.R.; Gillan, L.; Milmlow, D. The anti-glycolytic activity of 3-bromopyruvate on mature boar spermatozoa *in vitro*. *Contraception*, **1995**, *52*, 317-20.

[77] Pereira da Silva, A.P.; El-Bacha, T.; Kyaw, N.; dos Santos, R.S.; da-Silva, W.S.; Almeida, F.C.; Da Poian A.T.; Galina, A. Inhibition of energy-producing pathways of HepG2 cells by 3-bromopyruvate. *Biochem. J.*, **2009**, *417*, 717-26.

[78] Penso, J.; Beitner, R. Detachment of glycolytic enzymes from cytoskeleton of Lewis lung carcinoma and colon adenocarcinoma cells induced by clotrimazole and its correlation to cell viability and morphology. *Mol. Genet. Metab.*, **2002**, *76*, 181-8.

[79] Meira, D.D.; Marinho-Carvalho, M.M.; Teixeira, C.A.; Veiga, V.F.; Da Poian, A.T.; Holandino, C.; de Freitas, M.S.; Sola-Penna, M. Clotrimazole decreases human breast cancer cells viability through alterations in cytoskeleton-associated glycolytic enzymes. *Mol. Genet. Metab.*, **2005**, *84*, 354-62.

[80] Khalid, M.H.; Tokunaga, Y.; Caputy, A. J.; Walters, E. Inhibition of tumor growth and prolonged survival of rats with intracranial gliomas following administration of clotrimazole. *J. Neurosurg.*, **2005**, *103*, 79-86.

[81] van Wijk, R.; van Solinge, W.W. The energy-less red blood cell is lost: erythrocyte enzyme abnormalities of glycolysis. *Blood*, **2005**, *106*, 4034-42.

[82] Kim, J.W.; Dang, C.V. Multifaceted roles of glycolytic enzymes. *Trends Biochem. Sci.*, **2005**, *30*, 142-50.

[83] Chirgwin, J.M.; Parsons, T.F.; Noltmann, E.A. Mechanistic implications of the pH independence of inhibition of phosphoglucose isomerase by neutral sugar phosphates. *J. Biol. Chem.*, **1975**, *250*, 7277-9.

[84] Reitzer, L.J.; Wice, B.M.; Kennell, D. The pentose cycle. Control and essential function in HeLa cell nucleic acid synthesis. *J. Biol. Chem.*, **1980**, *255*, 5616-26.

[85] Horton, R.W.; Meldrum, B.S.; Bachelard, H.S. Enzymic and cerebral metabolic effects of 2-deoxy-D-glucose. *J. Neurochem.*, **1973**, *21*, 507-20.

[86] Manuel y Keenoy, B.; Zähner, D.; Malaisse, W.J. Dissociated effects of 2-deoxy-D-glucose and D-[2-^{3}H]glucose and D-[5-^{3}H]glucose conversion into ^{3}HOH in rat erythrocytes. *Biochem. J.* **1992**, *288*, 433-38.

[87] Liu, H.; Hu, Y.P.; Savaraj, N.; Priebe, W.; Lampidis, T.J. Hypersensitization of tumor cells to glycolytic inhibitors. *Biochemistry*, **2001**, *40*, 5542-7.

[88] Maschek, G.; Savaraj, N.; Pruebe, W.; Braunschweiger, P.; Hamilton, K.; Tudmarsh, G.F.; De Young, L.R.; Lampidis, T.J. 2-deoxy-D-glucose increases the efficacy of adriamycin and paclitaxel in human osteosarcoma and non-small cell lung cancers *in vivo*. *Cancer Res.*, **2004**, *64*, 31-4.

[89] Dwarakanath, B.S.; Khaitan, D.; Ravindranath, T. 2-deoxy-D-glucose enhances the cytotoxicity of topoisomerase inhibitors in human tumor cell lines. *Cancer Biol. Ther.*, **2004**, *3*, 864-70.

[90] Gupta, S.; Mathur, R.; Dwarakanath, B.S. The glycolytic inhibitor 2-deoxy-D-glucose enhances the efficacy of etoposide in Ehrlich ascites tumor-bearing mice. *Cancer Biol. Ther.*, **2005**, *4*, 87-94.

[91] Kang, H.T.; Hwang, E.S. 2-Deoxyglucose: an anticancer and antiviral therapeutic, but not any more a low glucose mimetic. *Life Sci.*, **2006**, *78*, 1392-9.

[92] Lynch, R.M.; Fogarty, K.E.; Fay, F.S. Modulation of hexokinase association with mitochondria analyzed with quantitative three-dimensional confocal microscopy. *J. Cell Biol.*, **1991**, *112*, 385-95.

[93] Dunaway, G.A.; Kasten, T.P.; Sebo, T.; Trapo, R. Analysis of the phosphofructokinase subunits and isoenzymes in human tissues. *Biochem. J.*, **1988**, *251*, 677-83.

[94] Rodríguez-Enríquez, S.; Juárez, O.; Rodríguez-Zavala, J.S.; Moreno-Sánchez, R. Multisite control of the Crabtree effect in ascites hepatoma cells. *Eur. J. Biochem.*, **2001**, *268*, 2512-9.

[95] González-Mateos, F.; Gómez, M.E.; García-Salguero, L.; Sánchez, V.; Aragón, J.J. Inhibition of glycolysis by amino acids in ascites tumor cells. Specificity and mechanism. *J. Biol. Chem.*, **1993**, *268*, 7809-17.

[96] Denis, C.; Paris, H.; Murat, J.C. Hormonal control of fructose 2,6-bisphosphate concentration in the HT29 human colon adenocarcinoma cell line. Alpha 2-adrenergic agonists counteract effect of vasoactive intestinal peptide. *Biochem. J.*, **1986**, *239*, 531-6.

[97] Loiseau, A.M.; Rousseau, G.G.; Hue, L. Fructose 2,6-bisphosphate and the control of glycolysis by glucocorticoids and by other agents in rat hepatoma cells. *Cancer Res.*, **1985**, *45*, 4263-9.

[98] Pezza, J.A.; Choi, K.H.; Berardini, T.Z.; Beernink, P.T.; Allen, K.N.; Tolan, D.R. Spatial clustering of isozyme-specific residues reveals unlikely determinants of isozyme specificity in fructose-1,6-bisphosphate aldolase. *J. Biol. Chem.*, **2003**, *278*, 17307-13.

[99] Biswas, S.; Ray, M.; Misra, S.; Dutta, D.P.; Ray, S. Selective inhibition of mitochondrial respiration and glycolysis in human leukaemic leucocytes by methylglyoxal. *Biochem. J.*, **1997**, *323*, 343-8.

[100] Sirover, M.A. Role of the glycolytic protein, glyceraldehyde-3-phosphate dehydrogenase, in normal cell function and in cell pathology. *J. Cell Biochem.*, **1997**, *66*, 133-40.

[101] Welch, J.E.; Brown, P.L.; O´Brien, D.A.; Magyar, P.L.; Bunch, D.O.; Mori, C.; Eddy, E. M. Human glyceraldehydes 3-phosphate dehydrogenase-2 gene is expressed specifically in spermatogenic cells. *J. Androl.*, **2000**, *21*, 328-38

[102] Jaroszewski, J.W.; Kaplan, O.; Cohen, J.S. Action of gossypol and rhodamine 123 on wild type and multidrug-resistant MCF-7 human breast cancer cells: 31P nuclear magnetic resonance and toxicity studies. *Cancer Res.*, **1990**, *50*, 6936-43.

[103] Tuszynski, G.P.; Cossu, G. Differential cytotoxic effect of gossypol on human melanoma, colon carcinoma, and other tissue culture cell lines. *Cancer Res.*, **1984**, *44*, 768-71.

[104] Oliver, C.L.; Miranda, M.B.; Shangary, S.; Land, S.; Wang, S.; Johnson, D.E. (-)-Gossypol acts directly on the mitochondria to overcome Bcl-2- and Bcl-X(L)-mediated apoptosis resistance. *Mol. Cancer Ther.*, **2005**, *4*, 23-31.

[105] Wu, Y.W.; Chik, C.L.; Knazek, R.A. An *in vitro* and *in vivo* study of antitumor effects of gossypol on human SW-13 adrenocortical carcinoma. *Cancer Res.*, **1989**, *49*, 3754-8.

[106] Bushunow, P.; Reidenberg, M.M.; Wasenko, J.; Lorenzo, B.; Lemke, S.; Himpler, B.; Corona, R.; Coyle, T. Gossypol treatment of recurrent adult malignant gliomas. *J. Neurooncol.*, **1999**, *43*, 79-86.

[107] Sakai, K.; Hasumi, K.; Endo, A. Inactivation of rabbit muscle glyceraldehyde-3-phosphate dehydrogenase by koningic acid. *BBA-Prot. Struct. Mol. Enzymol.*, **1988**, *952*, 297-03.

[108] Kumagai, S.; Narasaki, R.; Hasumi, K. Glucosa-dependent active ATP depletion by koningic acid kills high-glycolytic cells. *Biochem. Biophys. Res. Commun.*, **2008**, *365*, 362-68.

[109] Ralph, S.J. Arsenic-based antineoplastic drugs and their mechanisms of action. *Metal Based Drugs*., **2008**, *2008*, Article ID 260146.

[110] Lay, A.J.; Jiang, X.M.; Kisker, O.; Flynn, E.; Underwood, A.; Condron, R.; Hogg, P.J. Phosphoglycerate kinase acts in tumour angiogenesis as a disulphide reductase. *Nature*, **2000**, *408*, 869-73.

[111] Repiso, A.; Ramirez-Bajo, M.J.; Vives-Corrons, J.L.; Carreras, J.; Climent, F. Phosphoglycerate mutase BB isoenzyme deficiency in a patient with non-spherocytic anemia: familial and metabolic studies. *Haematologica*, **2005**, *90*, 257-9.

[112] Fundele, R.; Krietsch, W.K. Purification and properties of the phosphoglycerate mutase isozymes from the mouse. *Comp. Biochem. Physiol. B.*, **1985**, *81*, 965-8.

[113] Durany, N.; Joseph, J.; Campo, E.; Molina, R.; Carreras, J. Phosphoglycerate mutase, 2,3 bisphosphoglycerate phosphatase and enolase activity and isoenzymes in lung, colon and liver carcinomas. *Br. J. Cancer*, **1997**, *75*, 969–77.

[114] Durany, N.; Joseph, J.; Jimenez, O.M.; Climent, F.; Fernández, P.L.; Rivera, F.; Carreras, J. Phosphoglycerate mutase, 2,3-bisphosphoglycerate phosphatase, creatine kinase and enolase activity and isoenzymes in breast carcinoma. *Br. J. Cancer*, **2000**, *82*, 20–7.

[115] Kondoh, H.; Lleonart, M.E.; Gil, J.; Wang, J.; Degan, P.; Peters, G.; Martinez, D.; Carnero, A.; Beach, D. Glycolytic enzymes can modulate cellular life span. *Cancer Res.*, **2005**, *65*, 177-85.

[116] Pancholi, V. Multifunctional alpha-enolase: its role in diseases. *Cell. Mol. Life Sci.*, **2001**, 58, 902-20.

[117] Shimizu, A.; Suzuki, F.; Kato, K. Characterization of alpha alpha, beta beta, gamma gamma and alpha gamma human enolase isozymes, and preparation of hybrid enolases (alpha gamma, beta gamma and alpha beta) from homodimeric forms. *BBA-Prot. Struct. Mol. Enzymol.*, **1983**, *748*, 278-84.

[118] Imamura, K.; Tanaka, T. Pyruvate kinase isozymes from rat. *Methods Enzymol.*, **1982**, *90*, 150-65.

[119] Mazurek, S.; Grimm, H.; Boschek, C.B.; Vaupel, P.; Eigenbrodt, E. Pyruvate kinase type M2: a crossroad in the tumor metabolome. *Brit. J. Nutr.*, **2002**, *87*, S23-9.

[120] Christofk, H.R.; Vander-Heiden, M.G.; Wu, N.; Asara, J.M.; Cantley, L.C. Pyruvate kinase M2 is a phosphotyrosine-binding protein. *Nature*, **2008**, *452*, 181-6.

[121] Drent, M.; Cobben, N.A.; Henderson, R.F.; Wouters, E.F.M.; van Dieijen-Visser, M. Usefulness of lactate dehydrogenase and its isoenzymes as indicators of lung damage or inflammation. *Eur. Respir. J.*, **1996**, *9*, 1736-42.

[122] Buhl, S.N.; Jackson, K.Y.; Vanderlinde, R.E. The effect of temperature on the kinetic constants of human lactate dehydrogenase 1 and 5. *Clin. Chim. Acta*, **1977**, *80*, 265-70.

[123] Koukourakis, M.I.; Giatromanolaki, A.; Simopoulos, C.; Polychronidis, A.; Sivridis, E. Lactate dehydrogenase 5 (LDH5) relates to up-regulated hypoxia inducible factor pathway and metastasis in colorectal cancer. *Clin. Exp. Metastasis*, **2005**, *22*, 25-30.

[124] Elwood, J.C. Effect of oxamate on glycolysis and respiration in sarcoma 37 ascites cells. *Cancer Res.*, **1968**, *28*, 2056-60.

[125] Jow, G.M.; Wu, Y.C.;Guh, J.H.; Teng, C.M. Armepavine oxalate induces cell death on CCRF-CEM leukemia cell line through an apoptotic pathway. *Life Sci.*, **2004**, *75*, 549-57.

[126] Görlach, A.; Acker, H. pO2- and pH-gradients in multicellular spheroids and their relationship to cellular metabolism and radiation sensitivity of malignant human tumor cells. *BBA-Mol. Basis Dis.*, **1994**, *1227*, 105-12.

[127] Martin-Requero, A.; Ayuso, M.S.; Parrilla, R. Rate-limiting steps for hepatic gluconeogenesis. Mechanism of oxamate inhibition of mitochondrial pyruvate metabolism. *J. Biol. Chem.*, **1986**, *261*, 13973-8.

[128] Beutler, E.; Forman, L.; West, C. Effect of oxalate and malonate on red cell metabolism. *Blood*, **1987**, *70*, 1389-93.

[129] Fantin, V.R.; St-Pierre, J.; Leder, P. Attenuation of LDH-A expression uncovers a link between glycolysis, mitochondrial physiology, and tumor maintenance. *Cancer Cell*, **2006**, *9*, 425-34.

[130] Okar, D.A.; Manzano, A.; Navarro-Sabate, A.; Riera, L.l.; Bartrons, R.; Lange, A.J. PFK-2/FBPase-2: maker and breaker of the essential biofactor fructose-2,6-bisphosphate. *Trends Biochem. Sci.*, **2001**, *26*, 30-5.

[131] Halestrap, A.P.; Meredith, D. The SLC16 gene family-from monocarboxylate transporters (MCTs) to aromatic amino acid transporters and beyond. *Pflugers Arch.*, **2004**, *447*, 619-28.

[132] Izumi, H.; Torigoe, T.; Ishiguchi, H.; Yoshida, Y.; Tanabe, M.; Ise, T.; Murakami, T.; Yoshida, T.; Nomoto, M.; Kohno, K. Cellular pH regulators: potentially promising molecular targets for cancer chemotherapy. *Cancer Treat. Rev.*, **2003**, *29*, 541-9.

[133] Gallagher, S.M.; Castorino, J.J.; Wang, D.; Philp, N.J. Monocarboxylate transporter 4 regulates maturation and trafficking of CD147 to the plasma membrane in the metastatic breast cancer cell line MDA-MB-231. *Cancer Res.*, **2007**, *67*, 4182-9.

[134] Martín-Venegas, R.; Rodríguez-Lagunas, M.J.; Geraert, P.A.; Ferrer, R. Monocarboxylate transporter 1 mediates DL-2-Hydroxy-(4-methylthio)butanoic acid transport across the apical membrane of Caco-2 cell monolayers. *J. Nutr.*, **2007**, *137*, 49-54.

[135] Sonveaux, P.; Végran, F.; Schroeder, T.;Wergin, M.C. ; Verrax, J.; Rabbani, Z.N.; De Saedeleer, C.J.; Kennedy, K.M; Diepart, C.; Jordan, B.F.; Kelley, M.J.; Gallez, B.; Wahl, M.L.; Feron, O.; Dewhirst, M.W. Targeting lactate-fueled respiration selectively kills hypoxic tumor cells in mice. *J. Clin. Invest.*, **2008**,*118*, 3930-42.

[136] Bowman, E.J.; Bowman, B.J. V-ATPases as drug targets. *J. Bioenerg. Biomembr.*, **2005**, *37*, 431-5.

[137] Gerweck, L.E.; Vijayappa, S.; Kozin, S. Tumor pH controls the *in vivo* efficacy of weak acid and base chemotherapeutics. *Mol. Cancer Ther.*, **2006**, *5*, 1275-9.

[138] Sennoune, S.R.; Luo, D.; Martinez-Zaguilan, R. Plasmalemmal vacuolar-type H+-ATPase in cancer biology. *Cell Biochem. Biophys.*, **2004**, *40*, 185-206.

[139] Bowman, E.J.; Gustafson, K.R.; Bowman, B.J.; Boyd, M.R. Identification of a new chondropsin class of antitumor compound that selectively inhibits V-ATPases. *J. Biol. Chem.*, **2003**, 278, 44147-52.

[140] Lu, X.; Qin, W.; Li, J.; Tan, N.; Pan, D.; Zhang, H.; Xie, L.; Yao, G.; Shu, H.; Yao, M.; Wan, D.; Gu, J.; Yang, S. The growth and metastasis of human hepatocellular carcinoma xenografts are inhibited by small interfering RNA targeting to the subunit ATP6L of proton pump. *Cancer Res.*, **2005**, *65*, 6843-9.

[141] Fukuda, R.; Zhang, H.; Kim, J.W.; Shimoda, L.; Dang, C.V.; Semenza, G.L. HIF-1 regulates cytochrome oxidase subunits to optimize efficiency of respiration in hypoxic cells. *Cell*, **2007**, *129*, 111-22.

[142] Campian, J.L.; Gao, X.; Qian, M.; Eaton, J.W. Cytochrome *c* oxidase activity and oxygen tolerance. *J. Biol. Chem.*, **2007**, *282*, 12430-8.

[143] Moreno-Sánchez, R.; Saavedra, E.; Rodríguez-Enríquez, S.; Olín-Sandoval, V. Metabolic control analysis: a tool for designing strategies to manipulate metabolic pathways. *J. Biomed. Biotechnol.*, **2008**, *2008*, Article ID 597913.

[144] Roche, T.E.; Hiromasa, Y. Pyruvate dehydrogenase kinase regulatory mechanisms and inhibition in treating diabetes, heart ischemia, and cancer. *Cell Mol. Life Sci.*, **2007**, *64*, 830-49.

[145] Gudi, R.; Bowker-Kinley, M.M.; Kedishvili, N.Y.; Zhao, Y.; Popov, K. Diversity of the pyruvate dehydrogenase kinase gene family in humans. *J. Biol. Chem.,* **1995**, *270*, 28989-94.

[146] Bowker-Kinley, M.M.; Davis, W.I.; Wu, P.; Harris, R.A.; Popov, K.M. Evidence for existence of tissue-specific regulation of the mammalian pyruvate dehydrogenase complex. *Biochem. J.*, **1998**, *329*, 191-6.

[147] Korotchkina, L.G.; Patel, M.S. Site specificity of four pyruvate dehydrogenase kinase isoenzymes toward the three phosphorylation sites of human pyruvate dehydrogenase. *J. Biol. Chem.,* **2001**, *276*, 37223-9.

[148] Kolobova, E.; Tuganova, A.; Boulatnikov, I.; Popov, K.M. Regulation of pyruvate dehydrogenase activity through phosphorylation at multiple sites. *Biochem. J.*, **2001**, *358*, 69-77.

[149] Papandreou, I.; Cairns, R.A.; Fontana, L.; Lim, A.L.; Denko, N.C. HIF-1 mediates adaptation to hypoxia by actively downregulating mitochondrial oxygen consumption. *Cell Metab.*, **2006**, *3*, 187-97.

[150] Kim, J.W.; Tchernyshyov, I.; Semenza, G.L.; Dang, C.V. HIF-1-mediated expression of pyruvate dehydrogenase kinase: a metabolic switch required for cellular adaptation to hypoxia. *Cell Metab.*, **2006**, *3*, 177-85.

[151] McFate, T.; Mohyeldin, A.; Lu, H.; Thakar, J.; Henriques, J.; Halim, N.D.; Wu, H.; Schell, M.J.; Tsang, T.M.; Teahan, O.; Zhou, S.; Califano, J.A.; Jeoung, N.H.; Harris, R.A.;Verma, A. Pyruvate dehydrogenase complex activity controls metabolic and malignant phenotype in cancer cells. *J. Biol. Chem.*, **2008**, *283*, 22700-8.

[152] Bonnet, S.; Archer, S.L.; Allalunis-Turner, J.; Haromy, A.; Beaulieu, C.; Thompson, R.; Lee, C.T.; Lopaschuk, G.D.; Puttagunta, L.; Bonnet, S.; Harry, G.; Hashimoto, K.; Porter, C.J.; Andrade, M.A.; Thebaud, B.; Michelakis E.D. A mitochondria-K+ channel axis is suppressed in cancer and its normalization promotes apoptosis and inhibits cancer growth. *Cancer Cell*, **2007**, *11*, 37-51.

[153] Martínez-Sánchez, G.; Giuliani, A. Cellular redox status regulates hypoxia inducible factor-1 activity. Role in tumour development. *J. Exp. Clin. Cancer Res.*, **2007**, *26*, 39-50.

[154] Hossain, C.F.; Kim, Y.P.; Baerson, S.R.; Zhang, L.; Bruick, R.K.; Mohammed, K.A.; Agarwal, A.K.; Nagle, D.G.; Zhou, Y.D. *Saururus cernuus* lignans-potent small molecule inhibitors of hypoxia-inducible factor-1. *Biochem. Biophys. Res. Commun.*, **2005**, *333*, 1026-33.

[155] Zhang, H.; Qian, D.Z.; Tan, Y.S.; Lee, K.; Gao, P.; Ren, Y.R.; Rey, S.; Hammers, H.; Chang, D.; Pili, R.; Dang, C.V.; Liu, J.O.; Semenza, G.L. Digoxin and other cardiac glycosides inhibit HIF-1alpha synthesis and block tumor growth. *Proc. Natl. Acad. Sci. USA*, **2008**, *105*, 19579-86.

[156] Kong, D.; Park, E.J.; Stephen, A.G.; Calvani, M.; Cardellina, J.H.; Monks, A.; Fisher, R.J.; Shoemaker, R.H.; Melillo, G. Echinomycin, a small-molecule inhibitor of hypoxia-inducible factor-1 DNA-binding activity. *Cancer Res.*, **2005**, *65*, 9047-55.

[157] Takahashi, Y.; Nishikawa, M.; Takakura, Y. Inhibition of tumor cell growth in the liver by RNA interference-mediated suppression of HIF-1alpha expression in tumor cells and hepatocytes. *Gene Ther.*, **2008**, *15*, 572-82.

[158] Choi, H.J.; Eun, J.S.; Kim, B.G.; Kim, S.Y.; Jeon, H.; Soh, Y. Vitexin, an HIF-1alpha inhibitor, has anti-metastatic potential in PC12 cells. *Mol. Cells*, **2006**, *22*, 291-9.

[159] Puppo, M.; Battaglia, F., Ottaviano, C.; Delfino, S.; Ribatti, D.; Varesio, L.; Bosco, M.C. Topotecan inhibits vascular endothelial growth factor production and angiogenic activity induced by hypoxia in human neuroblastoma by targeting hypoxia-inducible factor-1alpha and -2alpha. *Mol. Cancer Ther.*, **2008**, *7*, 1974-84.

[160] Carmeliet, P.; Dor, Y.; Herbert, J.M.; Fukumura, D.; Brusselmans, K.; Dewerchin, M.; Neeman, M.; Bono, F.; Abramovitch, R.; Maxwell, P.; Koch, C.J.; Ratcliffe, P.; Moons, L.; Jain, R.K.; Collen, D.; Keshert, E. Role of HIF-1alpha in hypoxia-mediated apoptosis, cell proliferation and tumour angiogenesis. *Nature*, **1998**, *394*, 485-90.

[161] Blouw, B,; Song, H.; Tihan, T.; Bosze, J.; Ferrara, N.; Gerber, H.P.; Johnson, R.S.; Bergers G. The hypoxic response of tumors is dependent on their microenvironment. *Cancer Cell*, **2003**, *4*, 133-46.

[162] Ameln, H.; Gustafsson, T.; Sundberg, C.J.; Okamoto, K.; Jansson, E,; Poellinger, L.; Makino, Y. Physiological activation of hypoxia inducible factor-1 in human skeletal muscle. *FASEB J.*, **2005**, *19*, 1009-11.

[163] Critchley, H.O.; Osei, J.; Henderson, T.A.; Boswell, L.; Sales, K.J.; Jabbour, H.N.; Hiranio, N. Hypoxia-inducible factor-1alpha expression in human endometrium and its regulation by prostaglandin E-series prostanoid receptor 2 (EP2). *Endocrinology*, **2006**, *147*, 744-53.

[164] Neuzil, J., Zhao, M., Ostermann, G., Sticha, M., Gellert, N., Weber, C., Eaton, J.W., Brunk, U.T. Alpha-tocopheryl succinate, an agent with *in vivo* anti-tumour activity, induces apoptosis by causing lysosomal instability. *Biochem. J.*, **2002**, *362*, 709-15.

[165] Balinsky, D.; Platz, C.E.; Lewis, J.W. Isozyme patterns of normal, benign, and malignant human breast tissues. *Cancer Res.,* **1983**, *43*, 5895-901.

[166] Atsumi, T.; Chesney, J.; Metz, A.; Leng, L.; Donnelly, S.; Makita, Z.; Mitchell, R.; Bucala, R. High expression of inducible 6-phosphofructo-2-kinase/fructose-2,6-bisphosphatase (iPFK-2; PFKFB3) in human cancers. *Cancer Res.,* **2002**, *62*, 5881-7.

Received: 16 December, 2008 **Revised: 21 April, 2009** **Accepted: 23 April, 2009**

From: aneelafarooqi@benthamscience.org

To: morenosanchez@hotmail.com; rafael.moreno@cardiologia.org.mx
Subject: MRMC-192807: Dr. Gennari: Acceptance of Manuscript # 840 after Minor Changes
Date: Thu, 26 Mar 2009 09:21:40 +0500
March 25, 2009
Correspondence reference no. MRMC-192807

Dear Dr. Sanchez,

You will be pleased to know that your article entitled "HIF-1α modulates energy metabolism in cancer cells by modifying the status of glycolytic enzymes " will be accepted for publication in MRMC only after incorporation of the following minor changes suggested by the referees along with the confirmation letter for color figures, if any.
Best Regards
Ms. Aneela Farooqi
Manager Publications
Bentham Science Publications
E-mail: aneelafarooqi@benthamscience.org

Referees' comments: (1)

The review article entitled "HIF-1α modulates energy metabolism in cancer cells by modifying the status of glycolytic enzymes" is aimed at discussing the role of HIF-1a in the regulation of tumor glycolysis.

Growing body of evidences substantiate the metabolic switch of cancer cells to aerobic glycolysis. This metabolic modulation involves generation and utilization of cellular ATP under adverse conditions like diminished oxygen supply (hypoxia), cellular stress etc. Hypoxia inducible factor -1α (HIF-1α) has been known to be involved in the up regulation of several genes that favor tumor growth. This review article discusses about the role of HIF-1α in the up regulation of glycolytic enzymes.

However, the article does not enlighten how HIF-1α modulates the glycolytic up-regulation, except stating that HIF-1a induces the over-expression of key glycolytic enzymes.

Significantly, key references, which are relevant to the topic of this review, are not discussed. For example, the recent review by Denko (2008) in **Nat Rev Cancer,** and the report by Fulda and Debatin (2007) in **Cell Cycle** all discuss about Hypoxia, HIF-1 and glucose metabolism. Similarly, De Palma et al., (2007) have recently reported the metabolic modulation by hypoxia that would have been ideal for discussing the metabolic switch in hypoxia in this review. The pioneering work published by Semenza et al., (1994) which is entitled **"Transcriptional regulation of genes encoding glycolytic enzymes by hypoxia-inducible factor 1"** has not been referred. This reference is more appropriate and relevant for this review article, for a thorough discussion.

Table-1 does not cite any references from where those data were taken from.
It is unclear why the role of HIF-1 α has not been discussed for the glycolytic enzymes such as Hexosephosphate Isomerase (HPI), Phosphofructokinase type 1 (PFK-1), Triosephosphate Isomerase (TPI), Phosphofructokinase type 2 (PFK-2).

Regarding 3-bromopyruvate, the sentence on page-14, line-15 reads as follows citing a reference; " ..... the cytotoxic activity against cancer cells was of low potency (IC50~50uM) [76]". This is incorrect, as that reference does not relate to cancer cells, in fact that report is related to the activity of "boar spermatozoa".

Page 19, line 15 states " GAPDH is a homo-tetramer of 37 kDa subunits [102] with no isoforms". GAPDH has been reported to have different isoforms either at mRNA level or at post-translational levels, (e.g, Choudhary et al., (2000), Saunders et al., (1999), Glaser and Gross (1995)). It is erroneous to define that GAPDH has no isoforms.

Unfortunately, the review article does not mention about the inhibitors of GAPDH in detail. For example, Koningic acid has been known as an inhibitor of GAPDH and has been under in-depth investigation for its potential application as an anti-cancer agent.

Finally, on page-28, the first paragraph emphasizes that targeting cytosolic pH regulators, and v-type ATPase as very " ……. promising and novel therapeutic approach". On the contrary, in the abstract, the concluding sentence states as "……it is concluded that targeting the HIF1α-induced glucose transporter and hexokinase important to glycolytic flux control might provide better therapeutic targets for inhibiting tumor growth and progression than targeting HIF-1α itself ". There is no explanation or convincing justification why targeting hexokinase or glucose transporters is better or advantageous than other targets.

Referees' comments: (2)

I would suggest a few minor changes that might further clarify the work:

In the title, the phrase "by modifying the status of glycolytic enzymes" is confusing. This could be changed to "through precise effects on glycolysis" or "by facilitating a glycolytic phenotype" or something similar.

There are a few typographic errors: On page 6, the authors use PDH or PDH2 when they should use PHD to abbreviate prolyl hydroxylase. Also, the end of the sentence that starts page 30 is scrambled.

The authors point out that the drug 2-deoxyglucose (2-DOG) inhibits HPI, although it is usually referred to as a competitive inhibitor of hexokinase. The authors point out that in the presence of glucose, 2-DOG does compete with glucose at HK and elsewhere in the glycolytic pathway. Under standard conditions of culture or tumor growth *in vivo* (when glucose is present), is 2-DOG's primary effect on cell growth/survival exerted at the level of HPI or at these other sites?

PYK-M2's involvement in tumor cell metabolism is well-publicized but still difficult to explain and somewhat confusing as presented here. Do the oncoproteins pp60-v-src and HPV-16 E7 promote formation of the inactive dimer or the active tetramer? And can the authors resolve the issue of why the less active dimer seems to predominate in tumor cells, even when the Warburg effect (i.e. lactate production) is so prevalent in these same cells? Finally, many discussions of this topic hypothesize that PYK-M2 dimerization facilitates tumor growth by allowing upstream glycolytic intermediates to accumulate and be used for biosynthesis of nucleic acid and other macromolecules. But is there any good evidence that this occurs? The two papers cited do not provide any compelling evidence to this point. Reference 117, for example, shows an enhancement of conversion of glucose carbon into lipids in the presence of PYK-M2, but this activity presumably requires the forward activity of that enzyme, yielding pyruvate whose carbon can ultimately enter fatty acid synthesis. Can the authors resolve this question?

Although it is not known to be a HIF-1α target, MCT1 has been shown to support tumor growth in animal models (Sonveaux et al, *J Clin Invest* 118:3930-3942). This reference should be included.
In Figure 2, why is MCT4 shown as a filled symbol when it is the only MCT isoform shown?

Referees' comments: (3)
The first part describing glycolytic enzymes is very comprehensive and detailed. The second part, when the authors attempt to discuss HIF-1 is a target is poorly elaborated (pg 30). Either they remove this paragraph, which in n ay case seems to be at odd with the rest of the manuscript, or they expand it which might make the manuscript too long.

1) Pg 4: please check half-life of HIF under hypoxia.
2) Typos: pf 9 In 13: liomyomas; pg 10 In 13, sentence is unclear (down-regulate?); pg 30 In 1
revise sentence.
3) Reference for Topotecan as HIF inhibitor is missing.

Typographical errors
References incorrectly presented

21 April 2009

Ms. Aneela Farooqi
Manager Publications
Bentham Science Publications

Thank you for your kind letter of 25 March 2009, in which we were informed that our manuscript will be accepted for publication in ***Mini-Reviews in Medicinal Chemistry*** after incorporation of the changes suggested by the three reviewers. We would like to thank the reviewers for their favorable comments and minor criticisms. We have modified the text taking into account their suggestions. We have outlined our responses to each of the points they have made, in turn.
Due to the changes made and the addition (and deletion) of references, the reference numbering was modified. The reference format was also changed. A running header was included on the Title page. As required, we are re-submitting the revised manuscript in both a Word file, with all the changes made in bold letter, and a pdf file, with all the contents included and inserted as they should appear in the printed version.

Sincerely yours,

Rafael Moreno-Sanchez, Ph. D.

Response to reviewer 1
We agree with the reviewer comment that the paper does not enlighten on how HIF-1 modulates the glycolytic up-regulation. However, the genetic (molecular biological) mechanism by which HIF-1 modulates over-expression of specific glycolytic genes was outside the scope of our mini-review, and of the journal (focusing on Medicinal Chemistry). The central point of our review was to address the up-regulation of glycolytic gene isoforms and the possible biochemical (kinetic) reasons for this selection in tumor cells. Despite almost all the glycolytic pathway are up-regulated by HIF-1, the important point we make is in regard to those steps that play the most critical roles in controlling the glycolytic flux in cancer cells (a paragraph clearly stating the main focus of the paper was included on p. 4). It is these proteins that should therefore be considered the best targets for inhibitors as anti-cancer agents because blocking at such points would be predicted to show a stronger effect at inhibiting glycolysis (this was originally stated on the Abstract and p. 32).
Some of the references suggested by the reviewer [4,5] were included in the text. On the other hand, the De Palma paper is on skeletal muscle subjected to hypoxia, which is not a highly proliferative tissue like tumors; the Cell Cycle paper is a very short (two and a half pages) review on the subject. References were added to Table 1.
We have now modified the manuscript to mention that TPI gene is also up-regulated by HIF-1α (p. 19), and that HPI is over-expressed under hypoxia through a HIF-1α independent mechanism (p. 15). Discussion on HIF-1α-mediated PFK-1 and PFK-2 over-expression was included in the original manuscript on p. 17 and 26, respectively.
The incorrectly cited reference on 3BrPyr was changed (previous [76], now [74, 75]).
Isoform is defined as a protein encoded by a specific gene and hence, with amino acid sequence and kinetic and structural properties different to other proteins catalyzing the same physical (transporters) or chemical (enzymes) reaction. Therefore, the original statement, “GAPDH has no isoforms” was correct. The publications mentioned by the reviewer which use the word isoform are not isoforms, but concern post-translational modifications of GAPDH. However, another GAPDH isoform has been certainly found in spermatozoa. Then, the text was slightly modified (p. 20).
A detailed description of the properties of Koningic acid as a GAPDH inhibitor was incorporated on p. 21 and 22, as suggested.
The reviewer has taken out of context the conclusion that targeting HIF-1 versus GLUT or HK as a better option. This was one of the key proposals developed throughout the review and is quite distinct from the possibility of targeting cytosolic pH regulators and ATPases (p. 29 and 30) as the reviewer pointed out. Drugs targeting HIF have high toxicity in general to many cell types and this was outlined on p. 32, line 3 and again in the conclusion on p. 33, line 14. Consequently, targeting of the downstream targets of HIF,

particularly GLUT and HK could provide more specific targets with less side effects, as outlined and described on p. 12 for GLUT and p. 14 and 15 for HK, respectively. This proposal arises from the observations of the authors that GLUT and HK constitute potent regulatory points in the control of glycolytic flux in cancer cells. Hence, targeting these two sites would be predicted to have strong effects inhibiting glycolysis in cancer cells. This was discussed on p. 14 and 16? with two examples of drugs, 3-BrPyr and 2DOG that have been shown as potent glycolytic inhibitors.

Response to reviewer 2

1, 2, 6. These observations were corrected.

3. 2-DOG. The question on 2-DOG's primary effect was further elaborated on p. 16.

4. PYK-M. Interaction of oncogenes with this isoform induces the transition of tetramers to dimers. This was stated in the original version on p. 24, line 10. An explanation on why the dimer prevalence in cancer cells does not affect glycolysis was also added (p. 25, 3rd paragraph). Hard data on intermediary metabolite accumulation is still missing.

5. The Sonveaux et al reference was added (p. 29, 2nd paragraph) as suggested, and the associated text was slightly modified.

Response to reviewer 3

We consider to be inappropriate the point made by this reviewer about taking exception to the section on HIF-1 as a target being poorly elaborated. This section follows as a logical conclusion to the review and possible lead candidate for novel anti-cancer therapies aimed at targeting the subject of the review. Thus, we emphasize that it is NOT "at odds with the rest of the manuscript" but provides a purposeful flow to the logic addressed here. Unfortunately, there has not been significant development in the subject of targeting HIF yet, although some interesting initial results have been obtained with the manassantins as addressed on p. 32. Hence, this section is relatively short, but still remains highly pertinent to the themes developed in the review.

Again minor comments and typographical errors corrected.

Half life of HIF-1α under hypoxia. Values were checked and confirmed (p. 5, line 4).

Topotecan reference was not missing – Ref. 157.

2.1.1 Comentarios sobre el manuscrito No. 1

Este primer manuscrito nació de una idea que surgió al leer sobre los efectos del HIF-1α en el metabolismo de la glucosa en células tumorales. Una primera versión de este trabajo la publiqué como autor único en la Revista de Educación Bioquímica de la Facultad de Medicina de la UNAM (REB 2009, 28: 41-51) algunos meses antes.

En este manuscrito se analiza el papel que juega HIF-1α en la regulación de la glucólisis en las células tumorales, así como las ventajas que ofrece en estas células la expresión de isoformas diferentes de las enzimas (HKI, HKII, PFK-L, ALD-A, ALD-C, PGK1, ENO-α, PYK-M2, LDH-A y PFKFB-3) y transportadores (GLUT1 y GLUT3) glucolíticos inducida por este factor de transcripción. De este análisis concluimos que la expresión de HIF-1α facilita el desarrollo tumoral porque incrementa la glucólisis tumoral al promover la expresión de isoformas de las enzimas que tienen una menor afinidad por sus productos (ALD-A, ALD-C, MTC4) y una menor sensibilidad a sus inhibidores fisiológicos (PFK-L y PYK-M2), lo cual promueve el flujo hacia lactato y ATP. Además, algunas de estas enzimas al mantener funciones distintas contribuyen en la regulación de la transcripción (LDH-A), en la inhibición de la apoptosis (HKII) y en mediar la migración celular favoreciendo la metástasis (ENO-α).

Posteriormente, para publicar este manuscrito en la revista Mini Reviews in Medicinal Chemistry se incorporó información sobre inhibidores de HIF-1α y de las enzimas de la glucólisis, así como información sobre la regulación que ejerce HIF-1α sobre enzimas mitocondriales (piruvato deshidrogenasa cinasa y citocromo c oxidasa) que pueden modificar el funcionamiento de la mitocondria. Con base en la discusión de esta información concluimos en este trabajo que el HIF-1α, al tener la capacidad de

regular el metabolismo energético en las células tumorales, podría ser un blanco idóneo para el tratamiento del cáncer, aunque en paralelo sería necesario reducir específicamente al GLUT y a la HK, proteínas que controlan la glucólisis en células tumorales.

2.2 Genes supresores de tumores y oncogenes

Es interesante remarcar que aquellos genes (genes supresores de tumores y oncogenes) que conducen al desarrollo tumoral también están involucrados en el incremento de la glucólisis.

2.2.1 PTEN (Phosphatase and tensin homolog deleted on chromosome ten)

PTEN es una fosfatasa que específicamente remueve el fosfato en posición 3' del anillo de inositol de los fosfoinositidos. Como consecuencia reduce su actividad Akt/PKB y las PDK´s (1 y 2) disminuyendo la fosforilación de sustratos involucrados en el crecimiento y la supervivencia celular. En las células tumorales, la activación de esta vía se produce por mutaciones que inhiben la actividad de PTEN, las cuales son muy comunes en algunos tumores (Jones y Thompson, 2009; Robey y Hay, 2009).

El incremento en la glucólisis inducido por esta cascada de señalización se debe a que la activación de Akt promueve la expresión de varios transportadores de glucosa (GLUT1, GLUT2 y GLUT4) así como su translocación a la membrana plasmática e induce la asociación de la HKII a la membrana externa mitocondrial. Además, indirectamente activa la fosfofructocinasa tipo 1 (PFK-1) al activar por fosforilación directa a la fosfofrutocinasa tipo 2 (PFK2), cuyo producto es la fructosa -2,6- bisfosfato (F26BP), potente activador de la PFK-1. Al mismo tiempo, Akt evita la supresión de la transcripción de los genes glucolíticos al inhibir al factor de transcripción FoxO.

Finalmente con la activación de mTORC1, Akt incrementa la presencia de HIF-1α el cual, como ya se documentó en la sección anterior (y en el primer manuscrito publicado), es el principal factor de transcripción que regula la expresión de la mayoría de las enzimas y transportadores de la glucólisis (Yeung et al., 2008; Robey y Hay, 2009; Marin 2009).

2.2.2 p53

La proteína *p53* es un factor transcripcional inducido por estrés y encargado de mantener la estabilidad genética en la célula al modular la proliferación celular. Es importante señalar que en un gran número de tumores humanos esta proteína se encuentra inactiva por presentar mutaciones (Jones y Thompson, 2009; Olovnikov et al., 2009).

p53 inhibe la glucólisis a diversos niveles, reprime la transcripción de los genes de algunos transportadores de glucosa (GLUT1 y GLUT4) al unirse directamente al DNA inhibiendo a sus promotores; induce la ubiquitinación y la degradación de la fosfoglicerato mutasa (PGAM); y reduce la concentración de F2,6BP al inducir a la enzima *TIGAR* (*TP53-induced glycolysis and apoptosis regulator*) que es una isoforma especial de PFK-2 con actividad predominante de bisfosfatasa que convierte a la F2,6BP (potente activador de la PFK-1) en F6P, con lo cual se reduce la actividad de la PFK-1. Por lo tanto, la perdida de *p53* puede inducir un incremento en la glucólisis (Yeung et al., 2008; Jones y Thompson, 2009; Olovnikov et al., 2009).

2.2.3 c-Myc

c-Myc se transcribe activamente en diversos tipos de cáncer (linfomas de Burkitt), su producto, la proteína c-Myc, participa en la regulación de la apoptosis y de la

proliferación y diferenciación celular. c-Myc es un factor de transcripción que forma heterodímeros con la proteína MAX; estos heterodímeros se unen a sus genes blanco en la secuencia consenso 5´-CACGTG-3´ (Dang y Semenza, 1999). Diversos reportes indican que la activación de c-*Myc* altera el metabolismo de la glucosa, promoviendo el incremento de la glucólisis al aumentar la transcripción de varias enzimas (GLUT1, HPI, PFK, GAPDH, PGAM, ENO y LDH-A) (Shim et al. 1997; Osthus et al. 2000).

Otros oncogenes como *H-ras* y *src* pueden estimular la glucólisis indirectamente al estabilizar al HIF-1α (Kim y Dang, 2006).

2.3 Cambios en los mecanismos de regulación de la hexocinasa y de la fosfofructocinasa tipo 1.

Diversos grupos han descrito que en células no tumorales de mamífero (eritrocito humano, músculo de ratón y corazón de rata) el control del flujo de la glucólisis lo mantienen principalmente la hexocinasa (HK) y la fosfofructocinasa tipo 1 (PFK-1) (Rapoport et al., 1974; Kashiwaya et al., 1994; Jannaschk et al., 1999). El control que ejercen estas enzimas oscila alrededor del 70 y 30%, respectivamente (Rapoport et al., 1974; Kashiwaya et al., 1994; Jannaschk et al., 1999). En un estudio en corazón se señala que también el transportador de glucosa puede contribuir significativamente al control de la glucólisis (Kashiwaya et al., 1994).

2.3.1 Hexocinasa (HK)

La HK cataliza la reacción de fosforilación de la glucosa (Figura 1); existen cuatro isoenzimas (HKI, HKII, HKIII y HKIV), siendo la glucocinasa (HKIV) la única que

no es inhibida por su producto la glucosa 6-fosfato (G6P), mientras que las restantes mantienen constantes de inhibición (*Ki*) que oscilan entre 20 y 100 μM (Wilson, 2003).

En las células tumorales, la actividad de esta enzima, y predominantemente de la isoforma HKII, se llega a incrementar entre 5 y 500 veces en diversas líneas tumorales de rata (hepatomas de Morris, AS-30D, Novikoff, Erhlich-Lettre, glioma C6, células ovales de hígado, carcinoma de tiroides), de humano (MIA, adenocarcinoma de páncreas; K562, leucemia; LoVoD, carcinoma de colon), y en diversos tipos de tumores humanos (pulmón, mama, colon, recto) (Shonk et al., 1964; Kosow y Rose, 1968; Parry y Pedersen, 1983; Nakashima et al., 1988; Smith, 2000; Pedersen et al., 2002; Stubbs et al., 2003). La HKII se llega a encontrar unida a la membrana externa mitocondrial, lo que de acuerdo con varios autores permite que sea menos sensible a la inhibición por su producto la G6P (Bustamante et al., 1977; Nakashima et al., 1986; Widjojoatmadjo et al., 1990; Marín-Hernández et al., 2006).

2.3.2 Fosfofructocinasa tipo 1 (PFK-1)

La reacción que cataliza la PFK-1 produce fructosa 1, 6 bifosfato (F1,6BP) por medio de la fosforilación de la fructosa 6-fosfato (F6P) (Figura 1). Esta enzima se inhibe por el ATP, citrato y H^+, y se activa fuertemente por la fructosa 2,6 bisfosfato (F2,6BP), el AMP y Pi. De esta enzima se conocen tres isoformas (músculo M, plaqueta C o P e hígado L), las cuales difieren en su sensibilidad a los activadores e inhibidores y tienen pesos moleculares ligeramente diferentes.

En las células tumorales la PFK-1 incrementa su actividad hasta en 5 veces en algunos tumores y leucemias humanas (Vora et al., 1985; El-Bacha et al., 2003). En diversos modelos tumorales (carcinoma de tiroides, leucemia y gliomas) se ha

observado que la PFK-1 muestra entre 5 y 300 veces mayor sensibilidad por su activador la F2,6BP (Oskam et al., 1985; Colomer et al., 1987; Staal et al., 1987) y una menor sensibilidad al efecto inhibitorio inducido por el ATP y el citrato entre 1 y7 veces, respectivamente (Meldolesi et al., 1976; Oskam et al., 1985; Staal et al., 1987). Las diferencias observadas se han atribuido a la expresión preferencial de las isoformas C y L sobre la M (Oskam et al., 1985; Vora et al., 1985; Staal et al., 1987). Sin embargo, es sorprendente descubrir que no hay datos que apoyen esta última explicación, en particular porque la caracterización cinética de las isoenzimas de la PFK-1 en tejidos sanos indican que la isoforma M es la que tiene una mayor sensibilidad por la F2,6BP y se inhibe en menor proporción por el ATP y el citrato (Vora et al., 1985[b]; Dunaway et al., 1988).

Además, en células cancerosas existe un aumento significativo en la concentración de la F2,6BP debido a la expresión de una isoforma de la enzima bifuncional fosfofructocinasa tipo 2 (PFKB-3), que tiene la característica de mantener una elevada actividad de cinasa sobre la actividad de fosfatasa (es decir predomina la síntesis de F2,6BP sobre su degradación) (Yalsin et al., 2009). El que esta enzima mantenga esta elevada actividad de cinasa, de acuerdo a datos cristalográficos, se debe a que algunos residuos de su extremo N-terminal bloquean el sitio catalítico de fosfatasa. Además con respecto al resto de las isoformas, ésta presenta diferencias en las secuencias de unión del ATP y de la F6P que al parecer facilitan su unión. Asimismo, el dominio C-terminal que en el resto de las isoformas bloquea el sitio de cinasa, en esta enzima es flexible y no lo bloquea (Yalsin et al., 2009).

Como se sabe, la PFK-1 participa en el conocido efecto Pasteur, que consiste en la inhibición de esta enzima por algunos intermediarios mitocondriales como el citrato y el ATP que se producen activamente durante aerobiosis y por lo tanto la PFK-1 se inhibe y la glucólisis disminuye. Sin embargo, como en las células tumorales la concentración de F2,6BP se mantiene elevada, este activador bloquea el efecto inhibitorio del ATP, el citrato y el H^+ provocando que disminuya el efecto Pasteur (Eigenbrodt et al., 1985).

Capítulo 3. La glucólisis como un blanco terapéutico

3.1 La glucólisis como un blanco terapéutico en el tratamiento del cáncer

Como el incremento en la glucólisis es una de las alteraciones metabólicas que se mantiene en la mayoría de las células tumorales y está relacionada con resistencia a la quimioterapia y a la radioterapia (Fanciulli et al., 2000; Maschek et al., 2004; Xu et al., 2005; Lee et al., 2007), diversos grupos de investigación consideran que la inhibición de la glucólisis es una opción terapéutica (Pelicano, 2006), dado que podría disminuir el crecimiento de los tumores e incrementar la eficacia de la quimioterapia y la radioterapia. Aunque se propone inhibir, individualmente, a diversas enzimas (HKII, PFKFB3, GAPDH, LDH-A) o transportadores (GLUT1 and MCT) (Pedersen et al., 2002, Pelicano et al., 2006; Kumagai et al., 2008; Bartrons et al., 2007; Evans et al., 2008; Clem et al., 2008) de esta vía metabólica, no se ha determinado previamente el control que ejercen sobre la glucólisis. Para que la inhibición de la glucólisis sea efectiva, se debe considerar inhibir a las enzimas que controlan a esta vía ya que sólo reduciendo su actividad en una baja proporción, el flujo se reducirá drásticamente y no se necesitarán altas concentraciones del inhibidor.

Por lo tanto en esta tesis se consideró que como la HK y la PFK-1 presentan cambios en sus mecanismos de regulación en las células tumorales, era difícil suponer que la distribución del control de la glucólisis en las células tumorales fuera similar a aquella encontrada en las células normales. Por lo tanto, en este trabajo se determinó la distribución de control en células tumorales aplicando el análisis de control metabólico, para poder establecer cuáles serían las enzimas o transportadores que podrían ser considerados blancos terapéuticos.

3.2 Análisis de control metabólico

El análisis de control metabólico permite identificar a las enzimas que controlan a una vía metabólica, al determinar cuantitativamente el grado de control que ejercen cada una de ellas sobre el flujo de una vía metabólica o sobre la concentración de metabolitos. Para ello es necesario determinar la estructura de control, que está constituída por el coeficiente de control de flujo, por el coeficiente de control de concentración y por los coeficientes de elasticidad. El coeficiente de control de flujo indica el grado de control que ejerce una enzima sobre el flujo; en tanto que el coeficiente de control de concentración es el grado de control que ejerce una enzima sobre la concentración de un metabolito. Ambos coeficientes son propiedades de la vía metabólica y están determinados por los coeficientes de elasticidad, que se definen como la habilidad que tiene una enzima de variar su actividad al cambio en la concentración de alguno de sus ligandos (sustrato o producto).

El coeficiente de control de flujo se define como:

$$C_{vi}^{J} = \frac{dJ}{dvi} \bullet \frac{vi_0}{J_0}$$

la variación en el flujo (*J*) cuando se hace un cambio infinitesimal en la concentración o en la velocidad de una enzima (*vi*). Así que cuando un pequeño cambio en la velocidad de una enzima o transportador induce una variación proporcional en el flujo, la enzima ejerce un control elevado; pero si la variación en la actividad de la enzima no modifica el flujo, esta enzima no ejerce un control significativo (Fell, 1997; Moreno-Sánchez et al., 2008). Para obtener los valores de C^{J}_{vi} normalizados y adimencionales es necesario multiplicar por el factor escalar (vi_0 / J_0) que es la relación entre los valores iniciales de velocidad y flujo.

Para poder determinar el coeficiente de control de flujo de una enzima son necesarias pequeñas variaciones en su actividad, sin alterar el resto de la vía metabólica, midiendo los cambios en el flujo. Varias estrategias experimentales se han desarrollado para poder determinar el coeficiente de control de una enzima, de las cuales en este trabajo se emplearon el análisis de elasticidades y modelado matemático (*in silico* biology).

3.2.1 Análisis de elasticidades

El coeficiente de elasticidad (**ε**) se define como el cambio en la velocidad de una enzima o transportador cuando la concentración de uno de sus ligándos (sustrato, producto o activador) varía en una proporción infinitesimal. Los coeficientes de elasticidad son positivos para los metabolitos (sustratos y activadores) que incrementan la velocidad de una enzima o transportador y son negativos para los metabolitos que la disminuyen (productos e inhibidores) (Fell , 1997; Moreno-Sánchez et al., 2008).

Una enzima que tiene un coeficiente de elasticidad bajo no modifica su velocidad con el cambio en la concentración de sus ligandos y, por tanto, no modifica el flujo metabólico, lo que permite que mantenga un control alto sobre el flujo de la vía. En cambio una enzima con un coeficiente de elasticidad alto será muy sensible a los cambios en la concentración de sus ligandos, su actividad se ajustará a dichos cambios y, entonces, ejercerá un control bajo sobre el flujo. Esta relación inversa entre los coeficientes de elasticidad y los coeficientes de control se conoce como el teorema de conectividad (Fell, 1997; Moreno-Sánchez et al., 2008). Para simplificar el análisis teórico y experimental de una vía metabólica ésta se puede dividir en dos bloques, en

un bloque productor (E_P) y en un bloque consumidor (E_C) de un metabolito (m) (Fell, 1997; Moreno-Sánchez et al., 2008), quedando el teorema de conectividad como sigue:

$E_P \rightarrow m \rightarrow E_C$ $\qquad C_{EP}^{J}\varepsilon_m^{EP} + C_{EC}^{J}\varepsilon_m^{EC} = 0$

Para calcular los coeficientes de control es necesario determinar experimentalmente los coeficientes de elasticidad. Esto se puede lograr al variar la concentración del sustrato inicial (glucosa en el caso de la glucólisis) y de esta manera incrementar la concentración del metabolito de interés y el flujo (generación de láctico). Las concentraciones y los flujos son normalizados, considerando el punto de interés (que es la condición en la cual se quiere conocer la distribución de control) como el 100%. En nuestro caso el punto de interés fue 5 mM de glucosa (concentración fisiológica de glucosa en sangre). A partir de estos valores se obtiene la gráfica % metabolito vs % flujo (Figura 3.2.1) y se calcula la pendiente de la curva al punto de interés, que es el coeficiente de elasticidad del bloque consumidor (ε_m^{EC}). Finalmente, con el empleo de un inhibidor de alguna de las enzimas del bloque consumidor se determinan la concentración del metabolito y el flujo, y del gráfico se obtiene el coeficiente de elasticidad del bloque productor (ε_m^{EP}). Cabe señalar que los experimentos se tienen que realizar bajo condiciones de estado estacionario.

Los coeficientes de control son calculados a partir del teorema de conectividad, considerando que la suma de los coeficientes de control de una vía son igual a 1 ($C_P + C_c = 1$) (Fell, 1997; Moreno-Sánchez et al., 2008). Entonces tenemos que:

$$C_{EP}^{J} = \frac{\varepsilon_m^{C}}{\varepsilon_m^{C} - \varepsilon_m^{P}} \qquad C_{Ec}^{J} = -\frac{\varepsilon_m^{P}}{\varepsilon_m^{C} - \varepsilon_m^{P}}$$

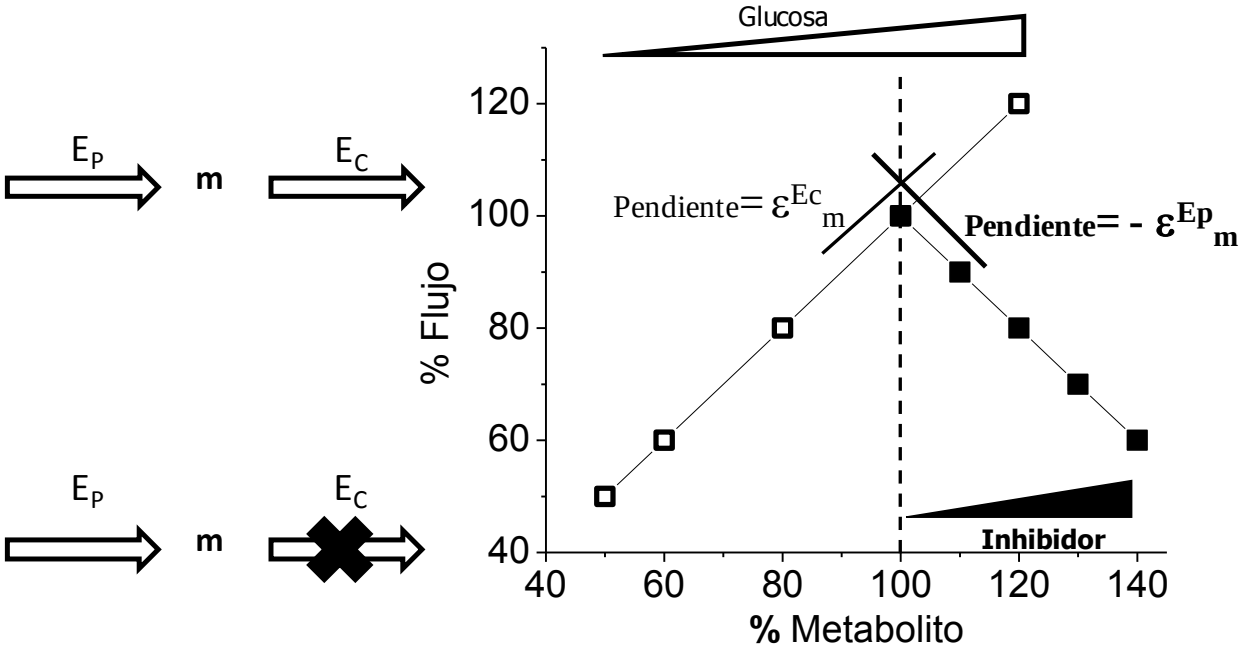

Figura 3.2.1 Gráfico para la obtención de los coeficientes de elasticidad. Una vía metabólica se puede dividir en dos bloques, en un bloque productor (Ep) y en un bloque consumidor (Ec) de un metabolito (m). Para determinar el coeficiente de elasticidad del Ec se tiene que variar la concentración del sustrato inicial de la vía (glucosa en el caso de la glucólisis) de esta manera se incrementa la concentración del metabolito de interés y el flujo. Mientras que para determinar el coeficiente de elasticidad del Ep se emplea un inhibidor de alguna de las enzimas del bloque consumidor con lo que se reduce el flujo y se incrementa la concentración del metabolito. Las concentraciones y los flujos son normalizados, considerando el punto de interés (que es la condición en la cual se quiere conocer la distribución de control) como el 100%. A partir de estos valores se obtiene la gráfica % metabolito vs % flujo y se calculan las pendientes de cada curva en el punto de interés, que corresponden al coeficiente de elasticidad del bloque consumidor ($\mathcal{E}_m^{E_C}$) y al coeficiente de elasticidad del bloque productor ($\mathcal{E}_m^{E_P}$).

A partir de aplicar el análisis a varios metabolitos de la vía es posible determinar los sitios que ejercen la mayor parte del control. El método tiene la ventaja de que no se necesitan inhibidores específicos de cada una de las enzimas o transportadores de la vía, ya que únicamente es necesario producir una variación en la concentración del metabolito de interés (Moreno-Sánchez et al., 2008). Sin embargo, para poder aplicar el análisis de elasticidades es necesario que los intermediarios de interés se encuentren

en concentraciones en las cuales se puedan detectar por los métodos analíticos convencionales.

El análisis de elasticidades se ha aplicado en diversos estudios entre los que se destacan los siguientes:

a) En hepatocitos se determinó que la piruvato carboxilasa (C^J_{Ei} = 0.83) controla la gluconeogénesis (a partir de lactato) estimulada por glucagon (Groen et al., 1986).
b) Posteriormente también en hepatocitos el grupo de Martin Brand estimó que la respiración dependiente de la oxidación de glucosa es controlada por el bloque productor de NADH entre el 15 y el 30% mientras que por el bloque consumidor de NADH entre un 70 y un 85% (Brown et al., 1990).
c) En el hepatoma AS-30D se determinó la distribución de control de la fosforilación oxidativa mostrándose que el complejo I y los sistemas consumidores de ATP mantienen un control significativo (C^J_{Ei}= 0.7) (Rodríguez-Enríquez et al., 2000).

Además de los estudios anteriores en células de mamíferos, este análisis se ha aplicado en diferentes vías metabólicas (fotosíntesis, la síntesis de serina y treonina la glucólisis y la síntesis de galactosa) en microorganismos como *E. coli* y levadura. (Moreno-Sánchez et al., 2008).

3.2.2 Modelos matemáticos de vías metabólicas (In silico biology)

Con la idea de hacer un análisis más profundo de una vía metabólica, se consideró el diseño de modelos matemáticos con los cuales se pudiera lograr reproducir su comportamiento en una gran variedad de condiciones experimentales (Poolman et al., 2004).

Existen dos tipos de modelado: modelado estructural y modelado cinético. El modelado estructural considera la estequiometría del conjunto de reacciones químicas que se llevan a cabo en la vía metabólica sin incluir datos cinéticos. En cambio, para el modelado cinético, además de la estequiometría es necesario conocer:

- la ecuación de velocidad con todos sus parámetros cinéticos (Km_S, Km_P, Vm_f, Vm_r, *Ki, Ka*),
- las constantes de equilibrio (Keq) (o en su caso las velocidades máximas en "forward" y "reverse" usando la ecuación de Haldane) de cada reacción,
- las concentraciones de intermediarios de la vía bajo una determinada condición de estado estacionario,
- un apropiado programa de computación en donde es construido el modelo. Entre los mas usados se encuentran "Copasi", "Gepasi", "Metamodel", "WinScamp", "Jarnac" and "PySCeS" (Poolman et al., 2004; Moreno-Sánchez et al., 2008).

El modelo cinético permite examinar y entender los mecanismos de regulación de una vía que no se logra con sólo atender a las propiedades cinéticas de cada enzima por separado (Moreno- Sánchez et al., 2008). Como el modelo se valida con datos experimentales, se asegura que las predicciones que arroja sobre la estructura de control de una vía metabólica sean confiables.

Capítulo 4

4.1 Planteamiento del problema

A nivel mundial y en nuestro país, el cáncer se encuentra entre las principales causas de muerte. Por tal motivo, diferentes grupos de trabajo han considerado que la glucólisis, por las ventajas que brinda a las células tumorales, puede ser un adecuado blanco terapéutico para reducir su crecimiento. Sin embargo, para lograr una reducción importante de la glucólisis es necesario inhibir a las enzimas que mantiene un control alto sobre el flujo de esta vía. El control de la vía en células normales recae principalmente en la HK y la PFK-1. Sin embargo, no se puede suponer que estas mismas enzimas sean los principales sitios de control de la glucólisis en células cancerosas, pues existe marcada sobre-expresión de ellas y presentan cambios en sus mecanismos de regulación. Por lo tanto, en este trabajo se consideró determinar, en una primera etapa, qué enzimas mantienen el control de la glucólisis tumoral y al mismo tiempo entender los mecanismos bioquímicos involucrados. Con la información generada se planteó una segunda atapa en la que se proponen los sitios más adecuados para intervención terapéutica y así estar en capacidad de diseñar nuevas estrategias antitumorales.

4.2 Hipótesis

El control de la glucólisis en las células tumorales de rápido crecimiento no recae totalmente en la hexocinasa y en la fosfofructocinasa tipo I por los cambios que presentan en su expresión y en sus mecanismos de regulación.

4.3 Objetivo general

Determinar la distribución de control en la glucólisis de células tumorales de rápido crecimiento.

4.4 Objetivos particulares

- Caracterización de la glucólisis en células tumorales (AS-30D y HeLa) y en células normales (hepatocitos de hígado de rata) a partir de la determinación de las concentraciones de intermediarios y de las actividades de cada una de las enzimas que forman parte de esta vía.
- Determinar la distribución de control en la glucólisis de las células AS-30D, al emplear el análisis de elasticidades.
- Construir modelos cinéticos de la glucólisis de las células AS-30D y HeLa.

Capítulo 5. Resultados

5.1 Distribución de control de la glucólisis en las células AS-30D

Como parte de nuestro primer objetivo, se realizó una caracterización de la glucólisis en modelos tumorales (hepatoma AS-30D de roedor y células HeLa de cáncer humano cérvico-uterino) y en un modelo de célula normal (hepatocitos de rata). Para ello determinamos las actividades de las enzimas, las concentraciones de algunos metabolitos y el flujo glucolítico en los tres modelos. Con base en los resultados de esta caracterización se consideró determinar la distribución de control en la glucólisis de las células AS-30D mediante el análisis de elasticidades, debido a la ausencia de inhibidores específicos para la glucólisis. Los resultados obtenidos fueron publicados en la revista ***FEBS Journal*** **2006, 273: 1975-1988.**

Factor de impacto 2009: 3.04
Citas:30

the FEBS Journal

Determining and understanding the control of glycolysis in fast-growth tumor cells

Flux control by an over-expressed but strongly product-inhibited hexokinase

Alvaro Marín-Hernández[1], Sara Rodríguez-Enríquez[1], Paola A. Vital-González[1], Fanny L. Flores-Rodríguez[1], Marina Macías-Silva[2], Marcela Sosa-Garrocho[2] and Rafael Moreno-Sánchez[1]

1 Instituto Nacional de Cardiología, Departamento de Bioquímica, Juan Badiano no. 1, Colonia Sección XVI, México, Mexico
2 Instituto de Fisiología Celular, Departamento de Biología Celular, Universidad Nacional Autónoma de México, Mexico

Keywords
elasticity coefficient; flux-control coefficient; hexokinase type 2; metabolic control analysis; phosphofructokinase type 1

Correspondence
R. Moreno-Sánchez, Instituto Nacional de Cardiología, Departamento de Bioquímica, Juan Badiano no. 1, Col. Sección XVI, Tlalpan, México 14080, Mexico
Fax: 52 55 55730926
Tel: 52 55 55732911 ext. 1422, 1298
E-mail: rafael.moreno@cardiologia.org.mx, morenosanchez@hotmail.com

(Received 17 October 2005, revised 21 February 2006, accepted 3 March 2006)

doi:10.1111/j.1742-4658.2006.05214.x

Control analysis of the glycolytic flux was carried out in two fast-growth tumor cell types of human and rodent origin (HeLa and AS-30D, respectively). Determination of the maximal velocity (V_{max}) of the 10 glycolytic enzymes from hexokinase to lactate dehydrogenase revealed that hexokinase (153–306 times) and phosphfructokinase-1 (PFK-1) (22–56 times) had higher over-expression in rat AS-30D hepatoma cells than in normal freshly isolated rat hepatocytes. Moreover, the steady-state concentrations of the glycolytic metabolites, particularly those of the products of hexokinase and PFK-1, were increased compared with hepatocytes. In HeLa cells, V_{max} values and metabolite concentrations for the 10 glycolytic enzyme were also significantly increased, but to a much lesser extent (6–9 times for both hexokinase and PFK-1). Elasticity-based analysis of the glycolytic flux in AS-30D cells showed that the block of enzymes producing Fru(1,6)P_2 (i.e. glucose transporter, hexokinase, hexosephosphate isomerase, PFK-1, and the Glc6P branches) exerted most of the flux control (70–75%), whereas the consuming block (from aldolase to lactate dehydrogenase) exhibited the remaining control. The Glc6P-producing block (glucose transporter and hexokinase) also showed high flux control (70%), which indicated low flux control by PFK-1. Kinetic analysis of PFK-1 showed low sensitivity towards its allosteric inhibitors citrate and ATP, at physiological concentrations of the activator Fru(2,6)P_2. On the other hand, hexokinase activity was strongly inhibited by high, but physiological, concentrations of Glc6P. Therefore, the enhanced glycolytic flux in fast-growth tumor cells was still controlled by an over-produced, but Glc6P-inhibited hexokinase.

It is well documented that fast-growth tumor cells have higher rates of lactate formation even under aerobic conditions than nontumorigenic cells. For instance, different types of hepatoma (Reuber, Morris, Dunings LC18) and fibrosarcoma 1929 exhibit rates of 0.2–2.7 μmol lactate·h^{-1}·(mg protein)$^{-1}$, whereas normal liver and kidney cells have rates of 0.05 μmol lactate·h^{-1}·(mg protein)$^{-1}$ [1,2].

The increase in tumor glycolysis has been associated with the activation of several oncogenes (*c-myc*, *ras* and *src*) or with the expression of the hypoxia-inducible factor (HIF-1α) in transformed human lymphoblastoid

Abbreviations
DHAP, dihydroxyacetone phosphate; G6PDH, glucose-6-phosphate dehydrogenase; GAPDH, glyceraldehyde-3-phosphate dehydrogenase; GluT, glucose transporter; LDH, lactate dehydrogenase; PFK-1, phosphofructokinase type 1.

and human U87 glioma [3,4]. As a result of oncogene activation and expression, the over-expression of several genes encoding eight glycolytic proteins, including the glucose transporter (GluT), takes place [5]. The over-expression of a plasma membrane H^+-ATPase in rat fibroblasts, to alter the cytosolic pH regulation, and presumably enhance ATP consumption, also promotes a sevenfold stimulation of glycolysis, in addition to inducing malignant transformation [6].

In comparison with hepatocytes, in several fast-growth tumor cells (AS-30D, Novikoff) there is over-expression of hexokinase-II [7,8], due to the activation of its own promoter, through a demethylation process [9] or through protein p53 activation (an abundant protein in fast-growth tumor cells) [10].

Binding of tumoral hexokinase-II to the mitochondrial outer membrane apparently changes its kinetic properties, compared with the cytosolic isoenzyme, i.e. mitochondrial hexokinase-II shows lower sensitivity ($\approx 30\%$) to inhibition by its product Glc6*P* [7]. The close vicinity of hexokinase-II to the adenine nucleotide translocase in tumor mitochondria ensures that mitochondrial ATP is preferentially used for hexose phosphorylation [8]. It has also been reported that hexokinase-II plays an important role in preventing apoptotic events, such as cytochrome *c* release in HeLa cells, by interfering with the binding of the pro-apoptotic protein Bax to the outer mitochondrial membrane [11].

In normal tissues, citrate and ATP are potent allosteric inhibitors of phosphofructokinase type 1 (PFK-1) [12], where it is mainly constituted by M subunits, but this does not occur when the predominant subunit is L or C [13]. The tumoral isoenzyme is less sensitive to the inhibitory effect of these two allosteric effectors [13,14]. In this regard, it has been observed that the subunit L or C content of tumor PFK-1 increases, whereas that of subunit M decreases, which explains the smaller effect of its negative modulators [15–17]. It has also been reported that the content of Fru(2,6)P_2 (a potent PFK-1 activator [12]) in HeLa cells, Ehrlich ascites cells and HT29 human colon adenocarcinoma is much higher than in normal hepatocytes [20–80 versus 6 pmol·(mg protein)$^{-1}$, respectively] [18–21]. These observations suggest that PKF-1 is highly active in tumors cells [13,20].

In mammalian nontumorigenic systems, such as human erythrocytes and rat perfused heart, glycolytic flux is mainly controlled by hexokinase (60–80%) and PFK-1 (20–30%) [22,23]. In tumor cells, an expected consequence of the over-expression of several glycolytic enzymes and glucose transporters, and kinetic changes in hexokinase and PFK-1, is a large modification of the regulatory mechanisms and fuctioning of the pathway. Hence, the assumption that control of the glycolytic flux in tumor cells is similar to that of normal cells is apparently not well supported. Therefore, to identify the flux-controlling sites of tumoral glycolysis, we firstly determined the V_{max} of each glycolytic enzyme from hexokinase to lactate dehydrogenase (LDH) in AS-30D and HeLa cells. Measurement of enzyme activity under V_{max} conditions ensures the determination of the content of active enzyme and allows the degree of over-expression compared with normal cells to be established. Secondly, we determined the steady-state concentrations of several intermediate metabolites to identify enzymes that may impose limitations on the glycolytic flux, although such inferences do not always hold, particularly for intermediates involved in more than two reactions.

To evaluate quantitatively flux control in tumoral glycolysis, we used the theory of the metabolic control analysis [24] by applying an elasticity analysis. This consists of the experimental determination of the sensitivity of segments of the pathway towards a common intermediate. Once we had identified the main sites of flux control, we performed experiments to determine which biochemical mechanisms are involved in establishing why some enzymes exert significant control and others do not.

Results

Maximal activities of glycolytic enzymes in hepatocytes and fast-growth tumor cells

In normal freshly isolated hepatocytes, the enzymes with lower activity (and hence less content) were hexokinase < PFK-1 < aldolase, enolase (Table 1). This activity pattern is in agreement with that found in hepatocytes by other authors [7,15]. In whole liver, the activities of all glycolytic enzymes were very similar, except for pyruvate kinase, which was 3 times lower than that obtained in isolated hepatocytes (data not shown). In an attempt to establish a proliferating, non-tumorigenic cell system, to make a more rigorous comparison with the tumor cell lines used in this work, we also isolated hepatocytes from regenerating rat liver; organ regeneration was induced by prior treatment with CCl_4 [0.39 g·(kg body weight)$^{-1}$] for 12 or 24 h. In two different cell preparations, the V_{max} values of the glycolytic enzymes were essentially identical with those found for normal isolated hepatocytes (data not shown).

In rat AS-30D hepatoma cells, the enzymes with lower activity were hexokinase, PFK-1 and aldolase, a

Table 1. Maximal activity of glycolytic enzymes in hepatocytes and tumor cells. AS-30D, HeLa and hepatocytes (65 mg protein·mL^{-1}) were incubated in lysis buffer as described in Experimental procedures. Activities of all enzymes were determined in the cytosolic-enriched fraction at 37 °C. Specific activities are expressed in U·(mg protein)$^{-1}$. The values shown represent the mean ± SD with the number of different preparations assayed in parentheses. HK, hexokinase; HPI, hexosephosphate isomerase; TPI, triosephosphate isomerase; GAPDH, glyceraldehyde-3-phosphate dehydrogenase; PGK, phosphoglycerate kinase; PGAM, phosphoglycerate mutase; PYK, pyruvate kinase; LDH, lactate dehydrogenase; G6PDH, glucose-6-phosphate dehydrogenase; α-GPDH, α-glycerophosphate dehydrogenase; PGM, phosphoglucomutase; ND, not detected.

Enzymes	Hepatocytes	AS-30D	AS-30D/ hepatocytes	HeLa
HK	0.003 ± 0.002 (3)	0.46 ± 0.1** (7)	153	0.02 ± 0.006†† (4)
HPI [a]	0.4 ± 0.05 (3)	1.6 ± 0.7* (4)	4	3.0 ± 1.7 (4)
PFK-1 [b]	0.01 ± 0.002 (3)	0.21 ± 0.1* (4)	22	0.09 ± 0.02 †(5)
Aldolase	0.09 ± 0.02 (3)	0.23 ± 0.07* (4)	2.7	0.2 ± 0.05 (5)
TPI [a]	15.6 ± 5.6 (3)	56 ± 15* (4)	3.6	42 ± 13 (3)
GAPDH	0.32 ± 0.07 (3)	1 ± 0.28* (3)	2.7	2 ± 0.74 (5)
GAPDH [a]	0.66 ± 0.23 (3)	0.9 (2)	1.4	2.5 ± 0.8 (5)
PGK	8.2 ± 5.8 (3)	27 ± 10* (4)	3.3	13 ± 6† (5)
PGAM	11 ± 2 (3)	20 ± 5* (4)	2.3	1.4 ± 1 (4)
Enolase	0.11 ± 0.03 (3)	0.51 ± 0.13* (3)	4.3	0.36 ± 0.15 (5)
PYK	0.8 ± 0.36 (3)	6.6 ± 1.5** (4)	8.1	3 ± 1.3 † (4)
LDH	4.4 ± 1.9 (3)	6.4 ± 3.7 (4)	1.5	1.7 ± 0.6 (3)
G6PDH	0.03 ± 0.003 (3)	0.05 ± 0.02 (3)	1.4	0.22 ± 0.08†† (5)
PGM [c]	0.37 (2)	0.21 ± 0.06 (5)	0.6	0.42 ± 0.13 (4)
α-GPDH [d]	0.11 (2)	0.002 ± 0.001 (3)	0.05	ND

*P < 0.05 versus hepatocytes, **P < 0.005 versus hepatocytes, †P < 0.05 versus AS-30D, ††P < 0.005 versus AS-30D. Student's t-test for nonpaired samples. [a] Activity in the reverse reaction. [b] Activity determined in the presence of 16–20 mM NH_4^+. [c] The PGM activity was determined in the absence of glucose-1,6- bisphosphate. [d] The reaction was started by adding DHAP.

pattern that also agrees with that reported for the same cells [7] and for other tumor cell types [25]. The AS-30D/hepatocyte activity ratio revealed that hexokinase and, to a lesser extent, PFK-1 were the enzymes that were most over-expressed in tumor cells; all other glycolytic enzymes, including glucose-6-phosphate dehydrogenase (G6PDH), were also over-expressed in AS-30D tumor cells (Table 1).

In HeLa cells, all glycolytic enzymes, except phosphoglycerate mutase, also exhibited a higher activity than that shown by hepatocytes. However, in these human tumor cells neither hexokinase nor PFK-1 were highly over-expressed as they were in rodent AS-30D cells. In HeLa cells, hexosephosphate isomerase, PFK-1, triosephosphate isomerase and pyruvate kinase, together with G6PDH, showed greater over-expression compared with hepatocytes (Table 1). V_{max} for phosphoglycerate mutase in HeLa cells was 14 and 8 times lower than that found in AS-30D cells and hepatocytes, respectively; such low phosphoglycerate mutase activity has also been observed by other authors [25]. Negligible α-glycerophosphate dehydrogenase activity was found in both tumor cell types. A similar observation has been described for the Morris hepatomas 3924A, 5123D, 7793 and 44 [26], which are fast or moderate-growth tumor lines [27].

Glycolytic flux and intermediary concentrations

As expected from the general increase in glycolytic enzymes, steady-state generation of lactate in the presence of 5 mM glucose was markedly higher in AS-30D and HeLa cells (9–13 times) than in hepatocytes (Table 2). In the absence of added glucose, the glycolytic flux diminished drastically in both tumor cell types, being negligible in AS-30D cells. The difference between the rates of lactate formation with and with-

Table 2. Glycolysis in hepatocytes and tumor cells. AS-30D and HeLa cells (15 mg protein·mL^{-1}) and hepatocytes (30 mg protein·mL^{-1}) were incubated in Krebs–Ringer medium as described in Experimental procedures. Under these conditions, the rate of lactate formation in AS-30D cells was constant after 2 min and up to 10 min from glucose addition (i.e. steady-state glycolysis). The intracellular concentration of Fru(1,6)P_2 was also invariant between the 2- and 10-min points, after the addition of glucose (data not shown). Glycolytic fluxes are expressed in nmol·min^{-1}·(mg cell protein)$^{-1}$. The values shown represent the mean ± SD with the number of different preparations assayed in parentheses. The negative flux value indicates lactate consumption.

Condition	Hepatocytes	AS-30D	HeLa
+ Glucose	2.4 ± 1.7 (6)	21 ± 9 (40)	32 ± 10 (8)
− Glucose	− 0.4 ± 1 (6)	− 2.2 ± 2.6 (17)*	7 ± 9 (6)

out added glucose indicates that net glycolytic flux depends on external glucose, which was 8–9 times higher in AS-30D and HeLa cells than in hepatocytes.

The elevated glycolytic flux in HeLa cells in the absence of added glucose was probably sustained by endogenous sources, i.e. glycogen degradation. The content of glycogen was apparently not depleted in HeLa cells by the 10 min preincubation at 37 °C. In contrast, the total dependence of the glycolytic flux on external glucose in AS-30D cells suggests depletion of glycogen induced by the 10 min preincubation at 37 °C. The glycolytic flux values reported in this work are in the same range as reported for other tumor cell types [2].

The steady-state concentrations of all glycolytic metabolites in AS-30D tumor cells also significantly increased, except for phosphoenolpyruvate and pyruvate (Table 3). In particular, Fru(1,6)P_2 increased 250 times and dihydroxyacetone phosphate (DHAP) 16.6 times. The cytosolic pyridine nucleotide redox state (NADH/NAD^+), estimated from the lactate/pyruvate ratio, was more reduced in AS-30D cells, a situation that favors flux through biosynthetic pathways. The concentration of ATP was also higher in AS-30D cells than in hepatocytes; however, the ATP/ADP ratio was similar (2.3 and 2.4). The latter values are similar to those previously reported [28] for normal organs such as rat heart (5.7) and liver (4.9), as well as mouse Erhlich ascites cells (2.3) and 3924A hepatoma cells (1.2).

Table 3. Steady-state concentrations (mM) of glycolytic intermediates in normal rat hepatocytes and hepatoma cells. See legend to Table 2 and Experimental procedures for experimental details. Values shown are the mean ± SD. The number of experiments is shown in parentheses. ND, not detected; NM, not measured; DHAP, dihydroxyacetone phosphate; G3P, glyceraldehyde 3-phosphate; PEP, phosphoenolpyruvate; Lac, lactate; Pyr, pyruvate.

Metabolite	Hepatocytes	AS-30D	HeLa
Glucose	NM	6.2 ± 1 (3)	NM
Glc6*P*	0.96 ± 0.16 (3)	5.3 ± 2.6**(23)	0.6 ± 0.16††(4)
Fru6*P*	0.4 ± 0.03 (3)	1.5 ± 0.7**(22)	0.22 ± 0.09†† (4)
Fru(1,6)P_2	0.1 ± 0.05 (3)	25 ± 7.6**(19)	0.29 ± 0.06†† (4)
DHAP	0.6 ± 0.1 (3)	10 ± 2.3**(14)	0.93 ± 0.07†† (3)
G3P	0.09 ± 0.01 (3)	0.9 ± 0.4*(7)	ND
PEP	0.1 (2)	0.1 ± 0.02 (3)	0.32 (2)
Pyr	1.6 ± 0.7 (3)	2.1 ± 1 (7)	8.5 ± 3.6†† (5)
Lac [a]	9.6 ± 1.3 (3)	27 ± 11* (3)	33 (2)
ATP	3.6 ± 0.24 (3)	5.6 ± 1.2* (9)	9.2 ± 1.9† (4)
ADP	1.6 ± 0.6 (4)	2.4 ± 0.7 (7)	2.7 ± 1.3 (3)
Lac/Pyr ratio	6.3	12.9	3.9

[a] L-Lactate was intracellularly located. *$P < 0.05$ versus Hepatocytes, **$P < 0.005$ versus Hepatocytes, †$P < 0.05$ versus AS-30D, ††$P < 0.005$ versus AS-30D.

In contrast with AS-30D cells, the steady-state concentrations of Glc6*P*, Fru6*P*, Fru(1,6)P_2 and DHAP in HeLa cells were similar to those observed in hepatocytes, whereas the ATP and pyruvate concentrations were 1.6 and 4 times higher than in AS-30D cells (Table 3).

Determination of flux control coefficients for glycolysis in hepatoma cells

Metabolic control analysis establishes how to determine quantitatively the degree of control (named flux control coefficient, C^J_{Ei}) that each enzyme Ei exerts over the metabolic flux J [24]. In the oxidative phosphorylation pathway, C^J_{Ei} values can be determined by titrating the flux with specific inhibitors [24,29,30]. However, there are no specific, permeable inhibitors for each glycolytic enzyme.

An alternative approach called elasticity analysis [31–34] consists of experimental determination of the sensitivity of enzyme blocks towards a common intermediate metabolite m. By applying the summation and connectivity theorems of metabolic control analysis (see Eqns 1 and 2 in Experimental procedures), the C^J_{Ei} values can be calculated. Variations in the steady-state activity of the enzyme blocks can be attained by adding different concentrations of the initial substrate or inhibitors of either block, which do not have to be specific for only one enzyme but they do have to inhibit only one block. The block of enzymes that generates the common intermediate is named the producer block, whereas the block of enzymes consuming that metabolite is named the consumer block.

For glycolysis, and other pathways, any metabolite may be used as the common intermediate that connects producer and consumer branches. However, to reach consistent results, it is more convenient to use, as common intermediates, metabolites that are present at relatively high concentrations and that are only connected to the specific pathway, such as Fru(1,6)P_2. Although other metabolites such as Glc6*P*, Fru6*P* and DHAP may be present at high concentrations, they are connected with other pathways (glycogen synthesis and degradation, pentose phosphate cycle, glycerol and triacylglycerol synthesis). However, this last group of metabolites may still be used in elasticity-based analysis as long as the flux through the other pathways is low (or it is assumed to be negligible) [33,35,36] or by actually determining the effect of the branching pathways on the main flux and on the concentration of the connecting metabolite [23].

To determine the elasticity coefficients of the consumer block for the common metabolite (ε^{Ei}_m), we

incubated hepatoma cells with different glucose concentrations (4–6 mM) or with the hexosephosphate isomerase inhibitor 2-deoxyglucose (0.5–10 mM), which induced variations in flux and in the steady-state concentrations of the metabolite. The elasticity of the producer block was determined by titrating flux with the LDH inhibitor, oxalate (0.5–2 mM), or the glyceraldehyde-3-phosphate dehydrogenase inhibitor, arsenite (5–100 μM). Thus, the glycolytic flux (measured as the rate of lactate formation) and the concentration of several intermediates [Glc6*P*, Fru6*P*, Fru(1,6)P_2 and DHAP] were determined under both conditions. The tangents to the curves, or the straight lines, taken at the reference, control points (100%) in the normalized plots of flux versus [metabolite] obtained with glucose and oxalate, or 2-deoxyglucose and arsenite, represent the elasticities towards the intermediate metabolite of the consumer and producer blocks, respectively.

We are aware that the experimental points in the flux versus [metabolite] plot should be fitted to a hyperbolic curve rather than to a straight line, as most of the glycolytic enzymes and transporters follow a Michaelis–Menten kinetic pattern; a near-linear relation between rate and substrate concentration might be attained when the product concentration varies concomitantly. However, the lack of sufficient experimental points near the reference, unaltered state may generate high, unrealistic slope values ($\gg$ 2) for the estimation of elasticity coefficients (Fig. 1) either by fitting to hyperbolic or linear equations. The definitions of the elasticity and flux control coefficients as well as the theorems of metabolic control analysis are based on differentials. However, it was not easy to produce small changes (and much less infinitesimal changes) of flux and metabolite concentration by using the experimental protocols described. In consequence, slope values were calculated with both approximations, nonlinear hyperbolic fitting and linear regression. In general, similar elasticity coefficients resulted from either approximation, although less dispersion was attained with the linear regression (see legend to Table 4 for values).

Titration of the glycolytic flux with exogenous glucose and oxalate (Fig. 1A), or with 2-deoxyglucose and arsenite (Fig. 1B), induced changes in flux and the Fru(1,6)P_2 concentration. Analysis of both segments showed that the Fru(1,6)P_2 consumer block (formed by enzymes from aldolase to LDH) showed a higher elasticity than the producer block (comprising GluT to PFK-1). In the first case (with glucose or 2-deoxyglucose), the slope had a positive value because Fru(1,6)P_2 is a substrate for the consumer block. On the other hand, with oxalate or arsenite titration, the slope had a negative value because Fru(1,6)P_2 is a product of the producer block, i.e. Fru(1,6)P_2 accumulation inhibits the producer activity.

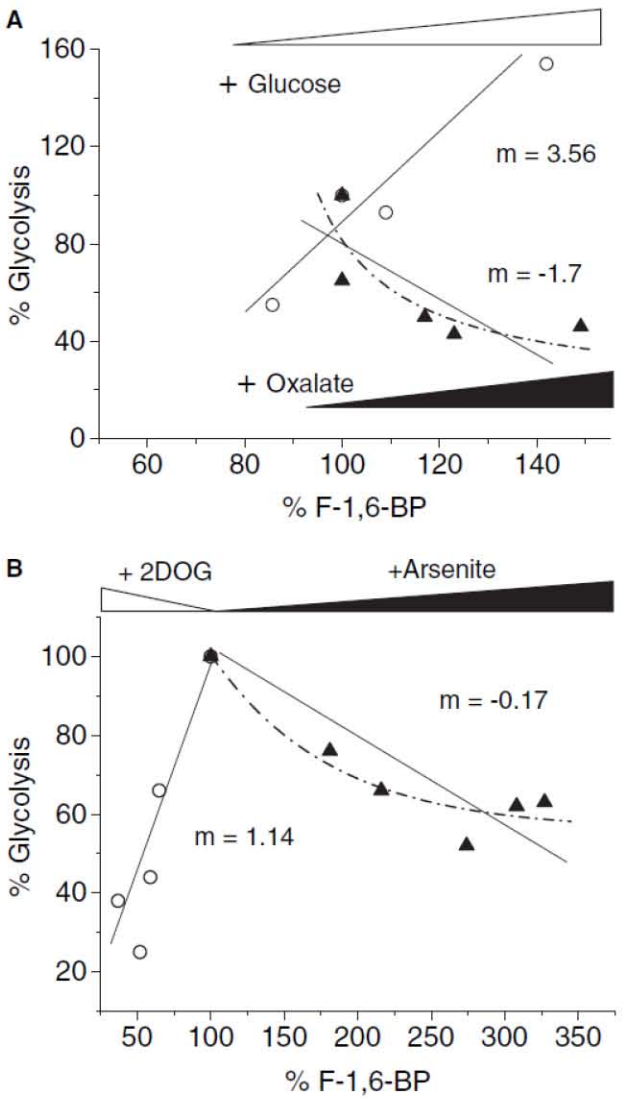

Fig. 1. Experimental determination of elasticity coefficients for glycolytic intermediates in tumor cells. AS-30D hepatoma cells (15 mg protein·mL^{-1}) were incubated in Krebs–Ringer medium at 37 °C. After 10 min, different concentrations of glucose (○, 4–6 mM) and oxalate (▲, 0.5–2 mM) in (A), or 2-deoxyglucose (○, 0.5–10 mM) and arsenite (▲, 5–100 μM) in (B), were added to the cell suspension. When a glycolytic inhibitor was added, glucose was kept constant at 5 mM. The hexokinase and PFK-1 activities, which are part of the Fru(1,6)P_2-producing block, were not affected by 10 mM oxalate or 1 mM arsenite (data not shown). Thus, the effect of these two inhibitors on flux was due to their interaction with enzymes of the Fru(1,6)P_2-consuming block, most likely LDH [66] (data not shown) and glyceraldehyde-3-phosphate dehydrogenase [67]. The values of the straight lines, or the tangents to the curves, at 100% Fru(1,6)P_2 (m), which are the elasticity coefficients in these normalized plots, are shown on the traces.

Table 4. Control (C) and elasticity (ε) coefficients values of AS-30D hepatoma cells. Control coefficients were calculated from elasticity coefficients, derived from data such as those shown in Fig. 1, and applying summation and connectivity theorems (Eqns 1 and 2; see Experimental procedures). ε^{P}_{m}, elasticity of producer block; ε^{C}_{m}, elasticity of consumer block; C^{J}_{p}, control coefficient of producer block; C^{J}_{c}, control coefficient of consumer block. All the elasticity coefficients shown in the table were calculated by using slope values derived from linear regression, although similar values were attained by nonlinear regression. For instance, the nonlinear regression for the titrations with 2-deoxyglucose and arsenite gave ε^{C}_{FBP} and ε^{P}_{FBP} of 1.99 ± 0.79 and −1.5 ± 1.6, which yielded the C^{J}_{c} and C^{J}_{P} of 0.39 ± 0.24 and 0.61 ± 0.24, respectively. The number of experiments is shown in parentheses, and values are mean ± SD. DHAP, Dihydroxyacetone phosphate.

Metabolite	ε^{C}_{m}	C^{J}_{C}	ε^{P}_{m}	C^{J}_{P}
	+ Glucose		+ Oxalate	
Glc6*P*	2.1 ± 1.7 (6)	0.29 ± 0.17 (3)	− 0.86 ± 0.41 (3)	0.71 ± 0.17 (3)
Fru6*P*	1.2 ± 0.45 (4)	0.31 ± 0.14 (3)	− 0.67 ± 0.43 (3)	0.69 ± 0.14 (3)
Fru(1,6)P_2	2.2 ± 0.95 (5)	0.44 ± 0.08 (5)	− 1.35 ± 0.66 (6)	0.62 ± 0.08 (5)
DHAP	1.27 ± 0.47 (5)	0.49 ± 0.18 (5)	− 1.5 ± 1 (5)	0.51 ± 0.18 (5)
	+ 2-Deoxyglucose		+ Arsenite	
Fru(1,6)P_2	0.93 ± 0.2 (3)	0.24 ± 0.06 (3)	− 0.25 ± 0.1 (3)	0.75 ± 0.05 (3)
	+ Glucose		+ Arsenite	
DHAP	1.18 ± 0.2 (3)	0.37 ± 0.15 (3)	− 0.5 ± 0.1 (3)	0.63 ± 0.14 (3)

It is worth emphasizing that, owing to the multitude of variables involved in determining flux and intermediary concentrations, which have to be kept constant during the experimental determination of elasticities towards one metabolite, the dispersion of the experimental points can be considerable in some cell preparations. This can be appreciated in Fig. 1 and in the values shown in Table 4. Nonetheless, it is possible to reach relevant conclusions about which steps exert significant flux control of glycolysis and which steps have low or negligible control (Table 5).

The elasticity coefficients, estimated from experiments such as those shown in Fig. 1, are summarized in Table 4. The flux control coefficients derived from the elasticity coefficients are also shown. These data clearly established that the main control of the glycolytic flux in AS-30D cells resides in the upstream part of the pathway. The experiments with glucose and oxalate show a high value for the flux control coefficient of the Glc6*P* producer block [$C^{J}_{P(Glc6P)}$], which indicates that GluT, hexokinase and perhaps the degradation of glycogen, steps that lead to the formation of Glc6*P*, were the sites that exerted most of the flux control. In turn, the experiments with 2-deoxyglucose and arsenite revealed that the producer block of Fru(1,6)P_2 exerted most of the control, which indicates that flux control was mainly located in GluT, hexokinase and glucogenolysis together with hexosephosphate isomerase and PFK-1.

The same conclusion may be drawn from the high $C^{J}_{P(Fru6P)}$ value (Table 4). However, the glycolytic flux was negligible in the absence of added glucose (Table 2), indicating that Glc6*P* and Fru6*P* formation from glycogen degradation was not significant in AS-30D cells. Hence, from the difference between the values of $C^{J}_{P(Glc6P)}$ and $C^{J}_{P(Fru6P)}$, which were determined under the same experimental conditions with glucose and oxalate, it was possible to calculate a specific flux control value of −0.02 for the Glc6*P* branches, pentose phosphate cycle and glycogen synthesis (Table 4).

Because of the less than perfect match of C^{J}_{C} and C^{J}_{P} values estimated from three different experimental protocols (Table 4), it was difficult to obtain a reliable flux control coefficient for the DHAP consumer branch. With 2-deoxyglucose and arsenite, the $C^{J}_{P(Fru(1,6)P2)}$ value of 0.75 suggests that the rest of the pathway (from aldolase to LDH) exerts a flux control of 0.25 (Table 5). However, the $C^{J}_{C(DHAP)}$ values with glucose and oxalate or with glucose and arsenite were 0.49 and 0.37, respectively, which revealed some discrepancy with the 2-deoxyglucose and arsenite protocol. If the total summation of C^{J}_{Ei} values was higher than 1.0, then branching in the middle and lower segments of glycolysis might be significant, bringing about negative flux control coefficients.

Table 5. Distribution of control of glycolysis in AS-30D cells. GluT, Glucose transporter; HK, hexokinase; HPI, hexosephosphate isomerase; TPI, triosephosphate isomerase; GAPDH, glyceraldehyde-3-phosphate dehydrogenase; PGAM, phosphoglycerate mutase; PYK, pyruvate kinase; LDH, lactate dehydrogenase.

Enzymes or branches	C^{J}_{Ei}
GluT + HK	0.71
Pentose phosphate cycle + HPI + glycogen synthesis	−0.02
PFK-1	0.06
Aldolase, TPI, GAPDH, PGAM, enolase, PYK, LDH, Pyr branches, ATP demand	0.25
$\Sigma C^{J(glycolysis)}_{Ei}$ =	1.00

The flux control coefficient of PFK-1 (Table 5) was estimated from the $C^{J}_{P(Fru(1,6)P2)}$ value attained with 2-deoxyglucose and arsenite minus the $C^{J}_{P(Glc6P)}$ value attained with external glucose and oxalate (Table 4). Only positive differences between C^{J}_{P} values are to be taken into account for elucidating flux control for specific enzymes. With negative differences [for instance, with $C^{J}_{P(Fru(1,6)P2)}$ minus $C^{J}_{P(Fru6P)}$ both attained with glucose and oxalate], the explanation is that there is a pathway branch at the measured metabolite concentration, or that the experimental dispersion masks small differences, or that indeed there is no difference between the enzyme blocks analyzed.

Kinetic analysis of tumoral hexokinase and PFK-1

To understand why hexokinase retained a significant degree of control on glycolytic flux, despite its high over-expression, and why PFK-1 control became negligible, the kinetic properties of the two enzymes were analyzed in cell extracts. The affinity of hexokinase for glucose and ATP in both the cytosolic and mitochondrial fractions (Table 6) was in the same range as reported by Wilson [37] for hexokinase from nontumorigenic mammalian tissues. Hexokinase was equally distributed between the cytosol and mitochondria in AS-30D hepatoma cells. Both hexokinase isoenzymes, cytosolic and mitochondrial, were 81–93% inhibited by 1 mM Glc6*P* (Fig. 2A).

The PFK-1 in the cytosolic-enriched fraction from AS-30D cells exhibited K_m and $K_{0.5}$ values for ATP and Fru6*P* (Table 6) similar to those reported for PFK-1 from other tumor cell lines [13,15]. In the absence of added effectors, the PFK-1 kinetic pattern was sigmoidal with respect to Fru6*P* [although $\approx$8–12 mM $(NH_4)_2SO_4$ coming from the coupling enzymes was present], and hyperbolic with respect to low concentrations of ATP (0.01–1 mM). At high concentrations (> 1 mM), ATP was inhibitory for PFK-1 activity. Citrate was also inhibitory at relatively low (< 1 mM) Fru6*P* concentrations. However, when 1.5 mM Fru6*P* (physiological concentration) or higher concentrations were used, citrate was innocuous, even at concentrations as high as 10 mM (data not shown), in the presence of 8–10 mM $(NH_4)_2SO_4$. Fru(2,6)P_2 was the most potent activator of tumoral PFK-1, followed by AMP and NH_4^+ (Table 6).

The mean ± SD intracellular concentrations of AMP and citrate determined under glycolytic steady-state conditions in AS-30D cells were 3.3 ± 1.4

Table 6. Tumoral hexokinase and PFK-1 kinetic parameters. The activities of hexokinase and PFK-1 were determined at 37 °C as described in Experimental procedures. For hexokinase, the K_m value for ATP was determined in the presence of 5 mM glucose, whereas that for glucose was determined with 10 mM ATP. For PFK-1, the K_m value for ATP was determined in the presence of 10 mM Fru6*P*, whereas the $K_{0.5}$ value for Fru6*P* was determined with 0.25 mM ATP. The ammonium concentration in the assay mixture, proceeding from the coupling enzymes, was 16–20 mM. The $K_{0.5}$ values for NH_4^+, AMP and Fru(2,6)P_2 were determined in the presence of 2 mM Fru6*P* and 0.8 mM ATP, and with lyophilized coupling enzymes (i.e. in the absence of contaminating ammonium). The number of independent experiments is shown in parentheses. Units of K_m and $K_{0.5}$ are μM; V_{max}, U·(mg protein)$^{-1}$.

	ATP		Glucose	
Hexokinase	K_m	V_{max}	K_m	V_{max}
Mitochondrial	696 ± 180 (3)	1.96 ± 0.4 (3)	146 ± 12 (3)	1.65 ± 0.18 (3)
Cytosolic	990 ± 50 (3)	0.52 ± 0.1 (3)	180 ± 40 (3)	0.44 ± 0.1 (3)
Type I [a]	500		30	
Type II [a]	700		300	
Type III [a]	1000		3	
	ATP		Fru6*P*	
PFK-1	K_m	V_{max}	$K_{0.5}$	V_{max}
	14 ± 2 (3)	0.2 ± 0.09 (3)	200 (2)	0.2 (2)
	NH_4^+		AMP	
	$K_{0.5}$	V_{max}	$K_{0.5}$	V_{max}
	1400 ± 800 (3)	0. 51 ± 0.2 (3)	100 ± 50 (4)	0.58 ± 0.14(4)
	Fru(2,6)P_2			
	$K_{0.5}$	V_{max}		
	0.96 ± 0.3 (3)	0.52 ± 0.16 (3)		

[a] Values taken from [37].

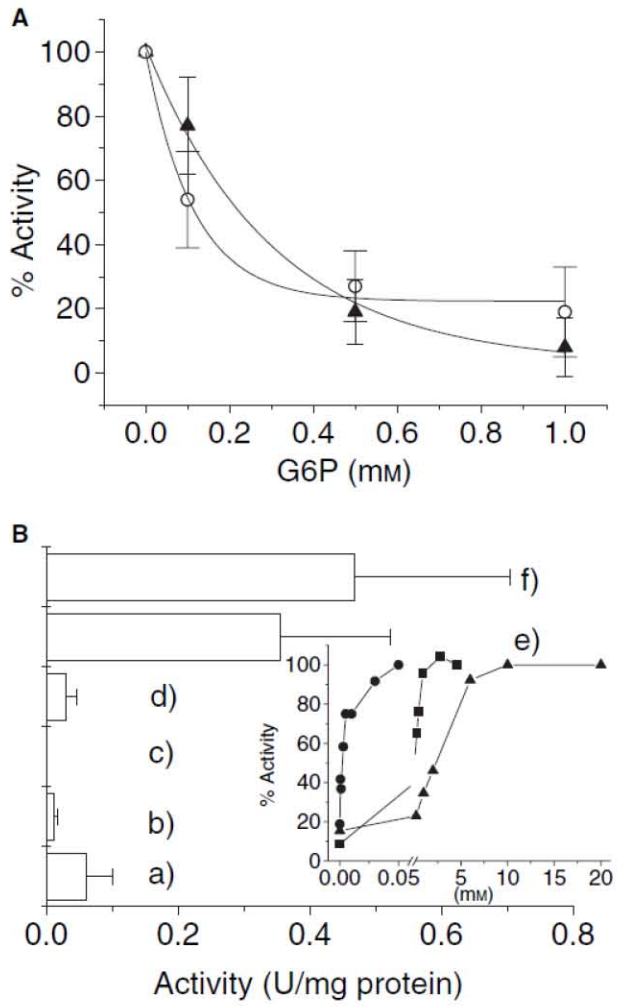

Fig. 2. Effect of modulators on tumoral hexokinase and PFK-1. (A) Inhibition of mitochondrial bound (○) and cytosolic hexokinase (▲) by Glc6*P*. Values shown represent the mean ± SD from three different preparations assayed, except for the experiments with cytosolic hexokinase at 0 and 1 mM Glc6*P*, in which nine different preparations were analyzed. (B) Effect of modulators of PFK-1. PFK-1 activity was determined in the presence of 1.5 mM Fru6*P* and (a) 0.8 mM ATP; (b) 3.9 mM ATP; (c) 3.9 mM ATP +1.7 mM citrate; (d) 3.9 mM ATP +1.7 mM citrate + 3.2 mM AMP; (e) 3.9 mM ATP + 1.7 mM citrate + 3.2 mM AMP + 5 μM Fru(2,6)P_2; and (f) 3.9 mM ATP + 1.7 mM citrate + 3.2 mM AMP + 50 μM Fru(2,6)P_2. Values shown represent the mean ± SD from three different preparations assayed. Inset: Activation of PFK-1 by different concentrations of Fru(2,6)P_2 (●), AMP (■) and NH_4^+ (▲), in the presence of 2 mM Fru6*P* and 0.8 mM ATP.

($n = 10$) and 1.7 ± 0.7 mM ($n = 6$), respectively. Thereafter, the PFK-1 activity was determined in the presence of the intracellular concentrations of its substrates (ATP, Fru6*P*), inhibitors (ATP, citrate) and activators [AMP, Fru(2,6)P_2]. PFK-1 activity was fully inhibited in the presence of ATP and citrate; this activity was only partially restored by AMP (Fig. 2B). The potent ATP + citrate inhibition was totally overcome, or even surpassed, by Fru(2,6)P_2 at concentrations found in tumor cells [18–21].

Discussion

Distribution of glycolytic flux control

Metabolic control analysis has been applied to determine the control structure of glycolysis in several normal mammalian systems, such as human erythrocytes, rat heart and mouse skeletal muscle extracts [22,23,38]. With this quantitative framework, hexokinase and PFK-1 have been identified as the main controlling steps. Fast-growth tumor cells develop a nontypical metabolism [39,40], which includes an accelerated glycolytic flux. As glycolysis in different tumor lines has been considered to be an extremely fast pathway [39], the identification of which enzyme(s) controls glycolytic flux becomes clinically relevant.

The 10 enzymes of the AS-30D hepatoma glycolytic pathway showed higher activity than in normal rat hepatocytes. Despite showing the greatest over-expression, hexokinase and PFK-1, together with aldolase, had the lowest V_{max} values (Table 1). Other groups have described a similar pattern for AS-30D [7] and other tumor cell types [25]. However, in all previous papers [7,15,25,41,42] it was difficult to establish a strict activity sequence order, as not all glycolytic activities were determined; moreover, the activity assays were performed at nonphysiological pH (>7) and temperature (<37 °C). Indeed, determining V_{max} under near-physiological conditions establishes the true content of active enzyme, which is not possible when mRNA, or protein, is measured.

The tumoral hexokinase and PFK-1, enzymes that in normal tissues control the flux (100% in human erythrocytes, 59% in isolated rat heart, and 100% in rat skeletal muscle reconstituted pathway) [22,23,38], exhibited the highest activity enhancement (306-fold and 22–56-fold increase versus hepatocytes; Table 1). In addition, the cytosolic concentrations of Glc6*P* and Fru(1,6)P_2, which are products of hexokinase and PFK-1, respectively, increased by fivefold and 250-fold (Table 3). The upper limits of activity increment were established by taking into account both the cytosolic and mitochondrial hexokinase activities (Table 6), and the PFK-1 maximal activity attained in the presence of the activator Fru(2,6)P_2 (Fig. 2B inset).

The flux control coefficients calculated from elasticities are, to a great extent, determined by the definition of producing and consuming blocks [24,43,44]. Elasticity-based analysis requires that (a) the metabolic

pathway reaches a quasi-steady-state (see legend to Table 2 for experimental details on how the glycolytic steady-state flux was established), and (b) the intermediates that link the blocks are not significantly affected by other pathways. However, some of the glycolytic intermediates used in this work for the estimation of elasticity coefficients such as Glc6*P*, Fru6*P* and DHAP are indeed connected to other pathways, and hence changes in the flux of glycogen synthesis and degradation, pentose phosphate cycle, and glycerol and triacylglycerol synthesis might affect the concentrations of these metabolites.

Another important assumption (c) in this elasticity-based analysis is that producing and consuming blocks affect each other only through the common metabolite. However, the glycolytic segments analyzed in this work may also interact through the moiety-conserved pools of ATP–ADP–AMP and NAD(P)H–NAD(P)$^+$. The discrepancy in the calculated flux control coefficients for producing and consuming blocks of DHAP and Fru(1,6)P_2, by using different experimental protocols (Table 4), might partly be due to variation in the nicotinamide nucleotide redox state and adenine nucleotide energy state, respectively.

Furthermore, the elasticity-based analysis might be flawed, and the control distribution reported might be erroneous, if the concentrations of adenine nucleotides also varied in the titration experiments. It is worth mentioning that several other studies involving elasticity-based analysis have not taken into account the potential interactions between producing and consuming blocks mediated by the pool of adenine nucleotides [23,33–36,45]. Therefore, the variation in the concentrations of ATP, ADP and AMP was determined under the conditions of the experiments shown in Fig. 1. The results indicate that none of the adenine nucleotides changed significantly ($n = 4$) on varying either glucose (from 4.5 to 5.5 mM) or oxalate (from 0 to 1 mM); with 2 mM oxalate, a 10–30% increase in ATP, ADP and AMP was observed. Thus, these findings support the control distribution of glycolysis (Table 5) derived from the elasticity-based analysis shown in Table 4.

DHAP is certainly connected with nonglycolytic reactions that involve NAD$^+$ such as α-glycerophosphate dehydrogenase, which was however, negligible in AS-30D cells (Table 1). Likewise, Fru(1,6)P_2 formation may affect the ATP/ADP ratio, which in turn establishes communication with glycolytic downstream reactions (phosphoglycerate kinase, pyruvate kinase) and with other energy-dependent reactions (adenylate kinase, ATPases, biosynthetic pathways). Moreover, PFK-1 is activated by AMP (Table 6 and Fig. 2B), which connects with the adenylate kinase reaction. Therefore, the connectivity theorem used here for the calculation of the flux control coefficients from elasticities towards some intermediates [Eqn 2 in Experimental procedures] was apparently incomplete and too simplistic to describe all interactions, and it may be necessary to consider more complicated relationships [24,43,44].

Notwithstanding the above arguments, the elasticity-based analysis, as used here, revealed that the Glc6*P*-producing block (GluT and hexokinase) exerted the main control of flux. The finding that the intracellular concentration of free glucose was high and saturating for hexokinase (Table 3) suggests that most of the control exerted by the Glc6*P*-producing block might reside in hexokinase. Moreover, high over-expression of GluT has been documented for HeLa cells and other human tumor cell types [46,47]. However, before we can conclude that hexokinase is the main controlling step, we should further examine the content and activity of the GluT under physiological conditions, as product inhibition of the GluT activity has not been explored [48].

In HeLa cells, all glycolytic enzymes except LDH were also over-expressed compared with hepatocytes. However, it should be noted that to achieve a more rigorous comparison, a normal proliferating endothelial cell line should be used instead of hepatocytes. The over-expression in HeLa cells was much less than that in AS-30D cells (Table 1); however, the glycolytic rates were similar (Table 2). This was probably due to a high rate of degradation of glycogen (high lactate formation in the absence of added glucose; Table 2) and amino acids (elevated concentration of pyruvate; Table 3), the products of which bypass hexokinase, the presumed main controlling step, to enter the glycolytic pathway.

In HeLa cells, the control of glycolytic flux may also reside in hexokinase, as in normal hepatocytes and AS-30D cells, as well as in PFK-1, because the two enzymes have the lowest V_{max} values, and they are not highly over-expressed. The eightfold lower concentration of Glc6*P* in HeLa cells, compared with AS-30D cells, is expected to exert a low or negligible inhibition of hexokinase. The low Glc6*P* concentration in HeLa cells may be related to a higher activity of the Glc6*P* branches, glycogen synthesis and pentose phosphate cycle. Indeed, G6PDH activity was 4–7 times higher in HeLa cells than in hepatocytes and AS-30D cells (Table 1).

A higher ATP concentration in HeLa cells than in AS-30D cells suggests a lower activity of ATPases and other ATP-dependent cell processes or, alternatively, that ATP production by oxidative phosphorylation

was faster. Indeed, the rate of oligomycin-sensitive respiration, which reflects the rate of oxidative phosphorylation [40,49], in the presence of 5 mM glucose + 0.6 mM glutamine was 43 ± 4 ng-atoms oxygen·min^{-1}·10^{-7} cells ($n = 4$) in AS-30D cells and 92 ± 16 ng-atoms oxygen·min^{-1}·10^{-7} cells ($n = 6$) in HeLa cells. As the enzymatic assay of ADP determines total but not free ADP, the ATP/ADP ratio was not highly reliable as an indicator of the cellular energy status.

There are two α-glycerophosphate dehydrogenase isoenzymes in mammalian cells, one bound to the mitochondrial inner membrane and another in the cytosol, which regulate the cytosolic NADH/NAD$^+$ ratio and are involved in the synthesis of triacylglycerols [50]. The activity of the cytosolic isoenzyme decreases or becomes negligible in fast-growth hepatomas [26,27] and AS-30D and HeLa cells (Table 1), which may induce DHAP accumulation (Table 3). An alternative route for triacylglycerol synthesis has been described that does not require α-glycerophosphate. This pathway starts with the acylation of DHAP, in a reaction catalyzed by DHAP acyltransferase, which is present in rat liver, kidney, spleen and adipose tissue; at the subcellular level, this enzyme is localized in the mitochondrial and microsomal fractions [51]. Such a route might be operating in tumor cells.

Biochemical mechanisms underlying the evaluated distribution of flux control

It should be emphasized that the analysis of V_{max} values only (i.e. cellular content of active enzyme) to reach conclusions on the metabolic pathway control is certainly incomplete, as the enzymatic activities are determined in the absence of their physiological activators and inhibitors, at saturating substrate concentrations, and in the absence of products; these factors discard the role of the reversibility of reactions under physiological conditions on control of flux [52].

Accumulation of products may decrease the forward reaction. In this regard, it is well documented that Glc6*P* is a potent inhibitor of hexokinase-I, hexokinase-II and hexokinase-III [37]. In consequence, the increased hexokinase activity might be counterbalanced by stronger Glc6*P* inhibition. One way to circumvent this blockade is to over-express hexokinase-III, an isoenzyme with a higher K_i for Glc6*P* (0.1 mM). Alternatively, hexokinase binding to mitochondria may protect it against Glc6*P* inhibition [7,53]. However, the Glc6*P* inhibition was strong and similar for both mitochondrial and cytosolic hexokinase isoenzymes (Figure 2A), when the activity was assayed under near-physiological conditions of pH (7.0) and temperature (37 °C) and high concentrations of glucose (> 1 mM) and Glc6*P* (≥ 1 mM). On the other hand, Nakashima *et al.* [7] and Bustamante *et al.* [53] determined Glc6*P* inhibition of mitochondrial hexokinase at 22–30 °C, pH 7.9, and in a hypotonic medium with nonphysiological concentrations of glucose (< 1 mM) and Glc6*P* (< 1 mM). The presence of this Glc6*P* regulatory mechanism in tumoral hexokinase supports an essential role for this enzyme in the control of flux.

Four hexokinase isoenzymes have been identified in mammalian cells: Type-I, II, III and IV (glucokinase), from which the first three are Glc6*P*-sensitive [37]. Hexokinase-I and hexokinase-II may bind to the outer mitochondrial membrane, as they have a specific hydrophobic N-terminal segment [54]. Hexokinase-I is predominantly located in brain, kidney, retina and breast, whereas hexokinase-II is abundant in skeletal muscle and adipose tissue [8]. In tumor cells, hexokinase-II is apparently the main over-expressed isoenzyme [7,8,37], except for brain tumors, in which hexokinase-I is over-expressed [8].

Analysis of the hexokinase kinetic properties and subcellular redistribution towards mitochondria suggested that the isoenzyme over-expressed in AS-30D cells was type II, as previously suggested using a similar analysis [7]. The amount of mitochondrial hexokinase in AS-30D (50%) and HeLa cells (70%; data not shown) was also similar to that observed for Novikoff and AS-30D ascites tumor cells of 50–80% [55,56]. This observation explains, at least in part, the enhanced glycolytic flux (Table 2, [8]) and the resistance to apoptosis [11] in these tumor cells.

The kinetic analysis of PFK-1 revealed that the isoenzyme present in AS-30D cells was completely insensitive to the usual allosteric inhibitors, ATP and citrate, in the presence of a low, physiological concentration of Fru(2,6)P_2, and that it was highly sensitive to the activators NH_4^+, AMP and Fru(2,6)P_2. The high, physiological concentration of AMP in AS-30D did not suffice to potently activate PFK-1 in the presence of ATP and citrate. The expression of a PFK-2 isoenzyme with a low fructose-2,6-bisphosphatase activity in several human tumor lines has been described [57,58], which ensures a high concentration of Fru(2,6)P_2. Indeed, Fru(2,6)P_2 was the most potent activator of PFK-1 and blocked the inhibition by ATP and citrate (Fig. 2B and Table 6, and also [12]).

Therefore, its kinetic properties predict that PFK-1 activity cannot impose a flux limitation on glycolysis in AS-30D cells. Under near-physiological conditions, the estimated elasticity coefficient of PFK-1 for Fru6*P* was high ($\varepsilon^{PFK\text{-}1}_{Fru6P} = 1.2$), which provides the bio-

chemical mechanism for its low flux control coefficient (Table 5). The PFK-1 elasticity and kinetic properties also provide a biochemical basis for understanding the diminished Pasteur effect observed in AS-30D [49] and other tumor cell types [39].

Experimental procedures

Chemicals

Hexokinase, G6PDH, hexosephosphate isomerase, aldolase, α-glycerophosphate dehydrogenase, triosephosphate isomerase, glyceraldehyde-3-phosphate dehydrogenase, pyruvate kinase and LDH were purchased from Roche Co. (Mannheim, Germany). Recombinant enzymes enolase, pyruvate phosphate dikinase and phosphoglycerate kinase from *Entamoeba histolytica* were kindly provided by E Saavedra, Instituto Nacional de Cardiología, México. Glucose, Glc6*P*, Fru(1,6)P_2, glyceraldehyde 3-phosphate, 2-phosphoglycerate, phosphoenolpyruvate, Fru(2,6)P_2, pyruvate, citrate, ATP, AMP, ADP, GTP, dithiothreitol, cysteine, NADH, NAD^+, NADP and oxalate were from Sigma Chemical (St Louis, MO, USA). Fru6*P* and 3-phosphoglycerate were from Roche (Indianapolis, IN, USA). Methoxy[^{3}H]inulin was from Perkin–Elmer Life Sci (Boston, MA, USA). All other reagents were of analytical grade from commercial sources.

Isolation of tumor and liver cells

AS-30D hepatoma cells [(2–4) × 10^8 cells·mL^{-1}) were propagated in female Wistar rats (200 g) by intraperitoneal transplantation. Hepatoma cells were isolated as described elsewhere [59].

HeLa cells (1.5 × 10^4 cells·mL^{-1}) were grown in Dulbecco's minimal essential medium (Gibco Life Technologies, Rockville, MD, USA), supplemented with 10% fetal bovine serum (Gibco), 10 000 U·mL^{-1} streptomycin/penicillin, and fungizone (amphotericin B; Gibco) in 175-cm^2 flasks (Corning, New York, NY, USA) at 37 °C in 5% CO_2/95%O_2. Hepatocytes were isolated by perfusion of isolated liver with collagenase IV (Worthington, Lakewood, NJ, USA) from fed Wistar rats [60]. The cellular viability assayed by trypan blue exclusion was 80–85%. Experimental manipulation of human and rodent cells and animal specimens were carried out following the Instituto Nacional de Cardiología de Mexico guidelines in accordance with the Declaration of Helsinki and the US NIH guidelines for care and use of experimental animals.

Determination of steady-state concentrations of metabolites

Cells (15 mg protein·mL^{-1}) were incubated in Krebs-Ringer medium with orbital shaking (150 r.p.m.) at 37 °C in a plastic flask. After 10 min, 5 mM glucose was added to the cell suspension. The reaction was stopped 3 min later with ice-cold perchloric acid (3%, v/v, final concentration). For the determination of the intracellular L-lactate, an aliquot (1 mL) of the cell suspension was rapidly withdrawn and centrifuged at 20 800 ***g*** for 10–15 s at room temperature. The supernatant was discarded, and the pellet rinsed with fresh Krebs–Ringer medium and then resuspended in 3% perchloric acid. The samples were neutralized with 3 M KOH/0.1 M Tris. The concentrations of Glc6*P*, Fru6*P*, Fru(1,6)P_2, DHAP, glyceraldehyde 3-phosphate, phosphoenolpyruvate, pyruvate, ATP, ADP, AMP, citrate and L- lactate were determined by standard enzymatic assays [61].

Protein was determined by the biuret method using BSA as standard [62].

Determination of intracellular glucose

AS-30D cells (15 mg·mL^{-1}) were preincubated for 10 min in the absence of exogenous substrates at 37 °C. Exogenous glucose was added after 10 min, and the cells were incubated for 3 min more. Afterwards, an aliquot (0.5 mL) was carefully poured into microcentrifuge tubes containing, from bottom to top, 30% (v/v) perchloric acid (0.3 mL), 1-bromododecane (0.3 mL) and fresh Krebs–Ringer medium (0.3 mL). The sample was centrifuged for 2–3 min in a refrigerated Microfuge (Eppendorf centrifuge 5804 R, Eppendorf, Hamburg, Germany) at 20 800 ***g***. The bottom layer was collected and neutralized with 10% NaOH. Glucose was determined by enzymatic analysis [61].

To correct for the presence of exogenous glucose from the incubation medium in the cellular pellet, the content of external water was evaluated by using methoxy[^{3}H]inulin. An aliquot of cells (5–30 mg protein·mL^{-1}) was incubated in 0.5 mL Krebs–Ringer medium with [^{3}H]inulin (0.15 mg·mL^{-1}, specific radioactivity 5200 c.p.m.·μg^{-1}) for 15 s. Thereafter, the cell suspension was carefully layered into microcentrifuge tubes prepared as described above. The radioactivity of the bottom layer was measured in a liquid scintillation analyzer (Packard Instruments/Canberra, Meriden, CT, USA). The concentration of glucose carried from the extracellular milieu was 1.28 mM. This value was subtracted from the original intracellular concentration.

Determination of glycolytic flux in liver and tumor cells

Cells (15 mg protein·mL^{-1}) were incubated in 3 mL Krebs–Ringer medium with orbital stirring (150 r.p.m.) at 37 °C in a plastic flask. After 10 min, 5 mM glucose was added to the cells; the reaction was stopped with cold 3% perchloric acid 0 and 3 min later. The samples were neutralized with 3 M KOH/0.1 M Tris. L-Lactate generated was determined by enzymatic analysis [61].

Cell extracts of tumor and liver cells

Cells (65 mg protein·mL^{-1}) were resuspended in 25 mM Tris/HCl buffer, pH 7.6, with 1 mM EDTA, 5 mM dithiothreitol and 1 mM phenylmethanesulfonyl fluoride. The cell suspension was frozen in liquid nitrogen and thawed in a water bath at 37 °C; this procedure was repeated three times. Cell lysates were centrifuged at 39 000 ***g*** for 20 min and 4 °C. Afterwards, the supernatant was collected for determination of enzyme activity. Activities of hexokinase, hexosephosphate isomerase, PFK-1, triosephosphate isomerase, aldolase, glyceraldehyde-3-phosphate dehydrogenase, phosphoglycerate kinase, phosphoglycerate mutase, enolase, pyruvate kinase, LDH, α-glycerophosphate dehydrogenase, phosphoglucomutase and G6PDH were determined spectrophotometrically by standard assays [63,64]. The incubation buffer was 50 mM Mops, pH 7, at 37 °C. Phosphoglycerate kinase activity was determined in 50 mM potassium phosphate, pH 7, at 37 °C. To assay mitochondrial hexokinase, isolated mitochondria were prepared as described elsewhere [59]. The assays for both cytosolic and mitochondrial hexokinase isoenzymes were carried out at 37 °C in 1 mL KME buffer (100 mM KCl, 50 mM Mops, 0.5 mM EGTA, pH 7.0) plus 2 U G6PDH, 1 mM $NADP^+$, 5 mM $MgCl_2$, glucose (from 0.05 to 10 mM) and 1 μM oligomycin. The reaction was started by the addition of ATP (0.05–5 mM) after 2 min incubation.

Assay for hexokinase inhibition by Glc6*P* was carried out in 3 mL of KME buffer at 37 °C, in the presence of 3 mM ATP, 5 mM $MgCl_2$, 1 μM oligomycin and 0.2–1 mM Glc6*P*. Owing to the high unspecific oxidation of added NADH by the cytosolic-enriched and mitochondrial fractions (despite the addition of rotenone), the activity was calculated from the ADP generated, which was determined by a standard assay [61]. The hexokinase activity was corrected for the ADP formed in the absence of added glucose. Bound and free isoenzymes were preincubated for 2 min, and then the hexokinase reaction was started by adding 3 mM glucose. After 30 s, the reaction was stopped with ice-cold perchloric acid (3%, v/v, final concentration). The samples were neutralized with 3 M KOH/0.1 M Tris. The control activities for both hexokinase isoenzymes were comparable to those determined by the G6PDH coupling assay.

For PFK-1 activity, freshly prepared extracts were incubated at 37 °C in 50 mM Mops, pH 7. The reaction assay contained 0.15 mM NADH, 5 mM $MgCl_2$, 1 mM EDTA, Fru6*P* (from 0.01 to 10 mM) and ammonium sulfate suspensions of the following coupling enzymes: 0.36 U aldolase, 9 U triosephosphate isomerase, and 3.1 U α- glyceraldehyde-3-phosphate dehydrogenase. The reaction was started by the addition of exogenous ATP (from 0.01 to 2 mM). For the determination of $K_{0.5}$ for NH_4^+, AMP and Fru(2,6)P_2, as well as for the effect of activators and inhibitors, lyophilized (ammonium-free) coupling enzymes were used in KME buffer.

Determination of flux control coefficients

The flux control coefficients (C^J_{Ei}) were determined by using the elasticity-based analysis [31,34,45,65,]. This approach quantifies the sensitivity of a given enzyme or block of enzymes to variations in its substrate or product when the steady-state flux is modified. Glycolysis was stimulated by exogenous glucose (4–6 mM) or inhibited by oxalate (0.5–2 mM), 2-deoxyglucose (0.5–10 mM) or arsenite (5–100 μM). Under these conditions, the variation in the glycolytic flux and in several intermediates was determined. Flux control coefficients were estimated using the connectivity (Eqn 1) and summation theorems (Eqn 2) [24],

$$C^J_{E1}\varepsilon^{E1}_m + C^J_{E2}\varepsilon^{E2}_m = 0 \quad (1)$$

$$C^J_{E1} + C^J_{E2} = 1 \quad (2)$$

in which J is the glycolytic flux (rate of lactate formation), E1 is the enzyme block that produces the intermediate (m) and E2 is the enzyme block that consumes m.

Acknowledgements

This work was partially supported by grant no. 43811-Q from CONACyT-México.

References

1 Warburg O (1956) On respiratory impairment in cancer cells. *Science* **124**, 269–270.
2 Zu XL & Guppy M (2004) Cancer metabolism: facts, fantasy, and fiction. *Biochem Biophys Res Commun* **313**, 459–465.
3 Dang C & Semenza GL (1999) Oncogenic alterations of metabolism. *Trends Biochem Sci* **24**, 68–72.
4 Lu H, Forbes RA & Verma A (2002) Hypoxia-inducible factor 1 activation by aerobic glycolysis implicates the Warburg effect in carcinogenesis. *J Biol Chem* **277**, 23111–23115.
5 Osthus RC, Shim H, Kim S, Li Q, Reddy R, Mukherjee M, Xu Y, Wonsey D, Lee LA & Dang C (2000) Deregulation of glucose transporter 1 and glycolytic gene expression by c-Myc. *J Biol Chem* **275**, 21797–21800.
6 Gillies RJ, Martinez-Zaguillan R, Martinez GM, Serrano R & Perona R (1990) Tumorigenic 3T3 cells maintain an alkaline intracellular pH under physiological conditions. *Proc Natl Acad Sci USA* **87**, 7414–7418.
7 Nakashima R, Paggi M, Scott LJ & Pedersen PL (1988) Purification and characterization of a bindable form of mitochondrial bound hexokinase from the highly glycolytic AS-30D rat hepatoma cell line. *Cancer Res* **48**, 913–919.
8 Pedersen PL, Mathupala S, Rempel A, Geschwind JF & Hee Ko Y (2002) Mitochondrial bound type II

hexokinase: a key player in the growth and survival of many cancers and an ideal prospect for therapeutic intervention. *Biochim Biophys Acta* **1555**, 14–20.
9 Goel A, Mathupala SP & Pedersen PL (2003) Glucose metabolism in cancer. Evidence that demethylation events play a role in activating type II hexokinase gene expression. *J Biol Chem* **278**, 15333–15340.
10 Mathupala SP, Heese C & Pedersen PL (1997) Glucose catabolism in cancer cells. The type II hexokinase promoter contains functionally active response elements for the tumor suppressor p53. *J Biol Chem* **272**, 22776–22780.
11 Pastorino JG, Shulga N & Hoek JB (2002) Mitochondrial binding of hexokinase II inhibits Bax-induced cytochrome *c* release and apoptosis. *J Biol Chem* **277**, 7610–7618.
12 Depré C, Rider MH & Hue L (1998) Mechanisms of control of heart glycolysis. *Eur J Biochem* **258**, 277–290.
13 Staal GEJ, Kalff A, Heesbeen EC, Van Veelen CWM & Rijksen G (1987) Subunit composition, regulatory properties, and phosphorylation of phosphofructokinase, from human gliomas. *Cancer Res* **47**, 5047–5051.
14 Meldolesi MF, Macchia V & Lacceti P (1976) Differences in phosphofructokinase regulation in normal and tumor rat thyroid cells. *J Biol Chem* **251**, 6244–6251.
15 Oskam R, Rijksen G, Staal GEJ & Vora S (1985) Isozymic composition and regulatory properties of phosphofructokinase from well-differentiated and anaplastic medullary thyroid carcinomas of the rat. *Cancer Res* **45**, 135–142.
16 Vora S, Halper JP & Knowles DM (1985) Alterations in the activity and isozymic profile of human phosphofructokinase during malignant transformation *in vivo and in vitro*: transformation-and progression-linked discriminants of malignancy. *Cancer Res* **45**, 2993–3001.
17 Sánchez-Martínez C & Aragón JJ (1997) Analysis of phosphofructokinase subunits and isozymes in ascites tumor cells and its original tissue, murine mammary gland. *FEBS Lett* **409**, 86–90.
18 Denis C, Paris H & Murat JC (1986) Hormonal control of fructose-2,6-bisphosphate concentration in the HT29 human colon adenocarcinoma cell line. *Biochem J* **239**, 531–536.
19 Mojeda M, Bosca L & Hue L (1985) Effect of glutamine on fructose-2,6-biphosphate and on glucose metabolism in HeLa cells and in chick-embryo fibroblasts. *Biochem J* **232**, 521–527.
20 Loiseau AM, Rousseau GG & Hue L (1985) Fructose-2,6-bisphosphate and the control of glycolysis by glucocorticoids and by other agents in rat hepatoma cells. *Cancer Res* **45**, 4263–4269.
21 Nissler K, Petermann H, Wenz I & Brox D (1995) Fructose-2,6-bisphosphate metabolism in Ehrlich ascites tumour cells. *J Cancer Res Clin Oncol* **121**, 739–745.
22 Rapoport T, Heinrich R, Jacobasch G & Rapoport S (1974) A linear steady-state treatment of enzymatic chains. A mathematical model of glycolysis of human erytrocytes. *Eur J Biochem* **42**, 107–120.
23 Kashiwaya Y, Sato K, Tsuchiya N, Thomas S, Fell DA, Veech RL & Passonneau JV (1994) Control of glucose utilization in working perfused rat heart. *J Biol Chem* **269**, 25502–25514.
24 Fell D (1997) *Understanding the Control of Metabolism*. Plenum Press, London.
25 Wu R (1959) Regulatory mechanisms in carbohydrate metabolism. V. Limiting factors of glycolysis in HeLa cells. *J Biol Chem* **234**, 2806–2810.
26 Harding JW, Pyeritz EA, Morris HP & White HB (1975) Proportional activities of glycerol kinase and glycerol 3-phosphate dehydrogenase in rat hepatomas. *Biochem J* **148**, 545–550.
27 Pedersen PL (1978) Tumor mitochondria and the bioenergetics of cancer cells. *Prog Exp Tumor Res* **22**, 190–274.
28 Traut TW (1994) Physiological concentrations of purines and pyrimidines. *Mol Cell Biochem* **140**, 1–22.
29 Moreno-Sánchez R & Torres-Márquez ME (1991) Control of oxidative phosphorylation in mitochondria, cells and tissues. *Int J Biochem* **23**, 1163–1174.
30 Groen AK, Wanders RJ, Westerhoff HV, van der Meer R & Tager JM (1982) Quantification of the contribution of various steps to the control of mitochondrial respiration. *J Biol Chem* **257**, 2754–2757.
31 Kacser H (1983) The control of enzyme systems *in vivo*: elasticity analysis of the steady state. *Biochem Soc Trans* **11**, 35–40.
32 Moreno-Sánchez R, Bravo C & Westerhoff HV (1999) Determining and understanding the control of flux. An illustration in submitochondrial particles of how to validate schemes or metabolic control. *Eur J Biochem* **264**, 427–433.
33 Groen AK, van Roermund CW, Vervoom RC & Tager JM (1986) Control of gluconeogenesis in rat liver cells. Flux control coefficients of the enzymes in the gluconeogenic pathway in the absence and presence of glucagon. *Biochem J* **237**, 379–389.
34 Hafner RP, Brown GC & Brand MD (1990) Analysis of the control of respiration rate, phosphorylation rate, proton leak rate and protonmotive force in isolated mitochondria using the 'top-down' approach of metabolic control theory. *Eur J Biochem* **188**, 313–319.
35 Thomas S, Mooney PJ, Burrell MM & Fell DA (1997) Metabolic control analysis of glycolysis in tuber tissue of potato (*Solanum tuberosum*): explanation for the low control coefficient of phosphofructokinase over respiratory flux. *Biochem J* **322**, 119–127.
36 Ainscow EK & Brand MD (1999) Top-down control analysis of ATP turnover, glycolysis and oxidative phosphorylation in rat hepatocytes. *Eur J Biochem* **263**, 671–685.
37 Wilson JE (2003) Isozymes of mammalian hexokinase: structure, subcellular localization and metabolic function. *J Exp Biol* **206**, 2049–2057.

38 Jannaschk KD, Burgos M, Centerlles JJ, Ovadi J & Cascante M (1999) Application of metabolic control analysis to the study of toxic effects of copper in muscle glycolysis. *FEBS Lett* **445**, 144–148.

39 Eigenbrodt E, Fister P & Reinacher M (1985) New perspectives in carbohydrate metabolism in tumor cells. In. *Regulation of Carbohydrate Metabolism* (Reitner, R, ed.), vol. 2, pp 141–179. CRC Press, Boca Raton, FL.

40 Rodríguez-Enríquez S & Moreno-Sánchez R (1998) Intermediary metabolism of fast-growth tumor cells. *Arch Med Res* **29**, 1–12.

41 Mazuret S, Eigenbrodt E, Failing K & Steinberg P (1999) Alterations in the glycolytic and glutaminolytic pathways after malignant transformation of rat liver oval cells. *J Cell Physiol* **181**, 136–146.

42 Mazuret S, Michel A & Eigenbrod E (1997) Effect of extracellular AMP on cell proliferation and metabolism of breast cancer cell lines with high and low glycolytic rates. *J Biol Chem* **272**, 4941–4952.

43 Shuster S, Kahn D & Westerhoff HV (1993) Modular analysis of control of complex metabolic pathways. *Biophys Chem* **48**, 1–17.

44 Ainscow EK & Brand MD (1998) Control analysis of systems with reaction blocks that 'cross-talk'. *Biochim Biophys Acta* **1366**, 284–290.

45 Brown GC, Lakin-Tomas L & Brand MD (1990) Control of respiration and oxidative phosphorylation in isolated rat liver cells. *Eur J Biochem* **192**, 355–362.

46 Kitagawa T, Tsuruhara Y, Hayashi M, Endo T & Stanbridge EJ (1995) A tumor-associated glycosylation change in the glucose transporter GLUT1 controlled by tumor suppressor function in human cell hybrids. *J Cell Sci* **108**, 3735–3743.

47 Macheda ML, Rogers S & Best JD (2005) Molecular and cellular regulation of glucose transporter (GLUT) proteins in cancer. *J Cell Physiol* **202**, 654–662.

48 Colville C, Seatter MJ, Jess TJ, Gould GW & Thomas HM (1993) Kinetic analysis of the liver-type (GLUT2) and brain-type (GLUT3) glucose transporters in *Xenopus oocytes*: substrate specificities and effects of transport inhibitors. *Biochem J* **290**, 701–706.

49 Rodríguez-Enríquez S, Juárez O, Rodríguez-Zavala JS & Moreno-Sánchez R (2001) Multisite control of the Crabtree effect in ascites hepatoma cells. *Eur J Biochem* **268**, 2512–2519.

50 Houstek J, Cannon B & Lindberg O (1975) Glycerol-3-phosphate shuttle and its funtion in intermediary metabolism of hamster brow-adipose tissue. *Eur J Biochem* **54**, 11–18.

51 Hajra AK (1997) Dihydroxyacetone phosphate acyltransferase. *Biochim Biophys Acta* **1348**, 27–34.

52 Mendoza-Cozatl DG & Moreno-Sanchez R (2006) Control of glutathione and phytochelatin synthesis under cadmium stress. Pathway modeling for plants. *J Theor Biol* **238**, 919–936.

53 Bustamante E & Pedersen PL (1977) High aerobic glycolysis of rat hepatoma cells in culture: role of mitochondrial hexokinase. *Proc Natl Acad Sci USA* **74**, 3735–3739.

54 Smith TAD (2000) Mammalian hexokinases and their abnormal expression in cancer. *Br J Biomed Sci* **57**, 170–178.

55 Arora KK & Pedersen PL (1988) Functional significance of mitochondrial bound hexokinase in tumor cell metabolism. *J Biol Chem* **263**, 17422–17428.

56 Parry DM & Pedersen PL (1983) Intracellular localization and properties of particulate hexokinase in the Novikoff ascites tumor. *J Biol Chem* **258**, 10904–10912.

57 Atsumi T, Chesney J, Metz C, Leng L, Donnelly S, Makita Z, Mitchell R & Bucala R (2002) High expression of inducible 6-phosphofructo-2-kinase/fructose-2,6-bisphosphatase (iPFK-2; PFKFB3) in human cancers. *Cancer Res* **62**, 5881–5887.

58 Chesney J, Mitchell R, Benigni F, Bacher M, Spiegel L, Al-Abed Y, Han JH, Metz C & Bucala R (1999) An inducible gene product for 6-phosphofructo-2-kinase with an AU-rich instability element: role in tumor cell glycolysis and the Warburg effect. *Proc Natl Acad Sci USA* **96**, 3047–3052.

59 López-Gómez F & Torres-Márquez & Moreno-Sánchez R (1993) Control of oxidative phosphorylation in AS-30D hepatoma mitochondria. *Int J Biochem* **25**, 373–377.

60 Berry MN & Friend DS (1969) High-yield preparation of isolated rat liver parenchymal cells. A biochemical and fine structural study. *J Cell Biol* **43**, 506–520.

61 Bergmeyer HU (ed.) (1974) *Methods of Enzymatic Analysis*. Verlag Chemie, Weinheim.

62 Gornall AG, Bardwill CJ & David MM (1949) Determination of serum proteins by means of biuret reaction. *J Biol Chem* **177**, 751–766.

63 Bergmeyer HU (ed.) (1983) *Methods of Enzymatic Analysis*. Verlag Chemie, Weinheim.

64 Saavedra E, Encalada R, Pineda E, Jasso-Chávez R & Moreno-Sánchez R (2005) Glycolysis in *Entamoeba histolytica*. Biochemical characterization of recombinant glycolytic enzymes and flux control analysis. *FEBS J* **272**, 1767–1783.

65 Tager JM, Wanders JA, Groen AK, Kunz W, Bohnensack R, Küster U, Letko G, Böhme G, Duszynski J & Wojtczak L (1983) Control of mitochondrial respiration. *FEBS Lett* **151**, 1–9.

66 Simpson RJ, Brindle KM, Brown FF, Campbell ID & Foxall DL (1982) Studies of lactate dehydrogenase in the purified state and in intact erythrocytes. *Biochem J* **202**, 581–587.

67 Meunier JC & Dalziel K (1978) Kinetics studies of glyceraldehyde-3-phosphate dehydrogenase from rabbit muscle. *Eur J Biochem* **82**, 483–492.

FEBS Journal
27 Jan 06
Reference no.: FJ-05-1056.R1

Title: Determining and understanding the control of glycolysis in fast-growth tumor cells. Flux control by an over-expressed but strongly product-inhibited hexokinase. Authors: 1) Rafael Moreno-Sánchez 2) Alvaro Marín-Hernández 3) Sara Rodríguez-Enríquez 4) Paola Vital-González 5) Fanny Flores-Rodríguez 6) Marina Macías-Silva 7) Marcela Sosa-Garrocho.
Editor: Hans Westerhoff

Dear Dr. Moreno-Sánchez
Thank you for submitting your paper for publication in FEBS Journal.

I am pleased to inform you that your paper has received favourable comments from the referees and is likely to be acceptable for publication in the Journal after incorporation of their comments, copies of which are appended below. Please note in particular the comments from the Editor.

Editor's comments:
I think the following objection by one of the reviewers: "I am concerned upon the likely possibility that the consuming and producing blocks interact via metabolites other than those measured. The existence of such interactions would invalidate the approach used in this manuscript. Particularly the concentrations of ATP, ADP and AMP are likely to change during the titration experiments and are likely to affect the rate of enzymes on both, consuming and producing blocks. "is fully justified. I can also see that it may be hard to deal with this. However, you should clearly mention this as a limitation to your approach and come with suggested future work. You should also remove some of the speculations.

Please note that no guarantee of acceptance of the revised version can be given in advance. If accepted, the dates of receipt of both the original and revised papers will be printed.

We look forward to receiving the revised version of your manuscript.

Yours sincerely
Dr Vanessa Wilkinson
FEBS Journal
98 Regent St
Cambridge CB2 1DP, UK
Email: febsj@camfebs.co.uk

REFEREES' COMMENTS

Referee 1 Comments: None

Referee 2 Comments:
General comments:

This manuscript describes a series of experiments aimed at describing the flux control distribution in healthy and tumoral hepatocytes. This is achieved through elasticity-based analysis, in which the control of producing and consuming blocks may be calculated from the (measurable) elasticities of consuming and producing blocks to their common intermediate.

Although the manuscript has clearly improved, there are a number of speculations for which the authors offer no explanation and that hinder the comprehension of the manuscript. Examples of
such speculations are noted in the "particular comments".

An issue which concerns this reviewer is the likely possibility that the consuming and producing blocks interact via

metabolites other than those measured. Particularly: ATP, ADP and AMP. If
the concentrations of these metabolites change during the titration experiments, the elasticity based analysis will be flawed and the control distribution reported, erroneous.

Particular comments:
Page 8: The authors wrote: ". F1,6-BP increased 250 times and DHAP 16.6 times, which suggested a strong activation of PFK-1 and an attenuated utilization of DHAP for glycerol and tracylglyceride synthesis." The rationale behind this expectation is not explained. DHAP concentration depends also upon the glycolytic pathway downstream of glyceraldehydes-3-phosphate.

Page 10: The authors wrote: "However, this last type of metabolites may be still used in elasticity-based analysis as long as the flux through other pathways is low or negligible".
The question that follows immediately is whether these pathways indeed have a negligible effect on those metabolites. References of experiments should be given to support applicability of the
elasticity-based analysis.

Page 10: The authors, rightly, point out that the rate dependence upon a substrate (or product) is likely to be hyperbolic for most glycolytic enzymes. However, in these experiments both substrate(s) and product(s) may change simultaneously and the rate relation of the flux and, say, the substrate needs not to be hyperbolic if the concentration of the product is also varying during the titration.

Page 10: The authors wrote: ". only one point determines the value of the tangent.", when referring hyperbolic fits to the data. This is not true. The tangent's slope at a given operational point will depend upon the derivative of the function evaluated in that point, and would therefore depend upon the points on which the fit was based (i.e. all). This reviewer doubts that tangent slopes are an appropriate method for elasticity calculations when so few data points are available.

Page 15, second paragraph: The authors wrote that increased concentrations of G6P and F1-6BP suggest that HK and PFK-1 may exert a lower flux control in AS-30D cells than in hepatocytes.
The rationale for this suggestion is not explained.

20 February, 2006

Subject: Manuscript **FJ-05-1056.R1**

Dr. Vanessa Wilkinson
FEBS Journal
(European Journal of Biochemistry)

Dear Dr. Wilkinson:

Thank you for your kind letter of January 27, 2006 concerning our manuscript entitled "Determining and understanding the control of glycolysis in fast-growth tumor cells. Flux control by an over-expressed but strongly product-inhibited hexokinase". We were informed that the manuscript may become acceptable for publication after incorporation of the comments of the editor and referees. Therefore, the text was modified accordingly, in regard to the potential drawback in the elasticity analysis and to some speculations made in the original manuscript. New experimental data were also included in the revised manuscript. Corrections in the manuscript were highlighted in bold type, as requested.

The changes made to the manuscript are described below. We hope that the manuscript may be now found acceptable in its present form for its publication in FEBS Journal (European Journal of Biochemistry).

Sincerely,

Rafael Moreno-Sánchez, Ph. D.

Response to Referee No. 1

Referee 1 did not indicate any comment.

Response to Referee No. 2

We thank this reviewer for the many helpful and constructive criticisms of our manuscript.

General comments

Certainly the glycolytic consuming and producing blocks interact via metabolites other than those measured, particularly the adenine nucleotides. So, we fully agree with the reviewer that our elasticity analysis may be flawed if the concentrations of ATP, ADP and AMP also vary in the titration experiments. Therefore, to avoid further speculation in justifying our results, it was decided to determine the variation in the concentrations of the adenine nucleotides under the same conditions used in the titration experiments. This new experimentation was described, and the text modified, on p. 16, last paragraph, in which the reviewer's argument was incorporated. The concentrations of the adenine nucleotides (Table 3 for ATP and ADP; p. 14, line 8 for AMP) now include the values of the new results. A figure with the new results is enclosed in this letter.

Particular comments

The statements regarding the original speculations on p. 8 ("…which suggested a strong activation of PFK-1 and an attenuated utilization of DHAP for glycerol and tracylglyceride synthesis") and p. 15 ("These results suggested that HK and PFK-1 may exert a lower flux control in AS-30D cells than in hepatocytes") were removed, as recommended.

The statement on p. 9, last two lines, p. 10, first two lines ("…this last type of metabolites may be still used in elasticity-based analysis as long as the flux through…") was slightly modified and some references added.

The argument about the hyperbolic rate dependence upon substrate or product (p. 10, lines 17-19) was modified to include the observation made by the reviewer.

The statement "…only one point determines the value of the tangent" was erased and the text modified accordingly on p. 10, lines 19-22.

The statement on p. 8, lines 16-17 was modified because ATP/ADP rate change with the news values of ATP.

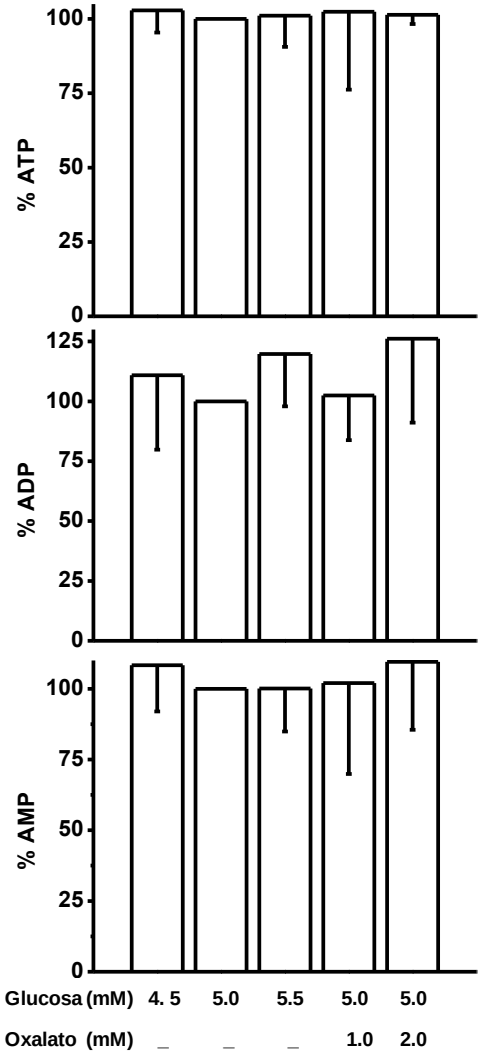

Figure 1. Concentrations of the adenine nucleotides under the same conditions used in the titration experiments. ATP 100 % was 7 ± 1 mM, n= 4; ADP 100 % was 2.1 ± 0.7 mM, n= 4; AMP 100 % was 3.3 ± 1.4 mM, n= 4.

5.1.1 Datos no mostrados

Para poder aplicar el análisis de elasticidades fue necesario establecer la condición de estado estacionario, la cual se define como aquella en la que el flujo de la vía y las concentraciones de intermediarios se mantienen constantes con respecto al tiempo. En la figura 5.2.1, se observa que el flujo (medido como la cantidad de lactato producido/ min) y la concentración de F1,6BP fueron constantes entre 2 a 10 minutos, después de haber agregado la glucosa. A partir de este resultado consideramos realizar nuestros experimentos incubando con glucosa por 3 minutos.

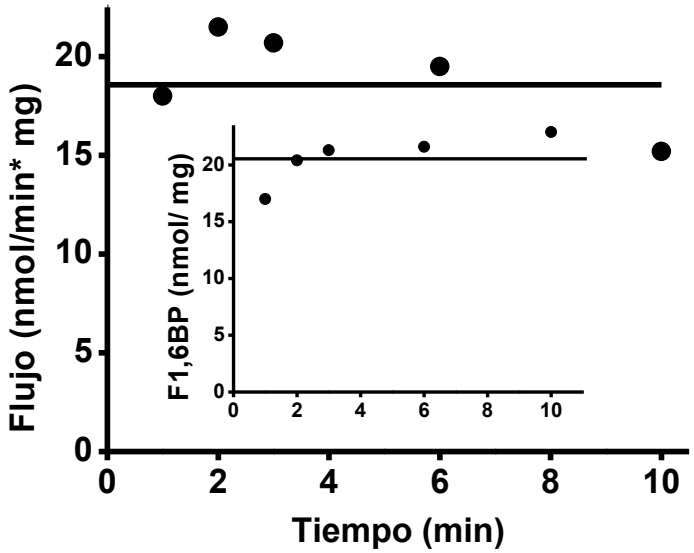

Figura 5.2.1. Establecimiento de la condición de estado estacionario en la glucólisis de las células AS-30D. Flujo (nmoles de lactato/min x mg proteína) y F1,6BP (nmoles/mg proteína). (n=2)

El siguiente paso fue determinar que los inhibidores empleados para reducir el flujo glucolítico (oxalato y arsenito) al inhibir enzimas de la parte baja de la glucólisis (GAPDH y LDH) no afectaran la actividad de alguna de las enzimas de la parte alta (HK y PFK-1). Se analizaron sobre la actividad de la HK y de la PFK-1 concentraciones de oxalato y de arsenito de 10 mM y 1 mM (5 veces las concentraciones empleadas en las

titulaciones 2 y 0.2 mM, respectivamente), las cuales no modificaron significativamente su actividad. En cambio, la LDH disminuyó su actividad en el intervalo de concentraciones de oxalato empleadas en los experimentos (0.5-2 mM) (Figura 5.2.2). El efecto del arsenito sobre la actividad de la GAPDH no se determinó.

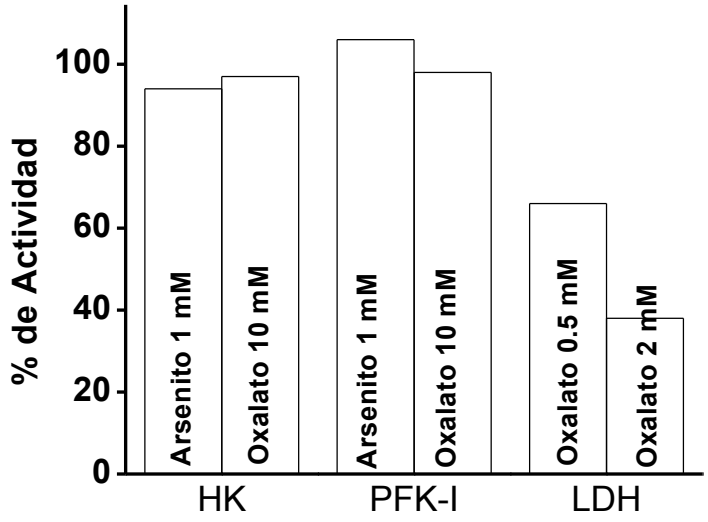

Figura 5.2.2. Efecto del arsenito y del oxalato sobre la actividad de la HK, PFK-1. (n=1)

Finalmente, debido a que la HK ejercía un control importante sobre la glucólisis tumoral, se consideró caracterizar a la enzima. Para ello se determinó su distribución entre el citosol y la mitocondria en células AS-30D (Tabla 5.2.1). Los resultados mostraron que el 50% de la HK estaba en el citosol y el resto estaba unido a la mitocondria, de manera similar a lo observado en otras líneas tumorales (Parry y Pedersen, 1983; Arora and Pedersen, 1988). En HeLa la HK se encontró en mayor proporción en la mitocondria (70%). Debido a que fue difícil obtener mitocondrias de estas células, se estimó primero la cantidad total de enzima en las células completas y luego en extractos celulares se determinó nuevamente la actividad en las fracciones

citosólica (citosol en la tabla 5.2.1) y mitocondrial (mitocondria en la tabla 5.2.1). Pero nos faltó medir la actividad de una enzima marcadora de la fracción mitocondrial como lo habíamos hecho para AS-30D.

Tabla 5.2.1 Distribución de la HK en las células AS-30D y HeLa.

	% de actividad	
Enzima	**Citosol**	**Mitocondria**
	AS-30D	
HK	52 ± 9 (3)	48 ± 9 (3)
HPI	88 (2)	12 (2)
Citocromo C oxidasa	15.5 (2)	84.5 (2)
	HeLa	
HK	31.7 (2)	67.8 (2)
HPI	92.8 (2)	7.3 (3)

Con base en nuestros resultados sobre el análisis de elasticidades se diseñó un problema que fue publicado en la Revista de Educación Bioquímica en la sección Problema Bioquímico (ver apéndice).

5.1.2 Comentarios sobre el manuscrito No. 2

En este manuscrito, por medio del análisis de elasticidades, logramos establecer que el bloque productor de G6P (GLUT + HK) es el que mantenía la mayor parte del control sobre la glucólisis. Además, también determinamos que la PFK-1 no ejercía un control significativo. Lo anterior nos llevó a caracterizar cinéticamente a la HK y a la PFK-1 para encontrar una explicación mecanística de estos resultados. La

caracterización reveló que la HK mantenía un control importante porque independientemente de su localización (citosol y membrana externa mitocondrial) no se modificaba la afinidad por sus sustratos (glucosa y ATP) ni tampoco su sensibilidad al efecto inhibitorio de la G6P: aunque había una sobre-expresión de la HK en células tumorales, su actividad incrementada producía más producto y por tanto más inhibición. Por otra parte, se demostró que la PFK-1 no controlaba porque la presencia de la F2,6BP y el AMP impedían que la enzima fuera inhibida por el citrato y el ATP. Estos resultados nos permitieron concluir que el GLUT y la HK son los principales puntos de control de la glucólisis tumoral y que al no ejercer un control significativo la PFK-1 se explicaba la ausencia del efecto Pasteur en las células tumorales.

Cabe señalar que no realizamos una caracterización cinética del GLUT en este estudio, sin embargo posteriormente en nuestro laboratorio se logró determinar que la isoforma que predomina en las células AS-30D del transportador de glucosa es el GLUT3 que tiene una alta afinidad por glucosa (*Km* = 0.5 mM) (Rodríguez-Enríquez et al., 2009), pero que con respecto al resto de las enzimas, es el transportador el que tiene la menor velocidad. Este resultado apoyaba nuestra propuesta de que el transportador ejercía un control significativo sobre la glucólisis.

A partir de la fecha de la publicación de nuestros resultados hasta estos momentos no se encuentran documentados estudios sobre el control de la glucólisis en células tumorales o estudios similares al nuestro aplicando el análisis de elasticidades u otra estrategia experimental derivada del análisis de control metabólico en otra vía metabólica. Esto puede deberse a lo complejo que puede resultar el aplicar el análisis de elasticidades, dado que los metabolitos que deben emplear son aquellos que se pueden considerar como metabolitos “esclavos”, es decir aquellos que únicamente son

producidos o consumidos en la vía de estudio o que su consumo por otras vías es limitado. Con ello se facilita el agrupar a las enzimas que forman la vía en dos bloques, el bloque productor y el bloque consumidor del metabolito de interés. Por ende, metabolitos como los adenin-nucleótidos (ATP, ADP y AMP) que son productos o sustratos de diversas vías metabólicas (metabolitos promiscuos) no pueden emplearse para este tipo de estudios.

Por otra parte, aunque podría considerarse ventajoso el empleo de inhibidores poco específicos para modular la actividad de los bloques, debe considerarse que únicamente deben observarse cambios en las concentraciones de los metabolitos esclavos, sin afectarse drásticamente las concentraciones de los metabolitos promiscuos.

5.2 Construcción de modelos cinéticos de la glucólisis tumoral

Debido a que por medio del análisis de elasticidades no era posible determinar el control que ejercía individualmente la HK y el GLUT en AS-30D por las dificultades técnicas para medir la glucosa libre intracelular y sobre todo porque para extender nuestro estudio a células tumorales humanas era necesario disponer de una gran cantidad de material biológico, se decidió construir en el programa "Gepasi" un modelo cinético de la glucólisis de las células AS-30D, considerando las ecuaciones cinéticas correspondientes para cada enzima. Para la validación experimental del modelo cinético, se determinaron en paralelo las concentraciones de los metabolitos y los flujos de la vía, además de comparar los valores de la distribución de control que el modelo predecía con aquellos obtenidos previamente por medio del análisis de elasticidades (Manuscrito No. 2 de esta tesis). Para construir el modelo fue necesario determinar los parámetros cinéticos (velocidades máximas "forward", V_{mf}; velocidades máximas "reverse", V_{mr}; afinidad por sustratos, K_{ms}; afinidad por productos, K_{mp}; constantes de activación, *Ka*; constantes de inhibición *Ki*) de cada una de las enzimas, la velocidad de la glucólisis, los flujos de algunas ramificaciones (síntesis-degradación de glucógeno y la vía de las pentosas fosfato) y las concentraciones en estado estacionario de todos los metabolitos de la vía . Una vez validado este modelo, se uso como base para la construcción de un modelo de la glucólisis en células tumorales humanas (HeLa, cáncer cervico-uterino). El manuscrito con estos resultados fue aceptado para su publicación en la Revista ***Biochimica et Biophysica Acta*-*Bioenergetics***.

Biochimica et Biophysica Acta xxx (2010) xxx–xxx

Factor de impacto 2009: 3.68

Contents lists available at ScienceDirect

Biochimica et Biophysica Acta

journal homepage: www.elsevier.com/locate/bbabio

Modeling cancer glycolysis☆

Alvaro Marín-Hernández, Juan Carlos Gallardo-Pérez, Sara Rodríguez-Enríquez, Rusely Encalada, Rafael Moreno-Sánchez *, Emma Saavedra *

Departamento de Bioquímica, Instituto Nacional de Cardiología, México D.F. 14080, Mexico

ARTICLE INFO

Article history:
Received 4 June 2010
Received in revised form 1 November 2010
Accepted 9 November 2010
Available online xxxx

Keywords:
Metabolic control analysis
Flux-control coefficient
Hexokinase
Phosphofructokinase type 1
Glucose transporter
Combined therapy

ABSTRACT

Most cancer cells exhibit an accelerated glycolysis rate compared to normal cells. This metabolic change is associated with the over-expression of all the pathway enzymes and transporters (as induced by HIF-1α and other oncogenes), and with the expression of hexokinase (HK) and phosphofructokinase type 1 (PFK-1) isoenzymes with different regulatory properties. Hence, a control distribution of tumor glycolysis, modified from that observed in normal cells, can be expected. To define the control distribution and to understand the underlying control mechanisms, kinetic models of glycolysis of rodent AS-30D hepatoma and human cervix HeLa cells were constructed with experimental data obtained here for each pathway step (enzyme kinetics; steady-state pathway metabolite concentrations and fluxes). The models predicted with high accuracy the fluxes and metabolite concentrations found in living cancer cells under physiological O_2 and glucose concentrations as well as under hypoxic and hypoglycemic conditions prevailing during tumor progression. The results indicated that HK ≥ HPI > GLUT in AS-30D whereas glycogen degradation ≥ GLUT > HK in HeLa were the main flux- and ATP concentration-control steps. Modeling also revealed that, in order to diminish the glycolytic flux or the ATP concentration by 50%, it was required to decrease GLUT or HK or HPI by 76% (AS-30D), and GLUT or glycogen degradation by 87–99% (HeLa), or decreasing simultaneously the mentioned steps by 47%. Thus, these proteins are proposed to be the foremost therapeutic targets because their simultaneous inhibition will have greater antagonistic effects on tumor energy metabolism than inhibition of all other glycolytic, non-controlling, enzymes. This article is part of a Special Issue entitled Bioenergetics of Cancer.

1. Introduction

Cancer treatments are mostly based on the higher susceptibility of tumor cells to damage caused by radiation and chemotherapy compared to normal non-proliferating cells. However, their severe side effects in the patients and the frequent lack of tumor response (due to inherent or acquired resistance) make necessary the development of novel therapeutic strategies to fight this deadly disease. Hence, the identification of the main differences at the molecular and functional levels between normal and tumor cells is essential in the search for new therapeutic targets.

In this regard, the most frequent metabolic alteration in the majority of tumor cells is a higher glucose consumption (with a concomitant higher lactate production) compared to normal cells [reviewed in 1,2]. The accelerated glycolysis rate can provide the required glycolytic intermediary precursors for DNA, protein and lipid synthesis necessary to sustaining the active proliferation of tumor cells. Moreover, glycolysis can be the main energy-generating pathway under conditions where mitochondrial function is absent or diminished such as in the initial non-vascular stages of tumor progression where hypoxic conditions prevail.

The cellular mechanisms involved in augmenting the glycolytic flux are the simultaneous increased transcription of the genes encoding glycolytic enzymes and transporters in processes mediated by the hypoxia-inducible factor 1α (HIF1α) and other oncogenes [reviewed in 3–5]. The higher transcription coupled to higher translation are responsible for the increased contents and activities of glycolytic

Abbreviations: AlaTA, alanine transaminase; ALDO, fructose 1,6 bisphosphate aldolase; $C^{J_i}_{E_i}$ concentration control coefficient; DHAP, dihydroxyacetone phosphate; ENO, enolase; Ery4P, erythrose-4-phosphate; FBP, fructose-1,6-bisphosphate; F6P, fructose-6-phosphate; F2,6BP, fructose-2,6-bisphosphate; $C^{J}_{E_i}$, FCC, flux control coefficient; GAPDH, glyceraldehyde-3-phosphate dehydrogenase; G1P, glucose-1-phosphate; G3P, glyceraldehyde-3-phosphate; G6P, glucose-6-phosphate; G6PDH, glucose-6-phosphate dehydrogenase; GLUT, glucose transporter; αGPDH, α-glycerophosphate dehydrogenase; HK, hexokinase; HPI, hexose-6-phosphate isomerase; LDH, lactate dehydrogenase; MPM, mitocondrial pyruvate metabolism; PEP, phosphoenolpyruvate; PFK-1, phosphofructokinase type 1; PGAM, 3-phosphoglycerate mutase; PGK, 3-phosphoglycerate kinase; PGM, phosphoglucomutase; PPP, pentose phosphate pathway; Pyr, pyruvate; PYK, pyruvate kinase; Rib5P, ribose 5-phosphate; TPI, triosephosphate isomerase; TA, transaldolase; TK, transketolase; Xy5P, xylulose 5-phosphate; 2PG, 2-phosphoglycerate; 3PG, 3-phosphoglycerate; 6PG, 6-phosphogluconate; 3PGDH, 3 phosphoglycerate dehydrogenase

☆ This article is part of a Special Issue entitled Bioenergetics of Cancer.

* Corresponding authors. Departamento de Bioquímica, Instituto Nacional de Cardiología, Juan Badiano No. 1, Col, Sección XVI, Tlalpan, México D.F. 14080, Mexico. Tel.: +52 555573 2911x1298.

E-mail addresses: rafael.moreno@cardiologia.org.mx (R. Moreno-Sánchez), emma_saavedra2002@yahoo.com (E. Saavedra).

0005-2728/$ – see front matter © 2010 Elsevier B.V. All rights reserved.
doi:10.1016/j.bbabio.2010.11.006

enzymes and transporters which result in an increased pathway flux. HIF-1α induces the expression of specific glycolytic protein isoforms (*i.e.*, GLUT1, GLUT3, HKI and II, PFK-L, ALDO-A and C, PGK1, ENO-a, PYK-M2, LDH-A and PFKFB-3) which are not usually found together in normal cells. Some of these isoforms show lower sensitivity to physiological inhibitors and lower affinity for products, thus favoring a higher forward (glycolytic) rate compared to normal cells [reviewed in 5].

Because of its relevance on tumor metabolism, inhibition of glycolytic flux has been considered an alternative strategy for cancer treatment [reviewed in 6]. However, since both tumor and non-tumor cells contain a similar set of glycolytic enzymes, it is mandatory to find striking differences in pathway control so that the tumor enzyme(s) with the highest control be different to those in normal cells. Perhaps some of the side-effects induced by anticancer glycolytic drugs have derived from their lack of specificity, targeting both cancer and non-cancer cells.

Metabolic Control Analysis (MCA) has shown that the control of a pathway flux or a metabolite concentration is distributed in different degrees among all the pathway enzymes, thus circumventing the misleading and qualitative concept of the "rate-limiting step" and moving into a quantitative analysis of the control of metabolic pathways [7–9]. MCA allows for the quantitative determination of the degree of control that each enzyme has over the pathway flux and the intermediary concentrations, namely, the flux control coefficient (C^J_{Ei}) and the concentration control coefficient (C^M_{Ei}), respectively, where *J* is flux, *M* is a metabolite concentration and *Ei* is a pathway enzyme. A practical definition of these coefficients is the percentage of change in flux or metabolite concentration when a 1% change in a pathway enzyme activity is attained.

By applying different experimental approaches such as elasticity analysis and metabolic modeling, the control distribution of a metabolic pathway can be determined [7,8]. The advantages of the elasticity analysis strategy are that it allows determining of the control distribution in living cells, and that it is not required to know the complete set of the kinetic parameters of the pathway enzymes. In a previous work, elasticity analysis was applied to glycolysis in rodent AS-30D hepatoma [10]. The results indicated that the pathway was mainly controlled by the glucose transporter (GLUT) *plus* hexokinase (HK) segment (71%; *i.e.*, $C^J_{GLUT+HK}=0.71$), with lesser control attained by phosphofructokinase 1 (PFK-1) ($C^J_{PFK\text{-}1}=0.06$). The rest of the control ($C^J_{Ei}=0.25$) resided within the aldolase (ALDO) to lactate dehydrogenase (LDH) segment [10].

As elasticity analysis relies on quantifiable small changes in pathway intermediary concentrations, thus dividing the analyzed pathway in segments, this approach determines control coefficients only by group of enzymes. Hence, in our previous study it was not possible to define in the glucose-6-phosphate producing segment which individual step, GLUT, HK or even glycogen degradation, was exerting the main flux control.

Kinetic modeling of a metabolic pathway integrates all available information (detailed kinetic properties of the individual enzymes and transporters, metabolite concentrations and pathway fluxes) into a functional, cross-talking network that attempts to simulate what occurs in the intracellular milieu [reviewed in 8,11]. Thus, the aim of kinetic modeling is to construct a model able to predict the fluxes and concentrations found in a cell under different specific metabolic steady-states. Validated models allow for the identification of the mechanisms by which a metabolic pathway is controlled and also provide the individual C^J_{Ei} and C^M_{Ei} for each pathway step. By extending this approach to normal (host, normal cells) and pathologic systems (tumor cells, parasites) the enzymes and transporters with the highest control in the latter and low control in the former can be identified and hence proposed as the best and most adequate therapeutic targets [8,12].

In the present work, we report on the kinetic modeling of glycolysis in rat AS-30D hepatoma and in human HeLa tumor cells under normoxic and physiological glucose concentration conditions characteristics of *in vitro* culture experimentation and under hypoxic and glucose deprivation conditions prevailing during tumor formation. The results indicated that in the evaluated conditions, the flux control was shared mainly among HK ≥ HPI > GLUT in AS-30D cells and glycogen degradation ≥ GLUT > HK in HeLa cells. Further modeling analysis showed that simultaneous inhibition of these controlling steps has greater negative effects on tumor glycolysis than inhibition of non-controlling reactions.

2. Experimental procedures

2.1. Enzymes and chemicals

HK, G6PDH, HPI, ALDO, GAPDH, αGPDH, αGPDH/TPI, PYK/LDH, LDH, G1P; G6P and F6P were purchased from Roche (Manheim, Germany). Recombinant enzymes ENO, PPi-PFK and PGK from *Entamoeba histolytica* were those previously described [13]. Glucose (Glu), 6PG, FBP, G3P, 2PG, 3PG, PEP, Pyr, Rib5P, Ery4P, Xy5P, ATP, ADP, GTP, DTT, cysteine, NADH, NAD^+, $NADP^+$, 6PGDH, amyloglucosidase, TK, TA, $MgCl_2$ and lyophilized ALDO, αGPDH and TPI were from Sigma (St Louis, MO, USA). DHAP was from Fluka (Buchs, Switzerland). Mops and Hepes were from Research Organics (Cleveland, Ohio, USA). Potato PPi-PFK was purified as previously described [14].

2.2. Enzyme activities

Clarified cytosolic extracts from AS-30D and HeLa cells were prepared as previously described [10]. Glycolytic enzyme activities and affinity constants were determined for the forward (glycolytic) and reverse (gluconeogenic) reactions in 50 mM Mops buffer pH 7.0 (assay buffer) at 37 °C by following the $NAD(P)^+$ reduction or NAD(P)H oxidation at 340 nm in a spectrophotometer (Agilent; Santa Clara, CA, USA). Standard kinetic assays were initially used [15,16], but the substrate concentrations were always adjusted to ensure they were saturating for the tumor cell enzymes. The activities were determined under initial-rate conditions; the reactions were started by adding the specific substrates and the absorbance baseline in the absence of one substrate was always subtracted. PGM, AlaTA and 3PGDH activities were determined by standard assays [15,16]. TK and TA were measured according to [17].

The Ery4P, FBP and 6PG inhibition on HPI in the forward direction was determined in assay buffer containing 5 mM $MgCl_2$, 1 mM PPi, 0.15 mM NADH, 1 U *E. histolytica* PPi-PFK, 0.36 U ALDO, 9 U TPI, 3.1 U αGPDH and 0.003–0.014 mg of cytosolic extract *plus* 13.8–28 μM Ery4P, 30–60 μM 6PG or 3–10 mM FBP. The reaction was started by adding G6P (0.1–7 mM). HPI inhibition was also evaluated in the reverse reaction in assay buffer containing 1 mM $NADP^+$, 2 U G6PDH, and 13–55 μM Ery4P, 40–90 μM 6PG or 3–10 mM FBP, and 0.001–0.01 mg of extract. The reaction was started with the addition of 0.05–10 mM F6P.

PFK-1 activity was determined according to [10] with lyophilized (ammonium-free) coupling enzymes.

2.3. Steady-state metabolite concentrations

AS-30D hepatoma cells were collected from rat ascites fluid. HeLa cells were cultured under normoxic (95% air–5% CO_2) conditions in Dulbecco-MEM medium at 37 °C as previously described [18]. For hypoxic conditions, HeLa cells were initially grown under normoxia; then at 75–90% confluency, cells were subjected for 24 h to 0.1–0.2% oxygen in a humidified hypoxia incubator chamber (Billups-Rothenberg, California, USA) as described before [19].

The experimental protocol to attain glycolytic flux under steady-state conditions was described elsewhere [10]. Briefly, the cells were harvested, washed and re-suspended in Krebs–Ringer medium (125 mM NaCl, 5 mM KCl, 1 mM $MgCl_2$, 1.4 mM $CaCl_2$, 1 mM KH_2PO_4, and 25 mM Hepes, pH 7.4). The cells were incubated at 37 °C under orbital shaking; after 10 min, 5 mM glucose (or 1 mM for AS-30D under

low glucose concentration) was added and incubated for another 3 min and the reaction was terminated by perchloric acid (3% v/v, final concentration) extraction.

Glycolytic metabolite concentrations were determined as previously described [10]. The concentrations of NAD^+, G1P, alanine and 6PG were determined in neutralized extracts as described before by using LDH; PGM plus G6PDH; AlaTA plus LDH and 6PGDH, respectively [20]. The Ery4P concentration was determined in 50 mM Hepes, 1 mM EGTA, pH 7.4, *plus* 0.7 mM Xy5P, 5 mM $MgCl_2$, 0.5 mM $NADP^+$, 0.04 mM thiamine pyrophosphate (TPP), 1 U/ml of each HPI and G6PDH, and 0.5 U/ml of TK.

For F2,6BP determination, after the 3 min incubation with glucose, the cells were quickly spun down; the pellet was re-suspended in 25 mM Tris–HCl pH 7.6 and the cells were disrupted by freezing in liquid N_2 and thawing at 37 °C three times. The homogenate was centrifuged at 20,800×*g* for 3 min at 4 °C. The supernatant was alkalinized with NaOH to a final concentration of 0.1 mM and heated at 80 °C for 5 min. The sample was centrifuged and the supernatant was neutralized with acetic acid. F2,6BP was determined by using potato PPi-PFK as described elsewhere [14].

For determination of the total intracellular Pi, cells were incubated for 3 min with glucose, and then a sample of 1 ml was withdrawn and centrifuged at 800×*g* for 30 s. The cell pellet was washed three times with saline (0.9% NaCl) and re-suspended in 1 ml of the same solution. The cellular suspension was divided into two; the first sample was centrifuged at 20,800×*g* for 1 min and the supernatant was recovered whereas the second sample was extracted with perchloric acid (3% v/v final volume), centrifuged for 5 min as above and the supernatant was recovered. Pi was determined in the supernatants as described elsewhere [21]. The intracellular total Pi content was calculated from the difference between the Pi present in the first supernatant (extracellular Pi) from that in the second supernatant (extracellular plus intracellular Pi). The concentration of cytosolic free Pi was calculated assuming that only 53% of the total content was in its free form, as previously determined in hepatocytes [22].

2.4. Metabolic fluxes

For the determination of the glycogen synthesis and degradation fluxes, AS-30D cells (15 mg protein/ml) were pre-incubated at 37 °C for 10 min in Krebs–Ringer medium. Then, an aliquot was withdrawn (t = 0) and 5 mM glucose was added to the cellular suspension and kept under the same conditions. Aliquots were taken at 10 and 30 min, immediately centrifuged, and the cellular pellet was frozen in liquid N_2 and kept at −70 °C until use. The pellet was further re-suspended in 0.3 ml of 30% KOH and heated for 30 min at 90 °C; afterwards, the sample was mixed with 0.1 ml 6% Na_2SO_4 and 0.9 ml 100% ethanol and centrifuged at 20,800 *g* for 5 min. The pellet was washed once with 1 ml of 80% ethanol and let dry at room temperature. Then, the pellet was re-suspended in 0.5 ml 0.2 M acetate buffer pH 4.8 *plus* 5 U amyloglucosidase and incubated for 1 h at 37 °C. Glucose units derived from glycogen breakdown were determined by enzymatic analysis by using HK and G6PDH [20] and reported as nmol of glucose equivalents. After the addition of glucose, the glycogen degradation rate was calculated from the difference of glucose equivalents in glycogen from the 10 min *minus* 0 min incubation, whereas the glycogen synthesis rate was calculated from the difference of glucose equivalents in glycogen from the 30 min *minus* 10 min incubation. For HeLa cells, glycogen synthesis and degradation rates were determined in cells (5–7 mg protein) incubated with and without glucose, respectively. The samples were taken at 0 and 3 min and treated as described above.

For the pentose phosphate pathway (PPP) flux, AS-30D cells were incubated as described above for glycogen metabolism analysis. After glucose addition, samples were withdrawn at 2, 4 and 6 min and immediately precipitated with perchloric acid, centrifuged and the supernatant neutralized. The 6PG content was determined in the neutralized extracts by using a 6PGDH assay [20]. The rate was calculated from the differences in 6PG concentrations at different time points.

The pyruvate consumption rate by mitochondria (mitochondrial pyruvate metabolism; MPM) was estimated from the total cellular oxygen consumption rate *minus* that in the presence of 5 μM oligomycin, and assuming that the main substrate consumed by mitochondria was the endogenous pool of pyruvate generated by the cells (equivalent to 4 mg cellular protein) incubated with 5 mM glucose for 5 min. For the calculations it was assumed that 6 mol of O_2 (12 atoms oxygen) are consumed *per* mol of completely oxidized glucose. It is noted that the MPM flux is the result of the coordinated activities of the pyruvate transporter, pyruvate dehydrogenase complex, Krebs cycle enzymes, respiratory chain complexes, adenine nucleotide translocator, Pi carrier and ATP synthase.

For the majority of the parameters described above (enzyme activities, metabolite concentrations and fluxes) at least two different batches of cells were assayed. The high dispersion in the experimental data is very common when using non-chemostat cultures and when using different batches of cellular cultures. On the other hand, lower dispersions can be certainly obtained by measuring triplicates of one homogeneous cell culture, but such results only represent one independent sampling.

2.5. Construction of the kinetic models

The models were constructed by using the software Gepasi v 3.3 [23] available at the web site http://www.gepasi.org/. Fig. 1 diagrammed the pathway reactions considered in both models. The reactions were written in the program as described in Table S1 and a summary of all the used kinetic parameters is provided in Tables S2, S3, and S4 of supplementary material.

All glycolytic reactions (including those of HK, PFK-1 and PYK) were considered reversible. For most of them, their *Vm* values were determined in cytosolic extracts in the forward and reverse reactions (Table 1) thus avoiding the use of *Keq* values taken from the literature in the rate equations (see below). Since these *Vm* values actually corresponded to those of the enriched cytosolic fractions, these were also experimentally determined in whole cells which were solubilized with 0.02% Triton X-100 to obtain the corresponding *Vm* in total cellular protein units (Table S3); the latter *Vm* values were used in the models.

The kinetic parameters *Vmf*, *Vmr* and *Km* for substrates, products and modulators were all determined under the same conditions of pH (7.0) and temperature (37 °C) (Table 1), whereas those of the glucose transporters were previously determined by our research group [24].

The oxidative and non-oxidative PPP sections, the glycogen synthesis and degradation pathways and the MPM branches were simplified and considered as non-reversible reactions with the constant flux values shown in Table 2. The glycogen metabolism reactions only included the initial substrates and the final products without considering the intermediate reactions catalyzed by PGM. The oxidative PPP section did not include the NADPH production whereas the non-oxidative section only included the reaction catalyzed by TK.

The cellular ATP consuming processes (ATPases) were represented as a mass-action irreversible reaction with an adjusted *k* value of 0.0042. To maintain the pyridine and adenine nucleotide balances, the DHases and adenylate kinase (AK) reactions were used, respectively, with mass-action reversible kinetics whose values were adjusted at $k_1 = 250$ and $k_2 = 1$ and $k_1 = 1$ and $k_2 = 2.26$, respectively. Conserved moieties were $[ATP] + [ADP] + [AMP] = 11.3$ mM and $[NADH] + [NAD^+] = 1.35$ mM.

In the pathway modeling, metabolite concentrations were initialized at the values found in the cells (Tables 3 and 4). Fixed metabolite concentrations were used for lactate, glycogen, 6PG, Ery4P, F2,6BP, Pi, citrate and Xy5P at the values shown in Tables 2–4 (summarized in Table S4 of supplementary material) except for Pi, for which only 53% of the total Pi content was assumed to be free Pi [22].

Please cite this article as: A. Marín-Hernández, et al., Modeling cancer glycolysis, Biochim. Biophys. Acta (2010), doi:10.1016/j.bbabio.2010.11.006

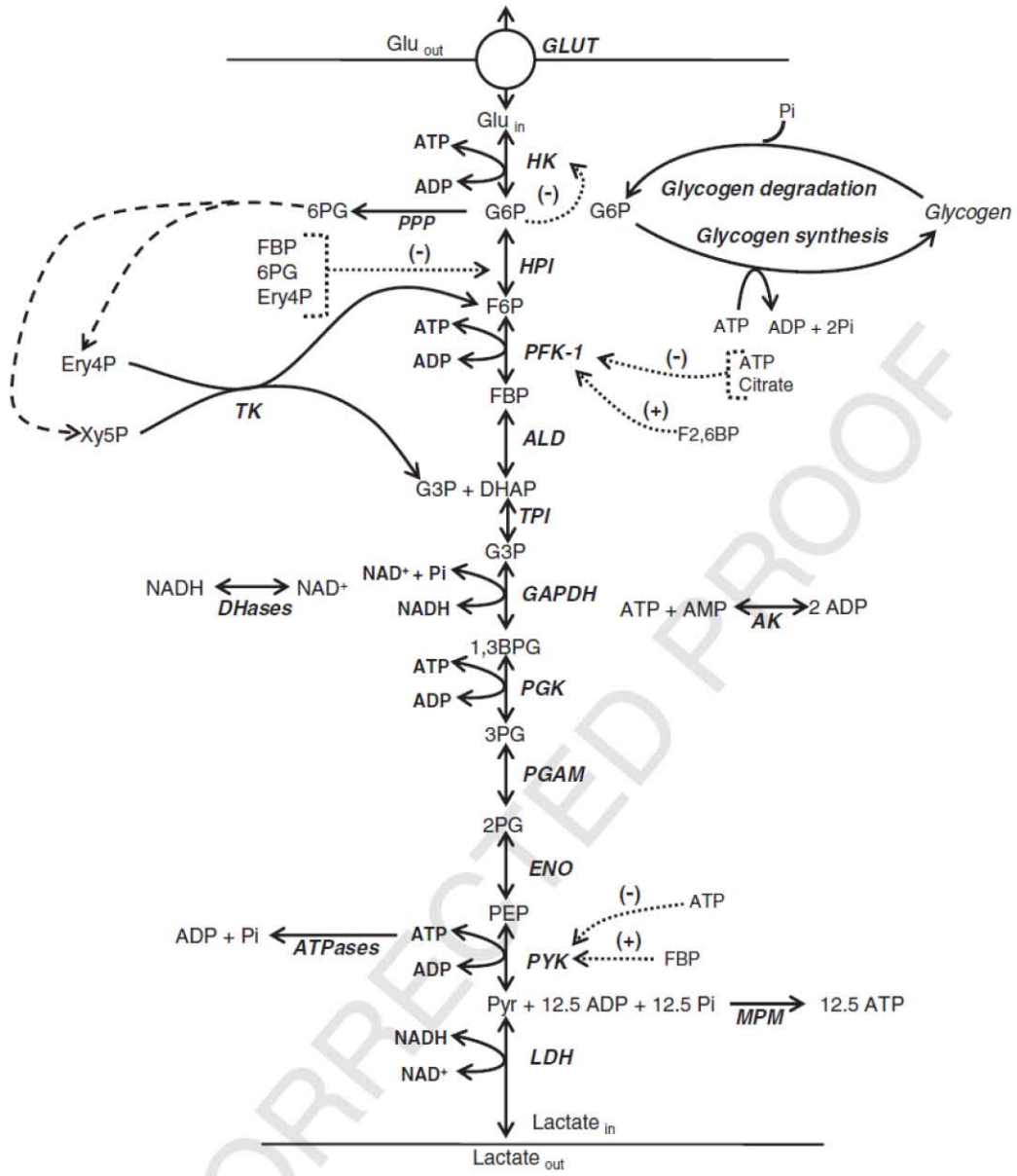

Fig. 1. Pathway reactions included in the kinetic models of glycolysis in AS-30D and HeLa tumor cells. Solid arrows indicate whether reactions are considered non-reversible or reversible in Gepasi; dotted arrows indicate allosteric modulators; dashed arrows indicate PPP existing reactions not included in the model. DHases; NADH consuming enzymes; ATPases, ATP-consuming processes; PPP, pentose phosphate pathway; MPM, mitochondrial pyruvate metabolism. ATP stoichiometry was calculated by using P/O ratios of 2.5 and 1.5 for NADH and $FADH_2$, respectively.

2.6. Rate-equations

The rate-equations used for each reaction are described below.

The kinetics of GLUT was introduced as a monosubstrate reversible Michaelis–Menten equation (Haldane's equation) [25]:

$$v = \frac{Vmf\left([Glu_{out}] - \frac{[Glu_{in}]}{Keq}\right)}{K_{Gluout}\left(1 + \frac{[Glu_{in}]}{K_{Gluin}}\right) + Glu_{out}}$$

in which Glu_{out} and Glu_{in} and K_{Gluout} and K_{Gluin} are the extra- and intra-cellular glucose concentrations and the enzyme's affinity constants (*Km* values), respectively; Keq is the equilibrium constant; and *Vmf* is the maximal velocity in the forward reaction.

The HK rate equation was described as random bi-substrate Michaelis–Menten [25]:

$$v = \frac{\frac{Vmf}{KaKb}\left([A][B] - \frac{[P][Q]}{Keq}\right)}{1 + \frac{[A]}{Ka} + \frac{[B]}{Kb} + \frac{[A][B]}{KaKb} + \frac{[P]}{Kp} + \frac{[Q]}{Kq} + \frac{[P][Q]}{KpKq} + \frac{[A][Q]}{KaKq} + \frac{[P][B]}{KpKb}}$$

in which [A] and [B] represent the substrate concentrations (Glu and ATP, respectively), whereas [P] and [Q] represent the product concentrations (G6P and ADP, respectively). *Ka*, *Kb*, *Kp* and *Kq* represent the enzymes *Km* values for their respective ligands.

The HPI rate equation was introduced as a monoreactant reversible equation with competitive inhibition by Ery4P, 6PG and FBP:

$$v = \frac{Vmf\frac{[G6P]}{K_{G6P}} - Vmr\frac{[F6P]}{K_{F6P}}}{1 + \frac{[G6P]}{K_{G6P}} + \frac{[F6P]}{K_{F6P}} + \frac{[ERY4P]}{K_{ERY4P}} + \frac{[6PG]}{K_{6PG}} + \frac{[FBP]}{K_{FBP}}}$$

Please cite this article as: A. Marín-Hernández, et al., Modeling cancer glycolysis, Biochim. Biophys. Acta (2010), doi:10.1016/j.bbabio.2010.11.006

Table 1
Kinetic parameters of AS-30D and HeLa glycolytic enzymes and transporter.

Enzyme		AS-30D	HeLa	Enzyme		AS-30D	HeLa
GLUT	Vm_f	0.055[a,e]	0.017[a,e]	GAPDH	Vm_f	1[b]	2[b]
	Km_{Glu}	0.52[a]	9.3[a]		Vm_r	0.9[b]	2.5[b]
HK	Vm_f	0.46[b]	0.06[a]		Km_{G3P}	0.29	0.19
	$K_{m\ Glu}$	0.18[b]	0.1		$Km_{1,3BPG}$	0.02	0.022
	Km_{ATP}	0.99[b]	1.1		Km_{NAD+}	0.08	0.09
	Ki_{G6P}	0.02[c]	0.02[c]		Km_{NADH}	0.004	0.01
HPI	Vm_f	4.9 ± 1.9 (3)	1.2 ± 0.2 (3)		**Km_{Pi}**	**11 ± 1 (3)**	**29**
	Vm_r	3.4 ± 1.1 (6)	2.8 (2)	PGK	Vm_f	27[b]	13[b]
	Km_{G6P}	0.9 ± 0.2 (4)	0.4 ± 0.03 (3)		Vm_r	4.3	3.8
	Km_{F6P}	0.07 ± 0.03 (6)	0.05 (2)		$Km_{1,3DPG}$	0.035	0.079
PFK-1	Vm_f	0.273[d]	0.078[d]		Km_{3PG}	0.12	0.13
	Km_{F6P}	4.6[d]	1.0[d]		Km_{ADP}	0.67	0.04
	Km_{ATP}	0.048[d]	0.021[d]		Km_{ATP}	0.15	0.27
	Ki_{ATP}	1.75[d]	20[d]	PGAM	Vm_f	20[b]	1.4[b]
	Ki_{CIT}	3.9[d]	6.8[d]		Vm_r	1.3	0.53
	Ka_{F26BP}	1.8×10^{-4}[d]	8.4×10^{-4}[d]		Km_{3PG}	0.18 (2)	0.19
ALDO	Vm_f	0.23[b]	0.2[b]		Km_{2PG}	0.04	0.12
	Vm_r	0.18	NM	ENO	Vm_f	0.51[b]	0.36[b]
	Km_{FBP}	0.01	0.009		Vm_r	0.74	0.4
	Km_{G3P}	0.16	NM		Km_{2PG}	0.16	0.038
	Km_{DHAP}	0.08	NM		Km_{PEP}	0.04	0.06
TPI	Vm_f	5.6	5	PYK	Vm_f	6.6[b]	3[b]
	Vm_r	56[b]	42[b]		Km_{PEP}	0.4	0.014
	Km_{DHAP}	1.9	1.6		Km_{ADP}	0.3	0.4
	Km_{G3P}	0.41	0.51	LDH	Vm_f	13.4	11.4
					Vm_r	1.8	NM
					Km_{Pyr}	0.13	0.3
					Km_{Lac}	4.7	NM
					Km_{NAD}	0.07	NM
					Km_{NADH}	0.002	NM

Vm in the forward (Vm_f) and reverse (Vm_r) reactions in U×(mg cytosolic protein)$^{-1}$; *Km* in mM. Values taken from [a][24]; [b][10]; [c][66], [d][Moreno-Sánchez R, Marín-Hernández A, Encalada R and Saavedra E, unpublished results]. [e]*Vm* in U×(mg total cellular protein). The number of independent batches of cells assayed is shown in parentheses; the absence of parenthesis indicates one assayed preparation. NM, not measured.

Table 2
Properties of some glycolytic branches in tumor cells.

	AS-30D	HeLa
Glycogen metabolism		
PGM activity[1]	0.32 ± 0.1 (3)	0.75 ± 0.2 (3)
Km^3_{G1P}	NM	0.07
glycogen content[2]	33 ± 30 (5) (26 mM)[c]	171 ± 55 (4) (135 mM)[c]
G1P content[3]	0.08 ± 0.04 (3)	NM
glycogen synthesis flux[4]	2.2 ± 0.3 (3)	2.4 (2)
glycogen degradation flux[4]	1.2 (2)	12 ± 2 (3)
Pentose phosphate pathway		
G6PDH activity[1]	0.05[a]	0.22[a]
6PG content[3]	0.35 ± 0.13 (5)	0.39
PPP flux[4]	0.096 ± 0.03 (3)	NM
TA activity[1]	0.043 ± 0.006 (3)	0.033 (2)
TK activity[1]	0.010 ± 0.001 (3)	0.037
Ery4P content[3]	1 ± 0.3 (3)	0.016[b]
Xyl5P content	NM	0.016[b]
Triglyceride synthesis		
αGPDH activity[1]	ND[a]	ND[a]
Amino acid metabolism		
3PGDH activity[1]	ND	ND
AlaTA activity[1]	0.046 ± 0.022 (3)	0.012 (2)
Alanine content[3]	ND	ND
Mitochondrial pyruvate metabolism		
Flux of pyruvate consumed by mitochondria[4]	1.8 (2)	NM

[1]U (mg cytosolic protein)$^{-1}$; [2]nmol glucose equivalents (mg total cellular protein)$^{-1}$; [3]in mM; [4]nmol min^{-1} (mg total cellular protein)$^{-1}$. Values were taken from [a][10] and [b][39]. [c]The glycogen concentration was calculated by assuming that 1.8 mg total cellular protein has a volume of 2.28 μl [38]. The values are mean ± SD and the number of independent batches of cells assayed is shown in parentheses: the absence of parenthesis indicates one preparation assayed. NM, not measured; ND, not detected.

Table 3
Glycolytic flux and intermediary concentrations obtained *in vivo* (cells) and by *in silico* modeling for AS-30D cells.

Metabolite	5 mM glucose		1 mM glucose[c]	
	In vivo[a]	Model	*In vivo*[b]	Model
Glu_{in}	6.2 ± 1	3.4	NM	0.8
G6P	5.3 ± 2.6	**6.5**	2 ± 0.5 (4)	3.0
F6P	1.5 ± 0.7	0.03	0.7 ± 0.2 (4)	0.016
FBP	25 ± 7.6	**5.2**	0.6 ± 0.3 (3)	**0.36**
DHAP	10 ± 2.3	**14**	1 ± 0.3 (3)	**4.0**
G3P	0.9 ± 0.4	**0.3**	0.38 (2)	**0.09**
1,3BPG	ND	**0.01**	NM	**0.002**
3PG	ND	**0.01**	NM	**0.005**
2PG	ND	**0.04**	NM	**0.016**
PEP	0.1 ± 0.02	**0.003**	NM	**0.001**
Pyr	2.1 ± 1	**0.84**	**0.72 (2)**	0.78
lactate	27 ± 11	Fixed	NM	Fixed
F2,6BP (×10^{-3})	6 ± 1(3)[b]	Fixed	NM	Fixed
citrate	1.7 ± 0.7	Fixed	NM	Fixed
ATP	5.6 ± 1.2	**7.9**	6 (2)	4.9
ADP	2.4 ± 0.7	**2.1**	**1.5 (2)**	2.9
AMP	3.3 ± 1.4	**1.3**	NM	3.9
Pi	**4.8 ± 1.9 (3)[b]**	**Fixed[d]**	**5 (1)[b]**	**Fixed[d]**
NADH	NM	0.005	NM	0.005
NAD^+	1.3 ± 0.5 (4)[b]	1.34	NM	1.34
Glycolytic flux	21 ± 9	29	10.5 (2)	14

Metabolite concentrations in mM; flux in nmol lactate min^{-1} (mg cellular protein)$^{-1}$. Values taken from [a][10]. [b]This study. [c]In the model, when this condition was simulated, Glu_{out} concentration and glycogen synthesis flux were fixed at values of 1 mM and 1 nmol min^{-1} (mg of cellular protein)$^{-1}$, respectively. **[d]53% of the total Pi concentration shown was assumed to be free Pi [22] which was used for pathway modeling.** Figures in parentheses indicate number of independent cellular extracts assayed. NM, not measured; ND, not detected. Fixed values in the model were at those experimentally determined in cells.

Table 4
Glycolytic flux and intermediary concentrations obtained *in vivo* (cells) and by *in silico* modeling for HeLa cells.

Metabolite	Normoxia		Hypoxia[c]	
	In vivo[a]	Model	*In vivo*[b]	Model
Glu_{in}	NM	**0.61**	NM	**1.4**
G6P	1.3 ± 0.4 (5)[b]	**0.66**	1.4 ± 0.4 (5)	**1.0**
F6P	0.5 ± 0.2 (5)[b]	0.01	0.5 ± 0.2 (5)	0.02
FBP	0.38(2)[b]	**0.14**	0.23 (2)	**0.52**
DHAP	0.93 ± 0.07	**2.0**	0.54	**3.6**
G3P	ND	**0.08**	NM	**0.14**
1,3BPG	ND	0.0009	NM	0.001
3PG	ND	0.006	NM	**0.009**
2PG	ND	0.003	NM	0.004
PEP	0.32	**0.0002**	NM	**0.0003**
Pyr	8.5 ± 3.6	2.5	4.2 (2)	2.6
lactate	33	Fixed	NM	Fixed
F2,6BP ($\times 10^{-3}$)	4.2 ± 0.8 (3)[b]	Fixed	NM	Fixed
citrate	NM	Fixed	NM	Fixed
ATP	8.7 ± 3 (5)[b]	8.4	7.9 ± 4 (5)	**7.7**
ADP	2.7 ± 1.3	2.2	1.8 (2)	**2.1**
AMP	0.4 (2)[b]	1.3	NM	**1.2**
Pi	**7.5 (2)[b]**	**Fixed**	**7.8 (2)[b]**	**Fixed**
NADH	NM	0.005	NM	0.005
NAD^+	NM	1.34	NM	1.34
Glycolytic flux	16 ± 12 (5)[b]	20	21 ± 9 (5)[b]	**29**

Metabolite concentrations in mM; flux in nmol lactate min^{-1} (mg cellular protein)$^{-1}$. Values taken from [a][10]. [b]Present study. [c]For this condition, HK and HPI activities were determined in cells exposed to hypoxia by 24 h; GLUT activity was estimated from the protein content obtained by Western-blot analysis (Fig. 2); the ATPase rate was also adjusted to a value of 4.5×10^{-3}. Figures in parentheses indicate number of independent cellular batches assayed. NM, not measured; ND, not detected. The fixed values used for modeling were those experimentally determined in cells, **except for Pi which was adjusted to the free concentration.**

with Vm_r as the maximal rate in the reverse (gluconeogenic) direction.

The kinetics for TPI, PGAM and ENO were depicted by mono-substrate simple reversible Michaelis–Menten equation:

$$v = \frac{Vmf\dfrac{[S]}{Ks} - Vmr\dfrac{[P]}{Kp}}{1 + \dfrac{[S]}{Ks} + \dfrac{[P]}{Kp}}$$

in which [S] and [P] are the respective concentrations of substrates and products with their respective affinity constants.

PFK-1 is an allosteric enzyme showing cooperative behavior with respect to F6P and hyperbolic kinetics with respect to ATP. The rate equation for this tetrameric enzyme was the concerted transition model of Monod, Wyman and Changeux for exclusive ligand binding (F6P, activators, and inhibitors) [25] together with mixed-type activation (F2,6BP or AMP or Pi) and simple Michaelis–Menten terms for ATP and reverse reaction. ATP (at high concentrations) and citrate are the allosteric inhibitors. L is the allosteric transition constant; Ka_{F26BP} is the activation constant for F26BP; Ki_{CIT} and Ki_{ATP} are the inhibition constants for citrate and ATP; α and β are the factors by which K_{F6P} and Vm change when an activator is bound to the active enzyme form (R conformation in the Monod model).

$$v = Vm\left(\left(\frac{\frac{[ATP]}{K_{ATP}}}{1+\frac{[ATP]}{K_{ATP}}}\right)\left(\frac{1+\frac{\beta F26BP}{\alpha Ka_{F26BP}}}{1+\frac{F26BP}{\alpha Ka_{F26BP}}}\right)\left(\frac{\frac{F6P\left(1+\frac{F26BP}{\alpha Ka_{F26BP}}\right)}{K_{F6P}\left(1+\frac{F26BP}{Ka_{F26BP}}\right)}\left[1+\frac{F6P\left(1+\frac{F26BP}{\alpha Ka_{F26BP}}\right)}{K_{F6P}\left(1+\frac{F26BP}{Ka_{F26BP}}\right)}\right]^3}{L\left(1+\frac{[CIT]}{Ki_{CIT}}\right)^4\left(1+\frac{[ATP]}{Ki_{ATP}}\right)^4}{\left(1+\frac{F26BP}{Ka_{F26BP}}\right)^4}+\left[1+\frac{F6P\left(1+\frac{F26BP}{\alpha Ka_{F26BP}}\right)}{K_{F6P}\left(1+\frac{F26BP}{Ka_{F26BP}}\right)}\right]^4}\right)\right.$$
$$\left.-\left(\frac{\frac{[ADP][FBP]}{K_{ADP}K_{FBP}Keq}}{\frac{[ADP]}{K_{ADP}}+\frac{[FBP]}{K_{FBP}}+\frac{[ADP][FBP]}{K_{ADP}K_{FBP}}+1}\right)\right).$$

The ALDO rate equation was the reversible Uni–Bi Michaelis–Menten equation.

$$v = \frac{Vmf\dfrac{[FBP]}{K_{FBP}} - Vmr\dfrac{[DHAP][G3P]}{K_{DHAP}K_{G3P}}}{1 + \dfrac{[FBP]}{K_{FBP}} + \dfrac{[DHAP]}{K_{DHAP}} + \dfrac{[G3P]}{K_{G3P}} + \dfrac{[DHAP][G3P]}{K_{DHAP}K_{G3P}}}$$

The GAPDH kinetics was described by a simplified ordered Ter–Bi reversible Michaelis–Menten equation:

$$v = \frac{Vmf\dfrac{[NAD][G3P][Pi]}{K_{NAD}K_{G3P}K_{Pi}} - Vmr\dfrac{[DPG][NADH]}{K_{DPG}K_{NADH}}}{1 + \dfrac{[NAD]}{K_{NAD}} + \dfrac{[NAD][G3P]}{K_{NAD}K_{G3P}} + \dfrac{[NAD][G3P][Pi]}{K_{NAD}K_{G3P}K_{Pi}} + \dfrac{[DPG][NADH]}{K_{DPG}K_{NADH}} + \dfrac{[NADH]}{K_{NADH}}}.$$

Rate equations for PGK and LDH were represented by the random Bi–Bi reversible Michaelis–Menten equation for non-interacting substrates (α and β = 1).

$$v = \frac{Vmf\dfrac{[A][B]}{\alpha KaKb} - Vmr\dfrac{[P][Q]}{\beta KpKq}}{1 + \dfrac{[A]}{Ka} + \dfrac{[B]}{Kb} + \dfrac{[A][B]}{\alpha KaKb} + \dfrac{[P][Q]}{\beta KpKq} + \dfrac{[P]}{Kp} + \dfrac{[Q]}{Kq}}.$$

PYK kinetics was represented by the concerted transition model of Monod, Wyman and Changeux rate equation for exclusive ligand binding including PEP as well as FBP activation and ATP inhibition, with simple Michaelis–Menten terms for ADP and reverse reaction.

$$v = Vm\left(\left(\frac{\frac{[ADP]}{K_{ADP}}}{1+\frac{[ADP]}{K_{ADP}}}\right)\left(\frac{\frac{PEP}{K_{PEP}}\left[1+\frac{PEP}{K_{PEP}}\right]^3}{L\left(1+\frac{[ATP]}{Ki_{ATP}}\right)^4}{\left(1+\frac{FBP}{Ka_{FBP}}\right)^4}+\left[1+\frac{PEP}{K_{PEP}}\right]^4}\right)-\left(\frac{\frac{[ATP][PYR]}{K_{ATP}K_{PYR}Keq}}{\frac{[ATP]}{K_{ATP}}+\frac{[PYR]}{K_{PYR}}+\frac{[ATP][PYR]}{K_{ATP}K_{PYR}}+1}\right)\right).$$

The ATPases rate defined as the ATP-consuming cellular processes was depicted as mass-action irreversible reaction, in which k was the rate constant and Si was the substrate concentration.

$$v = k\prod_i Si.$$

The DHases and AK were included as reversible mass-action reactions, in which k_1 and k_2 are the rate constants, Si is the concentration of substrate and Pj is the concentration of product.

$$v = k1\prod_i Si - k2\prod_j Pj$$

The rest of glycolytic branches were adjusted to irreversible constant flux.

3. Results and discussion

3.1. Glycolytic enzyme activities, intermediary concentrations and fluxes in tumor cells

A recurrent difficulty encountered in building kinetic models of metabolic pathways is the lack of all the required kinetic data of the pathway under study, evaluated in the same cellular model, and determined under the same experimental conditions. Despite these inconveniences, some models have been reported for glycolysis in erythrocytes [26,27], yeast [28] and the human-infecting parasites *Trypanosoma brucei* [29] and *Entamoeba histolytica* [16].

Although there is sufficient kinetic information on glycolytic enzymes from a wide variety of tumor cells, most studies are not

Please cite this article as: A. Marín-Hernández, et al., Modeling cancer glycolysis, Biochim. Biophys. Acta (2010), doi:10.1016/j.bbabio.2010.11.006

usually accompanied by thorough cellular metabolic characterizations reporting metabolite concentrations and metabolic fluxes. This is particularly evident in studies based only on determinations of transcriptional changes, from which hypotheses and explanations are formulated about changes in metabolic fluxes and cellular function [reviewed and discussed in 9]. Hence, in order to have a complete kinetic characterization of the glycolytic pathway and its branches in the tumor cells studied here, the maximal velocities in the forward (Vm_f) and reverse (Vm_r) reactions and *Km* values for substrates (Km_s), products (Km_p) and effectors for each glycolytic enzyme were determined in cytosolic extracts from AS-30D and HeLa cells at 37 °C and pH 7.0 (Table 1). A pH value of 7.0 was chosen because the intracellular pH varies from 7.2 to 6.8 when cells are actively consuming glucose [30]. Due to thermodynamic constraints, HK, PFK-1 and PYK activities were only determined for the forward reaction.

In general, most of the enzyme activity (*i.e.*, *Vm*) values (Table 1) were in agreement with those previously reported for the same tumor cell lines [31,32]. In tumor cells, approximately 50–70% of HK activity is bound to mitochondria [10,33,34]; thus, to have an accurate determination of the total HK activity, detergent-permeabilized cells were used (Table S3). Remarkably, HK, PFK-1 and PGAM activities found in cytosolic extracts were 7.6, 3.5 and 14 times higher in AS-30D than in HeLa cells; which contrasted with the similar values obtained for the rest of the pathway enzymes in both cells (Table 1). HK and PFK-1 are 153 and 27 times lower in rat normal hepatocytes (3 and 10 mU/mg protein, respectively) than in the AS-30D hepatocarcinoma [10]. On the other hand, HK activity in human muscle cells is 10 times lower whereas PFK-1 activity in human brain is 3 times higher than in HeLa cells (6 and 258 mU/mg protein, respectively) [35,36]; however, for a more rigorous comparison with HeLa cells, normal proliferating cervix epithelial cells from which these tumor cells derived, should be used.

The *Km* values were similar in the two cell types (Table 1) and were within the same interval found in the BRENDA database (http://www.brenda-enzymes.info/) determined for normal and tumor cells.

The previously reported value for the glycolytic flux in AS-30D cells under normoxia and 5 mM glucose was 21 nmol min^{-1} (mg cellular protein)$^{-1}$ [10] which was used as reference in the present study (Table 3). On the other hand, in HeLa cells a value of 16 ± 12 nmol min^{-1} (mg cellular protein)$^{-1}$ (n = 5) under normoxic conditions was obtained in the present study (Table 4), which was lower than the previously reported value of 32 ± 10 nmol min^{-1} (mg cellular protein)$^{-1}$ [10], indicating variability within the same cell line from culture passage to culture passage. For comparison, normal rat hepatocytes and normal Chinese hamster ovary cells (CHO-K1) show glycolytic flux values of 2.4 and 8 nmol min^{-1} (mg cell protein)$^{-1}$, respectively [10,37]. Thus, the tumor cells used here indeed exhibit increased glycolysis rates compared to normal cells. Glycolytic metabolite concentrations were also previously reported for AS-30D cells incubated with 5 mM glucose [10] and used as reference (Table 3), whereas for HeLa cells under normoxia, values for some metabolites were re-determined (Table 4), finding no statistical difference with those previously reported [10].

The enzyme activities, fluxes and intermediary concentrations of the main glycolytic branches were also evaluated (Table 2): glycogen synthesis and degradation, PPP, triglyceride and serine synthesis, and MPM.

Regarding glycogen, HeLa cells showed 5.2 fold higher content than AS-30D cells and 2.3 fold increased PGM activity (Table 2). The glucose-1-phosphate (G1P) intracellular concentration (0.08 mM; Table 2) was lower than its glycolytic precursor G6P in AS-30D cells (5.3 mM; Table 3). Under the steady-state conditions used, in which extracellular glucose concentration is 5 mM (see Experimental procedures section), the glycogen synthesis and degradation rates were 10–18 times lower (Table 2) than the glycolytic fluxes (Tables 3 and 4) in both tumor cells; with the exception of the glycogen degradation flux in HeLa cells which was 75% the glycolytic flux. The most probable reason for the higher activity in the glycogen degradation branch in HeLa cells was that these are cultured in Dulbecco-MEM medium containing 25 mM glucose, whereas the glucose concentration found in AS-30D ascites fluid is 0.026 mM [38]. Cultivation of HeLa cells under high (25 mM) glucose induces the expression of the ~~low glucose affinity~~ GLUT1, whereas AS-30D hepatoma developed intra-peritoneally in rats predominantly express the ~~high glucose affinity~~ GLUT3 [24]. In consequence, the incubation of HeLa cells in fluxes assay medium containing lower glucose (compared to culture medium) most probably promoted strong activation of glycogen degradation to compensate for the diminished glucose uptake; this compensatory mechanism was apparently not required in AS-30D hepatoma.

In the oxidative section of PPP (Table 2), higher G6PDH activity was found in HeLa than in AS-30D cells, but similar 6PG concentrations. On the other hand, the activities of the PPP non-oxidative section enzymes TA and TK were similar to reported values for the same and other tumor cells (0.019–0.208 and 0.022–0.108 U (mg protein)$^{-1}$, respectively) [17,39]. A lower Ery4P concentration in comparison to that of glycolytic intermediaries (G6P, FBP, and DHAP) was determined, which was slightly higher than the previously reported value for Krebs ascites hepatoma cells (0.5 nmol/mg cellular protein) [40]. The lower PPP flux and enzyme activities (Table 2) compared to glycolytic flux (see text above for values) and enzyme activities (Table 1) suggested low nucleotide synthesis and hence negligible cellular proliferation, as expected from incubations made in a saline buffer for short times (3–10 min). For A549 lung carcinoma and C6 rat glioma, PPP fluxes of 1 and 6 nmol/min*mg protein, respectively, were determined by using radio-labelled glucose and lengthy incubations of 4–6 h in culture medium with glucose and fetal bovine serum, conditions under which cellular growth is favored [41,42]. Then, it seems possible that the PPP fluxes, determined here from 6PG changes (Table 2), were underestimated as the variation in the cellular 6PG content was small and close to the lower detection limit of the method used. Further evaluation of the PPP flux in AS-30D and HeLa cells either with radio-labelled glucose or under cell growth conditions for longer times should resolve this apparent discrepancy.

Low or negligible αGPDH activities, which are involved in triglyceride synthesis, have been reported for several tumor cells [43]; accordingly, αGPDH activity was not detected in AS-30D and HeLa cells [10]. Triglyceride synthesis can also be initiated by DHAP acylation in a reaction catalyzed by DHAP-acyltransferase [44]; however, this enzyme was not determined in the present study and this branch was not included in the model.

A previous report indicated that serine metabolism is accelerated in tumor cells [45]; however, the activity of 3-phosphoglycerate dehydrogenase was not detected when measured in the 3PG oxidation direction (Table 2) and thus, this branch was not included in the model. Alanine transaminase activity (AlaTA) measured in the pyruvate synthesis direction was low in both AS-30D and HeLa cells (Table 2). These low activities correlated with undetectable alanine levels in cellular extracts.

The MPM rate was 11.7 fold lower than the lactate production rate, suggesting that anaerobic glycolysis was favored. It might be possible that the mitochondrial pyruvate transporter expressed in AS-30D cells also has low affinity and low rate as described for Morris 44 and 3924A hepatomas (Vm = 5–12 mU/mg mitochondrial protein and Km_{Pyr} = 0.74–1.1 mM) [46]. The expression of a low activity/low affinity pyruvate transporter would favor a higher pyruvate flux towards lactate because of LDH higher activity and affinity (Vm = 2.0 U/mg cellular protein, Table S3; Km_{Pyr} = 0.13 mM, Table 1). Contributing to the unusually high endogenous pyruvate pool (Tables 3 and 4) may be the active oxidation of alternative substrates such as glutamine, glutamate and proline, which generate malate and hence pyruvate by the action of over-expressed malic enzyme in cancer cells [38,47]. In addition, the onset of the Crabtree effect (OxPhos inhibition by external glucose) should also promote an elevation in the intracellular pyruvate pool [30].

3.2. Building and refinement of the kinetic model of AS-30D glycolysis

The kinetic model of glycolysis in AS-30D cells was constructed by using the Gepasi software. The kinetic parameters *Vm*, *Km* for substrates, products and modulators for the pathway enzymes and glucose transporter from external glucose to lactate production as well as the enzyme activities and fluxes of the pathway branches experimentally determined were used to fulfill the parameters of the rate-equations describing each reaction as detailed in the Experimental procedures section. The metabolite concentrations and the pathway fluxes of glycolysis determined *in vivo* under steady-state conditions (Table 3) and the control distribution obtained by elasticity analysis previously reported by our research group [10] (Table 5) were used as reference parameters for model validation.

In consequence, for model building and validation, a refinement process was recurrently necessary, which in turn prompted an experimental re-evaluation of the kinetic properties of some enzymes as well as the determination of neglected metabolite concentrations and the inclusion of some branches to improve model reproduction of *in vivo* pathway behavior. Thus, this dynamic interplay between modeling and experimentation led to several model and rate equation modifications, from which the three most important are described below.

3.2.1. Kinetics of PFK-1

The first draft of the model included the reactions from external glucose to lactate production and the branch of glycogen metabolism (Fig. 1), in which a simplified version of the PFK-1 rate-equation (hyperbolic kinetics) was used. However, G6P level was too high whereas those of DHAP and G3P were too low. Thus, an improvement of the PFK-1 reaction was necessary.

There is a lack of detailed kinetic analyses of PFK-1 in normal and tumor cells, in which a simple Hill equation for only one modulator is used. Hence, a kinetic characterization of PFK-1 was carried out in AS-30D and HeLa cells (see Experimental procedures section), resulting in a rate-equation that followed the concerted transition model of Monod, Wyman and Changeux together with non-essential activation by F2,6BP (or any other allosteric activator) (Moreno-Sánchez R., Marín-Hernández A., Encalada R. and Saavedra E., unpublished results). The intracellular concentrations of F2,6BP, AMP, ATP and citrate were also determined (Tables 3 and 4). As the activating effect of F2,6BP overcame the inhibitory effect of citrate and ATP, at the tumor physiological concentrations of these modulators (see a simulation in Fig. S1 in supplementary material), the PFK-1 rate in the presence of physiological F2,6BP was 2 fold higher with the concomitant increased in FBP and DHAP to near-physiological levels. However, a marked decrease in the Glu_{in}, G6P and F6P concentrations was attained.

3.2.2. Kinetics of HPI

Through modeling it was noted that a decrease in the HPI activity resulted in a better prediction of the G6P concentration and the glycolytic flux. Hence, the effect of a wide variety of metabolites (ATP, AMP, Pi, PPi, citrate, Ery4P, DHAP, G1P, lactate, 6PG, FBP and F2,6BP) on HPI activity was examined. Most of them showed no effect (Table S5 in supplementary material); in contrast low *Ki* values for Ery4P (0.8–2.5 μM), 6PG (6.8–18 μM) and FBP (60–170 μM) were determined (Table S6). Thus, multiple competitive-type inhibition by Ery4P (Fig. S2), 6PG and FBP was incorporated in the HPI rate-equation. The potent HPI inhibition by these metabolites was not particular of the tumor enzyme, since it was previously reported for the normal rat brain, and rabbit liver and muscle HPIs [48–50] and they also modulated the enzymes from rat hepatocytes, yeast and *E. histolytica* (Table S6). Therefore, the intracellular concentrations of 6PG and Ery4P were also determined in the tumor cells, and in consequence the oxidative section of PPP and TK reaction with their corresponding fluxes (Table 2) and metabolite interactions with HPI were also included in the model (Fig. 1).

3.2.3. Kinetics of the FBP consuming block of enzymes and GAPDH

By including the two modifications described above, the modeled FBP concentration was still several times lower than the physiological concentration, indicating an unrealistic high rate by the ~~consumption~~ block of this metabolite. Thus, the effects of G6P, F6P, Pi, ATP, AMP, Ery4P, F2,6BP and PPi on the enzymes of the ALDO–ENO segment were tested (see Table S5).

ALDO activity was not modulated by any of these metabolites. Although GAPDH was inhibited by ATP (with non-competitive inhibition, $Ki = 4.3$ mM) and ENO was inhibited by DHAP and ATP (non-competitive inhibition, $Ki = 31$ mM, and uncompetitive inhibition, $Ki = 14$ mM, respectively), these *Ki* values were far from the physiological concentrations, and their effects were not included in the rate-equations.

GAPDH from AS-30D cells showed low affinity for Pi (Table 1; Fig. S3) which suggested that Pi availability might regulate the enzyme activity. High Km_{Pi} values for GAPDH from bovine liver, human muscle and sarcoma [51,52] have also been documented. Thus, contrary to other glycolysis kinetic models in which Pi is considered saturating and hence it is not included as pathway metabolite, in the present model Pi was included in the GAPDH rate-equation. On the other hand, from the total intracellular Pi concentration determined (Table 3) only 53% [22] was assumed to be free (*i.e.*, 2.5 mM); this free Pi concentration was used for modeling and was in agreement with values previously determined by nuclear magnetic resonance in rat liver and heart (1.3–2.8 mM) [53,54].

3.2.4. Properties of the kinetic model of glycolysis in AS-30D hepatoma cells

By incorporating (i) the PFK-1 complex rate equation, (ii) the inhibition of FBP, 6PG and Ery4P on HPI, and (iii) Pi in the GAPDH rate-equation, the kinetic model was able to predict with high accuracy the concentration of most of the pathway metabolites and flux rate determined in living cells (Table 3). The most significant exceptions were the predicted FBP (4.8 times lower) and F6P (50 times lower) concentrations. It was found that the FBP steady state concentration directly depended on the Pi concentration within the reported physiological range (Table S7). On the other hand, only by decreasing to 20% the PFK-1 activity, the F6P reached the physiological level; however, this decrease was not experimentally supported because of the strong activation by F2,6BP, AMP and/or Pi. Moreover, under this last condition of 20% activity, PFK-1 became the main flux control step, which was in disagreement with the results obtained by elasticity analysis [10]. Hence, still another unknown kinetic mechanism seems to also modulate the *in vivo* PFK-1 rate.

3.2.5. Control distribution of glycolysis in AS-30D

The analysis performed by Gepasi provided the C^J_{Ei} of all the pathway steps (Table 5). Modeling indicated that the first three reactions of glycolysis exerted most of the flux-control with HK ≥ HPI > GLUT ($\Sigma C^J_{Ei} = 1.04$; Table 5). This control distribution was in agreement with the C^J_{Ei} obtained by elasticity analysis, which indicated that the G6P producer block (GLUT and HK) exerted the main flux-control ($\Sigma C^J_{Ei} = 0.65$–0.71) [10], whereas the C^J_{HPI} value was not possible to be discerned in the previous study, because the high experimental dispersion masked flux-control differences among the different blocks of enzymes analyzed.

HK and HPI showed high flux-control because they were strongly inhibited by glycolytic and PPP intermediaries. It was previously demonstrated [10] that HK exerted significant control on flux in cancer cells because it was strongly inhibited by its product G6P, despite its higher levels of expression compared to normal cells. In particular, AS-30D cells over-expressed the HK-II isoform [24] which partitioned between the cytosol and mitochondria, the latter showing the same affinity constants for glucose, ATP and G6P than the former, cytosolic HK II [10]. Thus, although a hallmark of tumor cells is the

Please cite this article as: A. Marín-Hernández, et al., Modeling cancer glycolysis, Biochim. Biophys. Acta (2010), doi:10.1016/j.bbabio.2010.11.006

Table 5
Flux control coefficients obtained *in vivo* (cells) and by kinetic modeling.

Enzyme	C^J_{Ei}				
	AS-30D	AS-30D model		HeLa model	
	In vivo[a]	5 mM Glucose	1 mM Glucose	Normoxia	Hypoxia
~~GLUT + HK~~		**0.2**	0.12	0.39	**0.32**
	0.71[a]	**0.44**	0.50	0.08	**0.2**
HPI + ~~PPP + glyc~~	−0.02[a]	**0.4**	0.46	0.05	**0.1**
~~synthesis~~		−0.004	−0.009	−0.009	−0.005
		−0.1	−0.1	−0.1	−0.06
Glycogen degradation	NM	0.05	0.11	0.57	**0.33**
PFK-1	0.06[a]	0.02	0.03	0.03	**0.12**
ALDO + TPI + GAPDH + PGK + PGAM + ENO + PYK + LDH	0.24[a]	**0.08** (GAPDH **0.05**)	0.009	0.01	**0.06**
MPM	NM	**0.003**	0.02	−0.004	−0.001
TK	NM	**0.01**	0.023	0.014	0.01
ATPases	NM	**−0.1**	−0.16	−0.02	−0.05

[a] Values taken from [10]. PPP, pentose phosphate pathway; MPM, mitochondrial pyruvate metabolism. NM, not measured. For AS-30D, both conditions were modeled under normoxia. For HeLa, both conditions were modeled in the presence of 5 mM glucose.

increased activity of the glycolytic enzymes, the same enzyme activity regulatory mechanisms are apparently preserved to avoiding unrestricted increase in flux, which in turn can lead to cell death because of the turbo design of glycolysis [55]. On the other hand, HK also exerts significant flux control in normal cells [26,56] making this step less suitable for specific drug targeting in cancer cells.

In turn, HPI displayed a high C^J_E, despite being one of the most active enzymes in the pathway when determined under *Vm* conditions in the absence of modulators (Table 1). However, the potent combined HPI inhibition by FBP and the PPP intermediaries 6PG and Ery4P led to severe activity decrease, becoming now limiting for pathway flux. The modulation of HPI activity by these metabolites might be a control mechanism of the G6P concentration which in turn may exert control on (a) the synthesis of glycogen; (b) the PPP flux for NADPH and ribose-5P syntheses; (c) the production of UDP-glucuronate for proteo-glycan and glycoproteins synthesis and xenobiotic detoxification; and (d) the cellular ATP homeostasis by avoiding its depletion through an enhanced HK reaction. Remarkably, this HPI inhibition was also present in the yeast and ameba enzymes. As the potent inhibition on HPI here described was not considered in previous published models of glycolysis, which might change the control distribution, the putative HPI controlling role remains to be experimentally evaluated in other biological systems. On the other hand, the significant HPI flux control in AS-30D cancer cells (*cf.* Table 5), and its negligible controlling role in normal cells [26,56], indicates that this step is a suitable therapeutic target.

The results on HPI and GAPDH kinetics emphasize the importance, for metabolic modeling, of an extensive knowledge of the enzyme kinetic properties, which should not be restricted to the sole characterization with their substrates, but also to its interaction with its products and with other pathway intermediaries, which are not always assayed when studying the purified enzymes. This has been previously demonstrated by reconstitution of pathway segments of amebal glycolysis [57], in which interactions with non-substrate metabolites but pathway glycolytic intermediaries were elucidated for several enzymes.

GLUT displayed significant flux control ($C^J_{GLUT}=0.2$; Table 5) as previously suggested by elasticity analysis [10] and its kinetic properties [24]. From the main four isoforms (GLUT1–4), AS-30D cells mainly express GLUT3 which has a high affinity for glucose ($Km=0.52$ mM) [24]. Moreover, by over-expressing all GLUT isoforms in *Xenopus* oocytes and determining the kinetics parameters with 2-deoxyglucose, it was previously concluded that GLUT3 is the transporter with the highest catalytic efficiency [reviewed in 5]. In AS-30D cells, GLUT displayed lower activity and catalytic efficiency (*Vm*/*Km*) than HK and HPI; however, the inhibitory effect on the latter two by glycolytic and PPP metabolites decreased their activities to levels that conferred flux-controlling roles. In contrast, in the kinetic models of glycolysis in yeast [28], *T. brucei* [29], *E. histolytica* [16] and heart [56], GLUT contributed by >50% to flux-control. This difference in GLUT flux control between tumor cells and heart indicates that this step might not be an adequate target for cancer treatment, because its inhibition would preferentially affect normal cells over tumor cells.

The rest of the flux-control (0.08) was found in the ALDO–LDH segment (Table 5), which was also in agreement with that obtained by elasticity analysis ($\Sigma C^J_{Ei}=0.24$) [10]. Within this segment, most of the control was accounted by GAPDH ($C^J_{GAPDH}=0.05$), due to its Pi low affinity and hence its dependence on the variation of the Pi concentration in AS-30D cells (Table S7). The ATP demand (ATPases) showed a low flux control but of the negative sign, indicating that this reaction competes with the glycolytic ATP-consuming steps for ATP thus inhibiting the glycolytic flux.

3.2.6. Why a step controls flux?

The HK elasticity coefficient (Table S8) and the catalytic efficiency for ATP (*Vm*/*Km*) were among the lowest in both AS-30D and HeLa glycolysis, indicating near-saturation with concomitant activity insensitivity to variations in ATP, relatively lower transformation efficiency and hence flux limitation at this level. In turn, the reasons for the HPI high flux control coefficient resided in its step-wise increasing elasticities (sensitivities) towards the potent inhibitors FBP, 6PG and Ery4P, and low elasticity for its product F6P, indicating saturation, and hence strong inhibition and prevalence of the reverse over the forward reaction. Similarly, GLUT catalytic efficiency was the lowest among the pathway steps, indicating strong flux restriction; in addition, in HeLa cells, GLUT elasticity for its product, Glu_{in}, was one of the lowest, indicating near-saturation and perhaps product-inhibition and significant reaction reversibility and correlating with a higher GLUT flux control in these cells. On the other hand, the low flux-control exerted by PFK-1 is explained by the low elasticity towards activators, indicating saturation and hence full activation. If PFK-1 were not fully activated, it would very likely the main controlling step as its elasticity towards F6P is the lowest. On the other hand, the PFK-1 elasticities for citrate, and for their products FBP and ADP, were extremely low because these metabolites were not sensed due to the high *Ki* and *Km*, and low intracellular levels.

3.2.7. Control of metabolite concentrations

The control of the concentration of G6P, PEP and ATP depended on GLUT, HK, HPI and ATPase activities in AS-30D glycolysis and on GLUT, glycogen degradation and ATPase in HeLa glycolysis (Table S9). For the F6P concentration, PFK-1 in both AS-30D and HeLa glycolysis was the predominant controlling step, as expected.

3.2.8. Model robustness

The modeled pathway behavior (*i.e.*, flux-control and concentration control distribution, flux rates and metabolite concentrations) was not significantly altered by changing (decreasing by half or increasing by 2 times) the kinetic parameters of most steps and PPP flux (data not shown). Exceptions were (i) control distribution and/or metabolite concentrations, which varied by more than 50% when changing the main controlling steps GLUT, HK, HPI, PFK-1 and GAPDH *Vm* values (AS-30D model) or GLUT, glycogen degradation, PFK-1 and GAPDH *Vm* values (HeLa model, see below); (ii) FBP concentration, which varied by 21–100% when changing ALDO *Vm* and *Km* values in both models; and (iii) DHAP concentration, which varied by 9–100% when changing TPI, GAPDH, PGK, PGAM, ENO and PYK *Km* values (AS-30D) or only TPI *Km* values (HeLa). Both models were also highly sensitive to changes in the ATPase kinetics, revealing that this step is the weakest component in conferring stability to the pathway.

Notwithstanding the enlisted exceptions, the predicted pathway behavior showed satisfactory robustness, further validating the models constructed for both cancer cell lines.

3.3. Kinetic model of glycolysis in HeLa tumor cells

The kinetic model for HeLa cells glycolysis was constructed based also on the experimental parameters determined in these cells regarding enzyme activities (Table 1), metabolite concentrations and fluxes of the glycolytic pathway (Table 4) and its branches (Table 2), and the rate equations used in the AS-30D model.

The majority of the metabolite concentrations and fluxes predicted by the model correlated well with the *in vivo* concentrations except for F6P and PEP, which were 50- and 1600-times lower, respectively (Table 4). These discrepancies indicated that some kinetic experimentation-based refinement was still needed, most probably at the level of PFK-1 and ALDO, and PYK.

According to the model, the main flux controlling steps in HeLa cells, grown under normoxic and high glucose (25 mM) conditions, and assayed in the presence of physiological glucose (5 mM), were the glycogen degradation pathway and GLUT ($C^J_{glycogen\ degradation} + C^J_{GLUT} = 0.96$), whereas the control exerted by the block of HK + HPI + PFK-1 was 0.16 (Table 5). The higher control attained by GLUT in HeLa cells compared to AS-30D was caused by the over-expression of the GLUT1 isoform, which displays low rate in these cells (0.017 nmol/min*mg cellular protein) and low affinity for glucose (9 mM), resulting in a lower catalytic efficiency than that of GLUT3 in AS-30D cells [24]. At physiological glucose concentration (5 mM), the rate equation for GLUT1 predicts an activity of 25% of its maximal activity (4 nmol min^{-1} mg cellular $protein^{-1}$), which cannot completely account for the observed glycolytic flux (16 ± 12 nmol lactate min^{-1} mg cellular $protein^{-1}$). In consequence, the glycogen degradation pathway activates to provide the bulk of glucose equivalents to reach the observed high glycolytic flux.

The high flux through the glycogen degradation pathway and the higher PGM activity determined in HeLa cells, compared to AS-30D cells, supported a relevant role for this pathway in delivering glucose equivalents for glycolytic flux (Table 2). In fact, HeLa cells incubated in the absence of glucose were able to produce lactate (7 nmol·min^{-1}·mg cellular $protein^{-1}$), which corresponded to 22% of the lactate produced in its presence. In contrast, lactate production in AS-30D cells was completely dependent on available external glucose [10]. On the other hand, at 25 mM glucose, the predicted GLUT1 rate in HeLa cells (11.7 nmol min^{-1} mg cellular $protein^{-1}$) can easily cope with the required glucose supply for the glycolytic pathway, which brings about a decreased flux control exerted by both glycogen degradation and GLUT (data not shown). Moreover, it is well documented that glycogen phosphorylase is inhibited by high glucose and G6P levels, with the consequent decrease in glycogenolytic flux [58]. It might be possible that when HeLa cells are incubated with 5 mM glucose, the intracellular concentrations of these metabolites concomitantly also diminish as a consequence of the low GLUT activity, thus favoring glycogen phosphorylase activation, increasing glycogenolysis and hence acquiring higher flux-control.

Thus, the different control distribution between AS-30D and HeLa cells was probably related to the environmental prevailing conditions in which cells were grown. The low glucose concentration encountered by AS-30D cells in the rat intraperitoneal cavity (0.026 mM) favored the expression of a high affinity GLUT and led to a relatively low glycogen content, whereas the HeLa cell high-glucose containing culture medium (25 mM) favored the expression of a low affinity GLUT and led to high glycogen content.

3.4. Kinetic modeling under different steady-states

It is worth emphasizing that the control distribution as obtained by modeling can only be applied to the specific steady-state condition analyzed, which depended on a particular set of enzyme activities expressed in the cells. Therefore, it was interesting to test the validity of the model predictions in cells subjected to other environmental conditions.

During tumor growth, cells localized far from blood vessels are exposed to hypoxia and nutrient starvation. It is well known that under hypoxia the transcription factor HIF-1α induces an increase in the transcription of most glycolytic genes resulting in an over-expression of the enzymes and transporters of this pathway [reviewed in 5]. On the other hand, under low glucose concentration, an increase transcription of HK-II, PFKB3, GLUT1 and GLUT3 induced by AMP kinase has been observed [59,60].

With the validated kinetic models, low availability of external glucose (for AS-30D) and hypoxia (for HeLa) conditions were examined. To this end, it seemed that only a small set of data was needed to be experimentally re-evaluated by focusing on the steps with the highest control. Although a generalized increased activity under hypoxia in the glycolytic enzymes has been documented for most tumor cells [reviewed in 1], a higher increase activity in non-controlling steps does not affect pathway flux rate and flux-control distribution (Section 3.2.8 above).

3.4.1. Modeling AS-30D glycolysis under low glucose concentration

Steady-state intermediary concentrations and glycolytic flux determined in AS-30D cells incubated with 1 mM glucose were ~50% lower for G6P, F6P, G3P and Pyr, and flux rate, and one order of magnitude lower for FBP and DHAP (Table 3). The AS-30D kinetic model predicted well the values for flux and G6P, FBP, G3P and Pyr concentrations found in the cells, but for DHAP and G3P the values were 4 times higher and 4.2 times lower, respectively (Table 3). Essentially the same flux-control distribution was attained under low glucose (HK ≥ HPI > GLUT), with the glycogen degradation branch gained more control, as expected (Table 5).

3.4.2. Modeling HeLa glycolysis under hypoxic conditions

HeLa cells exposed to hypoxia did not show significant changes in G6P, F6P and ATP steady-state concentrations, whereas a 31% increased glycolytic flux was indeed found compared to cells grown under normoxia (Table 4). Increased enzyme activities under hypoxia for HK and HPI were also determined (37% and 30%, respectively) whereas a 252% increased protein content for GLUT was determined by Western-blot analysis (Fig. 2) and then a corresponding increase in transport activity was assumed for modeling. By introducing these new parameters, the kinetic model satisfactorily predicted the flux rate and the metabolite concentrations (Table 4). In addition, hypoxia did not bring about a change in the control distribution (glycogen degradation > GLUT > HK), although the difference in the control exerted by glycogen degradation and GLUT compared to normoxia (31%) was mainly transferred to HK, PFK-1 and the final pathway segment (Table 5).

The experiment of subjecting HeLa cells to hypoxia and nutrient starvation and determining fluxes, activities and metabolite concentrations is difficult to achieve because of low cell number yields. Therefore, the HeLa model was used to predict the pathway behavior under both conditions (hypoxia and 1 mM glucose; data not shown). The results showed a similar control distribution to that obtained under normoxia and 5 mM glucose (column 5 of Table 5) although with decreases in flux and metabolite concentrations by 36–86%, compared to hypoxia alone (column 6 of Table 5). These accurate predictions under a variety of physiological steady-state conditions revealed again high robustness of the kinetic models adding further validation.

3.5. Enzyme titration for the identification of the best drug targets

The kinetic models allow the relationship between glycolytic flux and a given enzyme activity to be analyzed (Fig. 3). As long as the

Please cite this article as: A. Marín-Hernández, et al., Modeling cancer glycolysis, Biochim. Biophys. Acta (2010), doi:10.1016/j.bbabio.2010.11.006

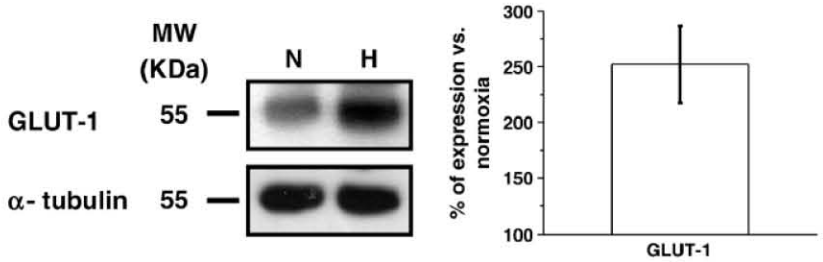

Fig. 2. Glucose transporter protein content after hypoxia treatment in HeLa cells. Bar data represent the mean ± SD of at least three different preparations. N, normoxia; H, hypoxia. Western-blot analysis was carried out according to reference [19].

models may reproduce the *in vivo* pathway behavior, they are a valid tool for identifying the drug targets with the highest therapeutic potential in a metabolic pathway. Thus, GLUT, HK, HPI, PFK-1, TPI and PYK activities were varied in the AS-30D hepatoma glycolysis model, or GLUT, HK, HPI, TPI and the glycogen degradation branch in the HeLa model, to establish how much these potential drug targets should be inhibited for attaining significant decrement in the glycolytic flux and ATP concentration. To decrease the pathway flux (or the ATP concentration; data not shown) by 50%, it was required to inhibit, individually, the main controlling steps HK, HPI or GLUT by 76–78% in AS-30D glycolysis (Fig. 3A), whereas those of HeLa glycolysis GLUT, HK, HPI or glycogen degradation required 87–99% inhibition (Fig. 3B). In contrast, to achieve a similar flux diminution, the non-controlling steps PFK-1, PYK or TPI in AS-30D glycolysis needed to be inhibited by 71%, 99.2% and 99.5%, respectively (Fig. 3A). Interestingly, 50% inhibition of flux (or ATP concentration) was attained, in AS-30D glycolysis, when GLUT + HK or GLUT + HK + HPI were decreased simultaneously by the same magnitude, 63% and 47% inhibition, respectively, whereas in HeLa glycolysis, when GLUT + glycogen degradation were decreased simultaneously by 48% (Fig. 3B).

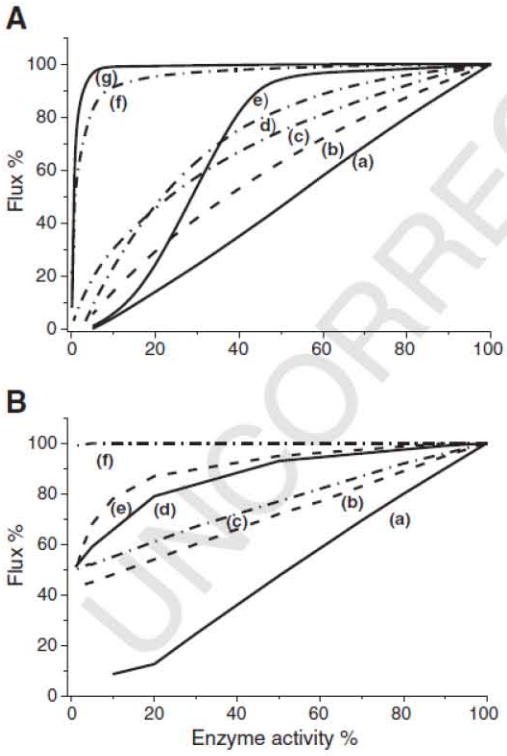

Fig. 3. Dependence of tumor glycolytic flux on enzyme activity. The reference 100% enzyme activity values were those corresponding to the respective *Vm* values for the forward reaction (Tables 1 and S3) whereas 100% fluxes were those predicted by each model (A for AS-30D; B for HeLa cells), which were the fluxes through LDH (29 and 20 nmol min^{-1} (mg cell protein)$^{-1}$, respectively; Tables 3 and 4). In A, enzymes, transporters and braches were (a) GLUT + HK + HPI; (b) GLUT + HK; (c) HK or HPI; (d)GLUT; (e) PFK-1; (f) PYK and (g)TPI. In B, (a) GLUT + glycogen degradation; (b) glycogen degradation; (c) GLUT; (d) HK; (e) HPI and (f) TPI. When two or more steps were titrated, identical variation in activity was applied. A decrease of the Vm_f value was accompanied by a proportional decrease in the Vm_r value.

4. Concluding remarks

The kinetic models for both tumor cells predicted reasonably well fluxes and metabolite concentrations found in living cells. To achieve high robustness, the models were built up with the kinetic properties of each individual enzyme determined experimentally including (a) the most common ligands (substrates, products and modulators), and (b) the interactions of several other pathway intermediaries with the enzymes (Fig. 1). Also, the great majority of the changes made to improve and refine the models were based on "wet" experimentation. This allowed us to identify some mechanisms by which a traditionally considered non-controlling enzyme such as HPI may exert significant control on tumor glycolysis. However, further rounds of model refinement are still necessary to reach more prediction accuracy, especially for F6P and PEP concentrations. Nevertheless, the present models may serve to predict the pathway behavior under other physiological conditions and in other cancer cell lines as long as the most controlling steps are experimentally evaluated.

Thus, kinetic modeling is a helpful theoretical–experimental approach to identifying the most promising therapeutic targets. It has been proposed that inhibition of glycolysis in tumor cells can be an alternative therapeutic strategy [6,61] and several therapeutic targets have been proposed (GLUT1, HKII, PFKFB3, GAPDH, LDH, and MCT) [37, reviewed in 62–65]. It then results of clinical relevance to experimentally evaluate whether such targets are indeed flux control steps of the tumor cells' pathway. Moreover, it would be desirable that such targets have high flux control in tumor cells, but low control in host, normal cells.

In normal cells, HK and PFK-1, together with GLUT, exert the main control on the glycolytic flux [reviewed in 8]. However, due to the different enzyme activity levels, different control distribution was expected, and demonstrated here, between HeLa (glycogen degradation ≥ GLUT > HK) and AS-30D (HK ≥ HPI > GLUT) cells; and between these and normal cells: PFK-1 played a minor role on flux- and metabolite-control in cancer cells, except for the hypoxia condition. The main flux-controlling steps are the targets with the higher potential to diminish the glycolytic flux in the two cancer cells examined. Although the glycogen degradation pathway was a high controlling step in HeLa glycolysis, it could not be an appropriate drug target because glycogen degradation cannot be sustained by prolonged periods of time.

In summary, drug-design studies targeting the most controlling enzymes or transporters in tumor glycolysis might have more promissory results than targeting non-controlling enzymes which usually require more potent and specific inhibitors to accomplish the required full inhibition to achieving effect on function. Another

Please cite this article as: A. Marín-Hernández, et al., Modeling cancer glycolysis, Biochim. Biophys. Acta (2010), doi:10.1016/j.bbabio.2010.11.006

strategy would be that of a multi-targeted therapy against the most controlling steps as previously suggested [*cf.* Fig. 3; see also 9].

From a therapeutic point of view, the kinetic models are useful for predicting how pathway fluxes and ATP concentration may vary when one or more steps are inhibited. The results of the simulations indicated that only the simultaneous inhibition of the controlling steps may have significant impact on glycolytic flux and ATP concentration. Other interventions such as inhibition of solely one controlling step, or worse, of non-controlling steps will bring about negligible effects on pathway behavior. For the latter, their negligible flux-control coefficients demand the design of highly potent and very specific inhibitors for the tumor steps or their full gene transcription or translation blockade.

Supplementary materials related to this article can be found online at doi:10.1016/j.bbabio.2010.11.006.

5. Uncited reference

~~[67]~~

Acknowledgements

This research was supported by CONACyT-México grants No. 80534 and 123636 to RMS and 83084 to ES, and Instituto de Ciencia y Tecnologia del Distrito Federal grant No. PICS08-5. AMH was supported by a CONACyT fellowship (No. 59991).

References

[1] R. Moreno-Sánchez, S. Rodríguez-Enríquez, A. Marín-Hernández, E. Saavedra, Energy metabolism in tumor cells, FEBS J. 274 (2007) 1393–1418.
[2] R. Moreno-Sánchez, S. Rodríguez-Enríquez, E. Saavedra, A. Marín-Hernández, J.C. Gallardo-Pérez, The bioenergetics of cancer: is glycolysis the main ATP supplier in all tumor cells? Biofactors 35 (2009) 209–225.
[3] C.V. Dang, J.W. Kim, P. Gao, J. Yustein, The interplay between MYC and HIF in cancer, Nat. Rev. Cancer 8 (2008) 51–56.
[4] S.J. Yeung, J. Pan, M.H. Lee, Roles of p53, Myc and HIF-1 in regulating glycolysis—the seventh hallmark of cancer, Cell. Mol. Life Sci. 65 (2008) 3981–3999.
[5] A. Marín-Hernández, J.C. Gallardo-Pérez, S.J. Ralph, S. Rodríguez-Enríquez, R. Moreno-Sánchez, HIF-1α modulates energy metabolism in cancer cells by inducing over-expression of specific glycolytic isoforms, Mini Rev. Med. Chem. 9 (2009) 1084–1101.
[6] S. Rodríguez-Enríquez, A. Marín-Hernández, J.C. Gallardo-Pérez, L. Carreño-Fuentes, R. Moreno-Sánchez, Targeting of cancer energy metabolism, Mol. Nutr. Food Res. 53 (2009) 29–48.
[7] D. Fell, Understanding the Control of Metabolism, Portland Press, London, 1997.
[8] R. Moreno-Sánchez, E. Saavedra, S. Rodríguez-Enríquez, V. Olín-Sandoval, Metabolic control analysis: a tool for designing strategies to manipulate pathways, J. Biomed. Biotech. 2008 (2008) 597913.
[9] R. Moreno-Sánchez, E. Saavedra, S. Rodríguez-Enríquez, J.C. Gallardo-Pérez, H. Quezada, H.V. Westerhoff, Metabolic control analysis indicates a change of strategy in the treatment of cancer. Mitochondrion ~~(in press)~~.
[10] A. Marín-Hernández, S. Rodríguez-Enríquez, P.A. Vital-González, F.L. Flores-Rodríguez, M. Macias-Silva, M. Sosa-Garrocho, R. Moreno-Sánchez, Determining and understanding the control of glycolysis in fast-growth tumor cells. Flux control by an over-expressed but strongly product-inhibited hexokinase, FEBS J. 273 (2006) 1975–1988.
[11] J.L. Snoep, The silicon cell initiative: working towards a detailed kinetic description at the cellular level, Curr. Opin. Biotechnol. 16 (2005) 336–343.
[12] J.J. Hornberg, F.J. Bruggeman, B.M. Bakker, H.V. Westerhoff, Metabolic control analysis to identify optimal drug targets, Prog. Drug Res. 64 (2007) 173–189.
[13] E. Saavedra, R. Encalada, E. Pineda, R. Jasso-Chávez, R. Moreno-Sánchez, Glycolysis in *Entamoeba histolytica*. Biochemical characterization of recombinant glycolytic enzymes and flux control analysis, FEBS J. 272 (2005) 1767–1783.
[14] E. van Schaftingen, B. Lederer, R. Bartrons, H.G. Hers, A kinetic study of pyrophosphate: fructose-6-phosphate phosphotransferase from potato tubers, Eur. J. Biochem. 129 (1982) 191–195.
[15] H.U. Bergmeyer, Methods of Enzymatic Analysis, Verlag Chemie, Winheim, 1983.
[16] E. Saavedra, A. Marín-Hernández, R. Encalada, A. Olivos, G. Mendoza-Hernández, R. Moreno-Sánchez, Kinetic modeling can describe in vivo glycolysis in *Entamoeba histolytica*, FEBS J. 274 (2007) 4922–4940.
[17] P.C. Heinrich, H.P. Morris, G. Weber, Behavior of transaldolase and transketolase activities in normal, neoplastic, differentiating and regenerating liver, Cancer Res. 36 (1976) 3189–3197.
[18] S. Rodríguez-Enríquez, P. Vital-Gónzalez, F.L. Flores-Rodríguez, A. Marín-Hernández, L. Ruiz-Ramírez, R. Moreno-Sánchez, Control of cellular proliferation by modulation of oxidative phosphorylation in human and rodent fast-growing tumor cells, Toxicol. Appl. Pharmacol. 215 (2006) 208–217.
[19] S. Rodriguez-Enriquez, L. Carreño-Fuentes, J.C. Gallardo-Pérez, E. Saavedra, H. Quezada, A. Vega, A. Marín-Hernández, V. Olín-Sandoval, M.E. Torres-Márquez, R. Moreno-Sánchez, Oxidative phosphorylation is impaired by prolonged hypoxia in breast but not in cervix carcinoma, Int. J. Biochem. Cell Biol. 42 (2010) 1744–1751.
[20] H.U. Bergmeyer, Methods of Enzymatic Analysis, Weinheim, Verlag Chemie, 1974.
[21] E.S. Baginski, P.P. Foà, B. Zak, Microdetermination of inorganic phosphate, phospholipids, and total phosphate in biologic materials, Clin. Chem. 12 (1967) 326–332.
[22] T.P.M. Akerboom, H. Bookelman, P.F. Zuurendonk, R. Meer, J.M. Tager, Intramitochondrial and extramitochondrial concentrations of adenine nucleotides and inorganic phosphate in isolated hepatocytes from fasted rats, Eur. J. Biochem. 84 (1978) 413–420.
[23] P. Mendes, GEPASI: a software package for modeling the dynamics, steady states and control of biochemical and other systems, Comput. Appl. Biosci. 9 (1993) 563–571.
[24] S. Rodríguez-Enríquez, A. Marín-Hernández, J.C. Gallardo-Pérez, R. Moreno-Sánchez, Kinetics of transport and phosphorylation of glucose in cancer cells, J. Cell. Physiol. 221 (2009) 552–559.
[25] I.H. Segel, Enzyme Kinetics, Wiley, New York, 1975.
[26] T. Rapoport, R. Heinrich, G. Jacobasch, S. Rapoport, A mathematical model of glycolysis of human erythrocytes, Eur. J. Biochem. 42 (1974) 107–120.
[27] F.B. du Preez, R. Conradie, G.P. Penkler, K. Holm, F.L.J. van Dooren, J.L. Snoep, A comparative analysis of kinetic models of erythrocyte glycolysis, J. Theor. Biol. 252 (2008) 488–496.
[28] B. Teusink, J. Passarge, C.A. Reijenga, E. Esgalhado, C.C. van der Weijden, M. Schepper, M.C. Walsh, B.M. Bakker, K. van Dam, H.V. Westerhoff, J.L. Snoep, Can yeast glycolysis be understood in terms of in vitro kinetics of the constituent enzymes? Testing biochemistry, Eur. J. Biochem. 267 (2000) 5313–5329.
[29] B.M. Bakker, M.C. Walsh, B.H. Ter Kuile, F.I.C. Mensonides, P.A.M. Michels, F.R. Opperdoes, H.V. Westerhoff, Contribution of glucose transport to the control of the glycolytic flux in *Trypanosoma brucei*, Proc. Natl Acad. Sci. USA 96 (1999) 10098–10103.
[30] S. Rodríguez-Enríquez, O. Juárez, J.S. Rodríguez-Zavala, R. Moreno-Sánchez, Multisite control of the Crabtree effect in ascites hepatoma cells, Eur. J. Biochem. 268 (2001) 2512–2519.
[31] R. Wu, Regulatory mechanisms in carbohydrate metabolism. V. Limiting factors of glycolysis in HeLa cells, J. Biol. Chem. 234 (1959) 2806–2810.
[32] R. Nakashima, M. Paggi, L.J. Scott, P.L. Pedersen, Purification and characterization of a bindable form of mitochondrial bound hexokinase from the highly glycolytic AS-30D rat hepatoma cell line, Cancer Res. 48 (1988) 913–919.
[33] D.M. Parry, P.L. Pedersen, Intracellular localization and properties of particulate hexokinase in the Novikoff ascites tumor, J. Biol. Chem. 258 (1983) 10904–10912.
[34] K.K. Arora, P.L. Pedersen, Functional significance of mitochondrial bound hexokinase in tumor cell metabolism, J. Biol. Chem. 263 (1988) 17422–17428.
[35] G.E.J. Staal, A. Kalff, E.C. Hessbeen, C.W.M. van Veelen, G. Rijksen, Subunit composition, regulatory properties and phosphorylation of phosphofructokinase from human gliomas, Cancer Res. 47 (1987) 5047–5051.
[36] L.J. Mandarino, R.L. Printz, K.A. Cusi, P. Kinchington, R.M. O'Doherty, H. Osawa, C. Sewell, A. Consoli, D.K. Granner, R.A. Defronzo, Regulation of hexokinase II and glycogen synthase mRNA, protein, and activity in human muscle, Am. J. Physiol. 269 (1995) E701–E708.
[37] S. Kumagai, R. Narasaki, K. Hasumi, Glucose-dependent active ATP depletion by koningic acid kills high-glycolytic cells, Biochem. Biophys. Res. Commun. 365 (2008) 362–368.
[38] S. Rodríguez-Enríquez, M.E. Torres-Márquez, R. Moreno-Sánchez, Substrate oxidation and ATP supply in AS-30D hepatoma cells, Arch. Biochem. Biophys. 375 (2000) 21–30.
[39] L.J. Reitzer, B.M. Wice, D. Kennell, The pentose cycle, J. Biol. Chem. 255 (1980) 5616–5626.
[40] K.A. Gumaa, P. McLean, The pentose phosphate pathway of glucose metabolism, Biochem. J. 115 (1969) 1009–1029.
[41] J.C. Portais, R. Schuster, M. Merle, P. Canioni, Metabolic flux determination in C6 glioma cells using carbon-13 distribution upon [1-^{13}C] glucose incubation, Eur. J. Biochem. 217 (1993) 457–468.
[42] C.M. Metallo, J.L. Walter, G. Stephanopoulos, Evaluation of ^{13}C isotopic tracers for metabolic flux analysis in mammalian cells, J. Biotechnol. 144 (2009) 167–174.
[43] J.W. Harding, E.A. Pyeritz, H.P. Morris, H.B. White, Proportional activities of glycerol kinase and glycerol 3-phosphate dehydrogenase in rat hepatomas, Biochem. J. 148 (1975) 545–550.
[44] B.W. Agranoff, A.K. Hajra, The acyl dihydroacetone phosphate pathway for glycerolipid biosynthesis in mouse liver and Ehrlich ascites tumor cells, Proc. Natl Acad. Sci. USA 68 (1971) 411–415.
[45] K. Snell, G. Weber, Enzymic imbalance in serine metabolism in rat hepatomas, Biochem. J. 233 (1986) 617–620.
[46] G. Paradies, F. Capuano, G. Palombini, T. Galeotti, S. Papa, Transport of pyruvate in mitochondria from different tumor cells, Cancer Res. 43 (1983) 5068–5071.
[47] S.J. Ralph, S. Rodríguez-Enríquez, J. Neuzil, R. Moreno-Sánchez, Bioenergetic pathways in tumor mitochondria as targets for cancer therapy and the importance of the ROS-induced apoptotic trigger, Mol. Aspects Med. 31 (2010) 29–59.
[48] J. Zalitis, I.T. Oliver, Inhibition of glucose phosphate isomerase by metabolic intermediates of fructose, Biochem. J. 102 (1967) 753–759.
[49] J.M. Chirgwin, T.F. Parsons, A.N. Ernst, Mechanistic implications of the pH independence of inhibition of phosphoglucose isomerase by neutral sugar phosphates, J. Biol. Chem. 250 (1975) 7277–7279.

[50] M.K. Gaitonde, E. Murray, V.J. Cunningham, Effect of 6-phosphogluconate on phosphoglucose isomerase in rat brain in vitro and in vivo, J. Neurochem. 52 (1989) 1348–1352.
[51] F. Heinz, K.D. Kulbe, Glyceraldehyde phosphate dehydrogenase from liver: I. Isolation and characterization of the bovine liver enzyme, Hoppe Seylers, Z. Physiol. Chem. 351 (1970) 249–261.
[52] S. Patra, S. Ghosh, S. Bera, A. Roy, S. Ray, M. Ray, Molecular characterization of tumor associated glyceraldehyde-3-phosphate dehydrogenase, Biochemistry (Mosc) 74 (2009) 717–727.
[53] A. Tanaka, B. Chance, B. Quistorff, A possible role of inorganic phosphate as a regulator of oxidative phosphorylation in combined urea synthesis and gluconeogenesis in perfused rat liver, J. Biol. Chem. 264 (1989) 10034–10040.
[54] L. Nascimben, J.S. Ingwall, B.H. Lorell, I. Pinz, V. Schultz, K. Tornheim, R. Tian, Mechanism for increased glycolysis in the hypertrophied rat heart, Hypertension 44 (2004) 662–667.
[55] B. Teusink, M.C. Walsh, K. van Dam, H.V. Westerhoff, The danger of metabolic pathways with turbo design, Trends Biochem. Sci. 23 (1998) 162–169.
[56] Y.K. Kashiwaya, K. Sato, N. Tsuchiya, S. Thomas, D.A. Fell, R.L. Veech, J.V. Passonneau, Control of glucose utilization in working perfused rat heart, J. Biol. Chem. 269 (1994) 25502–25514.
[57] R. Moreno-Sánchez, R. Encalada, A. Marín-Hernández, E. Saavedra, Experimental validation of metabolic pathway modeling. An illustration with glycolytic segments from *Entamoeba histolytica*, FEBS J. 275 (2008) 3454–3469.
[58] S. Aiston, B. Andersen, L. Agius, Glucose 6-phosphate regulates hepatic glycogenolysis through inactivation of phosphorylase, Diabetes 52 (2003) 1333–1339.
[59] H. Yun, M. Lee, S.-S. Kim, J. Ha, Glucose deprivation increases mRNA stability of vascular endothelial growth factor through activation of AMP-activated protein kinase in DU145 prostate carcinoma, J. Biol. Chem. 280 (2005) 9963–9972.
[60] M. Natsuizaka, M. Ozasa, S. Darmanin, M. Miyamoto, S. Kondo, S. Kamada, M. Shindoh, F. Higashino, W. Suhara, H. Koide, K. Aita, K. Nakagawa, T. Kondo, M. Asaka, F. Okada, M. Kobayashi, Synergistic up-regulation of hexokinase-2, glucose transporters and angiogenic factors in pancreatic cancer cells by glucose deprivation and hypoxia, Exp. Cell Res. 313 (2007) 3337–3348.
[61] H. Pelicano, D.S. Martin, R.H. Xu, P. Huang, Glycolysis inhibition for anticancer treatment, Oncogene 25 (2006) 4633–4646.
[62] P.L. Pedersen, S. Mathupala, A. Rempel, J.F. Geschwind, Y.H. Ko, Mitochondrial bound type II hexokinase; a key player in the growth and survival of many cancers and an ideal prospect for therapeutic intervention, Biochim. Biophys. Acta 1555 (2002) 14–20.
[63] M.L. Macheda, S. Rogers, J.D. Best, Molecular and cellular regulation of glucose transporter (GLUT) proteins in cancer, J. Cell. Physiol. 202 (2005) 654–662.
[64] S.P. Mathupala, C.B. Colen, P. Parajuli, A.E. Sloan, Lactate and malignant tumors: a therapeutic target at the stage of glycolysis, J. Bioenerg. Biomembr. 39 (2007) 73–77.
[65] A. Yalcin, S. Telang, B. Clem, J. Chesney, Regulation of glucose metabolism by 6-phosphofructo-2-kinase/fructose-2, 6-bisphosphatases, Exp. Mol. Pathol. 86 (2009) 174–179.
[66] J.E. Wilson, Isozymes of mammalian hexokinase: structure, subcellular localization and metabolic function, J. Exp. Biol. 206 (2003) 2049–2057.
[67] K. Imamura, T. Tanaka, Pyruvate kinase isoenzymes from rat, Methods Enzymol. 90 (1982) 150–165.

Please cite this article as: A. Marín-Hernández, et al., Modeling cancer glycolysis, Biochim. Biophys. Acta (2010), doi:10.1016/j.bbabio.2010.11.006

Supplementary Material

Table S1. Model reactions as written in Gepasi

Enzyme or branch	Reaction
GLUT	$Glu_{out} = Glu_{in}$
HK	Glu_{in} + ATP = G6P + ADP
HPI	G6P = F6P
PFK-1	F6P + ATP = FBP + ADP
ALDO	FBP = DHAP + G3P
TPI	DHAP = G3P
GAPDH	NAD + G3P + Pi = 13BPG + NADH
PGK	1,3BPG + ADP = 3PG + ATP
PGAM	3PG = 2PG
ENO	2PG = PEP
PYK	PEP + ADP = Pyr + ATP
LDH	NADH + Pyr = Lac + NAD
Glycogen synthesis	G6P + ATP -> glycogen + ADP + Pi + Pi
Glycogen degradation	Glycogen + Pi -> G6P
ATPases	ATP -> ADP + Pi
AK	ATP + AMP = ADP + ADP
DHases	NADH = NAD
PPP	G6P -> 6PG
TK	Xy5P + Ery4P -> G3P + F6P
MPM	Pyr + 13ADP + 13Pi -> 13ATP

PPP, pentose phosphate pathway; MPM, mitochondrial pyruvate metabolism; TK, transketolase. The computer program GEPASI used for building the pathway model only accepts entire figures and therefore the oxidative phosphorylation stoichiometry for ATP synthesis from pyruvate oxidation was included as 13 instead of 12.5.

Table S2. Summary of the kinetic parameter values used in Gepasi for kinetic models of glycolysis in AS-30D and HeLa tumor cells*

Enzyme		AS-30D	HeLa	Enzyme		AS-30D	HeLa
GLUT	Km_{GLU}	0.52 [a]	9.3 [a]	PGK	$Km_{1,3BPG}$	0.035 [e]	0.079 [e]
	K_{eq}	1 [b]	1 [b]		Km_{3PG}	0.12 [e]	0.13 [e]
	Kmp	10 [b]	10 [b]		Km_{ADP}	0.67 [e]	0.04 [e]
HK	$K_{m\,GLU}$	0.18 [c]	0.1 [e]		Km_{ATP}	0.15 [e]	0.27 [e]
	Km_{ATP}	0.99 [c]	1.1 [e]		α	1 [b]	1 [b]
	Ki_{G6P}	0.02 [d]	0.02 [d]		β	1 [b]	1 [b]
	K_{ADP}	3.5 [b]	3.5 [b]	PGAM	Km_{3PG}	0.18 [e]	0.19 [e]
	K_{eq}	651 [f]	651 [f]		Km_{2PG}	0.04 [e]	0.12 [e]
HPI	Km_{G6P}	0.9 [e]	0.4 [e]	ENO	Km_{2PG}	0.16 [e]	0.038 [e]
	Km_{F6P}	0.07 [e]	0.05 [e]		Km_{PEP}	0.04 [e]	0.06 [e]
	Ki_{Ery4P}	0.0017 [g]	0.001 [g]	PYK	Km_{PEP}	0.4 [e]	0.014 [e]
	Ki_{FBP}	0.17 [g]	0.06 [g]		Km_{ADP}	0.3 [e]	0.4 [e]
	Ki_{6PG}	0.0094 [g]	0.015 [g]		Km_{Pyr}	10 [j]	10 [j]
PFK-I	Km_{F6P}	4.6 [h]	1.0 [h]		Km_{ATP}	0.86 [j]	0.86 [j]
	Km_{ATP}	0.048 [h]	0.021 [h]		K_{eq}	195172 [k]	195172 [k]
	Ki_{ATP}	1.75 [h]	20 [h]		Ka_{F16BP}	4×10^{-4} [s]	4×10^{-4} [s]
	Ki_{CIT}	3.9 [h]	6.8 [h]		Ki_{ATP}	2.5 [s]	2.5 [s]

	Ka_{F26BP} β α L K_{eq} K_{ADP} K_{F16BP}	1.8 x10^{-4} [h] 2.35 [h] 4.47 [h] 13 [h] 247 [i] 5 [b] 5 [b]	8.4 x10^{-4} [h] 0.98 [h] 0.32 [h] 4.1 [h] 247 [i] 5 [b] 5 [b]		L	1 [b]	1 [b]
				LDH	Km_{Pyr} Km_{Lac} Km_{NADH} Km_{NAD} α β	0.13 [e] 4.7 [e] 0.002 [e] 0.07 [e] 1 [b] 1 [b]	0.3 [e] 4.7 [p] 0.002 [p] 0.07 [e, p] 1 [b] 1 [b]
				Glycogen degradation	v=	1.2x10 $^{-3}$ [m]	6x10 $^{-3}$ [m]
				Glycogen synthesis	v=	2.2x10^{-3} [m] 1 x 10^{-3} [q]	1.1x10 $^{-3}$ [m]
				ATPases	k=	4.2x10^{-3} [n]	0.003 [n] 0.0045 [r]
ALDO	Km_{F16BP} Km_{G3P} Km_{DHAP}	0.01 [e] 0.16 [e] 0.08 [e]	0.009 [e] 0.16 [p] 0.08 [p]	AK	$k1$= $k2$=	1 [n] 2.26 [n]	1 [n] 2.26 [n]
				DHases	$k1$= $k2$=	250 [n] 1 [n]	250 [n] 1 [n]
TPI	Km_{DHAP} Km_{G3P}	1.9 [e] 0.41 [e]	1.6 [e] 0.51 [e]				
GAPDH	Km_{G3P} $Km_{1,3BPG}$ Km_{NAD+} Km_{NADH} Km_{Pi}	0.29 [e] 0.02 [e] 0.08 [e] 0.004 [e] 11 [e]	0.19 [e] 0.022 [e] 0.09 [e] 0.01 [e] 29 [e]	PPP	v=	9.5x10^{-5} [m]	9.5 x 10^{-5} [m]
				MPM	v=	5 x 10^{-4} [m]	1 x 10^{-4} [m]
				TK	v=	9.5x10^{-5} [n]	9.5x 10^{-5} [n]

*The *Vm* values were those from Table S3. *Km, Ka and Ki* in mM.
[a] taken from [24].
[b] arbitrary value
[c] taken from [10]
[d] taken from [66]
[e] Present study
[f] recalculated from the $\Delta G^{\circ\prime}$ = - 16.7 KJ mol^{-1}.
[g] adjusted in the interval described in Table 2.
[h] Moreno-Sánchez, Marín-Hernández, Encalada & Saavedra, unpublished results.
[i] recalculated from the $\Delta G^{\circ\prime}$ = - 14.2 KJ mol^{-1}.
[j] taken from [15]
[k] recalculated from the $\Delta G^{\circ\prime}$ = - 31.4 KJ mol^{-1}.
[m] adjusted in the interval described in Table 2.
[n] adjusted
[p] values reported for AS-30D in Table 1.
[q] value used for 1 mM glucose condition
[r] values used for hypoxia condition
[s] taken from K. Imamura, T. Tanaka, Pyruvate kinase isoenzymes from rat, Methods Enzymol. 90 (1982) 150–165.

Table S3. Enzyme activity re-calculation per mg of total cellular protein

Enzyme activity		U (mg cytosolic protein) $^{-1}$	U (mg *total* cellular protein) $^{-1}$	*Vm* value used in the model
			AS-30D	
HK	Vm_f	0.46 [a]	0.35 ± 0.17 (3)	0.35
HPI	Vm_f	4.9 [b]	NM	1.42 [e]
	Vm_r	3.4 [b]	0. 98 ± 0. 46 (3)	0.98
PFK-1	Vm_f	0.273 [c]	NM	0.066[f]
ALDO	Vm_f	0.23 [a]	0.056 (1)	0.056
	Vm_r	0.18 [b]	NM	0.044 [e]
TPI	Vm_f	5.6 [b]	NM	1.39 [e]
	Vm_r	56 [a]	13.9 (1)	13.9
GAPDH	Vm_f	1 [a]	NM	0.38 [e]
	Vm_r	0.9[a]	0.34 (1)	0.34
PGK	Vm_f	27 [a]	NM	10.8 [g]
	Vm_r	4.3 [b]	NM	1.72 [g]
PGAM	Vm_f	20 [a]	NM	8 [g]
	Vm_r	1.3 [b]	NM	0.52 [g]
ENO	Vm_f	0.51[a]	0.29 (1)	0.29
	Vm_r	0.74 [b]	NM	0.42 [e]
PYK	Vm_f	6.6 [a]	4.2 (2)	4.2
LDH	Vm_f	13.4 [b]	2.0 (2)	2.0
	Vm_r	1.8 [b]	NM	0.27 [e]
			HeLa	
HK	Vm_f	0.06 [d]	0.04 ± 0.01 (3)	0.04
HPI	Vm_f	1.2 [b]	NM	0.4 [e]
	Vm_r	2.8 [b]	0.9 ± 0.1 (3)	0.9
PFK-1	Vm_f	0.078 [c]	NM	0.031[†]
ALDO	Vm_f	0.2 [a]	0.08 ± 0.02 (3)	0.08
	Vm_r	NM	NM	0.063 [i]
TPI	Vm_f	5 [b]	NM	3.4 [h]
	Vm_r	42 [a]	NM	28 [h]
GAPDH	Vm_f	2 [a]	0.58	0.58
	Vm_r	2.5 [a]	NM	0.72 [e]
PGK	Vm_f	13 [a]	NM	8.7 [h]
	Vm_r	3.8 [b]	NM	2.5 [h]
PGAM	Vm_f	1.4 [a]	NM	0.94 [h]
	Vm_r	0.53 [b]	NM	0.36 [h]
ENO	Vm_f	0.36 [a]	0.34 ± 0.07 (3)	0.34
	Vm_r	0.4 [b]	NM	0.38 [e]
PYK	Vm_f	3 [a]	1.9 ± 0.4 (3)	1.9
LDH	Vm_f	11.4 [b]	3.4 ± 0.5 (3)	3.4
	Vm_r	NM	NM	0.54 [i]

Values from [a] [10]; [b] Present study (Table 1); [c] activity in the absence of activators at pH 7.5 (Moreno-Sánchez, Marín-Hernández, Encalada & Saavedra, unpublished results) and [d] [24]. [e] By determining the *Vm* value in the indicated direction in the total cellular extract (fourth column), the *Vm* value in the other

direction (fifth column) was calculated from the *Vmf*/*Vmr* ratio determined in the cytosolic protein (first column). [f] The PFK-1 *Vm* was estimated from the ratio Vm cytosolic protein/Vm in total protein of the Vmf of ALDO. [g] The activities were estimated from the average ratio Vm cytosolic/ Vm total protein of the GAPDH and ENO in AS-30D cells and [h] ALDO and ENO for HeLa cells. [i]. These activities were based on the ratio Vmf/Vmr of ALDO and LDH in the cytosolic fraction of AS-30D. For the pathway modeling under hypoxia the *Vm* values used for GLUT, HK and HPI were 0.043, 0.055 and 0.52/1.17 U* mg of cellular protein, respectively.

Table S4. Fixed metabolite concentrations used in Gepasi for glycolysis kinetic models

Metabolites	AS-30D	HeLa
Glu_{out}	5	5
Lac	27 [a]	33 [a]
Glycogen	26 [b]	135 [b]
6PG	0.35 [b]	0.39 [b]
Citrate	1.7 [a]	1.7 [a]
F26BP	0.006 [c]	0.0043 [c]
Pi	2.5 [d]	4 [d]
Ery4P	1 [b]	0.016 [e]
Xy5P	0.54 [f]	0.016 [e]

Values (in mM) were taken from [a][10], [b] Table 2 , [c] Tables 3 and 4, [d] For modeling, free Pi was used instead of total Pi: 53% of the total Pi concentration determined in AS-30D (Table 3) and HeLa cells (Table 4) was considered as free Pi; [e] [39] and [f] adjusted.

Figure S1. Simulation of PFK-1 activity in the presence and absence of modulators

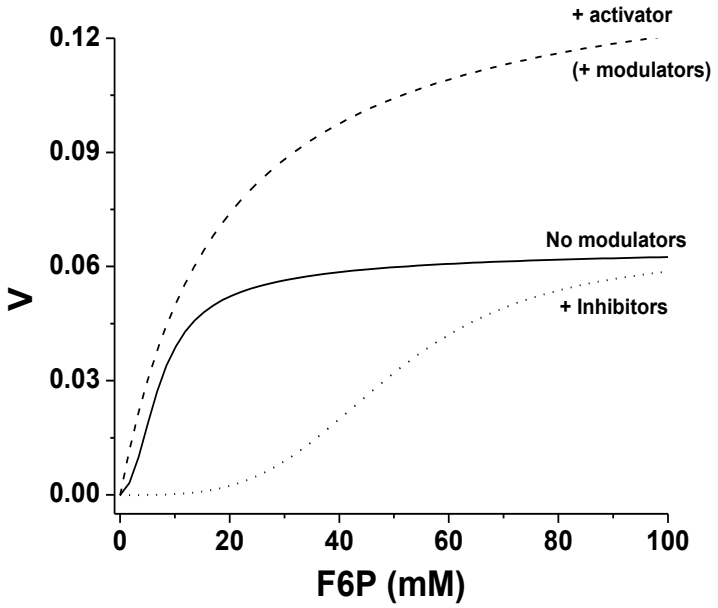

The values for simulation were taken from Table 3, Table S2 and Table S3. Simulation of the PFK-1 equation (see section 2.6 rate equations) was performed in the OriginPro 7.5 software with the following concentration values: 5.6 mM ATP + 1.7 mM citrate (+ inhibitors); 6 µM F26BP (+ activator).

Table S5. Effect of some metabolites on the activity of HPI, ALDO, ENO and GAPDH

Metabolite	Concentration (mM)	HPI [a]	ALDO [b]	ENO[c]	GAPDH[d]
		Remaining activity (%)			
AMP	5	100	90	*	*
ATP	5 + $MgCl_2$ 5mM	101	103	87	53
PPi	5 + $MgCl_2$ 5mM	87	73	*	*
Pi	5 + $MgCl_2$ 5mM	98	96	*	*
G6P	5	*	98	*	*
F6P	5	*	103	*	*
FBP	5	35	*	*	*
F26BP	0.006 [e]	86	96	*	*
6PG	0.093	56	*	*	*
Ery4P	0.055	16	84	*	*
Citrate	2	101	*	*	*
DHAP	2.2	93	*	*	*
	3	*	*	85	*
G1P	1[f]	74	*	*	*
L-lactate	25	95	*	*	*

Inhibitions were assayed in 50 mM Mops pH 7 at 37^{o} C. [a] F6P concentration was 1.5 mM. [b] FBP concentration was 0.2 mM. [c] 2PG concentration was 1 mM. [d] G3P and NAD^{+} concentrations were 1.5 mM and 1 mM, respectively. [e] physiological concentration. [f] 12 times the physiological concentration. * not measured.

Table S6. Inhibition of HPI from different biological sources

Cell type	*Ki* (μM)		
	FBP	6PG	Ery4P
	Forward reaction		
AS-30D	NM	12 (2)	2.5 ± 0.8 (3)
HeLa	NM	17.6	1± 0.07 (3)
hepatocytes	NM	NM	0.9
	Reverse reaction		
AS-30D	170 ± 110 (3)	6.8 ± 1.5 (3)	0.86 ± 0.3 (3)
HeLa	60	15.5 ± 4 (3)	0.79
hepatocytes	210 ± 190 (3)	8	1.2
yeast *	NM	47	6.7
*Entamoeba histolytica***	NM	15	5.9

The values represent the mean ± SD with the number of different preparations assayed in parentheses; the absence of parenthesis indicates one preparation assayed. NM, not measured. * commercial enzyme; ** recombinant purified enzyme [13]. *Ki* values were determined by nonlinear regression analysis of the experimental data, according to the competitive inhibition equation, by using the computer program Microcal Origin 5.0.

Figure S2. Hexose phosphate isomerase (HPI) inhibition by Ery4P

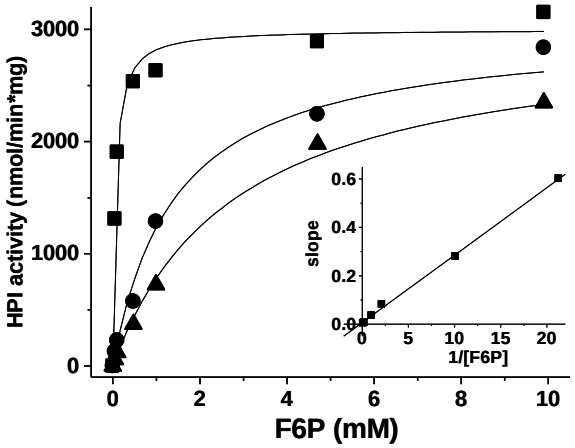

The concentration of Ery4P were 0 (■), 13.8 (●) and 28 (▲) μM. The inset shows a re-plot of the slopes obtained from a Dixon plot ([inhibitor] against 1/v at different substrate concentrations). The linear fitting, which intersects the origin, indicates that Ery4P is an HPI competitive inhibitor [25].

Figure S3. GAPDH affinity by Pi

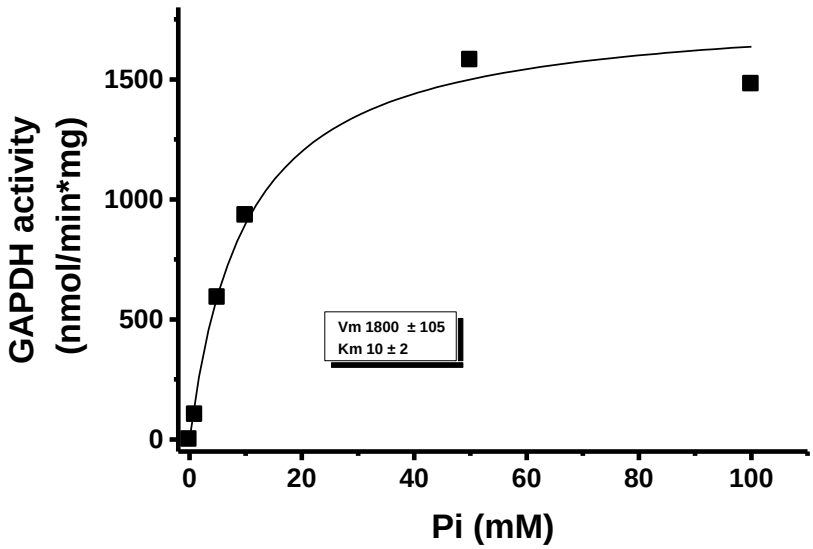

GAPDH activity in AS-30D cytosolic extracts was determined in 50 mM Mops pH 7 at 37^{o}C and in the presence of 1 mM NAD^{+}, 2.9 mM G3P and 5 mM cysteine. The experimental points were fitted to a Michaelis-Menten equation by using the software Microcal Origin v 5.

Table S7. Robustness for Pi concentration values in the AS-30D glycolysis kinetic model

	Pi (mM)			
Metabolite (mM)	2.5*	1.3	2	2.8
Glu_{in}	3.4	3.5	3.4	3.3
G6P	6.5	7.3	6.6	6.4
F6P	0.03	0.02	0.02	0.02
FBP	5.2	35	9.7	3.8
DHAP	14	39	19.4	11.8
G3P	0.3	0.8	0.41	0.25
1,3BPG	0.01	0.008	0.01	0.01
Pyr	0.84	0.82	0.83	0.84
ATP	7.9	7.2	7.8	8
ADP	2.1	2.4	2.2	2.1
AMP	1.3	1.7	1.4	1.3
NADH	0.005	0.005	0.005	0.005
NAD^+	1.34	1.34	1.34	1.34
glycolytic flux	29	26	29	29
Flux control coefficients				
GLUT	0.2	0.11	0.18	0.2
HK	0.44	0.27	0.4	0.45
HPI	0.4	0.25	0.37	0.41
PFK-1	0.02	0.01	0.02	0.02
GAPDH	0.05	0.33	0.1	0.04

*Pi concentration used in the main model.

Table S8. Elasticity coefficients for substrates (S), products (P) and modulators (M)

		ε^{Ei}_{S}			ε^{Ei}_{P}			ε^{Ei}_{M}	
		AS-30D	HeLa		AS-30D	HeLa		AS-30D	HeLa
GLUT	Glu_{out}	2.2	0.8	Glu_{in}	-2.1	-0.18			
HK	Glu_{in}	0.95	0.85	G6P	-0.94	-0.82			
	ATP	0.17	0.18	ADP	-0.06	-0.07			
							FBP	-0.05	-0.05
HPI	G6P	1.0	1.4	F6P	-0.04	-0.42	6PG	-0.06	-0.55
							Ery4P	-0.89	-0.34
PFK-1	F6P	0.65	0.66	FBP	-0.004	-4×10^{-5}	F26BP	0.001	0.003
	ATP	0.71	0.04	ADP	-0.003	-3×10^{-5}	CIT	-1×10^{-5}	-1.8×10^{-8}
ALDO	FBP	1.4	2.1	DHAP	-1.4	-2.1			
				G3P	-1.2	-1.6			
TPI	DHAP	75	177	G3P	-75	-177			
GAPDH	G3P	0.70	0.74	13BPG	-0.23	-0.03			
	NAD^+	0.29	0.1	NADH	-0.26	-0.06			
	Pi	1.1	0.99						
PGK	13BPG	5.7	3.0	3PG	-4.8	-2.0			
	ADP	5.7	2.3	ATP	-5.6	-2.3			
PGAM	3PG	8.9	1.3	2PG	-8.4	-0.38			
ENO	2PG	1.5	1.0	PEP	-0.75	-0.06			
PYK	PEP	0.99	0.98	Pyr	-8×10^{-5}	-4×10^{-5}	FBP		2×10^{-12}
	ADP	0.16	0.16	ATP	-9×10^{-5}	-9×10^{-5}			
LDH	Pyr	7.1	19.6	Lac	-7.0	-19.5			
	NADH	7.1	19.6	NAD^+	-7.0	-19.5			
ATPases	ATP	1	1						
DHases	NADH	2690	13447	NAD^+	-2689	-13446			

Table S9. Concentration control coefficients

	Model									
	AS-30D					***HeLa***				
	G6P	F6P	PEP	ATP	NADH	G6P	F6P	PEP	ATP	NADH
GLUT	0.25	0.12	0.24	0.18	*	0.5	0.57	0.47	0.3	*
HK	0.54	0.26	0.52	0.39	*	0.11	0.12	0.1	0.06	*
HPI	-0.48	0.24	0.48	0.36	*	-0.66	0.07	0.06	0.04	*
PFK-1	-0.03	-1.5	0.03	0.02	*	-0.42	-1.4	0.04	0.02	*
ALDO	-0.02	*	0.02	0.01	*	-0.02	*	*	*	*
GAPDH	-0.06	-0.01	0.06	0.04	*	-0.08	0.01	0.01	*	*
ENO	*	*	0.01	*	*	*	*	*	*	*
PYK	*	*	-1	*	*	*	*	-1	*	*
Glycogen degradation	0.07	-0.01	0.07	0.08	*	0.7	0.82	0.74	0.69	*
ATPases	-0.15	1.0	-0.35	-1.1	*	0.02	0.03	-0.26	-1.0	*
PPP	*	*	-0.01	*	*	-0.01	-0.01	-0.01	-0.01	*
Glycogen synthesis	-0.13	0.08	-0.15	-0.22	*	-0.13	-0.15	-0.15	-0.17	*
MPM	0.03	-0.2	0.07	0.21	*	*	*	0.01	0.05	*
TK	*	*	0.01	0.01	*	*	0.01	0.02	0.02	*

* The values were lower than 0.01. The respective TPI, PGK, PGAM, LDH, AK and DHases elasticity coefficients were lower than 0.01 and hence they were not included in the table.

----- Original Message ----- From: "BBA - Bioenergetics (ELS)" <bbabio@elsevier.com>
To: <morenosanchez@hotmail.com>; <rafael.moreno@cardiologia.org.mx>
Sent: Tuesday, September 21, 2010 5:20 PM
Subject: BBABIO-10-99: Decision

Manuscript No.: BBABIO-10-99
Title: Modeling cancer glycolysis
Article Type: Special Issue: Bioenergetics of Cancer
BBA Section: BBA - BBA - Bioenergetics
Corresponding Author: Dr. Rafael Moreno-Sanchez
All Authors: Alvaro Marín-Hernández, Ph. D.; Juan C Gallardo-Pérez, Ph. D.; Sara Rodríguez-Enríquez, Ph. D.; Rusely Encalada, B.S.; Rafael Moreno-Sanchez; Emma Saavedra, Ph. D.
Submit Date: Jun 04, 2010

Dear Dr. Moreno-Sanchez:

On behalf of the Executive Editors of Biochimica et Biophysica Acta, I would like to thank you for submitting the above-named article to BBA - Bioenergetics.

I am pleased to inform you that your paper may become acceptable for publication. The reviewers, whose comments are enclosed below, indicate that the manuscript is a valuable contribution to the field and recommend publication after modifications. However, before returning your revised paper, you should answer the points raised by the reviewers. We look forward to receiving your prompt response.

Thank you, and we look forward to receiving your revised manuscript.

Yours sincerely,

Rodrigue Rossignol, PHD (Guest Editor)
BBA - Bioenergetics

Please see below Reviewer(s') comments:

Reviewer #1: Cancer glycolysis is a subject of interest as a better knowledge of altered cancer metabolism could help to identify new drug targets. The work presented in this paper is a continuation of the previous work and propose possible therapeutic targets to inhibit tumour energy metabolism. The paper is suitable for publication in BBA provided that the authors take into account the following points:

- The HeLa cells are cultured at 25 mM and experiments are performed at 5 mM glucose. The authors discuss that the high flux of glycogen degradation observed in these cells can be influenced by this fact. The authors not discuss if the high control coefficients observed for glycogen degradation in HeLa cells could be influenced also by this change in glucose concentration. A discussion on how the change of glucose concentration can result in the high control coefficients observed for glycogen need to be included.

- The authors use an equation "random bi-substrate Michaelis-Menten" to describe the kientics of pyruvate kinase (PK). It has been well described that PK is an allosteric enzyme and that in tumors an specific isoform is overexpressed. The regulation of this enzyme by dimer-tetramer formation has also been reported in several papers (see: Robust metabolic adaptation underlying tumor progression. Vizán P., Mazurek S., Cascante M. Metabolomics (2008) 4:1-12. and also Mazurek S. Ernst Schering Found Symp Proc. 2007;(4):99-124.). Inclusion of this regulatory mechanism in the kinetic equation or a justification of why this mechanism of regulation has not been taken into account is necessary.

- Page 15: the authors comment that: "The low PPP flux and intermediary concentrations compared to

glycolytic flux and metabolites suggested low activity of the PPP indicating that tumor cells were not in proliferative stage". The authors compute the PPP from changes in 6PG which can result in an underestimation of the flux. It should be discussed the error associated with this method as well as why tracers as 14C or 13C labelled glucose has not been used to verify that this flux is so low.

- Page 18: The authors say that: "ALDO activity was not modulated by any of these metabolites. Although GAPDH was inhibited by ATP (with non-competitive inhibition, Ki = 4.3 mM) and ENO was inhibited by DHAP and ATP (non-competitive inhibition, Ki = 31 mM, and uncompetitive inhibition, Ki = 14 mM, respectively), these Ki values were far from the physiological concentrations, and their effects were not included in the rate-equations. However, GAPDH from AS-30D cells has low affinity for Pi (Km =10 mM) (Fig. S3) and the Pi concentration in the cells is 0.6 mM [23], suggesting low GAPDH activity. By decreasing the GAPDH activity to 15% of the Vmf and Vmr values showed in Table S3, because Pi was not included in the rate equation, accumulation of FBP was promoted reaching a near-physiological value of 11.4 mM (Table 3)". It should be justified why Pi is not included in the rate equation of GAPDH if the concentrations are available.

Page 24: The authors say that : "Increased enzyme activities under hypoxia for HK and HPI were also determined (37% and 30%, respectively) whereas a 225% increased protein content for GLUT was determined by western-blot analysis and then a corresponding increase in transport activity was assumed for modeling (data not shown)". Western-blot must be included in the paper instead of mention as data not shown.

- Figure 1: The positive and negative metabolite regulatory loops considered in the kinetic equations must be included in the figure.

- Pyruvate dehidrogenase reaction has not been included in the model. A justification for this fact need to be provided.

- HPI is a reversible enzyme described in general as in rapid equilibrium and Vmf and Vmf and Vmr arround 200 times higher than Vmf of HK have been described in muscle (Puigjaner J, et al. M. FEBS Lett. 1997 Nov 24;418(1-2):47-52.). Vmf and Vmr are difficult to determine due to the reversibility of enzyme and the high rates in both directions of this reaction. It is sourprising that here Vmr are the same order of magnitude for both enzymes in AS-30D. In HeLa the differences are more notorious. It will be interesting to verify in the model how much dependent is the control coefficient of HPI on the magnitudes of Vmf and Vmr for HPI (i.e. increase in an order of magnitude both Vmf and Vmi for HPI and see how much this fact affect the control coefficient).

Reviewer #2: Review BBABIO-10-99

The authors submitted an important paper dealing with the application of metabolic control theory on glycolysis of tumor cells. They measured in two tumor cells enzyme kinetics and steady state concentrations as well as fluxes of all relevant glycolytic enzymes put these data into a computer model calculated flux control and concentration control steps. This is a large and interesting work. Authors were able to detect the most limiting steps which could be used as targets for cancer therapy, also the approach to detect the extent of single enzyme inhibition which could the reduce glycolytic ATP formation by 50 %. They compared these new data with data from non tumor cells obtained from others using not such an elegant but laborious approach. I agree with the paper. However, I have a little problems with the concept of the paper. It would be more interesting to compare tumor data with data obtained with the same method from non tumor cells.
Moreover we know, that in tumors also the interaction between mitochondria and glycolysis is impaired. The tumor metabolism is also characterized by impaired mitochondria. Limitation on the glycolysis only, is therefore a limitation of possibilities. I know that is a large bigger task but the problem is known since more than 40 years ago. (The reviewer was to that time involved in the task to bring together the glycolytic and mitochondrial pathway of reticulocytes). Therefore I think it should at least discussed in the present paper, why the authors concentrated on the glycolysis only and only on two tumor cell lines.

Rodrigue Rossignol, Ph. D. November 1, 2010
BBA-Bioenergetics
Guest Editor
Dear Dr. Rossignol,

Thank you for your letter of September 21, 2010 regarding the submission of the manuscript (No. BBABIO-10-99) entitled “Modeling cancer glycolysis”. We were encouraged to resubmit a revised paper, in which the observations made by the two reviewers should be answered. Therefore, several modifications were made throughout the manuscript most of which required further experimentation and *in silico* modeling. We would like to also thank the reviewers, particularly reviewer 1, for their insightful observations and suggestions, which have enabled us to strengthen the paper on several points (enzyme kinetics, pathway modeling, and paper focus). The new experimental data, included in the revised manuscript, added further support to our findings and conclusions. The changes made to the manuscript were indicated in bold letter. A point-by-point response to the observations raised by the reviewers is shown below. Trusting that the manuscript will now be acceptable for publication in *BBA-Bioenergetics* special issue on Bioenergetics of Cancer, we remain.

Sincerely yours,

Emma Saavedra, Ph.D. Rafael Moreno-Sánchez, Ph. D.
Corresponding authors

Response to Reviewer 1

1. Discussion on how the change in glucose concentration may affect the contribution of glycogen degradation to the control of glycolysis was included, as suggested, on p. 25 2nd paragraph.

2. Full PYK kinetic description.
The PYK rate equation was changed to that of a cooperative enzyme regarding [PEP], [F1,6BP] and [ATP] (the Monod et al. equation for exclusive binding; p. 14). However, as expected from saturation with allosteric activator ($K_{A(F1,6BP)}$ = 0.4 □M in Table S2; [F1,6BP] = 5.2 mM in Table 3), and despite the presence of a relatively high concentration of an allosteric inhibitor ($Ki_{(ATP)}$ = 2.5 mM in Table S2; [ATP] = 7.9 mM in Table 3), no changes on PYK flux control, and on flux control distribution and metabolite concentrations were attained. Under maximal activation (*e.g.*, all enzyme molecules are in the active tetrameric conformation), an enzyme with sigmoidal kinetics shifts to hyperbolic behavior and therefore a simplified Michaelis-Menten equation can be used. However, for the sake of accuracy, the more complex Monod equation for PYK (instead of the previous Michaelis-Menten equation) was included in the pathway models, as suggested by the reviewer.

3. Pentose Phosphate Pathway flux.
In agreement with the reviewer’s observation, we have re-written the section describing and discussing the results of the PPP flux (p. 17, 1st paragraph). In there, we have (i) recognized the possibility of underestimating the PPP flux when evaluated from changes in the 6PG concentration and (ii) discussed an improvement in the PPP flux determination by using radio-labelled glucose, as suggested. Moreover, the robustness of the pathway models was tested for variation in the PPP flux to 10-20 times the original value (and assuming that our values were underestimated). However, no significant changes on fluxes or control coefficients were attained, and only a 20-40% decrease in FBP and DHAP concentrations was observed. These observations were concisely summarized on p. 24, 2nd paragraph. Thus, it seems that under the conditions used in the present study, the PPP flux is indeed low.

4. Inclusion of Pi in the GAPDH rate equation.
The GAPDH rate-equation was modified to a rapid equilibrium ordered Ter-Bi reversible Michaelis-Menten equation (p. 13) now including Pi. The inclusion of this metabolite prompted an experimental re-evaluation of the GAPDH affinity for Pi (Km_{Pi}) and the determination of the total Pi intracellular content under the conditions of the present study; the description of the method used for determination of Pi was now added on p. 8. These new data confirmed the high GAPDH Km_{Pi} (Table 1), described in the previous version of the manuscript, and showed a high total Pi level, even in the presence of glucose in both cancer cell lines (p. 20, 3th paragraph; Tables 3 and 4). For pathway modeling, free Pi was used which

was stated in the same paragraph and in the legends of Tables 3 and 4. The effect of varying the Pi concentration on the GAPDH control coefficient and FBP concentration was modeled and the results were included in Table S7 in supplementary material and discussed on section 4.4 of the main text.

5. GLUT content under hypoxia.
As suggested, the Western-blot analysis for the glucose transporter under normoxic and hypoxic HeLa cells was included in the revised paper as Figure 2 and mentioned on p. 27, 1st paragraph.

6. Figure 1 was modified, as suggested, including the positive and negative metabolite regulatory loops and new substrates in the modified rate-equations.

7. PDH was not included in the model.
The rate-reaction for this step was not specifically defined in the model. However, this enzyme was implicitly included as part of mitochondrial pyruvate oxidation, which was experimentally evaluated as the steady-state rate of O_2 consumption. A statement in this regard was added on p. 9, last four lines.

8. HPI Vm_f and Vm_r values.
HPI certainly catalyzes a near-equilibrium reaction under physiological conditions but its kinetic parameters are not difficult to determine using the appropriate conditions. In our assays we made sure to be under initial velocity conditions by using an excess of the coupling system (*i.e.*, G6PDH for the reverse reaction; recombinant PFK from *Entamoeba histolytica*, and commercial ALDO, TPI and □GPDH for the forward reaction) and making rate-limiting the HPI activity by adjusting the amount of cellular extract. Regarding the magnitude of the HPI *Vmf* and *Vmr*, and HK *Vm*, values in AS-30D cells: In muscle cells and in general in non-tumor cells, indeed very high HPI *Vmf* (or *Vmr*)/HK Vm ratios are commonly found. This activity ratio is still high in tumor cells, but lower than that found in non-tumor cells, as a consequence of the enhanced over-expression of all glycolytic enzymes, particularly HK, in tumor cells [see 10, 32, 40]. On the other hand, similar HPI Vmf and *Vmr* values (Table 1, AS-30D) have been also documented in other biological systems (see 40, 50, Blood Cells Mol. Dis. 1998, 24: 54-61). To address the reviewer concern regarding HPI *Vm* values, the AS-30D model was subjected to variations in this enzyme activity. Increasing HPI activity from 0.5 to 10 times (*i.e.*, simultaneously increasing both *Vmf* and *Vmr*) brought about a proportional decrease in the HPI flux control coefficient and increase in flux and the FBP and DHAP levels (see the Table S10 included in this letter but not in the paper). These data indicated that the model was not so robust when varying HPI, suggesting that HPI high activity has to be tightly modulated. However, this observation had already been noted in the previous version of the manuscript (section 4.8).

Table S10. Model Robustness regarding HPI *Vm* values.

Variation Fold	1X	0.5X	2X	10X
Vmf	1.42	0.71	2.84	14.2
Vmr	0.98	0.49	1.96	9.8
Metabolite				
Glu_{in}	3.4	3.8	3	2.7
G6P	6.5	9	4.9	4
F6P	0.03	0.02	0.03	0.03
FBP	5.2	1.3	26	374
DHAP	14	7.3	30	109
G3P	0.3	0.16	0.6	2.3
1,3BPG	0.01	0.005	0.03	0.15
Pyr	0.84	0.86	0.86	0.89
ATP	7.9	6	9.7	10.8
ADP	2.1	2.6	1.3	4.2
AMP	1.3	2.6	3.8	0.04
glycolytic flux	29	21.5	36.7	41.7
	Flux control coefficients			

GLUT	0.2	0.16	0.15	0.02
HK	0.44	0.51	0.25	0.03
HPI	0.4	0.49	0.22	0.02
Glycogen degradation	0.05	0.07	0.02	-0.02
PFK-1	0.02	0.02	0.02	0.003
ATPases	-0.1	-0.15	-0.18	0.88

Response to Reviewer 2

- *"It would be more interesting to compare tumor data with data obtained with the same method from non-tumor cells".*

We have now extended the comparison of the present results (*cf*. Table 5) with data from glycolysis in non-tumor cells, in which MCA was applied (p. 21, last 3 lines of 2nd paragraph; p. 14, 2nd paragraph from bottom; p. 22, lines 6-9; p. 22, last 4 lines of 2nd paragraph; p. 28, 3th paragraph). The main conclusion drawn from this analysis was that HPI was a more specific target for AS-30D cancer cells than GLUT or HK.

- *"…in tumors the interaction between mitochondria and glycolysis is impaired. The tumor metabolism is also characterized by impaired mitochondria".*

The second part of the Warburg hypothesis, that mitochondria in cancer cells are impaired (*Science* 1956, 123: 309-314), is by no means an established and universal fact, and is still a matter of controversy. Undoubtedly, the mitochondrial function is damaged or diminished in many tumors, whereas in some others it is well-documented that the mitochondrial function is not impaired and actually may surpass the activity found in non-tumor cells (see references 1, 2, 47 for reviews). Therefore, impaired mitochondria do not represent a generalized finding within the different cancers. Indeed, in recent studies with different cancer cell models, oxidative phosphorylation is active and may predominate for ATP supply (*Toxicol Appl Pharmacol* 2006, 215:208; Amino Acids 2008, 35:681; *J Cell Physiol* 2008, 216:189; *BBA-Bioenergetics* 2009, 1787: 1433-1443; *Int J Biochem Cell Biol* 2010, 42:1744; *J Bioenerg Biomembr* 2010 42:55). Regarding the impaired interaction between mitochondria and glycolysis, the reviewer is probably referring to the lower pyruvate dehydrogenase complex (PDH) activity found in some tumor cells and to its inactivation by a hypoxia-upregulated pyruvate dehydrogenase kinase (PDK) (see reference 5 for review). However, the proposal that PDH inactivation by PDK is the mechanism by which mitochondria become impaired in cancer cells incorrectly assumes that pyruvate is the main oxidizable substrate in cancer cells and that PDH is the rate-limiting step of the Krebs cycle and oxidative phosphorylation. Moreover, full PDH inactivation has not been observed. On the other hand, the aspartate/malate shuttle, which is also involved in the interaction between mitochondria and glycolysis, is similar in some cancer cells (Ehrlich hepatoma) with respect to normal cells (hepatocytes) (*Biochem J* 1995, 310: 665-671); decreased activity of this shuttle in cancer cells has not been described.

- *"why the authors concentrated on the glycolysis only".*

One of the most prominent metabolic alterations in cancer cells, in comparison with normal cells, is the enhanced glycolytic capacity (see references 1 and 2 for reviews). In fact, glycolysis in many cancer cells is the main ATP supplier, surpassing and/or replacing oxidative phosphorylation. Therefore, it is highly relevant, from the mechanistic and clinical standpoints, to fully understand how this pathway is controlled in cancer cells to thus facilitating the identification of the most controlling enzymes (and transporters) which, as pointed out by the reviewer, could be used as targets for cancer therapy. This was originally stated on p. 3, lines 1-6; p. 4, 2nd and 4th paragraphs; p. 6, 1st paragraph; p. 28, 2nd paragraph. Extension of the glycolytic model to include Krebs cycle and oxidative phosphorylation in an oxidative-type tumor cell can be a natural next step in modeling energy tumor metabolism.

- *"why the authors concentrated…only on two tumor cell lines"*

We decided to initiate the MCA of cancer glycolysis with the experimental AS30D hepatoma and the human cervix HeLa carcinoma because these cancer cell lines provide relatively high biomass yields for experimentation. It could have been any other cancer cell line with fast growth characteristics. One further development of the present study is that the validated cancer glycolysis kinetics models may now serve as platforms on which glycolysis from other cancer cells can be analyzed and predictions be made, as far as sufficient data from the respective tumors (*i.e*., relative enzyme contents; fluxes; metabolite concentrations) can be provided and poured into the models. Statements on this last regard were included in the main text on p. 26 3rd paragraph; p. 28 2nd paragraph.

5.2.1 Comentarios manuscrito No. 3

En este trabajo se construyeron los modelos cinéticos de la glucólisis de las líneas tumorales AS-30D y HeLa, a partir de los parámetros cinéticos de cada enzima y transportador en el programa Gepasi. Ambos modelos se validaron al lograr predecir el flujo glucolítico y las concentraciones de metabolitos en diferentes condiciones, que se determinaron experimentalmente. De esta manera, se identificaron a los principales sitios de control en la glucólisis de AS-30D (la HK, la HPI y el GLUT) y HeLa (degradación de glucógeno, el GLUT y la HK). En consecuencia, todos estos sitos de control deben inhibirse simultáneamente para reducir drásticamente el flujo glucolítico y la concentración de ATP en células cancerosas. Los modelos desarrollados en este trabajo lograron también predecir con gran precisión tanto los flujos y las concentraciones de metabolitos bajo hipoxia e hipoglucemia y nos permitieron comprender la importancia que pueden tener tanto la HPI en el control del flujo glucolítico, como la GAPDH en el control de la concentración de la F1,6BP. A partir de estos resultados concluimos que nuestros modelos son robustos pues predijeron con precisión los flujos y las concentraciones de metabolitos en diversas condiciones experimentales y que el GLUT, la HK y la HPI pueden ser considerados como posibles blancos terapéuticos para inhibir la glucólisis tumoral.

5.3 Inhibición de la hexocinasa

Una vez que habíamos establecido cuales eran los principales sitios de control en la glucólisis tumoral (manuscritos 2 y 3), el siguiente paso fue determinar si la inhibición de alguno de estos sitios reducía significativamente el flujo glucolítico en células tumorales.

En el siguiente trabajo (Manuscrito No. 4), se determinó el efecto que tiene la inhibición de la HK sobre el flujo de la glucólisis. Para inhibirla se empleo un nuevo fármaco antineoplásico la Casiopeína II-gly (CasII-gly) que pertenece a una familia de compuestos de coordinación con cobre. A continuación se muestra la primera versión del manuscrito en preparación con estos resultados.

Casiopeina II-gly and BromoPyruvate inhibition of tumor hexokinase

Alvaro Marín-Hernández[1], Juan Carlos Gallardo-Pérez[1], Sayra Yoselin López-Ramírez[1], Jorge Donato García-García[1], Lena Ruiz-Ramírez[2], Isabel Gracia-Mora[2], Alejandro Zentella-Dehesa[3], Rafael Moreno-Sánchez[1] and Sara Rodríguez-Enríquez[1*].

[1] Departamento de Bioquímica, Instituto Nacional de Cardiología, MEXICO.
[2] Departamento de Química Inorgánica y Nuclear, Facultad de Química, UNAM.
[3]Departamento de Bioquímica INNSZ y Departamento de Medicina Genómica y Toxicología Ambiental, Instituto de Investigaciones Biomédicas, UNAM.

Running Title: Casiopeina II-gly inhibits tumor hexokinase

[*]Author for correspondence: Sara Rodriguez-Enríquez, PhD
Instituto Nacional de Cardiología
Departamento de Bioquímica
Juan Badiano No. 1, Col. Sección XVI
Tlalpan, México D.F. 14080
MEXICO
Phone: 5552-55732911 ext. 1422
Fax: 5552-55730926
E-mail: saren960104@hotmail.com

Abbreviations: ALDO, Aldolase; 3BrPyr, 3-bromopyruvate; CasII-gly, Casiopeina II-gly; F6P, fructose-6-phosphate; F1,6BP, fructose-1,6-bisphosphate; F2,6BP, fructose-2,6-bisphosphate; GAPDH, glyceraldehyde 3-phosphate dehydrogenase; GK, glucokinase; G6P, glucose-6-phosphate; α-GPDH, α-glycerophosphate dehydrogenase; HK, hexokinase; HPI, hexosephosphate isomerase; OxPhos, oxidative phosphorylation; PFK-1, phosphofructokinase type 1; PGK, phosphoglycerate cinase ; PYK, pyruvate kinase; TPI, triosephosphate isomerase; TriP, trioses phosphate.

Key Words: Cisplatin; fast-growing tumor cells; glycolysis; hexokinase; 3-bromopyruvate.

Abstract

The copper-based drug Casiopeina II-gly (CasII-gly) shows potent anti-neoplastic effect on several human and rodent fast-growth tumors. At the metabolic level, CasII-gly affects the cellular ATP level and energy mitochondrial metabolism. In order to elucidate whether CasII-gly also affects tumor glycolysis, the effect of CasII-gly was assayed on flux through the complete glycolytic pathway and through the initial glycolytic segment as well as on the activities of glycolytic enzymes of AS-30D hepatocarcinoma cells. CasII-gly was 13-91 times more potent than 3-BromoPyruvate (3BrPyr), HK inhibitor, decreasing tumor cells proliferation, whereas no tumor cells were insensitive to CasII-gly. In tumor cells incubated with 100 μM CasII-gly for 30-60 min, lactate production was stimulated by 2- (glucose medium) and 14- (glucose-free medium) fold. However, glycogen breakdown also increased by 2.8 (glucose medium) and 2-fold (glucose-free medium), suggesting that CasII-gly induced increase in lactate production derived from glycogenolysis. Moreover, in CasII-gly treated cells soluble HK activity and the flux through the first segment of glycolysis (HK-TPI) were significantly inhibited (58- and 41-60 %, respectively), whereas PFK-1, GAPDH, PGK, PYK activities and the flux through the HPI-TPI segment were not affected. In extracts from non-treated cells, 10 μM CasII-gly inhibited both soluble and mitochondrial-bound HK activity, and flux though the HK-TPI segment by 50 %; whereas flux through the HPI-TPI segment was not affected. Furthermore, CasII-gly was a 1.3-21 times more potent inhibitor of tumor HK than 3BrPyr, whereas, cisplatin did not affect HK maximal rate. These data suggested that CasII-gly is a HK inhibitor and may be considered as an alternative chemotherapeutic drug for glycolytic tumors.

Introduction

For ATP supply, fast-growing tumor cells depend on glycolysis (human oligodendroglioma, meningioma and medulloblastoma; rat Novikoff hepatoma), OxPhos (human colon sarcoma, breast cancer melanoma, breast, lung, ovarian, cervix and uterus carcinomas; rat hepatomas (Reuber H-35, Morris, AS-30D) or both pathways (human glioblastoma multiforme; rat astrocytoma C6; rat hepatomas (Ehrlich lettré, Walker-256, Morris 3683 and Dunings LC18; mouse (ascites, sarcoma 27) (reviewed in Moreno-Sanchez et al., 2007; 2009).

In human carcinomas and lymphomas with severe mitochondrial defects (*i.e*., decreased content and activity in respiratory chain complexes), and in tumors subjected to prolonged hypoxia, high resistance to chemo- and radiotherapy is usually encountered (Carew and Huang, 2002; Simonnet et al., 2002; Xu et al., 2005; Pelicano et al., 2006). In these tumors, the glycolysis rate is exacerbated, suggesting that tumor resistance might be associated with the accelerated glycolysis, a metabolic characteristic related to the development of invasive, metastatic and aggressive phenotypes (Brizel et al., 2001; Simonnet et al., 2002; Robey et al., 2005). Thus, inhibition of glycolysis has been suggested as an alternative target to diminish tumor progression in circumstances where traditional therapy is not effective (Pedersen et al., 2002; Pelicano et al., 2006; Gatenby and Gillies, 2007).

Pedersen *et al.*,(2002) proposed HK as target for cancer treatment by considering that this enzyme regulates the G6P levels that feed synthesis of ribose 5-phosphate and glycogen synthesis and inhibits apoptosis in malignant cells. Accordingly, several groups have tried to manipulate tumor growth by using anti-neoplastic drugs that presumably inhibits HK. For example, lonidamine (5-75 μM) inhibits the HK activity by 17-85 % in rat Ehrlich ascites (Floridi et al., 1981), although doses 6-30 times higher are required to diminish human and rodent fibrosarcomas growth (IC_{50} = 155-467 μM) (reviewed in Rodríguez-Enríquez et al., 2009), thus suggesting that inhibition of HK activity is not relevant for the sarcoma development. The strong inhibition of HK by the alkylating agent 3-bromopyruvate (3BrPyr, 5 mM), also reduced the growth and viability in AS-30D hepatocarcinoma through ATP cellular depletion (Ko et al., 2001).

Moreover, both lonidamine and 3BrPyr are non-specific as they also affect the activity of other enzymes (PGK, GAPDH, pyruvate decarboxylase, isocitrate lyase and vacuolar H^+-ATPase) and metabolic pathways (acetylcholine synthesis) (Arendt et al., 1990; Dell' Antone, 2006; Pereira da Silva et al., 2009); and their toxicity profiles have not been evaluated in non-tumorigenic cells. In the case of the lonidamine has been reported numerous side effects in humans (Robustelli della Cuna and Pedrazzoli, 1991). Although the use of these drugs has shown inconveniences, the basic idea of considering HK as the principal target in anticancer therapy is supported by the observation that this enzyme is one of the steps controlling tumor glycolysis in human and rodent models (Marín-Hernández et al., 2006; 2010).

In the search for new anti-neoplastic drugs with high selectivity for specific enzymes in tumor cells but with null effect in the host cells, the copper-based drugs Casiopeinas® have shown strong anti-tumor activity in several human carcinoma lines (HeLa, SiHa, CaSki, C33-A, CH1, ovarian) and rodent tumors (leukaemia L1210, glioma C6) (De Vizcaya-Ruiz et al., 2000; Marín-Hernández et al., 2003; Trejo-Solís et al., 2005; Rodríguez-Enríquez et al., 2006) and, encouragingly, a moderate toxic effect on lymphocytes (Rodríguez-Enríquez et al., 2006) and heart (Hernandez-Esquivel et al., 2006). Similarly to cisplatin, carmustine, mitomycin c, melphalan, cyclophosphamide and dacarbazine (reviewed in Lawley and Phillips, 1996), casiopeinas interfere with DNA replication through the formation of DNA-adducts. However, at the doses used to block DNA replication (0.4 nM- 30 μM), casiopeina II-gly (CasII-gly) also severely affects tumor OxPhos (< 10 μM) through inhibition of mitochondrial 2 oxoglutarate-, pyruvate- and succinate-dependent dehydrogenases (Marín-Hernández et al., 2003; Hernández-Esquivel et al., 2006). In isolated human and rodent carcinomas and perfused-heart (Rodríguez-Enríquez et al., 2006; Hernández-Esquivel et al., 2006) CasII-gly also diminished the glycolytic flux. Therefore, the aim of this work was to determine the effect of CasII-gly on tumor glycolysis and HK activity. The results indicated that CasII-gly may indeed be considered as a promising multi-site metabolic drug that also targets the bioenergetics of glycolytic-dependent tumors.

Materials and methods

Chemicals

HK, G6P dehydrogenase, HPI, ALDO, α–GPDH, TPI, lactate dehydrogenase, G6P, F6P and F1,6BP were purchased from Roche Co. (Mannheim, Germany). Glucose, G3P, $MgCl_2$, ATP, NADH, NAD^+, NADP, 3BrPyr and amyloglucosidase were from Sigma Chemical (St Louis, MO, USA). Recombinant HK from *Entamoeba histolytica* was kindly provided by Dr. E. Saavedra, Instituto Nacional de Cardiología, México. Casiopeina II-gly (aqua (4-7 dimethyl-1, 10-phenanthroline) (glycine) copper (II) nitrate) was synthesized as previously described (Kachadourian et al., 2010) and dissolved in distilled water.

Isolation of tumor and no tumor cells

Human tumor cells (HeLa, PC-3, MDA-MB-231, TD47, HTC15, SK-LU, U87MG, glioma C6 and MCF-7) were grown in Dulbecco-MEM medium supplemented with 5% fetal serum and 10,000 U/ ml streptomycin/ penicillin at 37°C in 95% air/ 5% CO_2. After 90% confluence, cells were removed from each culture flask by adding 0.25% trypsin/ 1mM EDTA and washed once by centrifugation with Krebs Ringer buffer (125 mM NaCl, 5 mM KCl, 1 mM $MgCl_2$, 1.4 mM $CaCl_2$, 1 mM KH_2PO_4, 25 mM HEPES, pH 7.4). AS-30D hepatocarcinoma cells (4 X 10^8 cells/ml) were propagated in female 200-250 g Wistar rats by intraperitoneal inoculation. AS-30D cells were isolated by centrifugation as previously described (López-Gómez et al., 1993).

Human platelets were isolated from healthy donor blood. The platelet rich-plasma was separated by differential centrifugation at 200 g for 20 min. Platelets were washed twice with Krebs-Ringer medium and centrifuged at 1800 g for 10 min. Afterwards, cellular pellet was re-suspended in Krebs Ringer medium at a final concentration of 15-20 mg/ml (Vasta et al., 1987). Lymphocytes were isolated from donor volunteers as described elsewhere (Rodríguez-Enríquez et al., 2006). Primary human endothelial cells (HUVECs) were isolated from umbilical cords according to Jaffe et al (1973).

Cellular protein was determined by biuret assay using bovine serum albumin (BSA) as standard (Gornall, et al., 1949). Viability assessed by the trypan blue

exclusion assay. revealed less than 10-15% cellular death under all experimental conditions for tumor cells and normal cells .

Cell growth in cells exposed to CasII-gly and 3BrPyr

Cell growth inhibition was determined by the crystal violet method (Gallardo-Pérez et al., 2009).Briefly, cells (tumor and normal cells) were seeded at 2 x 10^5 cells/well in 96 and 24-well plates (for 24 and 72 hrs respectively), left for 24 h prior to the treatment with drugs. After, cells were exposed for 24 and 72 hrs to different concentrations (0.1-100 µM) of CasII-gly and 3BrPyr.

Isolation of rat hepatocarcinoma mitochondria

AS-30D mitochondria were isolated by differential centrifugation with digitonin (15 µg/ mg cellular protein; ICN, Ohio, USA) as previously described by López-Gómez et al (1993).

Determination of glycolytic fluxes and metabolite concentrations

Tumor cells (15 mg protein/ml) were incubated in Krebs-Ringer buffer under orbital shaking (150 rpm) at 37°C with or without 100 µM CasioII-gly. After 1 min pre-incubation, 5 mM glucose (+GLU) was added. One ml of cellular sample was taken immediately (time 0), and the rest was further incubated for 10, 20, 30 and 60 min. Each sample was mixed with perchloric acid (3%, v/v final concentration) and centrifuged at 1800 g by 1 min. The supernatant was neutralized with 3 M KOH/ 0.1 M Tris and centrifuged once to eliminate potassium salts. Supernatants were kept on ice for determination of G6P, F6P, F1,6BP, Trioses phosphate (TriP), ATP and L-lactate concentrations by using standard enzymatic methods (Bergmeyer, 1974). In parallel, cellular samples (1 ml) were taken after 30 and 60 min incubation, and frozen in liquid nitrogen and kept at -70 °C for determination of HK and PFK-1 activities, and fluxes from HK to TPI (first section of glycolytic pathway).

For glycogen determination, the cellular samples withdrawn after 30 and 60 min incubation were centrifuged at 20800 g for 20 s. The pellet was frozen in liquid nitrogen and kept at -70 °C until its use. The thawed cellular pellet was re-suspended in 30% KOH and heated for 30 min at 90°C. Afterwards, the sample was mixed with 6%

Na_2SO_4 and 100% ethanol and centrifuged at 20800 g for 5 min. Pellet was washed once with 1 ml of 80% ethanol and incubated at room temperature. Finally, the dried sample was re-suspended in 0.2 M acetate buffer, pH 4.8, plus 5 U amyloglucosidase and incubated for 1 h at 37°C (Hue et al., 1975). Glucose units derived from glycogen breakdown were determined by enzymatic analysis (Bergmeyer, 1974).

Enzyme activities and initial glycolytic segment fluxes

For determination of HK and PFK-1 activities, and fluxes from HK to TPI (first section of glycolytic pathway), aliquots of 1 ml (15 mg protein) were taken from cells incubated with CasII-gly at 30 and 60 min and centrifuged at 20800 g for 20 s. Cellular extracts were obtained from pellets re-suspended in 0.3 ml 25 mM Tris/HCl buffer plus 1 mM EDTA, 5 mM DTT and 1 mM PMSF (Marín-Hernández et al., 2006) and frozen in liquid nitrogen. Afterwards, three cycles of freezing/thawing at 37°C were carried out to obtain cellular lysates, which were centrifuged at 39000 g for 20 min at 4°C. Collected supernatants were stored in 10% (v/v) glycerol at -20°C until determination of enzyme activities and fluxes in KME buffer (100 mM KCl, 50 mM Mops and 1 mM EGTA) pH 7.0, at 37°C (Marín-Hernández et al., 2006).

For HK activity determinations in liver, brain and heart rat tissues, the organs were homogenized in 2 mL of SHE buffer (250 mM sucrose, 10 mM Hepes, 1 mM EGTA, pH 7.3) plus 1 mM EDTA, 0.5 mM DTT and 1 mM PMSF. Homogenates were centrifuged at 39 000 g for 20 min and 4 °C. Afterwards, the supernatant was collected for determination of enzyme activity.

The assays for both cytosolic and mitochondrial HK were carried out in 1 mL of KME (120 mM KCl, 20 mM Mops, EGTA 0.5 mM, pH 7) or KM (100 mM KCl, 50 mM Mops, pH 7) buffer plus 10 mM ATP, 15 mM $MgCl_2$, 1 mM NADP, 1 U/ml G6PDH and cellular extract (0.03 - 0.1mg). The reaction was started by adding 3 mM glucose. PFK-1 activity was determined in KME buffer plus 2 mM ATP, 5 mM $MgCl_2$, 5 µM F2,6BP, 0.15 mM NADH, 0.36 U aldolase/ml, 9 U triosephosphate isomerase/ml, 3 U α-GPDH/ml and cellular extract (0.03 – 0.1 mg protein). The reaction was started with 2 mM F6P.

GAPDH, PGK and PYK activities were determined according to Saavedra et al. (2004).

The flux through the first section of the glycolytic-pathway, *i.e*., from HK to TPI was determined by the method described by Torres *et al.*,(1988), modified as follows: The cellular extract (0.016- 0.5 mg protein) was pre-incubated for 5 min in KME buffer *plus* 10 mM ATP, 15 mM $MgCl_2$, 5 µM F2,6BP, 0.15 mM NADH and 6 U α- GPDH /ml; the reaction started by adding 3 mM glucose. To determine flux through the HPI-TPI segment, the reaction started by adding 10 mM G6P; for flux through the PFK-1-TPI segment, the reaction started by adding 5 mM F6P; and for flux through the ALDO-TPI segment, the reaction was started with 1 mM F1,6BP. In all assays, control experiments were undertaken to assess linearity of fluxes with respect to protein used. When the specific substrate was omitted, the flux rate was negligible. Also, coupling enzymes were insensitive to CasII-gly at the range of concentration used.

Statistical analysis

Student´s t-test for non-paired samples was used considering $P < 0.05$ as criterion of significance.

Results

Effects of CasII-gly and 3BrPir on the proliferation of normal and cancer cells

Due to that in preliminary essays were observed that CasII-gly inhibited HK activity in extracts of tumor cells, we decided to compare the effects of CasII-gly with 3-Bromo pyruvate (3BrPyr, aparently HK inhibitor) on the proliferation of several no-tumor and tumor cells lines. Both drugs decrease cells proliferation, in spite of presenting distinct effectiveness (Table1). It can be observed that CasII-gly was 13-91 times more potent than 3BrPyr decreasing tumor cells proliferation in 24 and 72 hrs. In contrast, normal cells (lymphocytes and endothelial cells) tested were relatively resistant to CasII-gly and 3BrPyr in comparison with tumor cells (Table1). Similar IC_{50} values of both drugs have been reported in other tumor and normal cells (Xu et al., 2005; Rodriguez-Enríquez, et al., 2006; Cao et al., 2008). These results are relevant because CasII-gly showed specificity by tumor cells over normal cells.

Effect of CasII-gly on tumor glycolytic flux and high energy-metabolites content

Treatment of tumor cells with CasII-gly and 3BrPyr induced a dramatic decrease in intracellular levels of gluthation (GSH) in function of protein concentration (data no shown). In consequence, we decided to determine optimal cellular protein concentration in which it was not observed modifications in the levels of GSH and this concentration was 15 mg /mL.

Titration of tumor glycolytic flux with CasII-gly (range 1-100 μM) (data not shown) revealed that 100 μM was an adequate concentration to induce changes in the glycolytic flux and glycolytic enzyme activities, without cellular viability alterations.

Therefore, the effect of 100 μM CasII-gly on the glycolytic flux was assayed in AS-30D carcinoma cells incubated in glucose-free medium (-GLU) or glucose-medium (+GLU) for 10-60 min (Fig. 1A). The incubation for 60 min without exogenous glucose did not change the lactate (Fig. 1A) and glycogen contents (Table 2), indicating depressed glycolysis and glycogenolysis rates. In the presence of CasII-gly for 60 min, the endogenous lactate increased 3.6-fold (Fig. 1A), suggesting drug activation of tumor glycolysis. In the presence of glucose, an increase of 13.7-times in lactate production was observed, in agreement with a previous report (Marín-Hernández et al., 2006), and the addition of CasII-gly did not modify significantly the production of lactate (Fig. 1A). Thereby, a significant increase in the glycolytic flux (12.2- and 1.9-fold) was attained in both –GLU and +GLU media between 30 and 60 min (Fig. 1B), indicating an active glycogen breakdown induced by the anti-neoplastic drug. To add support to the last hypothesis, the content of glycogen was determined. As expected, the drug significantly decreased (2-2.8times) the glycogen content (Table 2; Fig. 1C), which correlated well with the enhanced production of lactate (Fig. 1B) in cells stimulated by exogenous glucose, *i.e.*, when glycolysis is active; this correlation was less clear in cells incubated with no glucose.

Casiopeina II-gly did not modify the steady-state concentration of some glycolytic intermediates such as G6P, F6P, F1,6BP and TriP in glucose-incubated cells (Table 2), except for ATP, that was severely reduced by 60 % after 60 min incubation. In the absence of added glucose, the concentration of the glycolytic intermediates was below the limit of detection. However, although glycolysis was operating at a low rate, a high ATP level was still detected, which most likely derived from OxPhos; under these

conditions, CasII-gly also induced a significant diminution in the ATP content (78 %), indicating an inhibition of OxPhos as previously described (Marín-Hernández et al., 2003) (Table 2).

Effect of CasII-gly on the HK and PFK-1 activities and HK-TPI flux in drug-pretreated carcinoma cells

The observation that G6P levels were not modified by Cas-IIgly suggested (i) that the G6P pool was maintained by an activated glycogen breakdown (Table 2; Fig. 1C) or (ii) that HK was not a target for CasII-gly. Therefore, the activity of the soluble HK fraction (cytosolic enzyme) was determined in extracts of AS-30D tumor cells exposed for 60 min to 100 μM CasII-gly. Independently of the presence of glucose, CasII-gly drastically reduced the HK activity by 40-60%; in contrast, the PFK-1 activity (as control enzyme) was not affected by the drug (Fig. 2A). To further examine whether CasII-gly affects other enzymes of tumor glycolysis, the effect of the drug was assayed in both upper- and lower pathway segments (Fig. 2B). The flux of the first segment was assayed by feeding HK, HPI, PFK-1 or ALDO with its specific substrate (Fig. 2B) and measuring the α-GP produced under each experimental condition. CasII-gly inhibited the HK-TPI flux by 58%. On the contrary, the drug was ineffective on (i) the HPI-TPI (by adding G6P), PFK1-TPI (with F6P), and ALDO-TPI (with F1,6BP) fluxes, and (ii) the GAPDH, PGK and PYK activities (data no shown) . These observations clearly indicated that HK was the principal and exclusive CasII-gly target of tumor glycolysis.

Effect of CasII-gly on the HK activity and HK-TPI flux in non-drug treated tumor cells

To assess whether CasII-gly directly interacts with HK, mitochondrial and soluble HK fractions were prepared from non-drug treated AS-30D hepatoma. . To evaluate the effect of CasII-gly on the HK activity, the kinetics assays were performed in free-EGTA medium (Table 2). HK derived from different tumor sources was highly sensitive to CasII-gly or 3BrPyr, as well as HK derived from non-neoplastic tissues (Table 2). In the presence of EGTA, CasII-gly also promoted a significant inhibition of both soluble- and mitochondrial-HK AS-30D fractions at slightly higher concentrations (IC_{50} = 8 ± 3

μM; n=3; and 10 ± 2 μM; n=4; respectively) after 5 min incubation; in turn, 3BrPyr IC_{50} values for soluble-HK activity was similar in absent or in presence of EGTA (28 ± 8 (4) and 28 ± 10 (4) μM respectively).

Flux through the HK-TPI segment in non previously-treated cells was 48% inhibited by CasII-gly (10 μM), whereas flux through the HPI-TPI was unaffected (Fig. 3B), indicating that HK is a specific and direct CasII-gly target.

In order to evaluate whether other metal-based anti-neoplastic drugs, or the ion copper, have similar effect on HK activity as CasII-gly, cellular extracts were incubated for 5 min with 100 μM cisplatin (Fig. 3C,a) or 10-20 μM $CuCl_2$ (Fig 3C,b,c). Non-significant diminution in HK activity was attained with cisplatin, at same doses used to inhibit rabbit muscle Aldo (85%) and GAPDH (45%) (Aull, et al., 1979).

Copper is the metal involved in the coordination of the dimethyl-phenantroline rings in CasII-gly. In human erythrocytes, copper (15-100 μM) reacts with thiol-groups of several glycolytic enzymes promoting activity inhibition (Boulard et al., 1972). However, only at 20 μM Cu^{2+} HK activity was partially inhibited (Fig. 3C,c).

The activities of HK and other glycolytic enzymes (PFK, GAPDH, PGK and PYK) were also evaluated in extracs of cells incubated 60 min in the presence of 100 μM 3BrPyr or $CuCl_2$. However, none of the drugs, or ion, tested significantly modified the activity of these enzymes and lactate production (data not shown).Only 3BrPyr reduced GAPDH activity 25% (data not shown).

Discussion

Metabolic drugs have recently emerged as a suitable alternative therapeutic approach against malignant chemo- and radiotherapy-resistant tumors (Rodriguez-Enriquez et al., 2009). The action mechanism of the copper-based drug Casiopeina II-gly is to disturb DNA stabilization in HeLa, SiHa, Caski and C33-A tumors (Mejía and Ruiz, 2008; reviewed in Rodríguez-Enríquez et al., 2009) and to promote apoptosis in a process mediated by reactive oxygen species (Trejo-Solís et al., 2005; Mejía and Ruiz, 2008;). Moreover, CasII-gly affects mitochondrial ATP synthesis in rat AS-30D hepatocarcinoma, a highly OxPhos-dependent tumor (Rodríguez-Enríquez et al., 2006)

by interacting with the reactive thiol groups of Krebs cycle (pyruvate, 2-OG, succinate) dehydrogenases (Marín-Hernández et al., 2003; Hernández-Esquivel et al., 2006).

Glycogen breakdown-induced by CasII-gly is responsible of the increment in tumor glycolysis

After prolonged incubation with CasII-gly, lactate production significantly increased suggesting glycolysis activation. A similar pattern was observed in normal (mouse fibroblast 3T3-L1 adipocytes, L6 rat skeletal myoblasts) and HepG2 tumor cells after treatment with the anti-hyperglycemic drugs biguanides (buformin, phenformin), nefazodone (antidepressant) or the alkaloid berberine (Dykens et al., 2008a, 2008b; Yin et al., 2008). It was suggested that biguanides-, nefazodone- and berberine-glycolysis activation was the result of mitochondrial dysfunction (Dykens et al., 2008a, 2008b; Yin et al., 2008). However, glycogen degradation increased significantly in the presence of CasII-gly (*cf.*, Fig 1C), thus indicating that the increase in lactate production (*cf.*, Fig 1B) was the result of the drug-activated glycogen-breakdown. Although, the mechanism involved in the CasII-gly-activated glycogenolysis was not analyzed here, in rat isolated hepatocytes was demonstrated that non-steroidal anti-inflammatory drugs (Ibuprofen, indomethacin, meclofenamate) may promote glycogen degradation by interfering with the intracellular Ca^{2+} homeostasis (Brass and Garrity, 1985) and probably increasing glycogen phosphorylase A activity.

The glycogen breakdown after 60 min incubation with CasII-gly was 16 (-GLU) and 72 (+GLU) nmol/mg protein (*cf.* Table 1), which should theoretically generate 32 and 144 nmol lactate/mg protein, respectively. These predicted values matched the lactate production (*cf.* Fig. 1A, B) of 61 (-GLU) and 86 (+GLU) nmol/mg protein.

Mitochondrial and soluble-hexokinase are targets of CasII-gly

The majority of fast-growth tumor cells over-express HK-II, which is 30-50% located in the cytosol (Ko et al., 2001; Marín-Hernández et al., 2006) and the rest bound to the external mitochondrial membrane (Pastorino and Hoek, 2003) in a close vicinity to the adenine nucleotide translocator and VDAC (Pastorino and Hoek, 2003). Its

mitochondrial location is considered as a metabolic strategy of cancer cells to channel mitochondrial ATP for glycolysis (Pastorino and Hoek, 2003) and to inhibit apoptosis by blocking cytochrome c release (Pedersen et al., 2002; Pastorino and Hoek, 2003). Furthermore, HK is one of the main controlling steps of tumor glycolysis (Marín-Hernández et al., 2006; 2010). These characteristics make this enzyme an attractive target for anti-neoplastic therapy.

3BrPyr has shown potent inhibitory effect on the cellular proliferation of leukemia HL-60 cancer and AS-30D hepatocarcinoma (IC_{50}≈ 10- 50 μM) and Hep 3B and SNU449 hepatocarcinomas (50-200 μM) (Ko et al., 2004; Xu et al., 2005; Kim et. al., 2008). In VX-2 epidermoid rabbit and rat AS-30D tumors, 3BrPyr bolus of 1-25 ml of 0.5-2 mM significantly reduced the tumor progression *in vivo* (Geschwind et al., 2002; Ko et al., 2004). Although it has been claimed that 3BrPyr effect on tumor proliferation (including tumor progression, tumor toxicity) was the result of HK inhibition, it seems that other sites are involved as HK inhibition is attained at very high 3BrPyr concentration (2-10 mM) (Ko et al., 2001). In addition, several groups have described non-specific effects of 3BrPyr. For example, in HepG2 cells, 150 μM 3BrPyr does not affect HK activity but severely decreases (90 and 70 %) GAPDH and PGK activities (Pereira da Silva et al., 2009). Similar specific inhibition on GAPDH activity is reported in other human (Hep3B and SK-Hep1) and rabbit (Vx-2) hepatocellular carcinoma cell lines exposed to concentrations of 10 to 200 μM (Ganapathy-Kanniappan et al., 2009). In our study with 100 μM 3BrPyr only was observed 25% in the reduction of GAPDH activity (data no shown). These differences in results can be attributed to time of exposition (0.5-2 hr) and DTT concentration used in each case (0.5-5 mM). At 3BrPyr doses assayed to arrest tumor progression, pyruvate decarboxylase, isocitrate lyase, H^+ vacuolar ATPase, and acetylcholine synthesis are also affected (Arendt et al., 1990; Dell' Antone, 2006).

Several highly malignant tumors such as human melanoma, lymphoma, head and neck, breast, liver and colorectal cancers are apparently dependent on the glycolysis pathway to survive (Okada, et al, 1992; ;Lapela, et al, 1995; Abdel-Nabi, et al, 1998; Schwimmer, et al, 2000; Czernin and Phelps, 2002). In this context, the search for a potent, specific and permeable anti-glycolytic drug appears as a novel and promising

task. Encouragingly, CasII-gly inhibited both soluble (AS-30D, HeLa, MCF-7, MDA-MB-231, SK-LU, PC-3) and mitochondrial (AS-30D) HK isoforms (*cf.* Fig. 2A, 3A; Table 2). However, CasII-gly potency was reduced 2 times in presence of EGTA, probably because the copper is sequestrated by this agent. Therefore, tricarboxylic acid cycle intermediates as citrate and malate (physiological chelators) may reduce potency of CasII-gly *in vivo*.

The HK inhibition by Cas-IIgly was highly specific as other glycolytic enzymes were not affected. However, HKI, HKII and GK of normal rat tissues and human platelets were also inhibited (Table 2). But when normal and tumor cells were exposed to CasII-gly, this drug was more potent in reduced cellular proliferation on tumor cells than normal cells (see Table 1) This selective effect is not achieved by lonidamine, clotrimazol or 3BrPyr (Floridi et al., 1981; Penso et al., 2002; Pereira da Silva et al., 2009). The apparent higher selectively of CasII-gly towards tumor cells over normal cells seems related to its physico-chemical nature of lipophilic cation, which facilitates its entrance to tumor cells and mitochondria that maintain higher transmembrane electrical gradients (negative inside) across the plasma and inner mitochondrial membranes, in comparison with normal cells and mitochondria (Moreno-Sánchez et al., 2007; 2009; Rodríguez-Enríquez et al., 2009).

CasII-gly inhibits HK at lower doses than 3BrPyr and cisplatin

CasII-gly (IC_{50}= 4-10 μM) resulted to be a more potent HK inhibitor than 3BrPyr (IC_{50}=28 μM), cisplatin (*cf*, Fig 3B) and others anticancer drugs (clotrimazol or lonidamine) strongly suggesting that CasII-gly may be considered as a potent metabolic anti-cancer drug affecting energy metabolism. It is reported that 3BrPyr have the ability to interact with sulfhydryl groups (Ganapathy-Kanniappan et al., 2009). These groups apparently are critical for structural stability and catalytic activity of hexokinase isoforms (Hutny and Wilson, 1990; Tiedge et al., 2000) as consequence are higher susceptibility to several alquilant agents such as 3BrPyr (Connolly and Trayer, 1978; Fiorani et al., 2000; Tiedge et al., 2000). However in this study was not analyzed the mechanism of CasII-gly inhibition of HK, this inhibition can be atribute to cysteine interaction how has been establish for inhibition of mitochondrial 2 oxoglutarate-, pyruvate- and succinate-

dependent dehydrogenases (Marín-Hernández et al., 2003; Hernández-Esquivel et al., 2006).

However, we demonstrated that CasII-gly inhibits HK activity, it was observed a negligible effect on glycolysis. The results suggest that CasII-gly enhances glucose metabolism by stimulation of glycogen degradation, which is related to a mechanism to compensate the HK inhibition and lower ATP. The level of glycogen is function of the both its production and its breakdown, which are mediated by the enzymes glycogen synthase (GS) and glycogen phosphorylase (GP), respectively. The activity of these enzymes is regulated by phosphorylation and several effectors. GP catalizes the first step in intracellular degradation of glycogen, which may activated by AMP and is inhibited by ATP and other metabolites so that the enzyme is response to the levels of metabolites in the cell (Stalmans et al., 1974; Ercan et al, 1996). As the effect of ATP is counteracted by AMP concentration, we can propose that the glycogenolysis is activated because CasII-gly lead to ATP depletion (possibly as result of mitochondrial impairment), increasing availability of AMP. These changes in ATP and AMP concentrations could support the activation of the GP.Finally, the results suggested that CasII-gly may be considered as a potent and specific metabolic drug that affect energy metabolism and also indicated that the inhibition of solely one controlling step brought about negligible effects on glycolysis. Only the simultaneous inhibition of the other controlling steps (GLUT and HPI) may have significant impact on glycolytic flux (Marín-Hernández et al., 2010).

Acknowledgements

This work was partially supported by a CONACyT-Mexico grant (No 80534). AMH was supported by a CONACyT fellowship (No. 59991).

References

Abdel-Nabi, H., Doerr, R.J., Lamonica, D.M., Cronin, V.R., Galantowicz, P.J., Carbone, G.M., Spaulding, M.B., 1998. Staging of primary colorectal carcinomas with fluorine-18 fluorodeoxyglucose whole-body PET: correlation with histopathologic and CT findings. Radiology. 206, 755-60.

Aull, J.L., Allen, R.L., Bapat, A.R., Daron, H.H., Friedman, M.E., Wilson, J.F., 1979. The effects of platinum complexes on seven enzymes. Biochem. Biophys. Acta 571, 352-358.

Arendt, T., Schugens, M.M., Marchbanks, R.M., 1990. Reversible inhibition of acetylcholine synthesis and behavioural effetcs caused by 3-bromopyruvate. J. Neurochem. 55, 1474-1479.

Bergmeyer, H.U. (Ed.), 1974. Methods of Enzymatic Analysis, second English Ed. Verlag Chemie-Academic Press, New York.

Boulard, M., Blume, K.G., Beutler, E., 1972. The effect of copper on red cell enzyme activities. J. Clin. Inves. 51, 459-461.

Brass, E.P., Garrity, M.J., 1985. Effect of nonsteroidal anti-inflammatory drugs on glycogenolysis in isolated hepatocytes. Br. J. Pharmacol. 86, 491-496

Brizel, D.M., Schroeder, T., Scher, R.L., Walenta, S., Clough, R.W., Dewhirst, M.W., Mueller-Klieser, W., 2001. Elevated tumor lactate concentrations predict for an increased risk of metastases in head-and-neck cancer. Int. J. Radiat. Oncol. Biol. Phys. 51, 349-53.

Cao, X., Bloomston, M., Zhang, T., Frankel, W.L., Jia, G., Wang, B., Hall, N.C., Koch, R.M., Cheng, H., Knopp, M.V., Sun, D., 2008. Synergistic antipancreatic tumor effect by simultaneously targeting hypoxic cancer cells with HSP90 inhibitor and glycolysis inhibitor. Clin. Cancer Res. 14, 2008.

Carew, J.S., Huang, P., 200**2**. Mitochondrial defects in cancer. Mol. Cancer 1:9.Connolly, B.A., Trayer, I.P., 1979. Affinity labelling of rat-muscle hexokinase type II by a glucose-derived alkylating agent. Eur J Biochem. 93, 375-83.

Czernin, J., Phelps, M.E., 2002, Positron emission tomography scanning: current and future applications. Annu. Rev. Med. 53, 89-112.

Dell' Antone, P., 2006. Inactivation of H^+- vacuolar ATPase by the energy blocker 3-bromopyruvate, a new antitumor agent. Life Sci. 79, 2049-2055.

De Vizcaya-Ruiz, A., Rivero-Mueller, A., Ruiz-Ramírez, L., Kass, G.E., Kelland, L.R., Orr, R.M., 2000. Induction of apoptosis by a novel cupper-based anticancer compound, casiopeina II, in L1210 murine leukaemia and CH1 human ovarian carcinoma cells. Toxicol. In Vitro 14,1-5.

Dykens, J.A., Jamieson, J.D., Marroquin, L., Nadanciva, S., Xu, J.J., Dunn, M.C., Smith, A.R., Will, Y., 2008a. *In vitro* assessment of mitochondrial dysfunction and cytotoxicity of nefazodone, trazodone, and buspirone. Toxicol. Sci. 103, 335-345.

Dykens, J.A., Jamieson, J., Marroquin, L., Nadanciva, S., Billis, P.A., Will, Y., 2008b. Biguanide-induced mitochondrial dysfuntion yields incresed lactate production and cytotoxicity of aerobically-poised HepG2 cells and human hepatocites in vitro. Toxicol. Appl. Pharmacol. 233, 203-210.

Ercan, N., Gannon, M.C., Nuttall, F.Q.,1996. Arch Biochem Biophys. 328, 255-64.Fiorani, M., De Sanctis, R., Scarlatti, F., Vallorani, L., De Bellis, R., Serafini, G., Bianchi, M., Stocchi, V., 2000. Mol Cell Biochem. 209, 145-53.

Floridi, A., Paggi, M.G., D' Atri, S., Martino, C.D., Marcante, M.L., Silvestrini, B., Caputo, A., 1981. Effect of lonidamie on the energy metabolism of Erlich ascites tumor cells. Cancer Res. 41, 4661-4666.

Gallardo-Pérez, J.C., Espinoza, M., Ceballos-Cancino, G., Daniel, A., Rodríguez-Enríquez, S., Aviles, A., Moreno-Sánchez, R., Melendez-Zajgla, J., Maldonado, V., 2009. NF-kappa B is required for the development of tumor spheroids. J. Cell. Biochem. 108, 169-180.

Ganapathy-Kanniappan, S., Geschwind, J.F., Kunjithapatham, R., Buijs, M., Vossen, J.A., Tchernyshyov, I., Cole, R.N., Syed, L.H., Rao, P.P., Ota, S., Vali, M., 2009. Anticancer Res. 29, 4909-18.

Gatenby, R.A., Gillies, R.J., 2007. Glycolysis in cancer: a potential target for therapy. Int. J. Biochem. Cell Biol. 39, 1358-66.

Geschwind, J.F.H., Ko, Y.H., Torbenson, M.S., Magee, C., Pedersen, P.L., 2002.Novel therapy for liver cancer: direct intraarterial injection of a potent inhibitor of ATP production. Cancer Res. 62, 3909-3913.

Gornall, A.G., Bardwill, C.J., David, M.M., 1949. Determination of serum proteins by means of biuret reaction. J. Biol. Chem. 177, 751-766.

Hernández-Esquivel, L., Marín-Hernández, A., Pavon, N., Carbajal, K., Moreno-Sánchez, R., 2006. Cardiotoxicity of copper based antineoplastic drugs casiopeinas is related to inhibition of energy metabolism. Toxicol. Appl. Pharmacol. 212, 79-88.

Hue, L., Bontemps, F., Hers, H., 1975. The effects of glucose and of potassium ions on the interconversion of the two forms of glycogen phosphorylase and of glycogen synthetase in isolated rat liver preparations. Biochem. J. 152, 105-14.

Hutny, J., Wilson, J.E., 1990.Effect of ligand-induced conformational changes on the reactivity of specific sulfhydryl residues in rat brain hexokinase. Arch Biochem Biophys. 283, 173-83.

Jaffe, E., Nachmen, R.L., Becker, G.C., Minick, C.R., 1973. Culture of human endothelial cells from umbilical veins. J. Clin. Invest. 52, 2745-2756.

Kachadourian, R., Brechbuhl, H. M., Ruiz-Azuara, L., Gracia-Mora, I., Day, B.J., 2010. Casiopeína IIgly-induced oxidative stress and mitochondrial dysfunction in human lung cancer A549 and H157 cells. Toxicology, 268, 176-183.

Kim, J.S., Ahn, K.J., Kim, J.A., Kim, H.M., Lee, J.D., Lee, J.M., Kim, S.J., Park, J.H., 2008. Role of reactive oxygen species-mediated mitochondrial dysregulation in 3-bromopyruvate induced cell death in hepatoma cells. J. Bionerg. Biomembr. 40, 607-618.

Ko, Y.H., Pedersen, P.L., Geschwind, J.F., 2001. Glucose catabolism in the rabbit VX2 tumor model for liver cancer: characterization and targeting hexokinase. Cancer Lett. 173, 83-91.

Ko, Y.H., Smith, B.L., Wang, Y., Pomper, M.G., Rini, D.A., Torbenson, M.S., Hullihen, J., Pedersen, P.L., 2004. Advenced cancers: eradication in all cases using 3-bromopyruvate therapy to deplete ATP. Biochem. Biophys. Res. Commun. 324, 269-275.

Lapela, M., Grénman, R., Kurki, T., Joensuu, H., Leskinen, S., Lindholm, P., Haaparanta, M., Ruotsalainen, U., Minn, H., 1995. Head and neck cancer: detection of recurrence with PET and 2-[F-18]fluoro-2-deoxy-D-glucose. Radiology. 197, 205-11.

Lawley, P.D., Phillips, D.H., 1996. DNA adducts from chemotherapeutics agents. Mut. Res. 355, 13-40.

López-Gómez, F., Torres-Márquez, M.E., Moreno-Sánchez, R., 1993. Control of oxidative phosphorylation in AS-30D hepatoma mitochondria. Int. J. Biochem. 25, 373-377.

Marín-Hernández, A., Gracia-Mora, I., Ruiz-Ramírez, L., Moreno-Sánchez, R., 2003. Toxic effects of cupper-based antineoplastic drugs (Casiopeinas) on mitochondrial fuctions. Biochem. Pharmacol. 65, 1979-1989.

Marin-Hernandez, A., Rodriguez-Enriquez, S., Vital-Gonzalez, P.A., Flores-Rodriguez, F.L., Macias-Silva, M., Sosa-Garrocho, M., Moreno-Sanchez, R., 2006. Determining and understanding the control of glycolysis in fast-growth tumor cells. Flux control by an overexpressed but strongly product-inhibited hexokinase. FEBS J. 273, 1975–1988.

Marín-Hernández, A., Gallardo-Pérez, J.C., Rodríguez-Enríquez, S., Encalada, R., Moreno-Sánchez, R., Saavedra E., 2010. Modeling cancer glycolysis. Biochim Biophys Acta. 2010 “In Press”.

Mejia, C., Ruiz-Azuara, L., 2008. Casiopeinas IIgly and IIIia induce apoptosis in medulloblastoma cells. Pathol. Oncol. Res. 14, 467-472.

Moreno-Sánchez, R., Rodríguez-Enríquez, S., Marín-Hernández, A., Saavedra, E., 2007. Energy metabolism in tumor cells. FEBS J. 274, 1393-1418.

Moreno-Sánchez, R., Rodríguez-Enríquez, S., Saavedra, E., Marín-Hernández, A., Gallardo-Pérez, J.C., 2009. The bioenergetics of cancer: Is glycolysis the main ATP supplier in all tumor cells. Biofactors 35, 209-225.

Okada, J., Yoshikawa, K., Itami, M., Imaseki, K., Uno, K., Itami, J., Kuyama, J., Mikata, A., Arimizu, N., 1992. Positron emission tomography using fluorine-18-fluorodeoxyglucose in malignant lymphoma: a comparison with proliferative activity. J Nucl Med. 33, 325-9.

Pastorino, J.G., Hoek, J.B., 2003. Hexokinase II: The integration of energy metabolism and control of apoptosis. Curr. Med. Chem. 10, 1535-1551.

Pedersen, P.L., Mathupala, S., Rempel, A., Geschwind, J.F., Ko, Y.H., 2002. Mitochondrial bound type II hexokinase: a key player in the growth and survival of many cancers and an ideal prospect for therapeutic intervention. Biochim. Biophys. Acta 1555, 14-20.

Pelicano, H., Martin, D.S., Xu, R.H., Huang, P., 2006. Glycolysis inhibition for anticancer treatment. Oncogene 25, 4633-4646.

Penso, J., Beitner, R., 2002.Detachment of glycolytic enzyme from cytoskeleton of Lewis lung carcinoma and colon adenocarcinoma cells induced by clotrimazole and its correlation to cell viability and morphology. Mol. Genet. Metab. 76, 181-188.

Pereira da Silva, A.P., El-Bacha, T., Kyaw, N., dos Santos, R.S., da Silva, W.S., Almeida, F.C., Da Poian, A.T., Galina, A., 2009. Inhibition of energy –producing patways of HepG2 cells by 3-bromopyruvate. Biochem. J. 417, 717-726.

Robey, I.F., Lien, A.D., Welsh, S.J., Baggett, B.K., Gillies, R.J., 2005. Hypoxia-inducible factor-1alpha and the glycolytic phenotype in tumors. Neoplasia. 7, 324-30.

Rodríguez-Enríquez, S., Vital-González, P.A., Flores-Rodríguez, F.L., Marín-Hernández, A., Ruiz-Azuara, L., Moreno-Sánchez, R., 2006. Control of cellular proliferation by modulation of oxidative phosphorylation in human and rodent fast-growing tumor cells. Toxicol. Appl. Pharmacol. 215, 208-217.

Rodríguez-Enríquez, S., Marín-Hernández, A., Gallardo-Pérez, J.C., Carreño-Fuentes, L., Moreno-Sánchez, R., 2009. Targeting of cancer energy metabolism. Mol. Nutr. Food Res. 53, 29-48.

Robustelli della Cuna, G., Pedrazzoli, P., 1991. Toxicity and clinical tolerance of lonidamine. Semin. Oncol. 18, 18-22.

Saavedra, E., Encalada, R., Pineda, E., Jasso-Chávez, R., Moreno-Sánchez, R., 2004. Glycolysis in Entamoeba histolytica.Biochemical characterization of recombinant glycolytic enzymes and flux control analysis. FEBS J. 272, 1767-1783.

Schwimmer, J., Essner, R., Patel, A., Jahan, S.A., Shepherd, J.E., Park, K., Phelps, M.E., Czernin, J., Gambhir, S.S., 2000. A review of the literature for whole-body FDG PET in the management of patients with melanoma. Q. J. Nucl. Med. 44, 153-67.

Simonnet, H., Alazard, N., Pfeiffer, K., Gallou, C., Beroud, C., Demont, J., Bouvier, R., Schagger, H., Godinot, C., 2002. Low mitochondrial respiratory chain content correlates with tumor aggressiveness in renal cell carcinoma. Carcinogenesis 23, 759-768.

Stalmans, W., Laloux, M., Hers, H.G., 1974. The interaction of liver phosphorylase a with glucose and AMP. Eur J Biochem. 49, 15-27.Tiedge, M., Richter, T., Lenzen, S., 2000. Importance of cysteine residues for the stability and catalytic activity of human pancreatic beta cell glucokinase. Arch Biochem Biophys. 375, 251-60.

Torres, N.V., Mateo, F., Sicilia, J., Meléndez-Hevia, E., 1988. Distribution of the flux control in convergent metabolic pathways: theory and application to experimental and simulated systems. Int. J. Biochem. 234, 169-174.

Trejo-Solís, C., Palencia, G., Zuñiga, S., Rodríguez-Ropon, A., Osorio-Rico, L., Sánchez-Torres, L., Gracia-Mora, I., Marquez-Rosado, L., Sánchez, A., Moreno-García, M.E., Cruz, A., Bravo-Gómez, M.E., Ruiz-Ramírez, L., Rodríguez-Enríquez, S., Sotelo, J., 2005. Cas II gly induces apoptosis in glioma C6 cells *in vitro* and *in vivo* through caspase-dependent and caspase-independent mechanisms. Neoplasia 7, 563-574.

Vasta, V., Bruni, P., Farnararo, M., 1987. Mechanism of thrombin-induced rise in platelet fructose 2,6-bisphosphate content. Biochem. J. 244, 547-551.

Xu, R., Pelicano, H., Zhou, Y., Carew, J.S., Feng, L., Bhalla, K.N., Keating, M.J., Huang, P., 2005. Inhibition of glycolysis in cancer cells: a novel strategy to overcome drug resistance associated with mitochondrial respiratory defect and hypoxia. Cancer Res. 65, 613-621.

Yin, J., Gao, Z., Liu, D., Liu, Z., Ye, J., 2008. Berberine improves glucose metabolism througth induction of glycolysis. Am. J. Physiol. Endocrinol. Metab. 295, E148-156.

Figure legends

Figure 1. Effect of CasII-gly on glycolysis in AS-30D hepatocarcinoma cells
(A) AS-30D carcinoma cells (15 mg protein/ ml) were incubated in the presence (●, ■) or in the absence (○, □) of 100 μM CasII-gly in Krebs-Ringer buffer containing 5 mM glucose (+ GLU) or without glucose (- GLU). After 10, 20, 30, and 60 min, lactate (Lac) content was enzymatically determined. (B) Net lactate (Lac) production and (C) net variation in glycogen (Glyc) content were determined by subtracting values attained in the absence (Lac, Glyc) from values in the presence of 100 μM CasII-gly ($Lac_{CasII\text{-}gly}$; $Glyc_{CasII\text{-}gly}$) in AS-30D cells incubated for 30 and 60 min. Lactate is expressed in nmol/mg cellular protein and glycogen is expressed in nmol of glucose equivalents/mg cellular protein. Data show the mean ± SD of three different cellular preparations. * P< 0.05, **P<0.01,***P< 0.005 *vs*. $Lac_{CasII\text{-}gly}$-Lac or $Glyc_{CasII\text{-}gly}$- Glyc values is cero.

Figure 2. Effect of CasII-gly on HK and PFK-1 activities and on flux through the initial glycolytic segment AS-30D tumor cells were incubated for 60 min in the presence or in the absence of 100 μM CasII-gly in Ringer-Krebs buffer with (+Glu) or without (-Glu) 5 mM glucose. Afterwards, cellular extracts were obtained as described in the Material and Methods section. (A) 100 % activities of hexokinase (HK) and phosphofructokinase-1 (PFK-1) corresponds to 515 ± 140 and 152 ± 16 nmol/min/mg protein in the condition + GLU; 429 ± 96 and 140 ± 33 nmol/min/mg protein in condition - GLU, respectively. (B) Metabolic fluxes from HK to TPI in AS-30D cells (+GLU) treated with or without 100 μM CasII-gly. For the HK-TPI flux, 2 mM glucose was added; for the HPI-TPI, PFK-1-TPI and ALDO-TPI fluxes, the reaction was started with 10 mM G6P, 5 mM F6P, and 1 mM F1,6BP, respectively. 100 % control corresponds to 35 ± 25 (HK-TPI, GLU), 72 ± 57 (HPI-TPI, G6P), 153 ± 106 (PFK-TPI, F6P) and 438 ± 86 (ALD-TPI, F1,6BP) nmol/min/mg protein, respectively. Data show the mean ± SD of three different preparations.*P< 0.005 vs. no CasII-gly addition.

Figure 3. Activities of mitochondrial and soluble HK and fluxes of the first glycolytic segment at low CasII-gly concentration and 3BrPyr
A) Effect of CasII-gly and 3BrPyr on mitochondrial bound (●) and cytosolic HK activity (□, ■).B) Inhibition of flux from HK to TPI and from HPI to TPI by 10 μM CasII-gly (black bars) C) Effect of 100 μM cisplatin (a); 10 μM $CuCl_2$ (b) ; 20 μM $CuCl_2$ (c); 10 μM CasII-gly (d) on cytosolic tumor HK activity.*P<0.005 *vs* A) CasII-gly condition, B) 100% flux; **P<0.05 *vs* 100% HK activity.
The extracts were pre-incubated for 5 min with the indicated drug concentration. Afterwards, mitochondrial and cytosolic HK activities and segment fluxes were determined by adding 5 mM glucose (HK-TPI) or 5 mM G6P (HPI-TPI). In the absence of drug, the rates of mitochondrial bound- and cytosolic HKs were 1150 ± 996 and 648 ± 242 nmol NAD(P)H/min/mg protein; and the fluxes from HK to TPI and HPI to TPI were 55 ± 39 and 201 ± 103 nmol NAD(P)H/min/mg protein. Data show the mean ± SD of at least three different preparations.

Table 1.- Potency of Cas-IIgly and 3BrPyr on tumor and normal cells.

	IC_{50} (μM)			
Time	24 hr		72 hr	
	CasII-gly	3BrPyr	CasII-gly	3BrPyr
Rodent	Tumor cells			
Glioma C6	0.75 (1)	>100 (1)	ND	ND
Human				
HeLa	5 ± 2 (4)	> 100 (2)	0.66 (2)	48 (2)
MCF-7	5.7 ± 1 (3)	78 ± 15 (3)	0.76 ± 0.09 (3)	69 ± 27 (3)
PC3	6.7 (2)	>100 (2)	0.52 (2)	>100 (2)
SKLU	3.6 (2)	79 (2)	0.86 (2)	45 (2)
U87MG	5.7 (2)	74 (2)	1.9 (2)	79 (2)
HTC15	5.1 (1)	68 (1)	0.74 (1)	58 (1)
Human	Normal Cells			
Lymphocytes	>100 (3)	>100 (2)	>10 (3)	>10 (3)
Endothelial cells from umbilical cords	>100 (2)	>100 (3)	27 (1)	>100 (2)

Table 2 Effect of CasII-gly on the content of glycogen, glycolytic intermediates and ATP in AS-30D hepatocarcinoma

	+ GLU				- GLU			
	30 min		60 min		30 min		60 min	
		+ Cas-IIgly		+ Cas-IIgly		+ Cas-IIgly		+ Cas-IIgly
Glycogen	133 ± 8 (4)	105 ± 6* (4)	152 ± 14 (4)	81 ± 18* (4)	73 ± 7 (3)	65 ± 6 (3)	69 ± 2 (3)	53 ± 5 * (3)
G6P	0.4 ± 0.2 (3)	0.5 ± 0.3 (3)	0.5 ± 0.4 (6)	0.9 ± 0.6 (6)	N.D.	N.D.	N.D.	N.D.
F6P	0.4 ± 0.3 (5)	0.7 ±0.5(5)	0.2 ± 0.1 (6)	0.4 ± 0.2 (6)	N.D.	N.D.	N.D.	N.D.
F1,6BP	1 ± 0.8 (5)	2 ± 1.1(3)	0.4 ± 0.1(4)	0.6 ± 0.3 (3)	N.D.	N.D.	N.D.	N.D.
TriP	2 ± 1.1 (4)	1 ± 0.4(3)	0.6 ± 0.3 (3)	0.7 ± 0. 2(4)	N.D.	N.D.	N.D.	N.D.
ATP	9 ± 2.2 (3)	7 ± 1.1(3)	10 ± 1.5 (4)	4 ± 1.3**(4)	11 ± 0.7 (3)	7 ± 0.8**(3)	9± 2.6 (4)	2 ± 0.3 **(3)

Values are expressed in nmol/mg protein and represent the mean ± SD; number of different preparations assayed is shown in parentheses. N.D., not detected *P < 0.01 or **P< 0.005 vs. no CasII-gly at 30 or 60 min. .

Table 3. Potency of anti-neoplastic drugs on tumor and non-tumor cytosolic HK

	IC_{50} (μM)	
	CasII-gly	3BrPyr
Neoplasia		
Rodent		
AS-30D	4 ± 1 (4)	28 ± 8 (4)*
Glioma C6	17 ± 2 (3)	41 ± 8 (3)**
Human		
HeLa	16 (2)	34 (2)
PC-3	13 (2)	49 (2)
MDA-MB-231	19 (2)	>100 (3)
MCF-7	14 (2)	24 (2)
SK-LU	6 (2)	7.5 (2)
TD47	20 (1)	50 (1)
No tumorigenic tissues		
Rat brain (HKI)	6 ± 0.6 (3)	47 ± 13 (3)**
Rat heart (HKII)	9 ± 0.6 (3)	36 ± 13 (3)***
Rat liver (HKIV)	2 ± 0.8 (3)	43 ± 20 (3)***
Human platelets	4 ± 2 (3)	25 ± 8 (3)**

The values represent the mean ± SD; number of different preparations assayed is shown in parentheses. *P< 0.005, **P< 0.01 and ***P< 0.05 *vs*. CasII-gly.

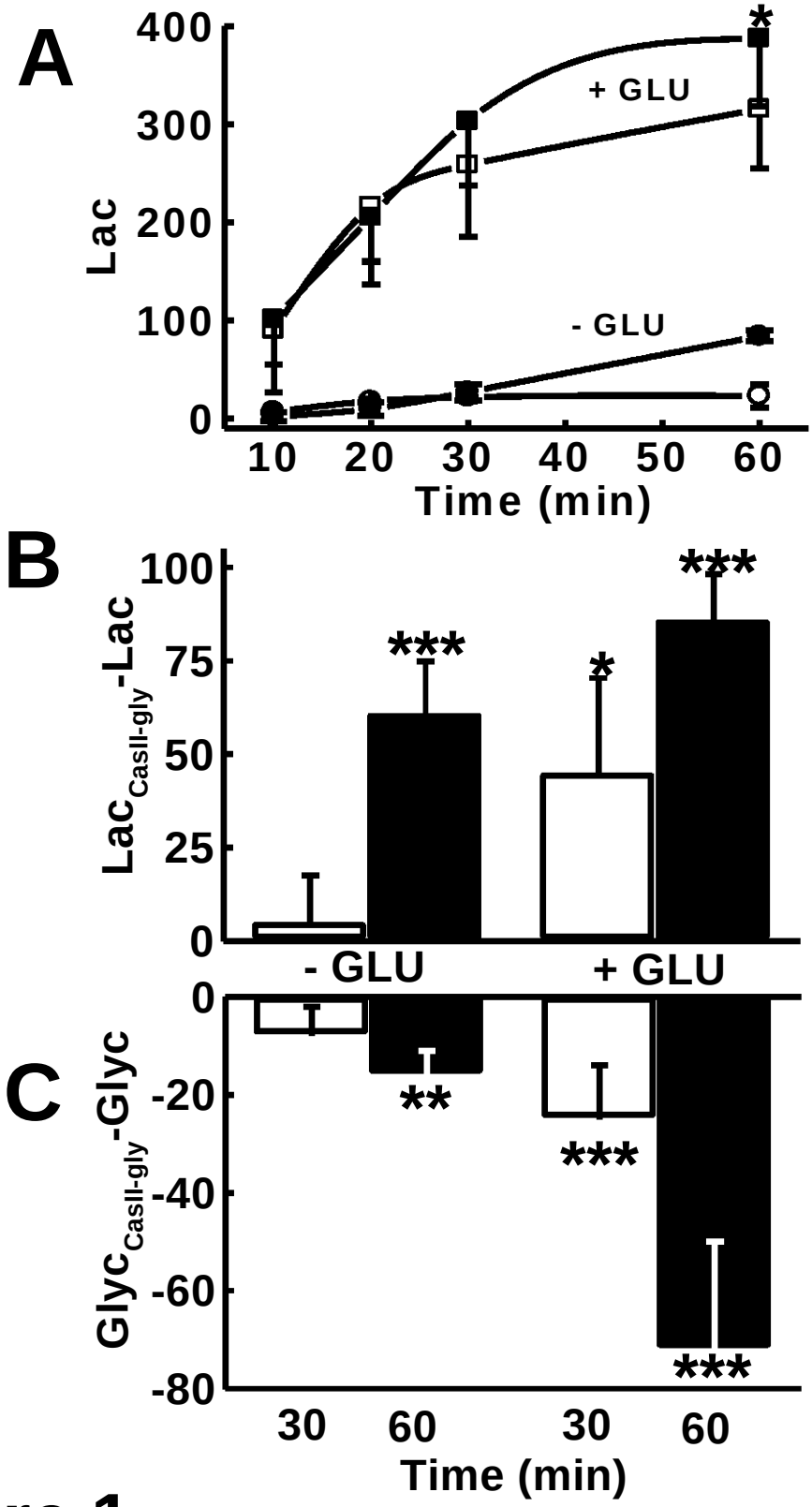
A
400
300
200
100
0
Lac
+ GLU
- GLU
*
10
20
30
40
50
60
Time (min)
B
100
75
50
25
0
Lac$_{CasII-gly}$-Lac
***
*
***
- GLU
+ GLU
C
0
-20
-40
-60
-80
Glyc$_{CasII-gly}$-Glyc
**
***
***
30
60
30
60
Time (min)

Figure 1

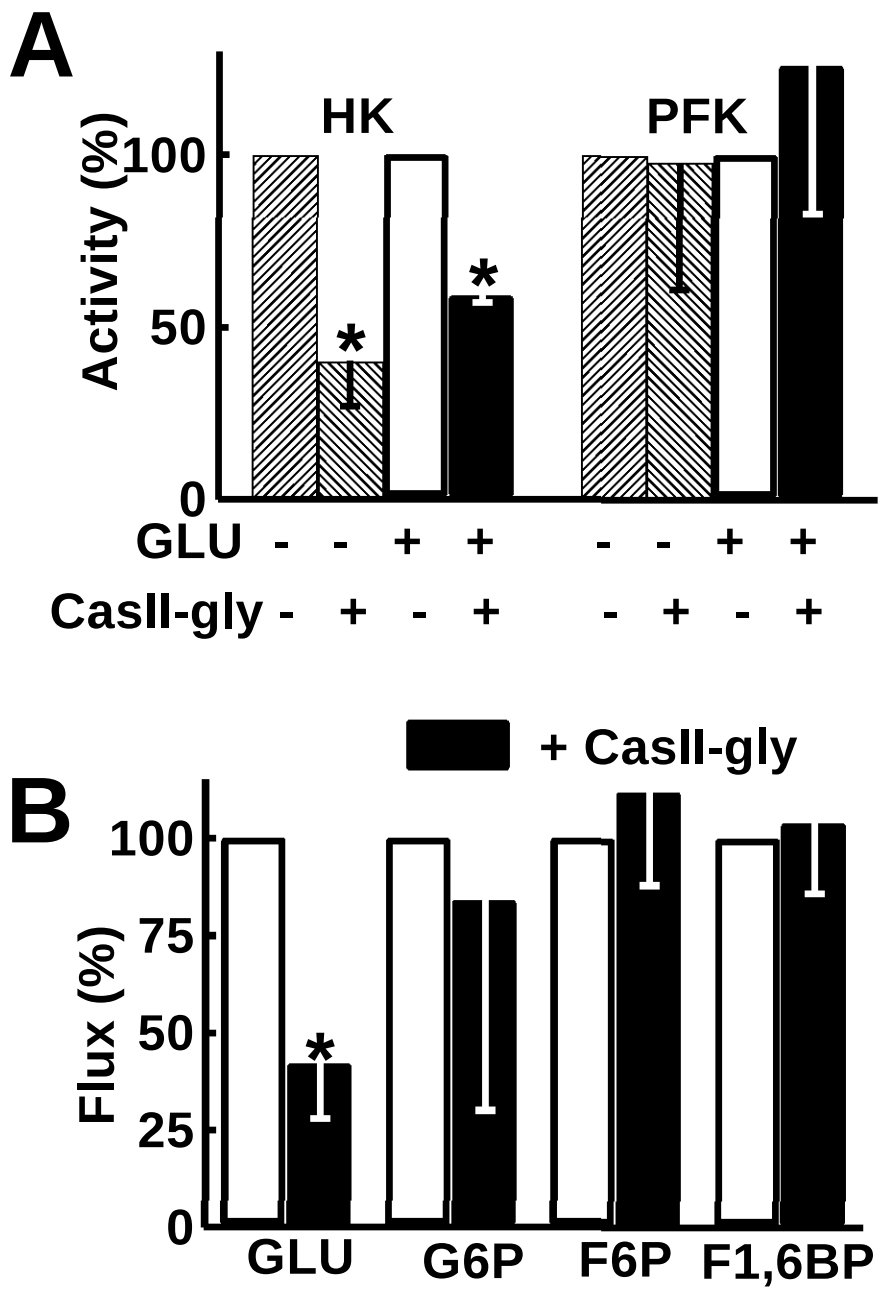
A
HK
PFK
Activity (%)
100
50
0
*
*
GLU - - + + - - + +
CasII-gly - + - + - + - +
+ CasII-gly
B
Flux (%)
100
75
50
25
0
*
GLU
G6P
F6P
F1,6BP

Figure 2

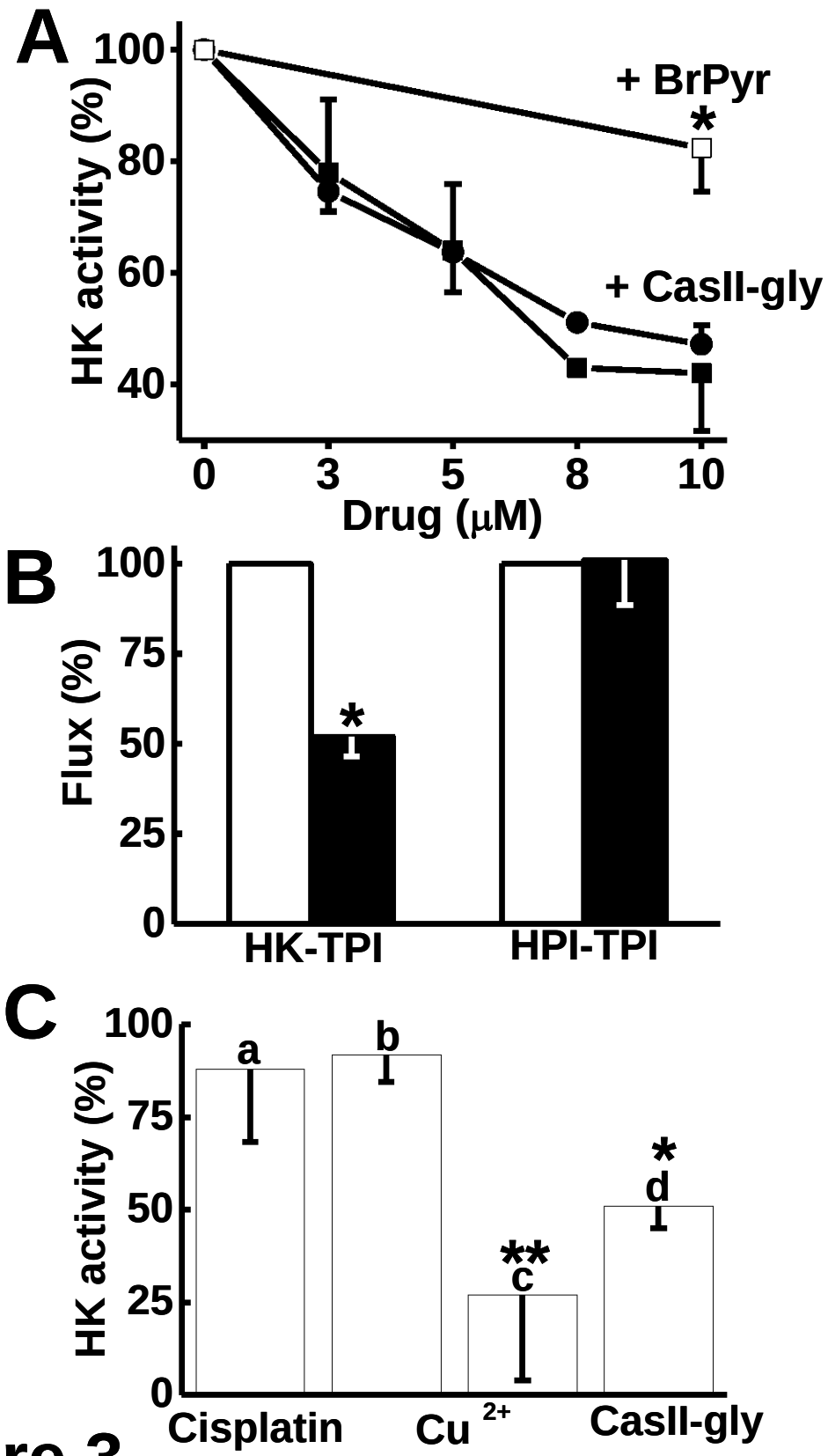
A
100
80
60
40
HK activity (%)
+ BrPyr
*
+ CasII-gly
0
3
5
8
10
Drug (μM)
B
100
75
50
25
0
Flux (%)
*
HK-TPI
HPI-TPI
C
100
75
50
25
0
HK activity (%)
a
b
**
c
*
d
Cisplatin
Cu 2+
CasII-gly

Figure 3

5.3.1 Comentarios manuscrito No. 4

Nuestro objetivo principal del manuscrito No. 4 era el determinar que la inhibición de la HK se traducía en una reducción en el flujo glucolítico y el de proponer a la CasII-gly como un fármaco antineoplásico que pueda específicamente reducir la proliferación celular en las células tumorales debido a que afecta su metabolismo energético. Sobre todo porque fue mas potente que el 3-bromopiruvato (inhibidor de la HK) entre 1-21 veces al inhibir la actividad de la HK y entre 13 -91 veces al inhibir la proliferación celular. Sin embargo, a pesar de haber demostrado que el fármaco inhibía específica y significativamente la actividad de la enzima, no se observó una reducción en la producción de láctico, debido a que se inducía una activa degradación de glucógeno. Estos resultados nos condujeron a concluir que con solo inhibir a esta enzima no se iba a lograr reducir el flujo glucolítico debido a que la vía metabólica, y la célula, tienen alternativas que disminuyen los estragos que pueda producir su inhibición. Por consiguiente, se tendrán mejores resultados si se inhiben al mismo tiempo al resto de las enzimas que controlan la glucólisis (GLUT y HPI).

Capítulo 6

6.1 Discusión general

En esta tesis, nuestra propuesta inicial consideraba que el control de la glucólisis tumoral no debería recaer en la HK y la PFK-1, a diferencia de lo que ocurre en las células normales en donde son los principales sitios de control, debido a los cambios en sus mecanismos de regulación y a sus niveles de sobre-expresión en células tumorales. Sin embargo, nuestros resultados (obtenidos en AS-30D y HeLa; Manuscrito No. 2) apoyaron parcialmente nuestra propuesta original, ya que únicamente en el caso de la PFK-1 se observó una reducción en su control, lo que atribuímos a que se encuentran concentraciones intracelulares saturantes de la F2,6BP (4-6 µM, *Ka*= 0.2-0.8 µM), el AMP y el Pi, activadores de la enzima que, además, bloquean la inhibición que ejercen el citrato y el ATP, y moderadamente el H^+ (datos no mostrados). Lo anterior concuerda con observaciones previas que sugerían que la enzima se encuentra muy activa en las células tumorales (Loiseau et al., 1985; Staal et al., 1987; Marín-Hernández et al., 2006), motivo por el cual se observa una pérdida en el efecto Pasteur (Eigenbrodt et al., 1985; Rodríguez-Enríquez et al., 2001).

Por otra parte, la HK mantiene un control significativo sobre la glucólisis tumoral debido a que, independientemente de su sobre-expresión (hasta en 300 veces en AS-30D) o su localización (membrana externa mitocondrial), su producto la G6P la inhibe fuertemente (Marín-Hernández et al., 2006; Manuscrito No. 2); el aumento en la actividad de la HK en células cancerosas trae como consecuencia un aumento concomitante en su producto, la G6P. Aparentemente, el que esta enzima se mantenga regulada de esta manera evita la disminución en los niveles de ATP intracelular.

Además, en esta tesis logramos establecer que en el control de la glucólisis pueden participan otros sitios como el GLUT, la HPI y la degradación de glucógeno, los cuales fueron visualizados por medio del modelado de la glucólisis, una vez que fueron construidos los modelos cinéticos de esta vía (ver sección 5.2; Manuscrito No. 3). Los modelos lograron predecir los flujos y las concentraciones de metabolitos encontradas en las células intactas. Sin embargo, su principal debilidad fue la predicción de la concentración de F6P, la cual fue 50 veces menor con respecto a lo detectado experimentalmente. Esto lo atribuimos a que en los modelos se simula a una PFK-1 muy rápida que reduce la concentración de F6P. Entonces consideramos que puede existir un freno cinético que aún no se ha identificado. Por ejemplo, en la PFK de músculo de conejo se ha reportado que el PEP, el 3PG y la creatina fosfato pueden incrementar el efecto inhibitorio del ATP (Colombo et al., 1975). Esto último sugiere la necesidad de caracterizar el efecto de éstos y otros metabolitos sobre la enzima tumoral.

Por un trabajo previo de nuestro grupo de trabajo se determinó que en las células tumorales AS-30D predomina el GLUT3 mientras que en HeLa predomina el GLUT1 (Rodríguez-Enríquez et al., 2009). En ambos tipos de células el GLUT ejerce un control significativo debido a su baja actividad con respecto al resto de los componentes de la vía, pero además, a ésto se suma la expresión de una isoforma del GLUT con una baja afinidad por la glucosa (Km = 9 mM) en el caso de las células HeLa.

Otra aportación importante de nuestro trabajo de tesis (Manuscrito No. 3) fue el de proponer a la HPI (una de las enzimas más rápidas de la glucólisis) como un sitio que controla el flujo glucolítico, debido a la fuerte y múltiple inhibición competitiva que ejercen sobre ella la F1,6 BP (intermediario de la glucólisis), la eritrosa-4P y el 6-

fosfogluconato (ambos intermediarios de la vía de las pentosas). Aunque cabe señalar que el efecto inhibitorio de estos metabolitos ya se había descrito previamente (Zalitis and Oliver, 1967; Chirgwin et al., 1975; Gaitonde et al., 1989), no se había evaluado la importancia que puede tener la inhibición de esta enzima en el control de la glucólisis.

Al mismo tiempo, sugerimos que la distribución de control puede verse influenciada por las condiciones en las que crecen las células tumorales, que pueden influir en la expresión de las enzimas y los transportadores de la glucólisis (Yun et al., 2005; Natsuizaka et al., 2007). Así, la degradación de glucógeno y el GLUT mantienen un alto coeficiente de control en las células HeLa, debido a que al cultivarse en 25 mM de glucosa, las células mantienen un alto contenido de glucógeno y además expresan una isoforma del GLUT con baja afinidad por glucosa (GLUT1, Km= 9 mM). En cambio, las células AS-30D que crecen en el espacio intraperitoneal de la rata, en donde se ven sometidas a una baja concentración (0.026 mM) de glucosa (Rodríguez-Enríquez et al., 2000) expresan un GLUT con alta afinidad (GLUT3, Km= 0.5 mM) y mantienen una baja concentración de glucógeno, que propicia que la glucólisis dependa únicamente de la glucosa exógena y por lo tanto el GLUT, la HK y la HPI controlen.

Otro aspecto interesante que debe señalarse es que aunque el control que ejerce la GAPDH sobre el flujo glucolítico no es significativo, éste depende de la concentración de fosfato libre presente en la célula, ya que puede limitar su actividad debido a la baja afinidad que tiene la enzima por éste (Heinz and Kulbe, 1970; Patra et al., 2009), lo cual no se ha considerado al analizar la glucólisis en otros organismos (levadura y tripanosoma) (Bakker et al., 1999; Teusink et al., 2000), en los que se supone que el fosfato no tiene ninguna relevancia en la actividad de esta enzima porque no limita su actividad.

Una vez que se han analizado los resultados obtenidos en esta tesis, la pregunta obvia es ¿Cuál es la enzima que se necesita inhibir para bloquear la glucólisis en las células tumorales? Como parte de la respuesta tenemos que el GLUT, la HK y la HPI pueden ser considerados como sitios adecuados para inhibir la glucólisis. En este caso no se propone inhibir la degradación de glucógeno porque el glucógeno se agotara eventualmente. Sin embargo, como único blanco específico para la glucólisis tumoral, la HK y el GLUT quedarían descartadas, ya que estas proteínas participan controlando la glucólisis en las células normales junto con la fosfofructocinasa tipo I (PFK-I), lo que deja como única opción de un posible blanco terapéutico a la HPI. Aunque al inhibir sólo a esta enzima la reducción en el flujo glucolítico no sería tan potente como lo sería inhibir al mismo tiempo a esta enzima junto con el GLUT y la HK, pero sí mayor con respecto a inhibir a enzimas que no controlan como la PFK-1, como lo predicen nuestros modelos. A esto se suma que experimentalmente demostramos que sólo inhibiendo a una enzima como la HK no basta para reducir la glucólisis (Manuscrito No. 4), porque la célula utiliza rutas alternativas para disminuir los estragos que pudo ocasionar la inhibición de esta enzima, lo cual se hubiera evitado al inhibir al mismo tiempo al GLUT y/o a la HPI.

Por lo tanto debe considerarse la necesidad de buscar en otras vías (metabólicas o de señalización) blancos terapéuticos potenciales que permitan una terapia multisitio, es decir buscar aquellos sitios (enzimas o transportadores) que contribuyan importantemente en el control de sus vías pero que en las células normales su control no sea significativo (Moreno-Sánchez et al., 2010).

En el campo de la biología del cáncer son pocos los estudios en los cuales se aplica el análisis de control metabólico para identificar blancos terapéuticos. Esto es

debido a que en general para el diseño de fármacos los grupos de investigación se enfocan en la búsqueda de un paso limitante, olvidando que este concepto no es aplicable en la mayoría de las vías metabólicas en las cuales más de una enzima puede controlar el flujo de la vía (Fell, 1997; Moreno-Sánchez et al., 2008; 2010). A esto se suma que en algunos casos la elección del blanco terapéutico se basa en la suposición de que es esencial en el crecimiento tumoral. Por lo tanto, se eligen sitios que no ejercen control, los cuales tienen que ver disminuida su actividad al menos un 80% para lograr observar cambios en el flujo de la vía que se desea inhibir. Esto provoca el empleo de concentraciones masivas de inhibidores que pueden conducir a afectos no deseados. Por este motivo el uso de inhibidores glucolíticos no ha tenido éxito en el tratamiento del cáncer. Esto se evitaría al inhibir sitios que controlan y que tienen la ventaja de que no es necesario abatir por completo su actividad para causar estragos en el flujo de una vía, con lo cual se emplearían concentraciones bajas de los inhibidores reduciendo los efectos adversos (Moreno Sánchez et al., 2010). Por todas estas razones, nuestro trabajo de tesis resulta relevante.

Finalmente, podemos indicar que el estudio de la glucólisis tumoral nos ha permitido determinar y entender los mecanismos bioquímicos involucrados en el control de esta vía, lo que nos permitirá extender nuestro estudio a otros tipos de cáncer para poder ayudar en la selección de nuevos blancos terapéuticos, y con ello el diseño de inhibidores más potentes y específicos.

6.2 Conclusiones generales

1. La HK ejerce un control significativo en la glucólisis tumoral debido a que sigue siendo inhibida fuertemente por su producto la G6P.
2. La PFK-1 no controla a causa de que la concentración intracelular de F2,6BP es suficiente para bloquear el efecto inhibitorio del citrato y el ATP.
3. El GLUT, la HPI y la degradación de glucógeno pueden participar en el control de la glucólisis.
4. La distribución de control depende del grado de expresión de las enzimas que controlan y de sus mecanismos de regulación así como del flujo de síntesis-degradación de glucógeno.
5. El análisis de control metabólico (mediante el empleo del análisis de elasticidades y el modelado cinético) nos permitió identificar a las enzimas que controlan la glucólisis así como entender los mecanismos bioquímicos involucrados. Entre estos últimos se destaca la inhibición de la HPI por metabolitos de la glucólisis y de la vía de las pentosas.
6. La inhibición de la HK no conduce a una reducción en el flujo de la glucólisis debido a que la célula usa el glucógeno para evitar los estragos que ocasiona la inhibición, a que la HK controla sólo parcialmente, y a que las otras enzimas controladoras compensan la disminución en la actividad de la HK y ajustan el flujo.

6.3 Perspectivas

En nuestro estudio establecimos que la distribución del control puede verse modificada como consecuencia de las condiciones en las que crecen las células y aunque con nuestros modelos cinéticos hicimos algunas aproximaciones al estudiar el efecto de la hipoxia y la hipoglucemia, una perspectiva de nuestro trabajo de tesis es el de explorar detalladamente los efectos que tiene sobre las células tumorales la exposición prolongada a la hipoxia y a la hipoglucemia. Esto es relevante si recordamos que en los tumores sólidos las células se ven sometidas a bajas concentraciones de oxígeno y de nutrientes (glucosa) por largos periodos de tiempo. Experimentalmente se han simulado estas condiciones en el laboratorio y otros grupos de investigación han observado un incremento en la expresión (RNAm) de los genes de algunas de las enzimas que hemos demostrado controlan la glucólisis como el GLUT y la HK, como consecuencia de la activación del HIF-1α y de la AMPK (Yun et al., 2005; Natsuizaka et al., 2007). Pero lamentablemente en estos estudios no se consideró evaluar los cambios en la actividad de las enzimas y el flujo de la glucólisis, por lo cual la pregunta que nos hacemos es: ¿Cómo se modifica el control de la glucólisis en hipoxia e hipoglucemia prolongada? ¿O no se modifica?

Para contestar la pregunta sería necesario someter a células HeLa en monocapa a periodos prolongados de hipoxia e hipoglucemia. En estas células habría que determinar las actividades del GLUT, HK y HPI, así como las concentraciones de sus moduladores y la concentración de glucógeno. Estos valores se vaciarían en los modelos de la glucólisis que hemos construido para establecer cuál es la distribución de control. Dado que los reportes indican que bajo estas condiciones el GLUT3 (transportador con alta afinidad por glucosa) llega a incrementar su expresión junto con

la HKII y si el contenido de glucógeno es bajo, se esperaría que las enzimas que controlen el flujo bajo estas condiciones sean, otra vez, el GLUT, la HK y la HPI como lo determinamos en las células AS-30D que están sometidas a bajas concentraciones de glucosa durante su crecimiento. Estos posibles resultados demostrarían que el control de una vía metabólica es robusto o, en otras palabras, el control es constante bajo diversas condiciones experimentales. Esta conclusión es relevante para el diseño de terapias anti-cancer, pues permitiría establecer con certeza los mejores sitios para inhibición específica.

Otro punto interesante es determinar cómo influyen en la glucólisis y en la distribución de control la activación de oncogenes y la falta de genes supresores de tumores, considerando que cada tipo de cáncer es una enfermedad diferente debido a que se han desarrollado por haberse apagado algunos genes supresores de tumores y al mismo tiempo se han encendido algunos oncogenes que sabemos pueden modificar la expresión de los componentes de la glucólisis. Por ello una perspectiva interesante es determinar si en cada tipo de cáncer existe una diferencia en la distribución del control y si esta diferencia es atribuida a la expresión de factores oncogénicos específicos.

Con este tipo de estudios parecería difícil conseguir resultados claros en líneas de células tumorales establecidas, pues varios oncogenes pueden encontrase activos al mismo tiempo y varios genes supresores de tumores inactivos. Entonces, la estrategia experimental sería emplear una línea celular no tumoral en la cual, por medio del empleo de siRNAs, apagar genes supresores de tumores o en su caso activar oncogenes (como se ha hecho para c-Myc o H-Ras en fibroblastos de rata) y evaluar los efectos sobre la glucólisis y la distribución de control. Se puede esperar que

aquellos factores que modifiquen la expresión de la HK y el GLUT puedan modificar la distribución de control.

Por otra parte, como nuestros resultados (Manuscritos No. 3 y 4) sugieren que para reducir el flujo glucolítico drásticamente es necesario inhibir al mismo tiempo a las enzimas que controlan (GLUT, HK y HPI), y como hasta el momento no se conocen inhibidores específicos de estas enzimas, se plantea el diseño de oligonucleótidos antisentido (que son secuencias específicas de un gen de interés que se unen al RNA mensajero de este gen, de tal forma que es inhibida la traducción y no hay proteína) para inhibir específicamente al GLUT3, a la HKII y a la HPI. Nuestro modelo para implementar estos experimentos serían las células AS-30D en las cuales esperaríamos una reducción drástica en el flujo glucolítico. Al mismo tiempo podríamos emplear estos oligonucleótidos antisentido en un modelo de célula no tumoral (hepatocitos) en el que se esperaría que debido a que el control sobre el flujo glucolítico no lo ejercen las mismas proteínas (GLUT, HPI y HK) no se vería disminuida la glucólisis.

Consideramos además que debe caracterizarse la glucólisis en modelos como las células rho y las células troncales. Esto debido a que las células rho son predominantemente glucolíticas ya que su mitocondria es disfuncional al carecer de DNA mitocondrial y podrían simular aquellas células tumorales que mantienen una reducción en la actividad de la mitocondria por el elevado número de mutaciones que presentan en su DNA mitocondrial (Carew y Huang, 2002). Mientras que el estudio de la glucólisis en las células troncales es relevante porque estas células son consideradas las precursoras de algunos tipos de cáncer (leucemias y cáncer de mama). Por lo cual, la caracterización de esta vía en ambos modelos con la aplicación del análisis de control metabólico podría permitir la identificación de blancos terapéuticos.

Finalmente, considerando que la muerte de la célula tumoral puede lograrse al disminuir los niveles de ATP y ésto sólo puede ocurrir al inhibir a la glucólisis y la fosforilación oxidativa, y aunque podría pensarse que en los tumores sólidos la inhibición de la fosforilación oxidativa no sería tan importante, hay reportes que indican que en los tumores sólidos pueden encontrarse poblaciones de células en las que predomina el metabolismo glucolítico por encontrarse lejos de los vasos o en zonas hipóxicas y otras en las que predomina el metabolismo mitocondrial por localizarse cerca de los vasos sanguíneos (Sonveaux et al., 2008). Por lo tanto nuestro modelo cinético se puede extender e incluir al ciclo de Krebs y a la fosforilación oxidativa para poder determinar los sitios que controlan el flujo de cada una de estas vías metabólicas y proponerlos para una terapia multisitio. El modelo experimental idóneo para poder encontrar estas dos poblaciones de células al mismo tiempo es el esferoide, que simula a un tumor en sus primeras etapas de desarrollo. En este modelo se pueden separar ambas poblaciones, lo que nos puede permitir hacer la caracterización de cada una de las vías metabólicas y obtener los datos suficientes para construir los modelos. En este modelo se ha reportado un incremento en la expresión de la HK y el GLUT en la población glucolítica con respecto a la población oxidativa (Rodríguez-Enríquez et al., 2008), por lo cual en las células oxidativas podría esperarse que el control de la glucólisis lo ejercieran el GLUT y la degradación de glucógeno (como ocurre en las células HeLa) mientras en la población glucolítica se podría esperar que fueran el GLUT, la HK y la HPI (como ocurre en AS-30D). Por otra parte aunque se ha estudiado el control de la fosforilación oxidativa en tumores es difícil establecer qué enzimas podrían ejercer el control sobre la fosforilación oxidativa dado que existen pocos datos sobre los flujos y actividades de las enzimas que participan en esta vía.

6.4 Referencias

- Arora KK, Pedersen PL (1988) Functional significance of mitochondrial bound hexokinase in tumor cell metabolism. J. Biol. Chem. **263**, 17422-17428.
- Bakker BM, Walsh MC, Ter Kuile BH, Mensonides FIC, Michels PAM, Opperdoes FR, Westerhoff HV (1999) Contribution of glucose transport to the control of the glycolytic flux in Trypanosoma brucei, Proc. Natl. Acad. Sci. USA **96**, 10098–10103.
- Bartrons R, Caro J (2007) Hypoxia, glucose metabolism and the Warbur´s effect. J. Bioenerg. Biomembr. **39**, 223-229.
- Bauer DE, Hatzivassiliou G, Zhao F, Andreadis C, Thompson CB (2005) ATP citrate lyase is an important component of cell growth and transformation. Oncogene **24**, 6314–6322.
- Brown GC, Lakin-Tomas L, Bran MD (1990) Control of respiration and oxidative phosphorylation in isolated rat liver cells. Eur. J. Biochem. **192**, 355-362.
- Bustamante E, Pedersen PL (1977) High aerobic glycolysis of rat hepatoma cells in culture: role of mitochondrial hexokinase. Proc. Natl. Acad. Sci. USA **74**, 3735-3739.
- Carew JS, Huang P (2002) Mitochondrial defects in cancer. Mol. Cancer **1**, 1-9.
- Chirgwin JM, Parsons TF, Ernst AN (1975) Mechanistic implications of the pH independence of inhibition of phosphoglucose isomerase by neutral sugar phosphates, J. Biol. Chem. **250**, 7277-7279.
- Clem B, Telang S, Clem A, Yalcin A, Meier J, Simmons A, Rasku MA, Arumugam S, Dean WL, Eaton J, Lane A, Trent JO, Chesney J (2008) Small-molecule inhibition of 6-phosphofructo-2-kinase activity suppresses glycolytic flux and tumor growth. Mol. Cancer Ther. **7**, 110-1120.
- Colombo G, Tate PW, Girotti AW, Kemp RG (1975) Interaction of inhibitors with muscle phosphofructokinase. J. Biol. Chem. **250**, 9404-12.
- Colomer D, Vives-Corrons JL, Pujades A, Bartrons R (1987) Control of phosphofructokinase by fructose 2,6 bisphosphate in B-lymphocytes and B-chronic lymphocytic leukemia cells. Cancer Res. **47**, 1859-1862.
- Dang CV, Semenza GL (1999) Oncogenic alterations of metabolism. TIBS. **24**, 68-72.
- DeBerardinis RJ, Lum JJ, Hatzivassiliou G, Thompson CB (2008) The biology of cancer: metabolic reprogramming fuels cell growth and proliferation. Cell Metab. **7**, 11-20.
- Dunaway GA, Kasten TP, Sebo T, Trapp R (1988) Analysis of the phosphofructokinase subunits and isoenzymes in human tissues. Biochem. J. **251**, 677-683.
- Eigenbrodt E, Fister P, Reinacher M (1985) New perspectives in carbohydrate metabolism in tumor cells. In. Regulation of carbohydrate metabolism (Reitner, R, ed.), vol. 2, pp 141-179. CRC Press, Boca Raton, FL.

- El-Bacha T, Sampaio de Freitas M, Sola-Penna M (2003) Cellular distribution of phosphofructokinase activity and implications to metabolic regulation in human breast cancer. Mol. Gen. Metab. **79**, 294-299.
- Evans A, Bates V, Troy H, Hewitt S, Holbeck S, Chung YL, Phillips R, Stubbs M, Griffiths J, Airley R (2008) GLUT1 as a therapeutic target: increased chemoresistance and HIF-1-independent link with cell turnover is revealed through compare analysis and metabolomic studies. Cancer Chemother. Pharmacol. **61**, 377-393.
- Fanciulli, M., Bruno, T., Giovannelli, A., Gentile, F.P., Di Padova, M., Rubiu, O. and Floridi, A (2000) Energy metabolism of human LoVo colon carcinoma cells: correlation to drug resistance and influence of Lonidamine. Clin. Cancer Res. **6**, 1590-1597.
- Fell D (1997) Understanding the control of metabolism. Plenum Press, London.
- Fisher K, Hoffmann P, Voelkl S, Meidenbauer N, Ammer J, Edinger M, Gottfried E, Schwarz S, Rothe G, Hoves S, Renner K, Timischl B, Mackensen A, Kunz-Schughart L, Andreesen R, Krause SW, Kreutz M (2007) Inhibitory effect of tumor cell-derived lactic acid on human T cells. Blood **109**, 3812-3819.
- Gaitonde MK, Murray E, Cunningham VJ (1989) Effect of 6-phosphogluconate on phosphoglucose isomerase in rat brain in vitro and in vivo. J. Neurochem. **52**, 1348-52.
- Gatenby R, Gillies RJ (2004) Why do cancers have high aerobic glycolysis?. Nature Rev. Cancer **4**, 891-899.
- Giatromanolaki A, Sivridis E, Gatter KC, Turley H, Harris AL, Koukourakis MI (2006) Lactate dehydrogenase 5 (LDH-5) expression in endometrial cancer relates to the activated VEGF/VEGFR2(KDR) pathway and prognosis. Gynecol. Oncol. **103**, 912-8.
- Gillies RJ, Robey I, Gatenby RA (2008) Causes and consequences of increased glucose metabolism of cancer. J. Nucl. Med. **49**, 24S-42S.
- Groen AK, van Roermund CW, Vervoom RC, Tager JM (1986) Control of gluconeogenesis in rat liver cells. Flux control coefficients of the enzymes in the gluconeogenic pathway in the absence and presence of glucagon. Biochem. J. **237**, 379-389.
- Heinz F, Kulbe KD (1970) Glyceraldehydephosphate dehydrogenase from liver. I. Isolation and characterization of the bovine liver enzyme. Hoppe Seylers Z Physiol Chem. **351**, 249-62.
- Horberg JJ, Bruggeman, FJ, Bakker BM, Westerhoff HV (2007) Metabolic control analysis to identify optimal drug targets. Progress in Drug Research, Vol 64.
- INEGI (2009) Estadísticas a propósito del día mundial contra el cáncer. www.inegi.org.mx.

- Jannaschk KD, Burgos M, Centerlles JJ, Ovadi J, Cascante M (1999) Application of metabolic control analysis to the study of toxic effects of copper in muscle glycolysis. FEBS Lett. **445**, 144-148.
- Jones RG and Thompson CB (2009) Tumor suppresors and cell metabolism: a recipe for cancer growth. Genes Dev. **23**, 537-548.
- Kashiwaya Y, Sato K, Tsuchiya N, Thomas S, Fell DA, Veech RL, Passonneau JV (1994) Control of glucose utilization in working perfused rat heart. J. Biol. Chem. **269**, 25502-25514.
- Kim WJ, Dang CV (2006) Cancer´s molecular sweet tooth and the Warburg effect. Cancer Res. **66**, 8927-8930.
- Kosow DP, Rose I (1968) Ascites tumor mitochondrial hexokinase II. Effect of binding on kinetic properties. J. Biol. Chem. **243**, 3623-3630.
- Kumagai S, Narasaki R, Hasumi K (2008) Glucose-dependent active ATP depletion by koningic acid kills high-glycolytic cells. Biochem Biophys. Res. Commun. **365**, 362-368.
- Lardner A (2001) The effects of extracellular pH on immune function. J. Leukoc. Biol. **69**, 522-530.
- Lee K A, Roth RA, LaPres JJ (2007) Hypoxia, drug therapy and toxicity. Pharmacol. Ther. **113**, 229-46.
- Liu Y, Zuckier LS, Ghesani NV (2010) Dominant uptake of fatty acid over glucose by prostate cells: a potential new diagnostic and therapeutic approach. Anticancer Res. **30**, 369-74.
- Loiseau AM, Rousseau GG, Hue L (1985) Fructose 2,6-bisphosphate and the control of glycolysis by glucocorticoids and by other agents in rat hepatoma cells. Cancer Res. **45**, 4263-9.
- Marín-Hernández A, Gallardo-Pérez JC, Ralph SJ, Rodríguez-Enríquez S, Moreno-Sánchez R (2009) HIF-1alpha modulates energy metabolism in cancer cells by inducing over-expression of specific glycolytic isoforms. Mini Rev. Med. Chem. **9**, 1084-101.
- Marín-Hernández A, Rodríguez-Enríquez S, Vital-González PA, Flores-Rodríguez FL, Macías-Silva M, Sosa-Garrocho M, Moreno-Sánchez R (2006) Determining and understanding the control of glycolysis in fast-growth tumor cells. Flux control by an over-expressed but strongly product-inhibited hexokinase. FEBS J. **273**, 1975-88.
- Maschek G, Savaraj N, Priebe W, Braunschweiger P, Hamilton K, Tidmarsh GF, De Young LR, Lampidis TJ (2004) 2-deoxy-D-glucose increases the efficacy of adriamycin and paclitaxel in human osteosarcoma and non-small cell lung cancers in vivo. Cancer Res. **64**, 31-4.
- Meldolesi MF, Macchia V, Laccetti P (1976) Differences in phosphofructokinase regulation in normal and tumor rat thyroid cells. J. Biol. Chem. **251**, 6244-6251.

- Moreno-Sánchez R, Rodríguez-Enríquez S, Marín-Hernández A, Saavedra E (2007) Energy metabolism in tumor cells. FEBS J. **274**,1393-1418.
- Moreno-Sánchez R, Saavedra E, Rodríguez-Enríquez S, Olín-Sandoval V (2008) Metabolic control analysis: a tool for designing strategies to manipulate pathways. J. Biomed. Biotech. 2008: 597913.
- Moreno-Sánchez R, Saavedra E, Rodríguez-Enríquez S, Gallardo-Pérez JC, Quezada H, Westerhoff HV (2010) Metabolic control analysis indicates a change of strategy in the treatment of cancer. Mitochondrion **10**, 626-39.
- Nakashima RA, Paggi MG, Scott LJ, Pedersen PL (1988) Purification and characterization of a bindable form of mitochondrial bound hexokinase from the highly glycolytic AS-30D rat hepatoma cell line. Cancer Res. **48**, 913-919.
- Natsuizaka M, Ozasa M, Darmanin S, Miyamoto M, Kondo S, Kamada S, Shindoh M, Higashino F, Suhara W, Koide H, Aita K, Nakagawa K, Kondo T, Asaka M, Okada F, Kobayashi M (2007) Synergistic up-regulation of Hexokinase-2, glucose transporters and angiogenic factors in pancreatic cancer cells by glucose deprivation and hypoxia. Exp. Cell Res. **313**, 3337-48.
- Nelson DL, Cox MM (2005) Lehninger Principles of Biochemistry, 4 edición, Editorial Freeman.
- Nishijima T, Nishina M, Fujiwara K (1997) Measurement of Lactate Levels in serum and bile using proton nuclear magnetic resonance in patients with hepatobiliary diseases: its utility in detection of malignancies. Jpn. J. Clin. Oncol. **27**, 13-17.
- Olovnikov IA, Kravchenko JE, Chumakov PM (2009) Homeostatic functions of the p53 tumor suppressor: Regulation of energy metabolism and antioxidant defense. Semi. Cancer Biol. **19**, 32-41.
- Oskam R, Rijksen G, Staal GEJ, Vora S (1985) Isozymic composition and regulatory properties of phosphofructokinase from well-differentiated and anaplastic medullary thyroid carcinomas of the rat. Cancer Res. **45**, 135-142.
- Osthus RC, Shim H, Kim S, Li Q, Reddy R, Mukherjee M, Xu Y, Wonsey D, Lee LA, Dang CV (2000) Deregulation of glucose transporter 1 and glycolytic gene expression by c-Myc. J. Biol. Chem. **275**, 21797–21800.
- Parry DM, Pedersen PL (1983) Intracellular localization and properties of particulate hexokinase in the Novikoff ascites tumor. J. Biol. Chem. **258**, 10904-10912.
- Patra S, Ghosh S, Bera S, Roy A, Ray S, Ray M (2009) Molecular characterization of tumor associated glyceraldehyde-3-phosphate dehydrogenase. Biochemistry (Mosc). **74**, 717-27.
- Pedersen PL, Mathupala S, Rempel A, Geschwind JF, Ko YH (2002) Mitochondrial bound type II hexokinase: a key player in the growth and survival of many cancers and an ideal prospect for therapeutic intervention. Biochem. Biophys. Acta **1555**, 14-20.

- Pedersen PL (1978) Tumor mitochondria and the bioenergetics of cancer cells. Prog. Exp. Tumor Res. **22**, 190-274.
- Pelicano H, Martin D S, Xu RH, Hung P (2006) Glycolysis inhibition for anticancer treatment. Oncogene **25**, 4633-4646.
- Plathow C and Weber WA (2008) Tumor cell metabolism imaging. J. Nucl. Med. **49**, 43S-63S.
- Poolman MG, Assmus HE, Fell DA (2004) Applications of metabolic modeling to plant metabolism. J. Exp. Bot. **55**,1177-1186.
- Rapoport T, Heinrich R, Jacobash G, Rapoport S (1974) A linear steady-state treatment of enzymatic chains. A mathematical model of glycolysis of human erythrocytes. Eur. J. Biochem. **42**, 107-120.
- Robey RB, Hay N (2009) Is Akt the "Warburg kinase"?-Akt-energy netabolism interactions and oncogenesis. Semin. Cancer Biol. **19**, 25-31.
- Rodríguez-Enríquez S, Gallardo-Pérez JC, Avilés-Salas A, Marín-Hernández A, Carreño-Fuentes L, Maldonado-Lagunas V, Moreno-Sánchez R (2008) Energy metabolism transition in multi-cellular human tumor spheroids. J. Cell Physiol. **216**, 189-97.
- Rodríguez-Enríquez S, Juárez O, Rodríguez-Zavala JS, Moreno-Sánchez R (2001) Multisite control of the Crabtree effect in ascites hepatoma cells. Eur. J. Biochem. **268**, 2512-9.
- Rodríguez-Enríquez S, Marín-Hernández A, Gallardo-Pérez JC, Moreno-Sánchez R (2009) Kinetics of transport and phosphorylation of glucose in cancer cells. J. Cell Physiol. **22**, 1552-9.
- Rodríguez-Enríquez S, Torres-Márquez ME, Moreno-Sánchez R (2000) Substrate oxidation and ATP supply in AS-30D hepatoma cells. Arch. Biochem. Biophys. **375**, 21-30.
- Shim H, Dolde C, Lewis BC, Wu CS, Dang G, Jungmann RA, Dalla-Favera R, Dang CV (1997) c-Myc transactivation of LDH-A: Implications for tumor metabolism and growth. Proc. Natl. Acad. Sci. **94**, 6658–6663.
- Shonk CE, Arison RN, Koven BJ, Majima H, Boxer GE (1964) Enzyme patters in human tissues. III. Glycolytic enzymes in normal and malignant tissues of the colon and rectum. Cancer Res. **25**, 1965.
- Smith TAD (2000) Mammalian hexokinase and their abnormal expression in cancer. Br. J. Biomed. Sci. **57**, 170-178.
- Sonveaux P, Végran F, Schroeder T, Wergin MC, Verrax J, Rabbani ZN, De Saedeleer CJ, Kennedy KM, Diepart C, Jordan BF, Kelley MJ, Gallez B, Wahl ML, Feron O, Dewhirst MW (2008) Targeting lactate-fueled respiration selectively kills hypoxic tumor cells in mice. J. Clin. Invest. **118**, 3930-42.

- Staal GEJ, Kalff A, Hessbeen EC, van Veelen CWM, Rijksen G (1987) Subunit composition, regulatory properties and phosphorylation of phosphofructokinase from human gliomas. Cancer Res. **47**, 5047-5051.
- Stubbs M, Bashford CL, Griffiths JR (2003) Understanding the tumor metabolic phenotype in the genomic era. Curr. Mol. Med. **3**, 49-59.
- Teusink B, Passarge J, Reijenga CA, Esgalhado E, van der Weijden CC, Schepper M, Walsh MC, Bakker BM, van Dam K, Westerhoff HV, Snoep JL (2000) Can yeast glycolysis be understood in terms of in vitro kinetics of the constituent enzymes? Testing biochemistry. Eur. J. Biochem. **267**, 5313-29.
- Tysnes B, Bjerkvig R (2007) Cancer initiation and progression: involvement of stem cells and the microenvironment. Biochim. Biophys. Acta **1775**, 283-297.
- Volgelstein B, Kinzler KW (2004) Cancer genes and the pathways they control. Nature Med. **10**, 789-799.
- Vora S, Halper JP, Knowles DM (1985) Alterations in the activity and prolife of human phosphofructokinase during malignant transformation in vivo and in vitro: transformation and progression-linked discriminants of malignancy. Cancer Res. **45**, 2993-3001.
- Vora S, Oskam R, Staal EJ (1985)[b] isoenzymes of phosphofructokinase in the rat. Biochem. J. **229**, 333-341.
- Walenta S, Mueller-Klieser WF (2004) Lactate: mirror and motor of tumor malignancy. Semin. Radiat. Oncol. **14**, 267-274.
- Widjojoatmodjo MN, Mancuso A, Blanch HW (1990) Mitochondrial hexokinase activity in a murine hybridoma. Biotech. Lett. **12**, 551-556.
- Wilson JE (2003) Isozymes of mammalian hexokinase: structure subcellular localization and metabolic function. J. Expert. Biol. **206**, 2049-2057.
- Xu RH, Pelicano H, Zhou Y, Carew JS, Feng L, Bhalla KN, Keating MJ, Huang P (2005) Inhibition of glycolysis in cancer cells: a novel strategy to overcome drug resistance associated with mitochondrial respiratory defect and hypoxia. Cancer Res. **65**, 613-21.
- Yalcin A, Telang S, Clem B, Chesney J (2009) Regulation of glucosa metabolism by 6-phosphofructo-2-kinase/fructosa-2,6-bisphosphatases in cancer. Exp. Mol. Pathol. 86, 174-179.
- Yeung SJ, Pan J, Lee MH (2008) Roles of p53, MYC and HIF-1 in regulating glycolysis - the seventh hallmark of cancer. Cell. Mol. Life Sci. **65**, 3981-99.
- Yun H, Lee M, Kim SS, Ha J (2005) Glucose deprivation increases mRNA stability of vascular endothelial growth factor through activation of AMP-activated protein kinase in DU145 prostate carcinoma. J. Biol. Chem. **280**, 9963-72.
- Zalitis J, Oliver IT (1967) Inhibition of glucose phosphate isomerase by metabolic intermediates of fructose. Biochem. J. **102**, 753-9.

6.5 Apéndice

Otras publicaciones durante el doctorado

PROBLEMA BIOQUÍMICO

Alvaro Marín Hernández y Rafael Moreno Sánchez
Correo E: marinhernndez@yahoo.com.mx

Análisis de control metabólico. Control de la glucólisis en células tumorales

La glucólisis en las células tumorales se encuentra incrementada con respecto a los tejidos normales. Esto se debe a un aumento en la actividad de todas las enzimas que forman parte de esta vía y a cambios en los mecanismos de regulación de las dos enzimas consideradas como sitios de control en células normales, la hexocinasa (HK) y la fosfofructocinasa tipo I (PFK-I), que las hacen menos sensibles a sus inhibidores fisiológicos (glucosa-6-fosfato, citrato y ATP) (1). Para evaluar la hipótesis de que estas enzimas no controlan la glucólisis en las células AS-30D (hepatoma ascítico), se utilizó el análisis de elasticidades, que permite calcular los coeficientes de control de flujo (CJ) a partir de los coeficientes de elasticidad. El coeficiente de elasticidad (E) es la capacidad de un bloque de enzimas de variar su velocidad al cambiar las concentraciones de su producto o sustrato (2). Experimentalmente se calcula a partir de la variación de la concentración de intermediarios (sustratos o productos de las enzimas de la vía) y del flujo de la vía en estado estacionario. Esto se logra mediante el empleo de inhibidores o al variar la concentración del sustrato de la ruta metabólica (glucosa en el caso de la glucólisis). En la Tabla 1 se muestran las velocidades de generación de láctico (velocidad de glucólisis) y las concentraciones en estado estacionario de glucosa-6-fosfato (G6P) y fructosa-1,6-bifosfato (F-1,6BP) a diferentes concentraciones de glucosa y en la Tabla 2, las velocidades de glucólisis y las concentraciones de ambos intermediarios, pero en presencia de diferentes concentraciones de oxalato (+ 5 mM de glucosa) (3).

TABLA 1

Velocidad de glucólisis, concentraciones de G6P y de F-1,6BP a diferentes concentraciones de glucosa

Glucosa (mM)	Velocidad de glucólisis (nmol/min/mg)	G6P (nmol/mg)	Velocidad de glucólisis (nmol/min/mg)	F-1,6BP (nmol/mg)
4	1.8	2.7	1.8	30
4.5	5.4	2.8	5.4	27
5	13.4	3.2	13.4	31
5.5	16.4	3.6	16.4	34
6	20.5	3.4	20.5	46

TABLA 2

Velocidad de glucólisis, concentraciones de G6P y de F-1,6BP a diferentes concentraciones de oxalato

Oxalato (mM)	Velocidad de glucólisis (nmol/min/mg)	G6P (nmol/mg)	Velocidad de glucólisis (nmol/min/mg)	F1,6BP (nmol/mg)
0	15	3	16	28
0.5	10.7	3.1	14.2	29.4
1.0	9.6	3.4	12.8	30.8
1.5	8	3.5	12.6	35.3
2.0	6.5	3.8	10.1	37.2

Con estos datos:

1. Determinar los coeficientes de control de flujo.
2. ¿Disminuyó el control que ejercen la HK y la PFK-I en la glucólisis de células tumorales, considerando que en eritrocito controlan 0.7 y 0.3, respectivamente (4)?
3. ¿Qué enzimas son las que ejercen mayor control?

El volumen intracelular en las células tumorales es de 2.28 µl/1.8 mg de proteína.

REFERENCIAS

1. Moreno-Sánchez R, Rodríguez- Enríquez S, Marín-Hernández A, Saavedra E. (2007) Energy metabolism in tumor cells. FEBS J. en Prensa.
2. Fell D (1997) Understanding the control of metabolism. Plenum Press, London.
3. Marín-Hernández A, Rodríguez-Enríquez S, Vital-González PA, Flores-Rodríguez FL, Macías-Silva M, Sosa-Garrocho M, Moreno-Sánchez R. (2006) Determining and understanding the control of glycolysis in fase-growth tumor cells. FEBS J. 273: 1975-1988.
4. Rapoport T, Heinrich R, Jacobasch G & Rapoport S (1974) A linear steady-state treatment of enzymatic chains. A mathematical model of glycolysis of human erytrocytes. Eur J Biochem 42: 107-120.

El Factor Inducido por la Hipoxia-1 (HIF-1) y la Glucólisis en las Células Tumorales*

Alvaro Marín-Hernández

RESUMEN

El factor inducido por la hipoxia 1 (HIF-1) tiene un papel fundamental en la respuesta a la baja tensión del oxígeno, ya que regula la expresión de una gran variedad de genes, cuyos productos participan en procesos como la angiogénesis, el metabolismo energético, la eritropoyesis y la proliferación celular. Diversos estudios indican que existe una relación estrecha entre el cáncer y el HIF-1, debido a que los mecanismos que regulan su expresión se encuentran alterados en las células tumorales. El HIF-1 es uno de los factores involucrados en el incremento de la glucólisis en las células tumorales, ya que aumenta la actividad de ciertas isoformas de las enzimas glucolíticas (GLUT1, GLUT3, HKI, HKII, PFK-L, ALD-A, ALD-C, PGK1, ENO-α, PYK-M2, LDH-A, PFKFB-3), promoviendo un aumento del flujo glucolítico (producción de lactato, H^+, ATP e intermediarios de la glucólisis). Por otra parte, algunas de estas isoformas participan activamente en otros procesos como son la inhibición de la apoptosis (HKI y HKII), la transcripción de histonas (LDH-A) y la migración celular (ENO-α), las cuales favorecen el desarrollo tumoral.

PALABRAS CLAVE: Hipoxia, glucólisis, HIF-1, isoenzimas glucolíticas, células tumorales.

ABSTRACT

The hypoxia-inducible factor 1 (HIF-1) is an important key mediator during low-oxygen cellular adaptation. Several genes involved in angiogenesis, erythropoiesis, energy metabolism and cell survival are up-regulated by HIF-1. In tumour cells, HIF-1 overexpression and activation is associated with malignancy, development and angiogenesis; whereas HIF-1 low expression has been determined in normal tissues and benign tumors. At metabolic level, HIF-1-activation stimulates transporters (GLUT1, GLUT3) and glycolytic enzymes (HKI, HKII, PFK-L, ALD-A, ALD-C, PGK1, ENO-α, PYK-M2, LDH-A, PFKFB-3) transcription. In consequence, a significant increment in the glycolytic flux (lactate ,ATP, and H+) and glycolytic intermediates levels are attained. An additional role of some of these HIF-induced isoforms as activators of survival, histones transcriptional activation (LDH-A), apoptotic inhibition (HKI y HKII) and cellular migration (ENO-α) pathways is discussed.

KEY WORDS: Hypoxia, glycolysis, HIF-1, glycolytic enzymes, tumour cells.

INTRODUCCION

La baja tensión de oxígeno altera la homeostasis de la célula, lo que conduce a la activación del factor inducido por la hipoxia 1 (HIF-1). El HIF-1 tiene como función incrementar la transcripción de genes cuyos productos son proteínas que participan en la angiogénesis, la eritropoyesis, la proliferación celular, la remodelación vascular y el metabolismo energético; permitiendo a la célula adaptarse a estas condiciones tan adversas (1).

En la mayoría de los tumores primarios de cerebro, páncreas, mama, colon, ovario, pulmón y próstata, y sus metástasis, se detectan altos niveles del HIF-1 comparados con los tejidos normales de los cuales provienen o tumores benignos (2). Las causas que promueven la sobreexpresión del HIF-1 en las células tumorales son la baja tensión de oxígeno presente en los tumores y las alteraciones en los mecanismos que regulan su expresión. Por lo anterior, el HIF-1 puede considerarse como un marcador tumoral y un blanco terapéutico.

En esta revisión se analiza el papel que juega el HIF-1 en la regulación de la glucólisis, así como las ventajas que ofrece a las células tumorales la expresión de las enzimas

*Recibido: 19 de agosto de 2008 Aceptado: 14 de abril de 2009
Instituto Nacional de Cardiología Ignacio Chávez". Departamento de Bioquímica. Juan Badiano No. 1. Col. Sección XVI. México DF, 14080. Correo E: marinhernndez@yahoo.com.mx

the FEBS Journal

REVIEW ARTICLE

Energy metabolism in tumor cells

Rafael Moreno-Sánchez, Sara Rodríguez-Enríquez, Alvaro Marín-Hernández and Emma Saavedra

Instituto Nacional de Cardiología, Departamento de Bioquímica, Tlalpan, México, Mexico

Keywords
casiopeinas; chemotherapy; glycolysis; metabolic control analysis; mitochondrial metabolism; PET; rhodamines

Correspondence
R. Moreno-Sánchez, Instituto Nacional de Cardiología, Departamento de Bioquímica, Juan Badiano no. 1, Tlalpan, México DF 14080, Mexico
Fax: +5255 55730926
Tel: +5255 55732911, ext. 1422, 1298
E-mail: rafael.moreno@cardiologia.org.mx or morenosanchez@hotmail.com

(Received 31 October 2006, revised 2 January 2007, accepted 10 January 2007)

doi:10.1111/j.1742-4658.2007.05686.x

In early studies on energy metabolism of tumor cells, it was proposed that the enhanced glycolysis was induced by a decreased oxidative phosphorylation. Since then it has been indiscriminately applied to all types of tumor cells that the ATP supply is mainly or only provided by glycolysis, without an appropriate experimental evaluation. In this review, the different genetic and biochemical mechanisms by which tumor cells achieve an enhanced glycolytic flux are analyzed. Furthermore, the proposed mechanisms that arguably lead to a decreased oxidative phosphorylation in tumor cells are discussed. As the O_2 concentration in hypoxic regions of tumors seems not to be limiting for the functioning of oxidative phosphorylation, this pathway is re-evaluated regarding oxidizable substrate utilization and its contribution to ATP supply versus glycolysis. In the tumor cell lines where the oxidative metabolism prevails over the glycolytic metabolism for ATP supply, the flux control distribution of both pathways is described. The effect of glycolytic and mitochondrial drugs on tumor energy metabolism and cellular proliferation is described and discussed. Similarly, the energy metabolic changes associated with inherent and acquired resistance to radiotherapy and chemotherapy of tumor cells, and those determined by positron emission tomography, are revised. It is proposed that energy metabolism may be an alternative therapeutic target for both hypoxic (glycolytic) and oxidative tumors.

In biochemical and physiological studies, tumor cells are usually classified according to their rate of growth: low; intermediate; or fast [1]. For tumors in experimental animals, the growth rate is determined by size and volume, mitotic count, degree of differentiation and thymidine incorporation [2]. Examples of fast-growth tumors in mice include several experimental cancers, such as Ehrlich ascites tumor, fibrosarcoma 1929 and lymphocytic leukemia L1210; and in rats, fast-growth tumors include the hepatomas of Morris (3924A, 7793, 7795, 7800, 7288C, 7316B, 3683), Reuber H-35, Novikoff, AH130 and AS-30D, breast carcinosarcoma Walker 256, hepatocellular carcinoma HC-252, hepatoma induced by dimethylazobenzene and DS-carcinosarcoma [1].

In human tumors, classification is based on their histological characteristics and stage of clinical progression. By their advanced developmental stage and metastatic properties, some human tumors considered to be of fast growth are breast carcinoma, ovarian carcinoma, melanoma, thyroid carcinoma, uterine carcinoma and lung carcinoma [1,3]. Human primary brain tumors, such as gliomas, glioblastomas and medulloblastomas, are also considered as fast-growth tumors because of their high rate of proliferation (average transfer in days or weeks) and their conversion to a poorly differentiated status [4,5].

Tumor cells exhibit profound genetic, biochemical and histological differences with respect to the original,

Abbreviations
ALD, aldolase; ANT, adenine nucleotide translocase; COX, cyclooxygenase; CT, computed tomography; F2,6BP, fructose-2,6-bisphosphate; FDG, ^{18}fluoro-deoxyglucose; GAPDH, glyceraldehyde-3-phosphate dehydrogenase; GLUT, glucose transporter; G6P, glucose-6-phosphate; HIF, hypoxia inducible factor; HK, hexokinase; LDH, lactate dehydrogenase; NSAID, nonsteroidal anti-inflammatory drug; PDH, pyruvate dehydrogenase complex; PET, positron emission tomography; PFK-1, phosphofructokinase type 1; PFK-2, phosphofructokinase type 2; Pyr, pyruvate.

Journal of Cellular Physiology

Energy Metabolism Transition in Multi-Cellular Human Tumor Spheroids

SARA RODRÍGUEZ-ENRÍQUEZ,[1]* JUAN CARLOS GALLARDO-PÉREZ,[1] ALEJANDRO AVILÉS-SALAS,[2] ALVARO MARÍN-HERNÁNDEZ,[1] LILIANA CARREÑO-FUENTES,[1] VILMA MALDONADO-LAGUNAS,[2] AND RAFAEL MORENO-SÁNCHEZ[1]

[1]*Departamento de Bioquímica, Instituto Nacional de Cardiología, Mexico, Mexico*

[2]*Departamentos de Biología Molecular y de Patología. Instituto Nacional de Cancerología, Mexico, Mexico*

It is thought that glycolysis is the predominant energy pathway in cancer, particularly in solid and poorly vascularized tumors where hypoxic regions develop. To evaluate whether glycolysis does effectively predominate for ATP supply and to identify the underlying biochemical mechanisms, the glycolytic and oxidative phosphorylation (OxPhos) fluxes, ATP/ADP ratio, phosphorylation potential, and expression and activity of relevant energy metabolism enzymes were determined in multi-cellular tumor spheroids, as a model of human solid tumors. In HeLa and Hek293 young-spheroids, the OxPhos flux and cytochrome *c* oxidase protein content and activity were similar to those observed in monolayer cultured cells, whereas the glycolytic flux increased two- to fourfold; the contribution of OxPhos to ATP supply was 60%. In contrast, in old-spheroids, OxPhos, ATP content, ATP/ADP ratio, and phosphorylation potential diminished 50–70%, as well as the activity (88%) and content (3 times) of cytochrome *c* oxidase. Glycolysis and hexokinase increased significantly (both, 4 times); consequently glycolysis was the predominant pathway for ATP supply (80%). These changes were associated with an increase (3.3 times) in the HIF-1α content. After chronic exposure, both oxidative and glycolytic inhibitors blocked spheroid growth, although the glycolytic inhibitors, 2-deoxyglucose and gossypol (IC_{50} of 15–17 nM), were more potent than the mitochondrial inhibitors, casiopeina II-gly, laherradurin, and rhodamine 123 ($IC_{50} > 100$ nM). These results suggest that glycolysis and OxPhos might be considered as metabolic targets to diminish cellular proliferation in poorly vascularized, hypoxic solid tumors.

J. Cell. Physiol. 216: 189–197, 2008.

The field of tumor energy metabolism seemed resolved by 1956, when Warburg proposed that an energy deficiency caused by an irreversible damage of the mitochondrial function induced increased glycolysis, which presumably supported the energy demand for tumor formation and growth. Since then, it has been thought that Warburg's hypothesis applied to all or most cancer cell types (Weber, 2001; Stubbs et al., 2003; Xu et al., 2005). Such an asseveration may indeed be particularly valid for solid tumors, in which the lower inner oxygen concentration activates, via the hypoxia inducible factor 1 (HIF-1), the transcription and translation of glycolytic genes (GLUT-1 and -3, HK, phosphofructokinase type 1, aldolase, GAPDH, phosphoglycerate kinase, enolase, pyruvate kinase, and lactate dehydrogenase) (Dang and Semenza, 1999), which in turn, stimulates the glycolytic flux. However, oxidative phosphorylation (enzyme activities and flux) has not been analyzed in parallel.

In this regard, recent data from numerous sources on the role of oxidative phosphorylation (OxPhos) during tumor development (Lampidis et al., 1983; Guppy et al., 2002; Zu and Guppy, 2004; Rodríguez-Enríquez et al., 2006a; Moreno-Sánchez et al., 2007) have prompted a re-evaluation of Warburg's hypothesis. For instance, it has been shown in human (HeLa, MCF-7, HL-60) and rodent (hepatoma AS-30D) tumors that mitochondrial ATP may indeed support the accelerated cellular proliferation rate (Sweet and Singh, 1995; Guppy et al., 2002; Rodríguez-Enríquez et al., 2006a) and, in consequence, anti-mitochondrial drugs are able to abolish tumor growth (Rodríguez-Enríquez et al., 2006a). For several aggressive metastasic human carcinomas (HeLa, CRL 1420 pancreas, MCF-7 breast, MB49 bladder) and osteosarcomas, OxPhos inhibitors alone, such as casiopeina II-gly and rhodamines (123, 6G), or in combination with glycolytic drugs have been effectively used to decrease the proliferation rate (reviewed in Moreno-Sánchez et al., 2007).

It should be noted, however, that most of the above-mentioned studies have been carried out with cellular suspensions or monolayer culture cells. It is usually assumed that energy metabolism of monolayer cultures (i.e., enzyme activity, metabolic pathway flux, and sensitivity to metabolic drugs) is similar to that found in solid tumors. Solid tumors maintain a complex physiological structure derived from their three-dimensional organization (i.e., cell-matrix interactions, variations in nutrient supply due to glucose, lactate, pH, and oxygen gradients; as well as variations in the expression of HIF-1α and c-Myc), which might result in gene regulation changes and, hence, in enzyme expression with respect to monolayer cultures and cell suspensions (Sutherland, 1988; Khaitan et al., 2006).

This article includes Supplementary Material available from the authors upon request or via the Internet at http://www.interscience.wiley.com/jpages/0021-9541/suppmat.

Abbreviations: ANT, adenine nucleotide translocator; casII-gly, casiopeina II-gly; COX, cytochrome *c* oxidase; GAPDH, glyceraldehyde 3P-dehydrogenase; GLUT-1, glucose transporter 1; HK, hexokinase; rhod 123, rhodamine 123; 2-DOG, 2-deoxyglucose.

Contract grant sponsor: CONACyT-Mexico;
Contract grant numbers: Salud-2002-C01-7677, SEP-2007-60517.

*Correspondence to: Sara Rodríguez-Enríquez, Departamento de Bioquímica, Instituto Nacional de Cardiología, Juan Badiano No. 1 Seccion XVI, Tlalpan, Mexico D.F. 14080, Mexico.
E-mail: saren960104@hotmail.com

Received 24 October 2007; Accepted 11 December 2007

DOI: 10.1002/jcp.21392

Review

Targeting of cancer energy metabolism

Sara Rodríguez-Enríquez, Alvaro Marín-Hernández, Juan Carlos Gallardo-Pérez, Liliana Carreño-Fuentes and Rafael Moreno-Sánchez

Departamento de Bioquímica, Instituto Nacional de Cardiología, Mexico, Mexico

The main purpose of this review is to update and analyze the effect of several antineoplastic drugs (adriamycin, apoptodilin, casiopeinas, cisplatin, clotrimazole, cyclophosphamide, ditercalinium, NSAIDs, tamoxifen, taxol, 6-mercaptopurine, and α-tocopheryl succinate) and energy metabolism inhibitors (2-DOG, gossypol, delocalized lipophilic cations, and uncouplers) on tumor development and progression. The possibility that these antineoplastic drugs currently used in *in vitro* cancer models, in chemo-therapy, or under study in phase I to III clinical trials induce tumor cellular death by altering also metabolite concentration (*i.e.*, ATP), enzyme activities, and/or energy metabolism fluxes is assessed. It is proposed that the use of energy metabolic therapy, as an alternative or complementary strategy, might be a promising novel approach in the treatment of cancer.

Keywords: Anticancer drugs / Glycolysis / Mitochondria / Oxidative phosphorylation

Received: November 19, 2007; revised: June 11, 2008; accepted: July 27, 2008

1 Introduction

The field of cancer energy metabolism seemed resolved by 1956 when Warburg [1] proposed that the prime cause of cancer was an energy deficiency caused by an irreversible damage to the mitochondrial function that induced an increased glycolysis. Since then, several researchers have thought that the Warburg hypothesis applies to all or most cancer cell types [2–14], because one of the most notorious and well-known alterations in tumor cells is certainly an increased glycolytic capacity, even in the presence of high O_2 concentration [3, 4, 15–18].

The observation that tumors have a higher glycolytic capacity than normal cells has found application in the use of positron emission tomography (PET) for diagnosis, monitoring, and treatment of cancer [19, 20]. With ^{18}fluoro-deoxyglucose (FDG) as tracer, PET has established that the vast majority of metastatic tumors (>90%) are highly glycolytic; and has also allowed for the accurate detection (>90%) of solitary pulmonary nodules, mediastinal and axillary lymph nodes, colorectal cancers, lymphomas, melanomas, breast cancers, and head and neck cancers [19].

2 Glycolysis in tumor cells

2.1 General

Fast-growth cancers from human (leukemia, HeLa) and rodent (AS-30D, Morris 7800, Dunings LC18, Novikoff hepatomas) show an increased glycolytic rate (2- to 17-times) in comparison with nontumorigenic cells [21–23]. This metabolic feature is the consequence of glycolytic enzymes over-expression induced by (i) oncogene *c-myc* (glucose transporter 1 (GLUT1), hexosephosphate isomerase (HPI), phosphofructo kinase type 1 (PFK1), glyceraldehyde 3-phosphate dehydrogenase (GAPDH), phosphoglycerate kinase (PGK), and enolase (ENO)) [5] and (ii) HIF-1α (hypoxia inducible factor 1α), GLUT1, glucose trans-

Correspondence: Dr. Sara Rodríguez-Enríquez, Departamento de Bioquímica, Instituto Nacional de Cardiología, Juan Badiano No. 1, Col. Sección 16, Tlalpan, Mexico, Mexico
E-mail: sara.rodriguez@cardiologia.org.mx
Fax: +5255-55-73-09-26

Abbreviations: ALDO, aldolase; **AMF,** autocrine motility factor; **Cas IIgly,** casiopeina II gly; **CCCP,** carbonyl cyanide-3-chlorophenylhydrazone; **CML,** chronic myelogenous leukemia; **CP,** cyclophosphamide; **DLC,** delocalized lipophilic cation; **2-DOG,** 2-deoxyglucose; **ENO,** enolase; **F1,6BP,** fructose 1,6 bisphosphate; **F2,6BP,** fructose 2,6 bisphosphate; **FDG,** ^{18}fluoro-deoxyglucose; **GAPDH,** glyceraldehyde 3-phosphate dehydrogenase; **GLUT1,** glucose transporter 1; **GLUT3,** glucose transporter 3; **G6P,** glucose 6-phosphate; **HK1,** hexokinase type I; **HKII,** hexokinase type II; **HPI,** hexosephosphate isomerase; **LDH,** lactate dehydrogenase; **6MP,** 6-mercaptopurine; **3MPA,** 3-mercaptopicolinic acid; **MPT,** mitochondrial permeability transition; **NSAID,** nonsteroidal anti-inflammatory drug; **PET,** positron emission tomography; **PFK1,** phosphofructo kinase type 1; **PFK2,** phosphofructo kinase type 2; **PGK,** phosphoglycerate kinase; **P-gly,** glycoprotein type P; **α-TOS,** α-tocopheryl succinate

Journal of Cellular Physiology

Kinetics of Transport and Phosphorylation of Glucose in Cancer Cells

SARA RODRÍGUEZ-ENRÍQUEZ*, ALVARO MARÍN-HERNÁNDEZ, JUAN CARLOS GALLARDO-PÉREZ, AND RAFAEL MORENO-SÁNCHEZ

Departamento de Bioquímica, Instituto Nacional de Cardiología Ignacio Chávez, Tlalpan, México City, Mexico

Metabolic control analysis of tumor glycolysis has indicated that hexokinase (HK) and glucose transporter (GLUT) exert the main flux control (71%). To understand why they are the main controlling steps, the GLUT and HK kinetics and the contents of GLUT1, GLUT2, GLUT3, GLUT4, HKI, and HKII were analyzed in rat hepatocarcinoma AS-30D and HeLa human cervix cancer. An improved protocol to determine the kinetic parameters of GLUT was developed with D-[2-^{3}H-glucose] as physiological substrate. Kinetic analysis revealed two components at low- and high-glucose concentrations in both tumor cells. At low glucose and 37°C, the V_{max} was 55 ± 20 and 17.2 ± 6 nmol (min × mg protein)$^{-1}$, whereas the K_m was 0.52 ± 0.7 and 9.3 ± 3 mM for hepatoma and HeLa cells, respectively. GLUT activity was partially inhibited by cytochalasin B ($IC_{50} = 0.44 \pm 0.1$; $K_i = 0.3 \pm 0.1$ μM) and phloretin ($IC_{50} = 8.7$ μM) in AS-30D hepatocarcinoma. At physiological glucose, GLUT1 and GLUT3 were the predominant active isoforms in HeLa cells and AS-30D cells, respectively. HK activity in HeLa cells was much lower (60 mU/mg protein) than that in AS-30D cells (700 mU/mg protein), but both HKs were strongly inhibited by G6P. HKII was the predominant isoform in AS-30D carcinoma and HeLa cells. The much lower GLUT V_{max} and catalytic efficiency (V_{max}/K_m) values in comparison to those of G6P-sensitive HK suggested the transporter exerts higher control on the glycolytic flux than HK in cancer cells. Thus, GLUT seems a more adequate therapeutic target.

J. Cell. Physiol. 221: 552–559, 2009.

The glycolytic rate of human and rodent fast-growing tumor cells, including those tumors depending on mitochondrial metabolism, is substantially higher than in non-tumorigenic cells (reviewed in Moreno-Sánchez et al., 2007). The activation of certain oncogenes (*c-myc*, *H-Ras*, *v-src*) and transcription factors, such as HIF-1α (hypoxia-inducible factor 1α), induces the over-expression and increase the activity of most glycolytic enzymes and glucose transporters (Dang et al., 1997).

Metabolic control analysis applied to non-tumorigenic mammalian cells (hepatocytes, erytrocytes, skeletal and cardiac muscle) shows that the main controlling steps of glycolysis (80–100%) are the glucose transport (GLUT), hexokinase (HK), and phosphofructokinase type-1 (PFK-1), whereas the remaining flux control is distributed among the other steps (Rapoport et al., 1976; Torres et al., 1989; Kashiwaya et al., 1994). However, in cancer cells a re-distribution of flux control might occur because such controlling steps are the most over-expressed glycolytic proteins (Moreno-Sánchez et al., 2007, 2008). In this regard, it was recently determined by using metabolic control analysis (Marín-Hernández et al., 2006) that AS-30D glycolysis was mainly controlled by HK and GLUT (up to 71% of flux control). The rest of the glycolytic enzymes (from HPI to LDH) and glycolysis branches (pentoses monophosphate, glycogen synthesis, pyruvate branches, and ATP-demand pathways) exerted the remaining flux control; PFK-1 showed negligible flux control (6%). Most of the flux control of the G6P-producing block in tumor cells might reside in HK because (i) the intracellular glucose concentration is high and saturating for HK (i.e., HK elasticity is low) and (ii) the enzyme is strongly inhibited by G6P.

HKII is the predominant isoform expressed in most cancer cells (Pedersen et al., 2002); this isoform may bind to the external mitochondrial membrane to rapidly consume the mitochondrial-derived ATP and generate G6P (Arora and Pedersen, 1988). It has been widely documented that the HK-maximal rate of human and rodent tumors is higher (60–420 mU/mg protein) than that of normal tissues (0.001–170 mU/mg protein) (Oskam et al., 1985; Mandarino et al., 1995; Marín-Hernández et al., 2006; Moreno-Sánchez et al., 2007). However, in the majority of the kinetic studies in cancer cells, the HK activity has been calculated from the free or cytosolic isoform, whereas the contribution of membrane-bound HK has not always been evaluated, thus, underestimating total HK activity.

HK is massively over-expressed by AS-30D hepatocarcinoma (300-times vs. hepatocytes); however, both HK isoforms, cytosolic and membrane-bound, are strongly inhibited by their product, G6P (Marín-Hernández et al., 2006). In consequence, HK becomes one of the main controlling steps of tumor glycolysis. To make well-informed statements and generalizations about the behavior of this relevant glycolytic step it is then required (i) to establish what HK isoform is expressed by each particular tumor cell line and (ii) to determine its kinetic properties.

GLUT1 is the most frequently isoform over-expressed in fast-growing and metastatic tumors (Medina and Owen, 2002). However, other GLUT isoforms (GLUT3 and GLUT5) not usually found in the original tissue may also be over-expressed (Higashi et al., 1997). GLUT over-expression has usually been determined as an mRNA or protein increase (Nagamatsu et al.,

Abbreviations: G6P, glucose-6-phosphate; GLUT, glucose transporter; HK, hexokinase; HPI, hexose-phosphate isomerase.

Additional Supporting Information may be found in the online version of this article.

Contract grant sponsor: CONACyT-México;
Contract grant numbers: 80534, 60085.

*Correspondence to: Sara Rodríguez-Enríquez, Departamento de Bioquímica, Instituto Nacional de Cardiología, Juan Badiano No. 1. Colonia Sección, XVI, Tlalpan 14080, México. E-mail: sara.rodriguez@cardiologia.org.mx

Received 13 May 2009; Accepted 22 June 2009

Published online in Wiley InterScience (www.interscience.wiley.com.), 13 August 2009.
DOI: 10.1002/jcp.21885

BioFactors

The bioenergetics of cancer: Is glycolysis the main ATP supplier in all tumor cells?

Rafael Moreno-Sánchez, Sara Rodríguez-Enríquez, Emma Saavedra, Alvaro Marín-Hernández, Juan Carlos Gallardo-Pérez*
Instituto Nacional de Cardiología, Departamento de Bioquímica, Juan Badiano 1, Tlalpan, México DF, Mexico

Abstract.

The molecular mechanisms by which tumor cells achieve an enhanced glycolytic flux and, presumably, a decreased oxidative phosphorylation are analyzed. As the O_2 concentration in hypoxic regions of tumors seems not limiting for oxidative phosphorylation, the role of this mitochondrial pathway in the ATP supply is re-evaluated. Drugs that inhibit glycoysis and oxidative phosphorylation are analyzed for their specificity toward tumor cells and effect on proliferation. The energy metabolism mechanisms involved in the use of positron emission tomography are revised and updated. It is proposed that energy metabolism may be an alternative therapeutic target for both hypoxic (glycolytic) and oxidative tumors.

Volume 35, Number 2, March/April 2009, Pages 209–225 •
E-mail: rafael.moreno@cardiologia.org.mx or morenosanchez@hotmail.com

Keywords: glycolysis, oxidative phosphorylation, mitochondrial function, PET, metabolic control analysis

1. Introduction

All tumor cell types show an altered energy metabolism in comparison to their tissue of origin (Figs. 1 and 2). The best characterized energy metabolism modification in tumor cells is an increased glycolytic capacity even in the presence of a high O_2 concentration ([1], reviewed in ref. 2). Several mechanisms for the enhanced glycolysis in tumor cells have been proposed (Table 1). However, each particular tumor cell line has its own combination of mechanisms to increase glycolysis and, therefore, generalizations should be avoided.

2. Genetic regulation of glycolysis

In tumor cells, there is an enhanced transcription of genes of several or all glycolytic pathway enzymes and transporters that is accompanied by an enhanced protein synthesis [2]. It is usually assumed that these transcriptional changes lead to increased activity and pathway flux. Unfortunately, the required biochemical (metabolic, kinetic) experimentation is considered "old-fashioned" and, only in few of the molecular biology studies, transporter and enzyme activities and flux rate have been determined.

In comparison with normal rat hepatocytes, the activity of all glycolytic enzymes are overexpressed in rat AS-30D hepatoma by 2–4 times (HPI, ALD, TPI, GAPDH, PGK, PGAM, ENO, and LDH), 8- to 10-fold for PYK, and 17–300 times for PFK-1 and HK (Fig. 1) [10]. For human cervix HeLa cells, all enzymes including HK and PFK-1 are overexpressed by 2–7 times, with the exception of PGAM and LDH which are 2–7 times lower than in rat hepatocytes [10]. However, for this last case a more rigorous comparison should be made with normal uterine cervix epithelial cells, the original source, when data become available. In rat Morris hepatomas, the activities of HK, PFK and PYK are 5- to 500-fold higher than in liver [26], whereas in human breast cancer, the activities of HK, ALD, PYK, and LDH are 3.7–7 times higher than in normal tissue [27]. In several human carcinomas, overexpression (Table 1) of GLUT [3], GAPDH, ENO-1, PYK, and LDH [28,29], correlates with a high glycolysis rate. In contrast, in human cartilage and bone marrow cancer, glycolysis is high but only sporadic expression of GAPDH, ENO-1, and PYK is observed [29]. Unfortunately, the expression pattern of the whole set of glycolytic enzymes is not always analyzed, which frequently leads to extend these observations to all types of cancer.

In cancer cells, the hypoxia inducible factor 1α (HIF-1α) is a transcriptional factor that upregulates the expression of specific isoforms of GLUT, HK, PFK-1, PFK-2, ALD, GAPDH,

Abbreviations: ALD, aldolase; AcCoA, acetyl CoA; Cit, citrate; DHAP, dihydroxyacetone phosphate; ENO, enolase; F6P, fructose-6-phosphate; F1,6BP, fructose-1, 6-bisphosphate; F2,6BP, fructose-2, 6-bisphosphate; Fum, fumarate; GAPDH, glyceraldehyde-3-phosphate dehydrogenase; αGPDH, α-glycerophosphate dehydrogenase; GLUT, glucose transporter; G6P, glucose-6-phosphate; Gln, glutamine; Glut, glutamate; HK, hexokinase; HPI, hexose-6-phosphate isomerase; LDH, lactate dehydrogenase; OxPhos, oxidative phosphorylation; 2-Oxo, 2-oxoglutarate; PDH, pyruvate dehydrogenase complex; PET, positron energy transfer; PFK-1, phosphofructokinase type 1; PGK, phosphoglycerate kinase; PGAM, phosphoglycerate mutase; PYK, pyruvate kinase; PEP, phospho*enol*pyruvate; 1,3 BPG, 1,3-bisphosphoglycerate; 2PG, 2-phosphoglycerate; 3PG, 3 phosphoglycerate; Pyr, pyruvate;TPI, triosephosphate isomerase.

*Address for correspondence: Rafael Moreno-Sánchez, Ph.D., Instituto Nacional de Cardiología, Departamento de Bioquímica, Juan Badiano No. 1, Col. Seccion XVI, Tlalpan, México DF 14080, Mexico. Tel: +5255 5573 2911 (ext. 1422, 1298); E-mail: rafael.moreno@cardiologia.org.mx or morenosanchez@hotmail.com.
Received 3 December 2008; accepted 18 January 2009
DOI: 10.1002/biof.31
Published online 11 March 2009 in Wiley InterScience (www.interscience.wiley.com)

The International Journal of Biochemistry & Cell Biology 42 (2010) 1744–1751

Contents lists available at ScienceDirect

The International Journal of Biochemistry & Cell Biology

journal homepage: www.elsevier.com/locate/biocel

Oxidative phosphorylation is impaired by prolonged hypoxia in breast and possibly in cervix carcinoma

Sara Rodríguez-Enríquez[a,*], Liliana Carreño-Fuentes[a], Juan Carlos Gallardo-Pérez[a], Emma Saavedra[a], Héctor Quezada[a], Alicia Vega[b], Alvaro Marín-Hernández[a], Viridiana Olín-Sandoval[a], M. Eugenia Torres-Márquez[b], Rafael Moreno-Sánchez[a]

[a] Departamento de Bioquímica, Instituto Nacional de Cardiología Ignacio Chávez, México D.F. 14080, Mexico
[b] Departamento de Bioquímica, Facultad de Medicina, UNAM, México D.F. 04510, Mexico

ARTICLE INFO

Article history:
Received 26 March 2010
Received in revised form 18 June 2010
Accepted 12 July 2010
Available online 21 July 2010

Keywords:
Glycolysis
Hypoxia
Mitochondria
Oxidative phosphorylation
Breast cancer

ABSTRACT

It has been assumed that oxidative phosphorylation (OxPhos) in solid tumors is severely reduced due to cytochrome *c* oxidase substrate restriction, although the measured extracellular oxygen concentration in hypoxic areas seems not limiting for this activity. To identify alternative hypoxia-induced OxPhos depressing mechanisms, an integral analysis of transcription, translation, enzyme activities and pathway fluxes was performed on glycolysis and OxPhos in HeLa and MCF-7 carcinomas. In both neoplasias exposed to hypoxia, an early transcriptional response was observed after 8 h (two times increased glycolysis-related mRNA synthesis promoted by increased HIF-1α levels). However, major metabolic remodeling was observed only after 24 h hypoxia: increased glycolytic protein content (1–5-times), enzyme activities (2-times) and fluxes (4–6-times). Interestingly, in MCF-7 cells, 24 h hypoxia decreased OxPhos flux (4–6-fold), and 2-oxoglutarate dehydrogenase and glutaminase activities (3-fold), with no changes in respiratory complexes I and IV activities. In contrast, 24 h hypoxia did not significantly affect HeLa OxPhos flux; neither mitochondria related mRNAs, protein contents or enzyme activities, although the enhanced glycolysis became the main ATP supplier. Thus, prolonged hypoxia (a) targeted some mitochondrial enzymes in MCF-7 but not in HeLa cells, and (b) induced a transition from mitochondrial towards a glycolytic-dependent energy metabolism in both MCF-7 and HeLa carcinomas.

1. Introduction

For growth, solid tumors have developed strategies to maintain the carbon source and oxygen supplies. Thus, tumors exhibit an active angiogenesis which, however, is highly inefficient generating chaotic networks, with unorganized, fragile, and leaky new vessels (reviewed by Nagy et al., 2009). In consequence, the dynamics of the blood flow is affected, leading to hypoxic regions at 100–200 μm away from a functional blood supply (Vaupel et al., 1989; Helmlinger et al., 1997; Nagy et al., 2009).

It has been determined that the oxygen concentration inside well-oxygenated areas of several carcinomas ranges from 30 to 80 mm Hg whereas in their hypoxic regions, it may reach a value of 2.5–10 mm Hg (equivalent to 3–13 μM O_2, calculated by Horan and Koch, 2001) (Kallinowski et al., 1989; Vaupel et al., 1991; Hunjan et al., 1998; Erickson et al., 2003). The development of hypoxic regions in solid tumors is a typical characteristic linked to malignant phenotype, metastasis, chemo-, immuno- and radio-therapy resistance, high genetic instability and apoptosis tolerance (Graeber et al., 1996; Bristow and Hill, 2008). Some of these processes are modulated by HIF-1α, a key transcriptional factor that regulates the gene transcription of proteins involved in angiogenesis, cellular proliferation, erythropoietic and vascularization pathways (Weidemann and Johnson, 2008), allowing tissues to adjust to scarce oxygen availability. At metabolic level, HIF-1α increases the gene transcription of specific isoenzymes of almost all glycolytic enzymes and transporters (reviewed in Marín-Hernández et al., 2009); in consequence, the glycolytic flux increases by at least 2-times in the majority of neoplasias (Altenberg and Greulich, 2004; Walenta et al., 2004).

In spite of the hypoxic-glycolytic activation, the tumor intracellular ATP pool drastically diminishes (30–60%) whereas phosphate augments (Mueller-Klieser et al., 1990; Heerlein et al., 2005;

Abbreviations: COX, cytochrome c oxidase; HIF-1α, hypoxia-inducible factor 1α; HK, hexokinase; GA, glutaminase; OxPhos, oxidative phosphorylation; PDH, pyruvate dehydrogenase complex; PDK1, pyruvate dehydrogenase kinase-1; 2-OGDH, 2-oxoglutarate dehydrogenase.

* Corresponding author at: Departamento de Bioquímica, Instituto Nacional de Cardiología, Juan Badiano No. 1, Col. Sección 16, Tlalpan, México D.F. 14080, Mexico. Tel.: +52 55 55 73 29 11.
E-mail address: saren960104@hotmail.com (S. Rodríguez-Enríquez).

1357-2725/$ – see front matter © 2010 Elsevier Ltd. All rights reserved.
doi:10.1016/j.biocel.2010.07.010